

# Targeted molecular engineering of PCE superplasticizers for OPC and slag blended cement

**Lin Zhang**

Vollständiger Abdruck der von der TUM School of Natural Sciences der Technischen Universität  
München zur Erlangung einer

**Doktorin der Naturwissenschaften (Dr. rer. nat.)**

genehmigten Dissertation.

Vorsitz: Prof. Dr. Thomas Brück

Prüfende der Dissertation:

1. Prof. Dr. Tom Nilges
2. Prof. Dr. Dr. h. c. Bernhard Rieger

Die Dissertation wurde am 14. 11. 2024 bei der Technischen Universität München eingereicht und  
durch die TUM School of Natural Sciences am 07. 01. 2025 angenommen.

---

---

## **Acknowledgments**

The present work, conducted between 2020 to 2024, was carried out under the instruction of **Prof. Dr. Johann Plank** at the Chair of Construction Chemistry, within the Chemistry Department of TUM School of Natural Sciences.

My four years of study at TUM have been an immensely valuable experience. It not only broadened my academic horizons but also had a profound impact on my life.

First, I want to express my sincere gratitude to my supervisor

### **Prof. Dr. Johann Plank**

Thank you for providing me the chance to work here and introduce me to this meaningful topic: PCE for OPC and low-carbon binders. I appreciate your insightful feedback on my work, helping me refine my research skills and academic writing. I am grateful for the chance to contribute to corporate projects, such as the Ecocem project, which bridged the gap between laboratory research and industrial applications and provided invaluable insights for my future endeavors. Your encouragement has motivated me to maintain a high work standard and refine my critical thinking skills.

Second, I want to thank my mentor **Prof. Dr. Lei Lei**, Thanks for your useful guidance and warm encouragement on my work. I am grateful for the positive impact you've had on both my academic and personal development.

Then, I want to thank the **China Scholarship Council** for the scholarship that financed my research and stay at TU München. Thanks to **Prof. Ziming Wang** and **Prof. Suping Cui** for the recommendation letters which help me a lot during my application for this scholarship.

Moreover, a special thanks to all colleagues at this chair. Thanks for your help in my research work, and getting to know you has made my life more colorful. Thanks to **Christopher Schiefer, Matthias Werani, Dr. Yue Zhang, Dominik Staude, Dagmar Lettrich, and My Linh Vo** for introducing the instruments in our group and showing me the operation of PCE synthesis and characterizations, mortar tests, and lab cleaning.

## Acknowledgments

---

I am grateful for the daily help given by my lab colleagues: **Dr. Ran Li, Wei-Chao Chen, Na Miao, Marlene Schmid, Hicran Güngör, Jingxian Yang, Yi Liu, Jie Shi, Yuexin Zhang, Zichen Guo, Dr. Matthias Theobald.** It is a pleasure to work with you and it is very interesting to learn the cultural customs of different countries and regions when talk with you. Thanks for your help again and wish you all the best.

Last but not the least, my cordial thanks go to my beloved family **Ying Zhang, Ying Li, Mingxiang Zhang** and extended family members. The warm, loving and nurturing environment you provided during my formative years have played a crucial role in shaping who I am today. Thank you for standing by me and supporting all my decisions, enabling me to embrace life happily and navigate life's challenges with courage and resilience.

I want to extend my appreciation to myself for the perseverance and hard working that have been instrumental in reaching this milestone. Thanks for never giving up, for embracing challenges with optimism, and for the courage to live life boldly.

München, January 09 2024.

Lin Zhang

## **List of publications**

### **Peer reviewed SCI journal paper**

Synthesis and performance of a non-air entraining polycarboxylate superplasticizer

Lei Lei, **Lin Zhang**

### **Peer reviewed data in brief paper**

Characterization data of reference industrial polycarboxylate superplasticizer VP 2020/15.2 used for Priority Program DFG SPP 2005 “Opus Fluidum Futurum - Rheology of reactive, multiscale, multiphase construction materials”

**Lin Zhang**, Ran Li, Lei Lei, Johann Plank

List of abbreviations

**List of abbreviations:**

<b>Abbreviation</b>	<b>Full name</b>
<b>AA</b>	Acrylic acid
<b>AAS</b>	Alkali-activated slag
<b>ALT</b>	Adsorbed layer thickness
<b>AMPS</b>	2-Acrylamido-2-methylpropane sulfonic acid
<b>APEG</b>	$\alpha$ -allyl- $\omega$ -methoxy polyethylene glycol
<b>APS</b>	Ammonium persulfate
<b>Bwob</b>	By weight of binders
<b>Bwoc</b>	By weight of cement
<b>°C</b>	Degree Celsius
<b>CEM I</b>	Portland cement (DIN EN 197-1)
<b>CEM II</b>	Composite cement (DIN EN 197-1)
<b>CEM III</b>	Composite cement (DIN EN 197-1)
<b>cm</b>	Centimeter
<b>CMC</b>	Critical micelle concentration
<b>CRP</b>	Controlled radical polymerization
<b>Da</b>	Dalton
<b>dRI</b>	Differential refractive index
<b>d10/50/90</b>	Unit of the grain size distribution (mass-averaged particle diameter)
<b>G</b>	Gram
<b>GGBFS</b>	Ground granulated blast-furnace slag
<b>g/L</b>	Gram per litre
<b>H</b>	Hour
<b>HLB</b>	Hydrophilic–lipophilic balance
<b>HPEG</b>	$\alpha$ -methallyl- $\omega$ -methoxy or - $\omega$ -hydroxy poly(ethylene glycol) ether

List of abbreviations

<b>Abbreviation</b>	<b>Full name</b>
<b>IFT</b>	Interfacial tension
<b>IPEG</b>	Isoprenyl oxy poly(ethylene glycol) ether
<b>Kg</b>	Kilogram
<b>L</b>	Litre
<b>LS</b>	Light scattering
<b>MAA</b>	Methacrylic acid
<b>MAH</b>	Maleic anhydride
<b>Mg</b>	Milligram
<b>mL</b>	Mililitre
<b>Min</b>	Minute
<b><math>M_n</math></b>	Number average molecular weight
<b><math>M_w</math></b>	Weight average molecular weight
<b>MPEG</b>	$\omega$ -methoxy polyethylene glycol
<b>OPC</b>	Ordinary Portland cement
<b>PCE</b>	Polycarboxylate ether/ ester
<b>PDI</b>	Polydispersity index
<b>PMAA</b>	Poly(methacrylic acid)
<b>Q-XRD</b>	Quantitative x-ray diffraction
<b>RI</b>	Refractive index
<b>Rpm</b>	Rotations per minute
<b>S</b>	Second
<b>SEC</b>	Size Exclusion Chromatography
<b>TOC</b>	Total organic carbon
<b><math>\mu\text{m}</math></b>	Micrometer
<b>VC</b>	Ascorbic acid
<b>wt. %</b>	Weight percent
<b>w/b ratio</b>	Water-to-binder ratio
<b>w/c ratio</b>	Water-to-cement ratio

List of abbreviations

<b>Abbreviation</b>	Full name
<b>XRD</b>	X-ray diffraction

**Content**

1. Introduction.....	- 1 -
2. Aims and scope .....	- 5 -
2.1 Non-air entraining PCE synthesized by grafting method .....	- 5 -
2.2 Non-air entraining PCE prepared through ion-pair complex.....	- 6 -
2.3 Synthesis of PCE composing maleic anhydride monomer .....	- 6 -
2.4 Characterization of low-carbon binders.....	- 7 -
2.5 PCE superplasticizers for ‘slag + cement’ binder system .....	- 7 -
2.6 Synthesis of novel structured PCE and their performance .....	- 7 -
3. Theoretical background.....	- 9 -
3.1 Composite cement and green binders .....	- 9 -
3.1.1 Classification of supplementary cementitious materials (SCMs) .....	- 9 -
3.1.2 Slag blended cement system .....	- 10 -
3.1.3 Composite cement CEMII/III .....	- 11 -
3.2 The workability of concrete .....	- 13 -
3.2.1 Interaction between cementitious materials and superplasticizer .....	- 13 -
3.2.2 Conventional methods to achieve slump retention for concrete .....	- 15 -
3.2.3 Conventional foam control agent for concrete.....	- 16 -
3.3 Polycarboxylate superplasticizers .....	- 18 -
3.3.1 Chemical composition and working mechanism of polycarboxylate superplasticizer.....	- 18 -
3.3.2 Copolymerization methods of polycarboxylate superplasticizer .....	- 25 -
3.3.3 Carbon emission of polycarboxylate superplasticizers .....	- 27 -
4. Experimental materials and methods .....	- 29 -
4.1 Materials .....	- 29 -
4.1.1 Cementitious materials.....	- 29 -
4.1.2 Chemicals .....	- 30 -
4.2 Experimental method .....	- 31 -
4.2.1 Size Exclusion Chromatography (SEC).....	- 31 -

## Content

---

4.2.2 FT-IR spectra .....	- 31 -
4.2.3 <sup>1</sup> H NMR .....	- 31 -
4.2.4 Specific anionic charge amount .....	- 31 -
4.2.5 Phase separation analysis of ion-pair system .....	- 32 -
4.2.6 Defoaming performance and foaming behavior .....	- 32 -
4.2.7 Defoaming performance in mortar .....	- 32 -
4.2.8 Dispersing effectiveness in paste .....	- 33 -
4.2.9 Dispersing effectiveness in mortar .....	- 33 -
4.2.10 Surface tension test .....	- 33 -
4.2.11 HLB value of the polymers .....	- 34 -
4.2.12 Compressive strength test in mortar .....	- 34 -
4.2.13 Isothermal heat-flow calorimetry .....	- 34 -
4.2.14 X-ray Diffraction analysis .....	- 34 -
4.2.15 Adsorption measurement .....	- 35 -
4.2.16 Zeta potential and pH values of cement paste .....	- 35 -
4.2.17 V-funnel empty times .....	- 36 -
4.2.17 Flow line test .....	- 36 -
5. Results and discussion .....	- 37 -
5.1 Synthesis and characterization of a non-air entraining PCE .....	- 37 -
5.1.1 Synthesis of conventional graft polymer G45PC3 and G45PC5 and non-air entraining PCE G45PC5-g-Jeffamine .....	- 37 -
5.1.2 Characterization of the synthesized graft PCE polymers .....	- 39 -
5.1.3 Phase separation of non-air entraining PCE .....	- 44 -
5.1.4 Dispersing effectiveness of non-air entraining PCE .....	- 45 -
5.1.5 Foaming behavior of non-air entraining PCE .....	- 47 -
5.1.6 Compressive strength of mortars .....	- 50 -
5.1.7 Isothermal heat-flow calorimetry test of cement paste .....	- 52 -
5.1.8 X-ray analysis of cement hydration .....	- 54 -
5.1.9 Summary of Section 5.1 .....	- 57 -

## Content

---

5.2 A novel defoaming system based on ion-pair complexes .....	- 59 -
5.2.1 Synthesis of PCE-Jeffamine ion-pair complexes .....	- 59 -
5.2.2 Characterization of PCE-Jeffamine ion-pair complexes .....	- 61 -
5.2.3 Phase separation test of PCE-Jeffamine ion-pair complexes .....	- 65 -
5.2.4 Foaming behavior of PCE-Jeffamine ion-pair complexes .....	- 65 -
5.2.5 Dispersing effectiveness of ion-pair complex .....	- 70 -
5.2.6 Compressive strength of mortars .....	- 71 -
5.2.7 Isothermal heat-flow calorimetry test of cement paste .....	- 73 -
5.2.8 Q XRD .....	- 75 -
5.2.9 Summary of Section 5.2 .....	- 80 -
5.3 Synthesis of HPEG-MAH PCE polymers.....	- 81 -
5.3.1 Synthesis of HPEG-MAH PCE by free radical copolymerization.....	- 81 -
5.3.2 HPEG-co-MAH copolymerization parameters .....	- 83 -
5.3.3 Ternary copolymerization system of MAH based PCE .....	- 86 -
5.3.4 Summary of Section 5.3 .....	- 88 -
5.4 Characterization and rheology of cementitious materials and their interaction with PCE polymers .....	- 89 -
5.4.1 Characterization data of VP 2020/15.2 PCE polymer.....	- 89 -
5.4.2 Interaction between PCE and cements .....	- 91 -
5.4.3 Phase composition and fluidity of composite cement CEM II/III .....	- 96 -
5.4.4 Summary of Section 5.4 .....	- 99 -
5.5 PCE superplasticizers for ‘slag + cement’ binder system .....	- 101 -
5.5.1 PCE for Na <sub>2</sub> SO <sub>4</sub> activated ‘slag + cement’ system .....	- 101 -
5.5.2 PCE superplasticizer for “Full binder” (w/b = 0.31).....	- 129 -
5.5.3 PCE superplasticizer for “Full binder” (w/c = 0.27).....	- 138 -
5.5.4 Summary of Section 5.5 .....	- 152 -
5.6 Novel structured PCE superplasticizers .....	- 154 -
5.6.1 Synthesis of PCE via free radical copolymerization.....	- 154 -
5.6.2 Characterization of PCE polymers.....	- 156 -

## Content

---

5.6.3 Performance of novel structured PCE in OPC .....	- 162 -
5.6.4 Summary of Section 5.6 .....	- 165 -
6. Summary and outlook .....	- 167 -
7. Zusammenfassung und Ausblick .....	- 171 -
Reference .....	- 175 -



## 1. Introduction

The ordinary Portland cement (OPC) has been used as an important ingredient of concrete material in construction field for even more than 200 years, and the increasing demand of building materials continues in pace with the urbanization development.

Nevertheless, the cement industry is one of the biggest energy consumer, and its carbon emissions account for ~ 8 % of the total global anthropogenic CO<sub>2</sub> emissions [1]. These CO<sub>2</sub> includes direct and indirect emissions emitted from the calcination of limestone (50 %), fossil fuels consumption (40 %) and transportation and electricity usage [2, 3].

**Figure 1** illustrated the carbon emissions originating from worldwide countries between 2000 and 2020.

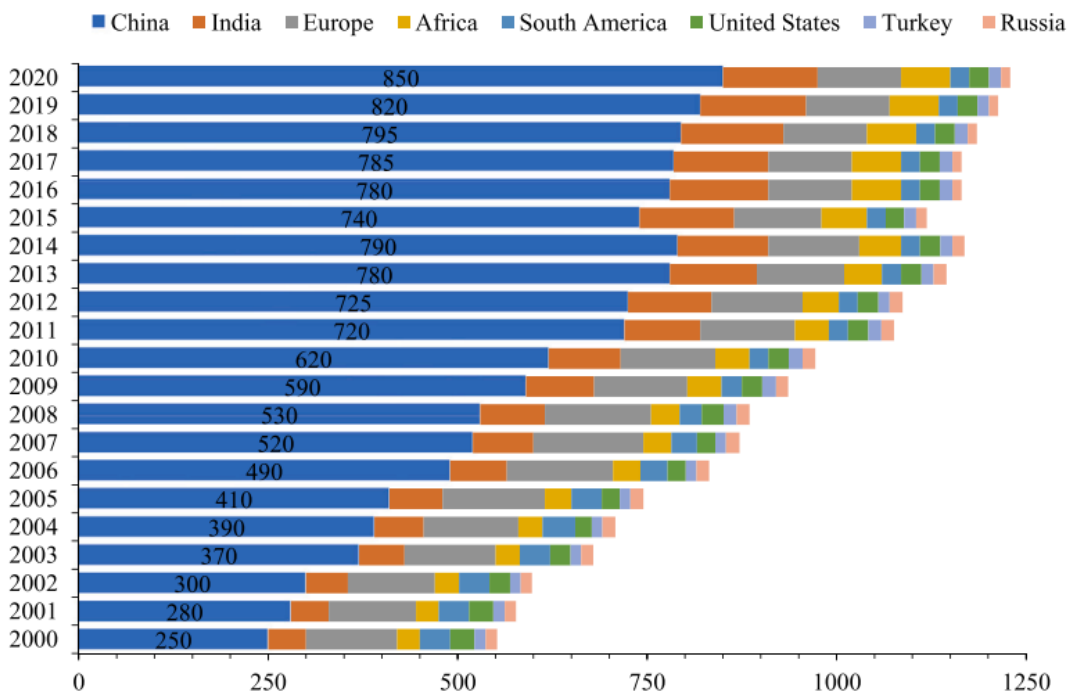


**Figure 1** Carbon emission of different countries between 2000 and 2020 [4, 5]

Cement industry needs to collaborate to tackle this massive challenge. Some sustainable development paths have been applied in the cement industry. Specifically, from the energy level, increasing energy efficiency and using some green fuels respectively

reduced the carbon emissions from energy consumption; carbon capture, use, and storage (CCUS) technology and CO<sub>2</sub> uptake approaches also effectively promote carbon recycling and reuse. The global CO<sub>2</sub> emission and uptake amount by cement from 1930 to 2019 is displayed in **Figure 2**.

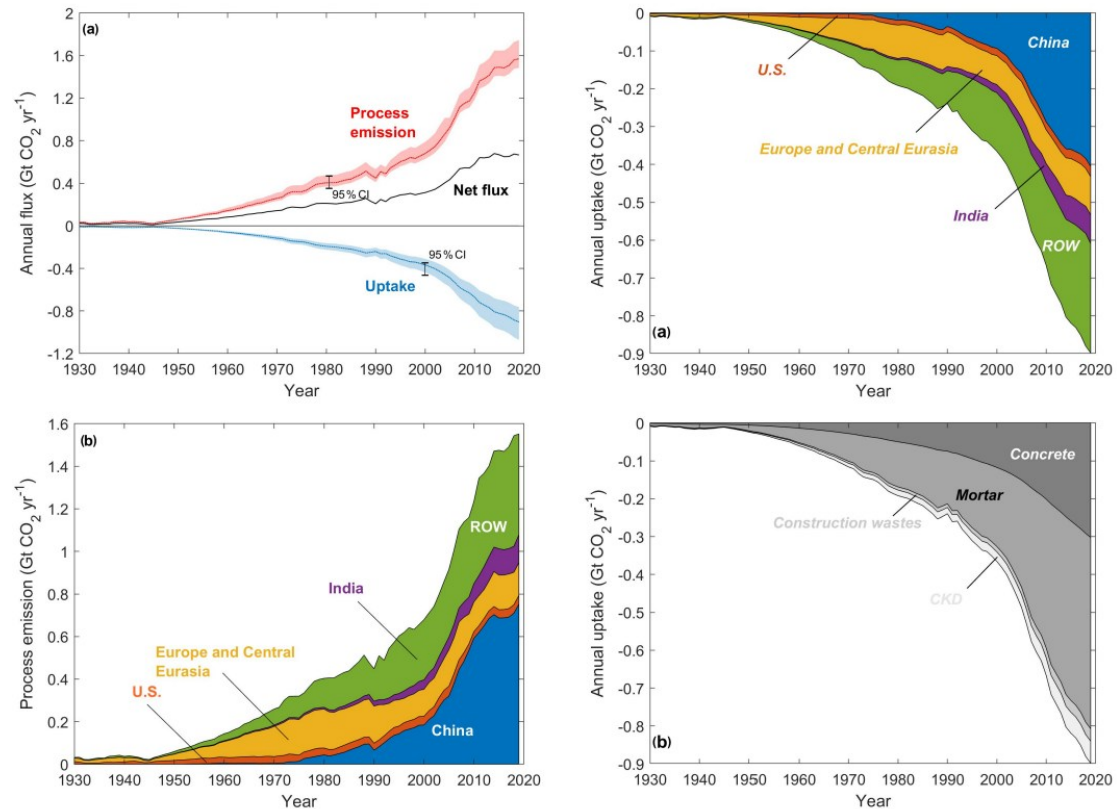


**Figure 2** Annual carbon emission (left a: total amount; b: different regions) and annual global uptake (right a: different regions; b: different cementitious materials) from cementitious materials between 1930 and 2019 [6]

From the material level, several strategies for cutting down carbon emissions have been reported [7, 8]. One direction is using waste products composed of high-content calcium oxides, such as slag, fly ash, and foundry sand to replace conventional clinker. Another direction is broadening novel alternative binders, including natural pozzolans, ground granulated blast-furnace slag (GGBFS), fly ash (FA), calcined clay, etc. The global trend to reduce carbon emissions from cement manufacturing and building materials

has promoted a gradual transition from OPC to a low-carbon cement system. Employing alternative raw materials in manufacturing Portland cement or partly replacing Portland clinker with low-carbon supplementary cementitious materials (SCMs) represent incremental improvements. Composite cements CEM II/III, which contain fly ash or slag SCMs, have been applied into production and application [9-12]. Such cements significantly reduce carbon emissions and provide improved durability, low heat of hydration, and sulfate resistance simultaneously [13-15].

Regarding the application of composite cement, both dispersing effectiveness and slump-retaining property are decisive aspects, especially for long-distance transition and pumping during concrete manufacturing. Therefore, Polycarboxylate ether superplasticizers (PCE) are essential and have become a standard component for cementitious materials. However, it is necessary to point out that low-carbon cement or supplementary cementitious materials have distinct particle sizes and surface charges compared with OPC. Conventional PCE superplasticizers designed for OPC may not be effective in low-carbon cement systems; therefore, novel structured PCE polymers are expected to disperse sustainable construction binders in the future.

Since its invention in 1981 [16], the PCE industry has continued to thrive and has never stopped improving its technology [17]. There are several avenues to enhance PCE's performance. First is adjusting the feeding molar ratio to give PCE different anionic charges or steric hindrance. Secondly, a great diversity of macromonomers exist have been produced for PCE synthesis: methacrylate ester-based PCEs (MPEG PCEs),  $\omega$ -methoxy- $\alpha$ -allyl poly(ethylene glycol) (APEG), vinyl ether-based PCEs (VPEG PCEs) including 2-hydroxyethyl poly(ethylene glycol) vinyl ether (EPEG) and ethylene glycol monovinyl polyethylene glycol ethers (GPEG), and isoprenyl oxy poly(ethylene glycol) ether (IPEG) and  $\alpha$ -methallyl- $\omega$ -methoxy (HPEG) monomers, which are remarkably popular macromonomers in most Asian countries. PCE superplasticizers synthesized from HPEG and IPEG present better performance and the synthesis process is much easier and more straightforward.

Furthermore, incorporating new functional groups such as amide or phosphate into PCE

or synthesizing zwitterionic PCE polymers provides additional properties. Zwitterionic PCEs were developed by K.C. Hsu et al. [18] and offered excellent performance in calcined clay blended composite cement systems. J. Stecher also reports that phosphate comb polymers can increase the flow speed of concrete [19]. Polycarboxylate superplasticizers (PCEs), as an indispensable admixture, have experienced modification by different macromonomers, small monomers, and functional groups. Nevertheless, all the PCEs keep a random chemical structure.

There are some reports related to novel structured PCEs like star-shaped or hyperbranched superplasticizers [20, 21]. Among all these novel structured PCE polymers, gradient structured superplasticizer was effective at relatively lower dosages. It showed lower sensitivity than random PCE at low sulfate ion concentrations [22, 23]. The reason is that the more concentrated distribution of carboxyl groups favors intense adsorption, and the adsorption conformation causes a more substantial steric effect. The synthesis of novel structured PCEs is often achieved through living radical polymerization techniques such as reversible addition-fragmentation chain transfer polymerization (RAFT), nitroxide-mediated polymerization (NMP), and atom transfer radical polymerization (ATRP) [24-26]. However, these methods are expensive and not practical for industrial production.

This dissertation focused on investigating the synthesis of defoamers based on PCE superplasticizer using grafting and ion pair methods. It also explores the free radical process for synthesizing a superplasticizer based on maleic anhydride. The study characterized low-carbon cement, including LCC, as well as three types of composite cement. Additionally, the research produces series of PCE samples designed for slag blended binder and PCE with novel structures that has potential in dispersing low-carbon composite cement.

## **2. Aims and scope**

The trend globally to reduce carbon emissions from cement industry has led to a shift from OPC towards low-carbon cement systems. PCE superplasticizer is an essential component for cementitious materials, and its unique properties such as slump retaining and less foaming are desirable for low-carbon binders. This dissertation focuses on developing novel structured PCEs by incorporating functional groups into typical PCE structures and investigating new chemical structures of PCE for OPC and low-carbon binders. Various synthesis methods, such as graft, free radical polymerization, and ion pair complex, have been studied. These investigations provide a diverse range of options for PCE synthesis and expand the scope of potential PCE products in the future. Moreover, the molecular design concept of PCE for low-carbon cement has been initially validated, and preparations have been made for further advancements in this area.

### **2.1 Non-air entraining PCE synthesized by grafting method**

This section deals with the synthesis and characterization of non-air entraining PCE samples, and their performances were evaluated in cement mortar. Specifically, conventional PCE exhibits polar backbones and hydrophilic polyethylene glycol (PEG) pendant chains. Such chemical structure offers great dispersing effectiveness through the adsorbed backbone and steric hindrance of PEG chains. On the other hand, the hydrophilic side chains stabilize the bubbles in mortar and concrete generated during the mixing process. The jeffamine monomers, which have EO/PO (hydrophilic/hydrophobic) repeat units, were grafted onto an MPEG PCE structure to realize the air control properties of PCE in mortar.

The graft PCE copolymers were characterized via SEC, FT-IR, <sup>1</sup>H NMR spectra, phase separation and foaming behavior tests to ensure they are high quality defoamers. The performance of such PCE samples was assessed and compared with conventional MPEG PCE in cement mortar through dispersing, air entrainment, compressive strength tests. For the mechanism analysis, the surface tension, HLB values of all PCE samples were measured. The isothermal heat-flow calorimetry and Q-XRD measurements were

also applied. The results suggested that the MPEG type PCE with extra Jeffamine side chains did not entrain any air and presents good dispersion power. The addition of such PCE polymer also promoted compressive strength development as it enhanced cement hydration, especially with respect to the silicate reaction.

The aim in this part is to bring a new concept to obtain non-air entraining PCE superplasticizer through grafting functional groups, and clarify the working mechanism of PCE polymer produced by graft method.

## **2.2 Non-air entraining PCE prepared through ion-pair complex**

In this part, the non-air entraining PCE samples were obtained by introducing Jeffamine monomer onto HPEG type PCEs through a simple ion pair reaction. Which can be realized by mixing PCE and Jeffamine, then adjusting the pH of the mixture solution.

Same as the MPEG type PCE defoamer, such ion-pair complexes were characterized via SEC, FT-IR, <sup>1</sup>H NMR spectra and phase separation. This study focuses on investigating the foaming behavior from different perspectives including foam stability, defoaming activity and durability. The dispersing mechanism of these ion pair complexes was explained through isothermal heat-flow calorimetry and Q-XRD measurements.

The purpose of this study is to obtain low-air entraining PCE product from simple ion-pair method and investigate the foaming behavior from different perspectives.

## **2.3 Synthesis of PCE superplasticizer composing maleic anhydride monomer**

The PCE superplasticizer contains maleic anhydride (MAH) with a high anionic charge. This helps to prolong the cement setting time and exhibits a good adsorption capacity. However, the MAH monomer has low activity and is not prone to copolymerization but homo-polymerization.

In this part, the APS-VC (Ammonium persulfate- ascorbic acid) redox initiators system was applied to synthesize MA-co-HPEG PCE superplasticizers in free radical method. SEC measurement was employed to verify the chemical information and conversion

rate of macromonomer. Different copolymerization parameters, such as feeding molar ratios, initiator amounts, HPEG macromonomer' molecular weight and third comonomers, were investigated to determine the optimal synthesis recipe.

The target of this part is to successfully synthesize MA-co-HPEG PCE superplasticizers through the free radical method and to increase the conversion rate to obtain high-quality PCE products.

#### **2.4 Characterization of low-carbon binders**

Nowadays, low-carbon binders have become increasingly prevalent in the construction industry. This part characterized LCC binder and three types of composite cement (CEM II/A-LL 32.5R; CEM III/A 42.5 N and CEM III/B 42.5 N). The interaction of VP 2020/15.2 PCE with LCC and OPC were determined by initial spread flow, slump retention, adsorption amount and zeta potential measurement. The particle size distribution, surface charges, pH values and fluidity of three types of composite cement were measured and compared with OPC cement.

The objective of this section is to fully comprehend the distinction between low-carbon binders and OPC cement. This will facilitate the advancement of PCE admixtures that are suitable for low-carbon cement.

#### **2.5 PCE superplasticizers for 'slag + cement' binder system**

This part aims to investigate the dispersing and slump retention performances of PCE polymers with different chemical compositions and PCE combinations in three 'slag + cement' systems possessing different slag content (85 %, 70 % and 60 %), and to check the potential retarding effect of these PCEs on the 1 d strength. Moreover, the fluidity of "Full binder" at very low water-to-binder ratio was evaluated, and the interaction between the microstructure of PCE superplasticizers and their performance was studied. These findings are valuable for developing PCE suitable for low-carbon cement-based materials, such as zwitterionic PCE and new structural PCE polymers.

#### **2.6 Synthesis of novel structured PCE and their performance**

PCE superplasticizer with novel structure exhibit distinct performance in cementitious materials. However, they are typically synthesized using controlled radical polymerization (CRP) techniques, including nitroxide mediated polymerization (NMP), atom transfer radical polymerization (ATRP) and reversible addition-fragmentation chain transfer (RAFT) methods. These methods are very useful but not easy to apply in the real industry. Therefore, this part investigates the potential of free radical methods to produce novel structured PCE copolymers.

Block-structured PCE was obtained from the free-radical method by changing the monomers' feeding sequence. Their dispersing effectiveness was tested in CEM I and low-carbon cement systems. The SEC, <sup>1</sup>H NMR and FT-IR spectra confirmed the distinct segment sequence between block and random PCE samples. It was found that PCE samples with block structure have higher dosage effectiveness especially in low-carbon cement system than random ones. This study confirms the possibility of controlling the performance of PCE polymers by changing the feeding sequence of monomers in free radical copolymerization.

### **3. Theoretical background**

#### **3.1 Composite cement and green binders**

##### **3.1.1 Classification of supplementary cementitious materials (SCMs)**

The sustainable development is currently the top priority for concrete industry. Among all energy-saving and emission-reduction measures, supplementary cementitious materials (SCMs) are considered good alternative materials and have been increasingly used to replace the OPC, which can reduce carbon emission as well as improve the durability of concrete [27-30]. The SCMs, such as ground granulated blast furnace slags (GGBFS) from the iron industry and fly ash from electricity production, have been widely employed as replacements in all types of concrete including lightweight concrete and ultra-high-performance concrete [31-33].

However, the supply of high-quality SCM by-products is limited and depends on local sources, as the availability of SCMs shown in **Figure 3**. In addition, a decline in production of GGBFS and fly ash is expected due to future developments in steel and electricity production. The main SCMs start shifting from slag and fly ash to limestone. Nowadays, more and more natural pozzolans and industry by-products are utilized to partly replace OPC clinker. Several SCM samples are introduced as follows [34-37]:

1. Natural pozzolans such as pumice, perlite, and vitric ash.
2. Calcined natural SCMs such as calcined metakaolin or kaolinite clay.
3. LC<sup>3</sup> materials which is a binder system including limestone, calcined clay and clinker.
4. Other industry by-product materials.

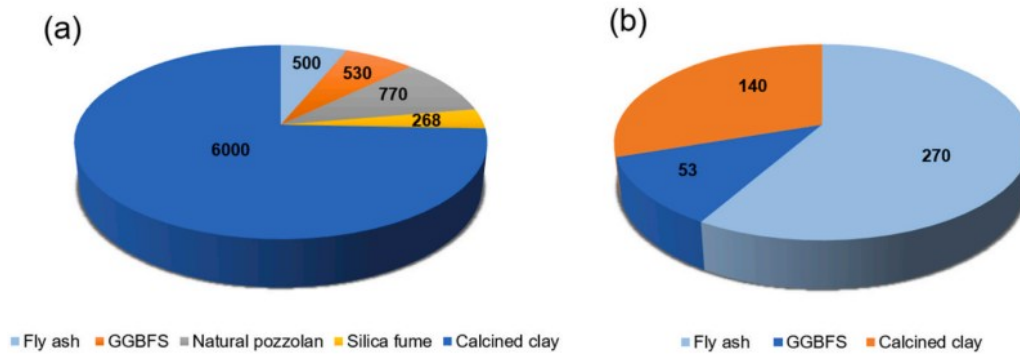


**Figure 3** Availability of different SCMs in million tons; (a) Global, (b) Indian [38-40]

It is worth to note, the physical properties of SCMs such as particle size distribution and specific surface area and chemical properties including oxide composition, phase composition and amorphous content, determine their hydration reactivity and water demand, which further influence the fluidity of the binder systems [41]. Specifically, the particle shape and size distribution of SCMs control their solid fraction and packing density, which are closely related to the strength development; the chemical surface properties drive PCE admixtures' adsorption behavior and interparticle forces, which affect the fluidity; both parts impact the hydration kinetics, the nucleation and growth of hydration products. Therefore, some characterizations of raw SCMs materials or binders are necessary before investigating their fluidity and interaction with PCE superplasticizers.

### 3.1.2 Slag blended cement system

Slag is a by-product from iron industry, it consists of calcium, magnesium aluminosilicates and has pozzolanic properties depending on quenching history. The carbon emission of slag is 0.07 ton CO<sub>2</sub>/ ton, which is much lower than that from OPC (1 ton CO<sub>2</sub>/ ton) [42].

GGBFS has a finer particle compare to OPC, the use of pure slag mineral admixtures could increase the fluidity of concrete and may reduce PCE dosages. Slag also has lower water demand, and exhibits enhanced workability compared with OPC. In addition, the

incorporation of these fine materials can optimize the particle size distribution and packing density, thus ensuring greater cohesiveness of binder [43, 44]. The hydrate product from slag, C-(A)-S-H gel, fills the pore and creates a denser microstructure during the hydration process, contributing to an enhanced durability [45].

However, the large amount of amorphous phase in slag determines its hydraulic properties. When dissolved in water, slag starts to hydrate at a very slow rate, therefore, alkaline activators, such as sodium hydroxide and sodium silicate, are necessary for slag-blended cement to promote the pozzolanic reactions [46]. Such activators increased the energy consumption and carbon emission, the production of 1 ton sodium hydroxide release 1.1 ton of CO<sub>2</sub>. For this reason, some green activators, including sodium carbonate, sodium sulphate, sodium aluminate, are used in alkaline activated slag system [47, 48]. In addition, potassium hydroxide is also suitable for slag activation, and it provides a faster setting time than sodium activator. The calcium activator, such as Ca(OH)<sub>2</sub>, can improve the durability of slag system. This three activators' effectiveness in strength development is in the order NaOH > KOH > Ca(OH)<sub>2</sub>, while in durability performance is Ca(OH)<sub>2</sub> > KOH > NaOH.

Previous publications have certificated that alkaline activated slag commits enhanced mechanical and durability properties of concrete but causes high shrinkage and quick setting problems [46, 49-51]. This characteristic makes it very suitable for use as aggregate in road surface layers, and its fire resistance performance extends the application in high-strength and refractory concrete.

The challenges related to the usage of alkaline-activated slag are exploring green activators, innovating novel superplasticizers that can maintain workability over long time, and keeping good compacity with a slag blended binder in the highly alkaline environment.

### **3.1.3 Composite cement CEMII/III**

The composite cement refers to cements produced by fine grinding of Portland clinker and industry byproduct, such as GGBFS and fly ash, and certain types of volcanic

material (natural pozzolanas) or limestone [9]. The CEM II or CEM III Portland cements are categorized based on the clinker replacement amount, CEM II Portland cement typically consists of up to 35% of SCM materials while the replacement of clinker in CEM III is even higher.

With respect to the interaction between PCE admixture and composite cement. Previous publications have consistently shown that slag blended cements present the lower affinity of slag for PCEs [52, 53]. The CEM III/B 42.5 N was reported to has the highest slag proportion (70.9 wt. %) [54]. Similarly, the addition of fly ash to the CEM II/A-LL will also favor the mortar fluidity but because of its smooth particles and reduced packing density [55-57].

LCC (or LC<sup>3</sup> cement) cement refers to the limestone calcined clay blended cement, which allows higher clinker replacement but excellent mechanical properties and better durability [58]. The phase composition of LC<sup>3</sup> and OPC cement is illustrated in **Figure 4**. The LC<sup>3</sup> cement with industrial waste materials reduced up to 40 % of CO<sub>2</sub> emissions by cutting half of the clinker content. That increases resource efficiency and reduces the utilization of scarce raw materials [59, 60].

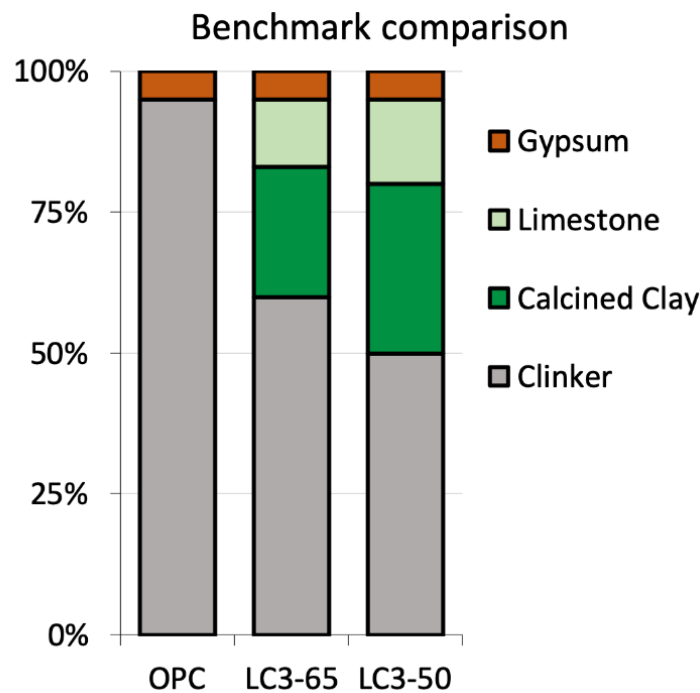


**Figure 4** Phase composition of LC<sup>3</sup> and OPC cements [61]

### 3.2 The workability of concrete

#### 3.2.1 Interaction between cementitious materials and superplasticizer

The cementitious materials trend to flocculate after contact with water due to the reaction to form C-S-H gel. The correlation between viscosity of cement paste and its solid content follow the ‘Krieger-Dougherty’ equation, which was later used in cement paste as **Equation 1** [62, 63].

$$\frac{\eta}{\eta_c} = \left(1 - \frac{\phi}{\phi_m}\right)^{-[\eta]\phi_m} \quad \text{Equation 1}$$

Here,  $\eta$  is viscosity,  $\eta_c$  is viscosity in continuous phase,  $\phi$  is volume solids content. The  $\phi_m$  value for OPC paste is from 0.40 to 0.45, and the viscosity of OPC increases with its solid content.

Adding PCE superplasticizers significantly reduces the viscosity at the same solid fraction, favoring the fluidity. The influence of different admixtures on viscosity reported by O. Burgos-Montes et al. is shown in **Figure 5**.

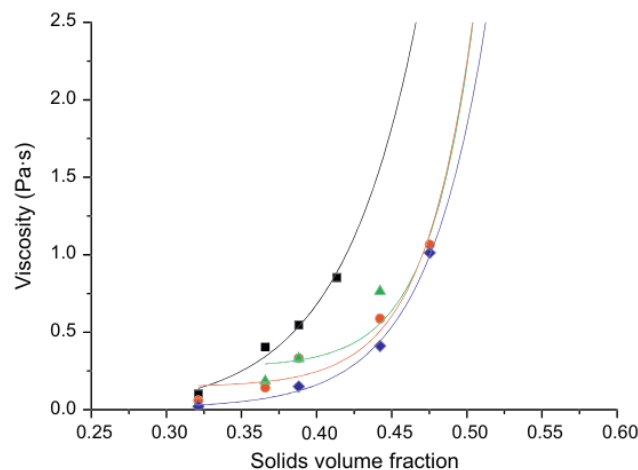


**Figure 5** The correlation between apparent viscosity and volume solid content of CEM I 52.5 R cement (black: without admixture) [64]

It is commonly accepted that PCE superplasticizer functions as a surfactant upon its adsorption on the surface of cement particles through complexation with  $\text{Ca}^{2+}$  ions. This decreases the water demand required to achieve the same fluidity by lowering the surface tension and preventing flocculation. Furthermore, the effectiveness of dispersion continues to increase with higher PCE dosages. The adsorption process of PCE is illustrate in **Figure 6** [17]. The investigations by Winnefeld et al. and Zingg et al. have established that the anionic charge density, side chains length, and molecular weight of PCE samples significantly impact their adsorption rate [65, 66]. Additionally, the particle charges and specific surface area of various supplementary cementitious materials (SCMs) also have discernible effects on the adsorption behavior [67]. The ternary diagram illustrating the composition of ordinary Portland cement (OPC) and SCMs materials is depicted in **Figure 7**.

The OPC cement displays a slightly positive surface charge, which facilitates the adsorption of anionic groups. SCMs with highly positive zeta potential, such as fly ash and limestone, accelerate the adsorption of PCE. Consequently, the incorporation of SCMs in blended cement leads to varying phases composition, particle sizes, and surface charges, thereby influencing the interaction with PCE polymers, resulting in diverse fresh and hardened properties [68].

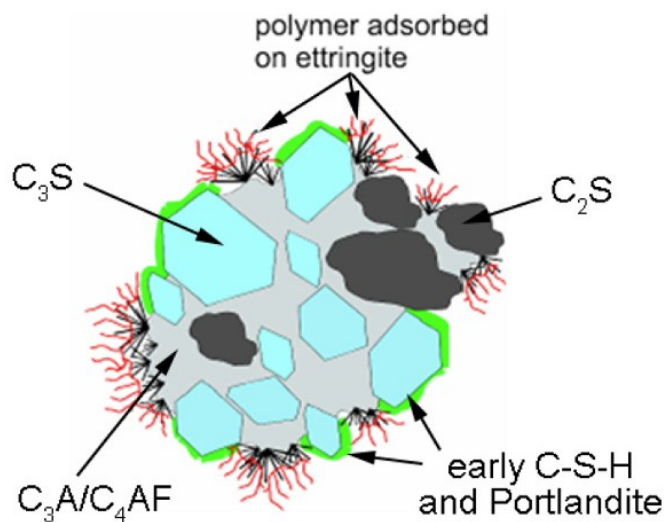


**Figure 6** Adsorption of PCE polymer on cement particles [17]

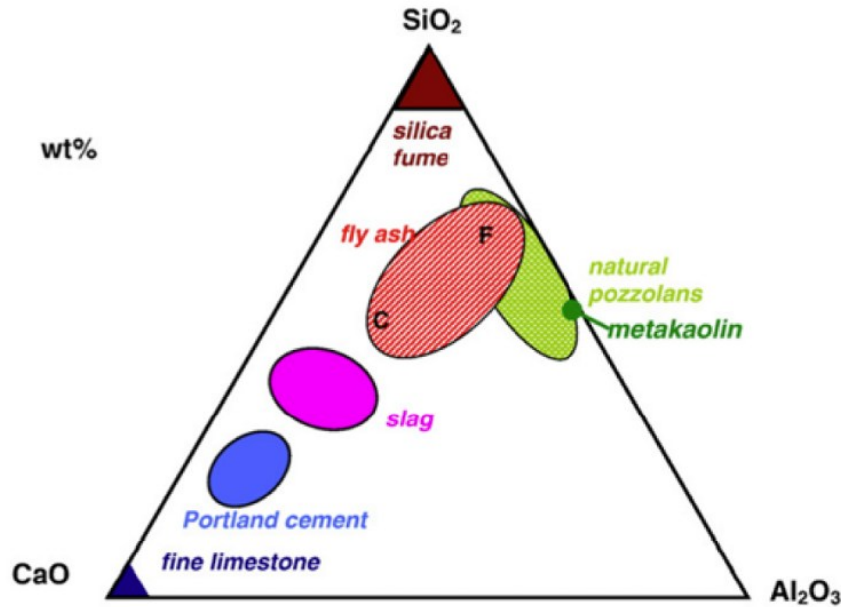


**Figure 7** Ternary diagram of OPC and SCMs materials [69]

### 3.2.2 Conventional methods to achieve slump retention for concrete

The workability over time, also called the slump retention property, is an important factor for the application of cementitious materials, especially for long-term transportation or super-high-rise pumping.

Retarder is the first concept that allows cementitious materials to remain workability for an extended time periods. There are several organic or inorganic retarders that have been used in this field, including sodium gluconate, zinc oxide, sucrose or calcium sulfate bearing material [70-73]. These retarders work by preventing hydrate formation through hindering the nucleation or growth of C-S-H.

PCE superplasticizers with higher side chains density also can be designed for the ready-mix concrete to maintain its workability [74]. The working mechanism is to reduce the initial adsorption amount of PCE polymers into the cement particles because of the steric hindrance from the higher side chains density; then more PCEs remaining in the cement pore solution are responsible for further dispersion over time [75]. Later, PCEs with hydrolyzing ester monomers, such as 2-hydroxyethyl acrylate (HEA),

hydroxypropyl acrylate (HPA), and maleic anhydride (MAH), are designed as the second generation of slump retaining PCEs based on a slow release mechanism [17, 76]. In detail, such ester functional groups hydrolyze slowly under the alkaline situation of the cement pore solution, providing  $\text{COO}^-$  groups continuously for further adsorption. Then the effective working time of the cement is extended. Recently, one more simple approach - delayed addition of PCE polymers - also achieved good slump retention in cement [77]. Li et al. reported a novel PCE-LDH nanocomposite can extend the slump retention of calcined clay blended cement through anion exchange reaction in pore solution, which gradually releases PCE superplasticizers [78].

It is worth to note that the pH value of PCE polymers also affect their slump retention performance, especially for the ester-based PCE superplasticizers. The operation of neutralization might destroy the dispersion of PCE with functional groups, as the alkaline treatment will release the  $\text{COO}^-$  group in advance. In addition, the neutralization will also cause extra carbon emissions from the NaOH solution, which is also undesirable. Previous publications from Chromy has reported the influence of pH values on the dispersing effectiveness of the precast type superplasticizers [79]. It was found that the acidic strongly anionic PCE polymers performed better, and in the presence of strongly anionic neutralized PCEs, more nano-ettringite was formed in cement paste than with the acidic counterpart, leading to a greater required dosage for an equal dispersing performance.

### **3.2.3 Conventional foam control agent for concrete**

The air voids control is another important topic related to the mechanical properties of concrete and its freeze-thaw resistance. Nevertheless, PCEs polymers containing polar carboxylic acid groups in the backbones and hydrophilic EO units in the side chains, is conducive to stabilize the foam which generated during the mixing of the aggregates [80, 81]. On the one hand, PCE polymers decrease the surface tension difference between the upper and lower layers of liquid film caused by the Gibbs-Marangoni effect [82]. On the other hand, when the water lamellar becomes thinner, PCE polymers get closer to each other, the electrostatic repulsion from carboxylic acid groups prevents

them from getting closer, and finally the foam becomes more stable. The entrained air significantly increases the porosity of concrete, which is harmful to its early mechanical properties and durability [83]. In this context, PCEs are highly requested to be combined with the defoamers in industrial applications.

The traditional defoamer is hydrophobic solid particles, oils or their mixtures, which can physically break the lamella of a foam bubble [84]. Later, amphiphilic molecules such as alcohols, fatty acids, fatty esters, and polymers based on oxyethylene, oxypropylene or oxybutylene units are used as defoamers [85]. Moreover, polymers with function groups, including Jeffamine derivatives (polyether amines) possessing amine groups and mixed PEO/PPO backbones, polyether modified silicone, n- or iso-tributylphosphate defoamers are also widely applied as highly effective foam control agents [86-90]. These defoaming polymers are low surface tension fluids, which break foam at a molecular level through adsorbing at the liquid-gas interface, replacing the foam-stabilizing surfactants until the bubble bursts. Considering the defoaming mechanism, three possible mechanisms including “bridging-stretching”, “bridging-dewetting” and “spreading-fluid entrainment”, have been identified that provide the destabilizing function of bubbles in cement [91-93].

However, there are still some problems need to be solved when utilizing the PCEs-defoamer combinations. First, as most defoamers are hydrophobic, the phase separation between PCEs and defoamers is a critical problem during storage, transport and application, and the insoluble defoamers can further cause unpredictable air voids over time, which greatly decrease the effectiveness of PCEs and defoamers. The intermittent mechanical mixing for defoamer and PCE admixtures can overcome the phase separation problem, but the cost of equipment and maintenance should take into consideration [94]. Shendy et al. invented a combination of a water-insoluble defoamer, a dispersant and an amine solubilizing agent, that significantly stabilizes the defoamer with the superplasticizers via a pre-mixing procedure [95]. Some chemical methods, including grafting or emulsification of the defoamer onto the superplasticizer molecule, can also provide the long terms storage stability for these PCE based defoamers, but the

chemical reactions are normally conducted under relatively higher temperature [96].

Second, adding defoamer in cement paste or mortar usually reduces the fluidity. One reason is the decreasing lubrication of the air bubbles. The other reason is the lower surface tension properties, as the size of bubbles decreases in the lower surface tension, more water is distributed on the surface of the pores. As a result, the amount of free water decreases, leading to lower initial fluidity [7]. Ma et al. investigated some block polyoxy polyether surfactants with different PO units, the results showed that the PO position and ratios had a remarkable effect on the foam properties, which makes it possible to apply this kind of surfactant as air voids regulator of concrete [38]. However, few researchers consider the effect of chemical structure, such as hydrophilic/hydrophobic properties resulting from different PEO/PPO ratios in the side chains of defoamer, on the defoaming and dispersing performance. Moreover, due to the wide variety of PCEs, it is difficult to find one kind of defoamer that has good compatibility with all of them.

### **3.3 Polycarboxylate superplasticizers**

#### **3.3.1 Chemical composition and working mechanism of polycarboxylate superplasticizer**

Generally, PCE superplasticizers exhibit comb-shaped chemical structures, which consisting carboxylic groups in the backbone and polyethylene oxide (PEO) side chains. Previous studies have reached consensus that the carboxylic groups act as anchors to adsorb on the surfaces of cement particles, and PEO side chains produce steric hindrance to prevent cement particles flocculating [97, 98]. The improvement of PCE structure for optimal performance can be achieved from several aspects: 1) adjust the acid to ether ratios and molecular weight, 2) explore new macromonomers, 3) graft novel functional groups, and 4) change the whole molecular structure of PCE polymers.

##### **1) Acid to ether ratios and molecular weight**

The dispersing effect of conventional PCE copolymers originates from the steric repulsion of their side chains besides the electrostatic repulsion from anionic backbone

[99, 100]. The chemical architecture parameters, such as side chains density, side chains length and molecular weight, affect their specific anionic charge amounts, resulting in distinct adsorption behavior and working mechanisms [65, 66, 101].

It is found in OPC cement, the fluidity of cement paste or mortar is well correlated with the adsorption amount of PCE, which relies on three factors: the cement pore solution, the polymer admixture and their solid interface [24]. From the polymer aspect, PCE polymers with higher acid-to-ether ratios and shorter side chains length present superior dispersing ability because of their excellent adsorption capability stemming from stronger anionic. While PCE admixtures with higher side chains density and longer side chains length are characterized as slump retaining polymers for ready mix type concrete due to its slowly adsorbing rate.

The molecular weight is another unignored factor for PCE, the optimal range of  $M_w$  used in OPC cement is 20000 - 50000 Da, in which range PCE polymer can forcefully disperse cementitious materials without causing undesired bridging effect between cement particles. Research from R. Flatt confirmed that increasing  $M_w$  of PCE also changes its adsorption conformation [102]. Li et al. demonstrated that PCE exhibiting higher anionic charge amount and higher molecular weight presents higher adsorption on the low carbon alkali-activated slag binder. Lei et al. found that PCE polymer with higher  $M_w$  improves the fluidity of alkaline activated slag due to a “loop” adsorption conformation [103].

## 2) Macromonomers

Besides adjusting the molecular architecture, the superplasticizer industry is also sparing no effort to develop new macromonomers for PCE preparation to cater to the needs of broadening market [104, 105]. MPEG-type PCE ( $\omega$ -methoxy polyethylene glycol) is the first generation of PCE and it is still dominate the superplasticizer market in Europe. Its chemical structure is displayed in **Figure 8**. Usually, this kind of PCE can be obtained through esterification or polymerization with a relative long reaction time. APEG ( $\alpha$ -allyl- $\omega$ -methoxy polyethylene glycol) macromonomer belongs to polyether macromonomers. Its application is limited due to its complex synthesis method and

inferior dispersing force. Additionally, the APEG macromonomer presents lower reactivity, making it unable to copolymerize with all acid monomers. Despite these limitations, the APEG-type PCE was reported to show a superior viscosity-reducing property, deriving from its highest HLB value [106].

HPEG (methylallyl polyoxyethylene ether) and IPEG (isopentenyl polyoxyethylene ether) types of PCE occupied Asia market because of their easy copolymerization synthesis procedure and their excellent dispersing performance in concrete [107]. These two types of comb-shaped polymers are highly effective in water reducing and retaining fluidity at lower dosages. Since 2009, they have been the most popular high-range superplasticizers in China. Later, the room temperature copolymerization of these PCE polymer expanded their application areas, and they are suitable for high-performance concrete, including high-strength and self-compacting concrete [108]. The only difference of HPEG and IPEG type PCE polymers come from the  $-\text{CH}_2-$  group as illustrated in **Figure 8**, which may affect their adsorption speed. For this reason, HPEG-type PCE is used for the preparation of precast-type PCE while IPEG-type PCE is designed for ready-mix concrete. One drawback of these two PCE is their excessive retardation effect from carboxyl groups, hindering the early strength development of concrete.

The VPEG-type PCE, which also known as MVA (consist of maleic anhydride, vinyl ether and acrylic acid monomers) was invented in 1996 [109]. Lei reported one vinyl ether-based polycarboxylate superplasticizer for concrete possessing clay tolerance [110]. EPEG and GPEG macromonomers contain vinyl oxy ether become popular in China because of their high reactivity during copolymerization at the chain growth stage [111-113]. Their copolymerization reactions require low-temperature control, and their reactions with AA monomer can be finished within one hour. Their chemical structures are displayed in **Figure 8**.

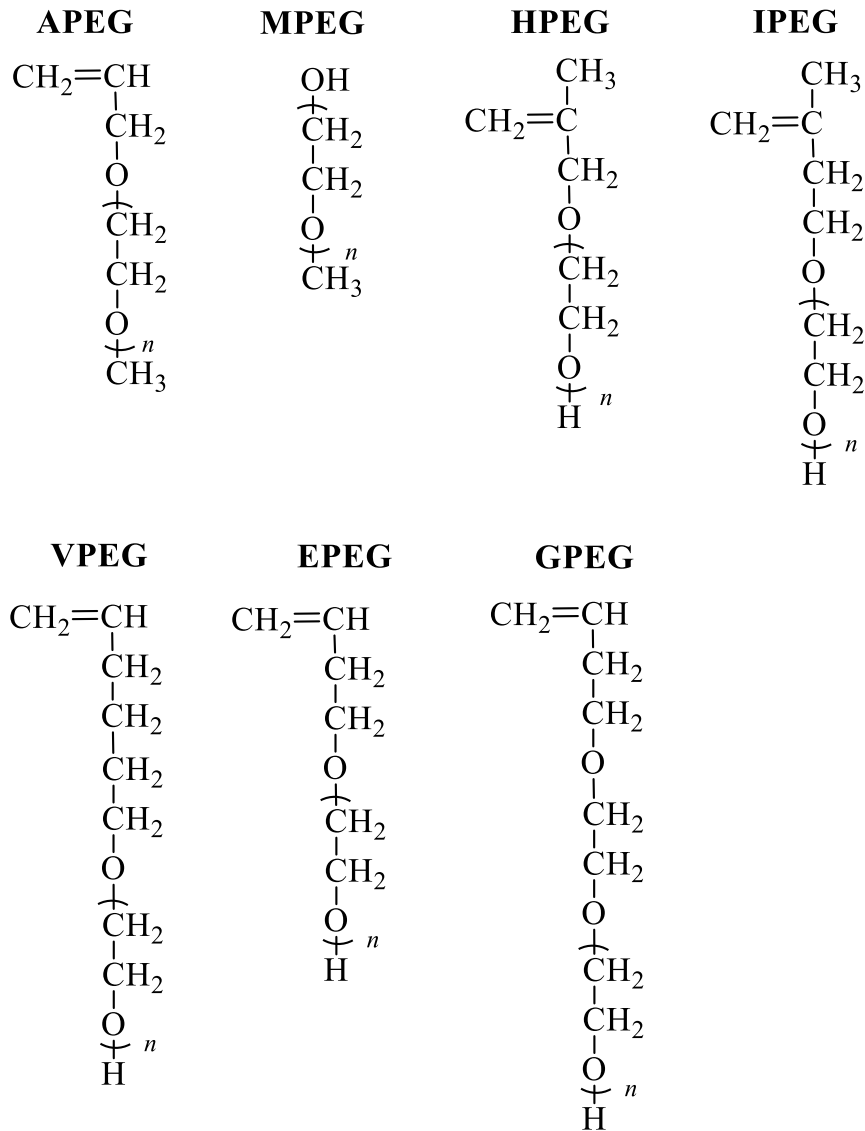


**Figure 8** Chemical structure of APEG, MPEG, HPEG, IPEG VPEG, EPEG and GPEG macromonomers

### 3) Modification with functional groups

The modification of PCE superplasticizer focuses on changing the anionic monomer in the backbone, which in turns affecting anionic charge density and rigidity of the PCE polymer chain. According to the dispersion mechanism, the calcium binding ability of different anchoring groups leads to varied PCE coverage on cement particles, thereby

influencing their adsorption capacity and ultimately contributing to disparate dispersing properties. There are various modifications of superplasticizers via partially substitute the carboxylate group with sulfonate, phosphonate, phosphate, silane, amide or quaternary ammonium groups [114-117]. Stecher et al. reported one series of phosphate modified MPEG-type PCE samples cause less retarding effect and display comparable robustness against sulfate and clay impurities [19]. Geert De Schutter published one research related to a TEMPO-based extension of PCE, this PCE enables a redox-controlled adsorption on the cement particles, allowing for the adjustment of rheological properties accordingly. This provides another route to adjust the rheology of fresh concrete in the post-mixing stage, which is very useful in the pumping and 3D printing concrete [118]. Lu et al. synthesized one silylated PCE via free radical copolymerization, which demonstrates better adsorption ability for the enhanced dispersing, sulfate resistance ability and minimized the retardation effect [119].

The introduction of maleic anhydride (MAH) monomer into PCE polymer composition effectively rise the  $-\text{COO}^-$  groups density on the backbone, as each MAH monomer can provide twice as many  $-\text{COO}^-$  groups as AA monomer. In addition, the adjacent carboxyl groups in MAH exist in different configuration representing stronger calcium binding capacity, that improves the adsorption rate and capacity of PCE samples [120, 121]. It was reported that PCE superplasticizer synthesized from MAH monomer exhibited good water solubility and higher hydrophilicity, this polymer also present higher sulfate robust due to a denser adsorption layer on the cement particles [122]. However, both MAH monomer and macromonomers exhibit relatively low reaction activity, it is hard for them to copolymerize and produce PCE copolymer with higher conversion rate. Some ternary copolymerization systems including highly active monomers such as MAA, HEA, AMPS are applied to improve the conversion rate of MAH based PCE copolymers [123, 124]. The introduction of amide functional group into PCE can change the air-entraining ability of PCE polymer. The air voids control is also an important topic for concrete, varies air voids in mortar alter its rheology at the fresh state and mechanical strength at the harden state [125-127]. The publication from

Liu et al. demonstrated that the concrete admixed with amide modified PCE exhibits better frost resistance [128]. The PCE superplasticizers with functional groups have been a hot research topic because they offer additional advantages such as the stickiness reduction, high sulfate tolerance, improved clay tolerance and robustness to different kinds of cement. The chemical structure of several small monomers utilized in this field is illustrated in **Figure 9**.

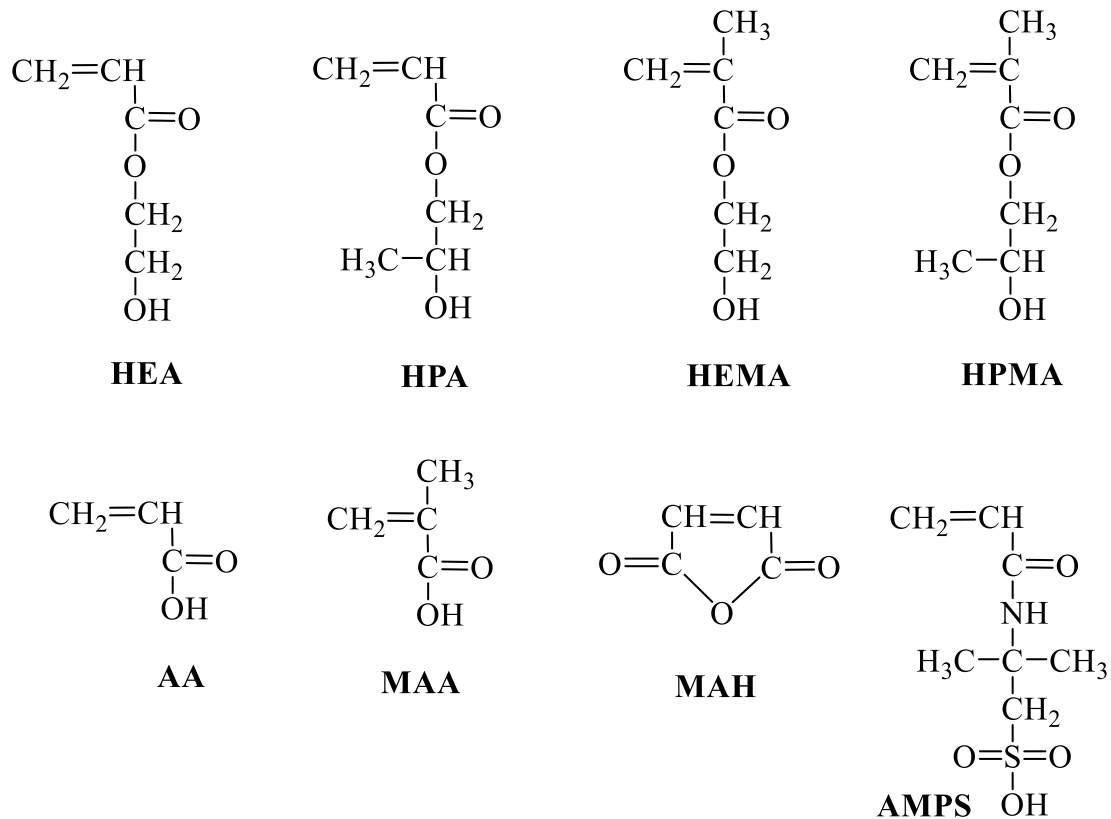


**Figure 9** Chemical structure of HEA, HPA, HEMA, HPMA, AA, MAA, MAH and AMPS small monomers

Recently, there has been a growing interest in developing zwitterionic (also called amphoteric) and cationic PCE copolymers. The introduction of positive and negative charged group on their backbones also affects their adsorption capacity. It can be date back to 2006, Hsu et al. reported a linear copolymer containing both anionic and cationic functional groups on the backbone. Such polymer present as a good concrete admixture because it requires less dosage to achieve good fluidity and provides better fluidity retention compared with naphthalene sulfonate formaldehyde (BNS)

superplasticizer [129]. Later, Schmid et al. confirmed the effectiveness of zwitterionic polymers in dispersing calcined clay blended cement. [130, 131]. However, the considerable expense associated with functional or cationic monomers limited the application of such PCE products. Nowadays, the transition of cement industry to low-carbon green binders provides modified PCEs a potential market in the future.

#### 4) Completely novel structured PCE superplasticizers

Innovations and breakthroughs in developing a completely new topological structure of PCEs are significantly sought after to meet the demand for low-carbon binders. The novel structured PCE superplasticizers, encompass block, gradient, or hyperbranched structures have been undertaken with the aim of boosting PCE performance [21, 74, 132]. A Y-shaped superplasticizer was synthesized by Zhou et al, this PCE exhibit better dispersing effectiveness than comb shaped PCE because its special adsorption conformation on the C-S-H hydration product [133]. The research from Liu et al. established that star-shaped PCE owns stronger calcium binding capacity and adsorbs more compact on cement surface than random PCE, resulting in lower yield stress and plastic viscosity of the cement paste [132].

Among the various novel structured PCEs, gradient PCE is currently attracting considerable attention due to its significant advantages for low-carbon cement. In detail, this type of PCE features a gradient distribution of anionic monomers along its backbones. The substantial anionic blocks located at one end of the polymer chains possess the strongly adsorb capability onto cement particles, altering both the adsorption amounts and conformation. Excellent sulfate resistance is another character of this type of polymers, it indicates stronger competitive adsorption capacity compared to  $\text{SO}_4^{2-}$  anions. As a result, gradient PCE contributes to a bigger fluidity of concrete and exhibits better compatibility with different types of cements [134].

The challenge related to such novel structured PCE superplasticizers is their synthesis approaches. Usually, living radical copolymerization (ATRP, RAFT and NMP) is involved to obtain a copolymer with specific sequence distribution, which is

unfortunately not so easy to realize industry production.

### 3.3.2 Copolymerization methods of polycarboxylate superplasticizer

PCE synthesis is conducted by copolymerizing unsaturated double bonds or distinct functional groups from macromonomers and small acid monomers, respectively. As discussed in **section 3.3.1**, there are various chemical macromonomers and small monomers, and the work on developing new monomers is still ongoing. The details related to the synthesis of macromonomers and small monomers will not be discussed in this study. The PCE superplasticizers are synthesized with macromonomer products and acid monomers via grafting, free radical or living copolymerization. The synthesis progress of these methods is introduced as follows:

#### 1) Graft Polymerization

Graft Polymerization of PCE polymer is a process that involves bonding side chains and main chain through esterification at elevated temperature. Take MPEG type PCE as an example [135-137]: to start the reaction, a mixture of PMAA, chain transfer agent, and initiator is added dropwise into the MPEG solution. The reaction temperature is usually raised to 120-180°C under N<sub>2</sub> protection, the water is continuously removed to prevent side effects. Copolymers obtained from graft copolymerization have a controlled molecular weight and acid-ether ratio. The drawbacks of this method is that limited monomers can be selected to conduct esterification, and it is also challenging to control the grafting rate due to its reversible equilibrium reaction.

#### 2) Free radical copolymerization

The vast majority of PCE polymers today are synthesized via free radical copolymerization with unsaturated monomers such as carboxylic acid and alkane macromonomers (HPEG, IPEG, EPEG and GPEG). Free radical copolymerization includes three steps: a slow chain initiation, a rapid chain growth and a fast chain termination [138].

In the chain initiation step, free radicals formed during the decomposition of initiator

and react with monomers to form the monomer radical during very short time periods. The initiation rate and degree depend on the initiator types and decomposition method. Then it comes to the chain growth step, also known as propagation, this step usually completed in few hours depending on the monomers' reactivities. In this period, the monomer radicals ( $M_1'$  and  $M_2'$ ) react with monomers ( $M_1$  and  $M_2$ ) to form the copolymer chains. The detail chain growth kinetics is illustrated in **Figure 10** [139]. The  $k_{11}$  value is the reaction rate of  $M_1$  radical with  $M_1$  monomer; The  $k_{12}$  value is the reaction rate of  $M_1$  radical with  $M_2$  monomer; The  $k_{22}$  value is the reaction rate of  $M_2$  radical with  $M_2$  monomer; The  $k_{21}$  value is the reaction rate of  $M_2$  radical with  $M_1$  monomer. Last is the chain termination step, the polymer chain can stop growing either by the reaction of two radicals to form a stabilized polymer or by transferring a radical to another polymer chain.

In the production process of PCE, the low-reactivity macromonomer is initially dissolved, followed by the gradual addition of AA and initiator APS. This method ensures an optimal chain growth rate and high conversion rate (see **Figure 10**). Free radical copolymerization can be realized at elevated or room temperature depending on the different initiator systems. Room temperature synthesis using redox initiator system, the PCE synthesized at room temperature has similar conversion rate and performance but wider molecular weight distribution compared to PCE obtained at elevated temperature.

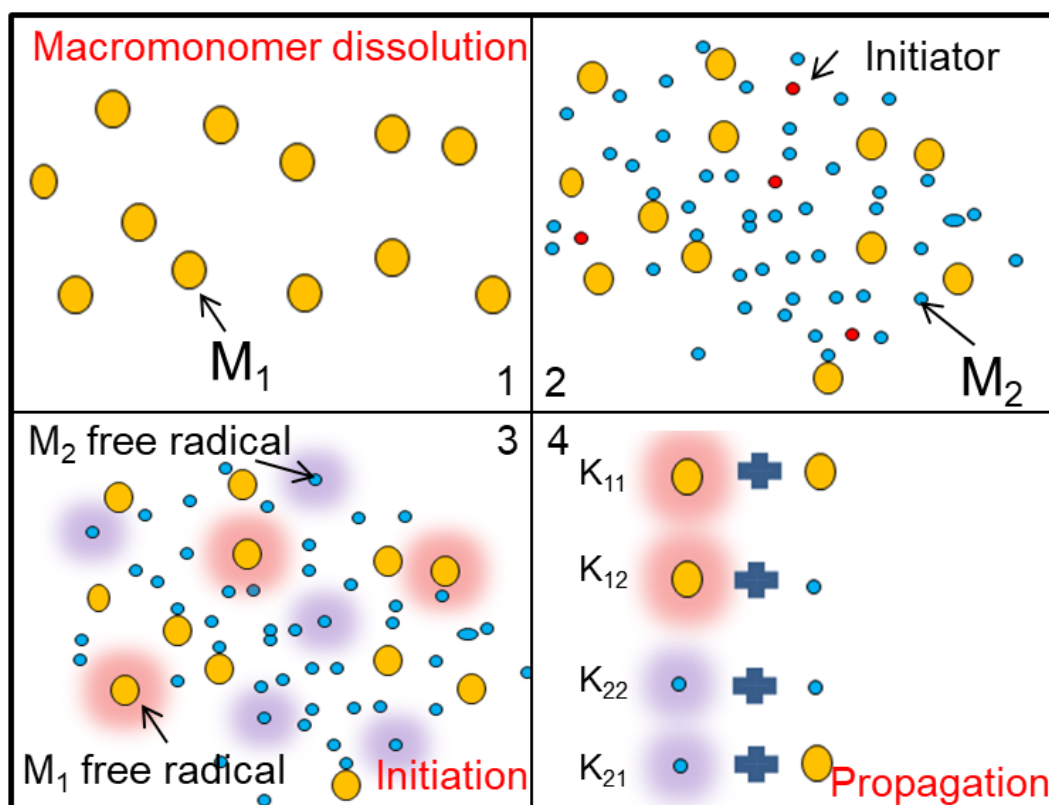


**Figure 10** Illustration of free radical copolymerization kinetics [139]

### 3) Living free radical copolymerization

Living free radical copolymerization is an effective method to prepare PCE polymers with narrow PDI and specific segment sequence [140]. The reversible addition-fragmentation chain transfer polymerization (RAFT), nitroxide-mediated polymerization (NMP), and atom transfer radical polymerization (ATRP) are commonly used methods [24-26]. Several transition metal complexes with central metal such as Cu, Fe, Ni are used as catalysts are applied to realize the controlled radical copolymerization. It is worth to note that these kinds of catalysts are used in large amounts and some of them have negative impact on environment [141, 142].

#### 3.3.3 Carbon emission of polycarboxylate superplasticizers

The carbon emission research in PCE superplasticizers filed focuses on examining electricity consumption during production, assessing raw material emissions, and evaluating the carbon emissions associated with different chemical structures of PCE

polymers. Flower and Sanjayan reported that the CO<sub>2</sub> emission from electricity consumption of superplasticizer is 5.2 (t CO<sub>2</sub>-e/L) [143]. Liu et al. published the life cycle assessment (LCA) of PCE superplasticizer, in their research, the solid PCE presents less carbon emission than the liquid PCE [144]. Schiefer et al. found that precast type PCE display higher carbon emission than ready-mix type PCE; MPEG-type PCEs reveal the higher footprint than HPEG and IPEG PCE samples [145, 146].

## 4. Experimental materials and methods

### 4.1 Materials

#### 4.1.1 Cementitious materials

Three ordinary Portland cement samples (CEM I) were used in this study, For **Section 5.2** and **Section 5.5**, the cement is provided by Ecocem company named ‘Ecocem’. Another two CEM I 42.5 R cement samples (‘CEM-1’ used in **Section 5.1** and **Section 5.3**; ‘CEM-2’ used in **Section 5.4.3** and **Section 5.6**) are obtained from Schwenk cement company. Their density and a  $d_{50}$  value in **Table 1** was determined by helium pycnometry and laser granulometry, respectively. The phases composition, which was determined by Q-XRD including *Rietveld* refinement, is also shown in **Table 1**. These measurements were conducted at the Construction Chemistry Group at the Technical University of Munich.

**Table 1** Phase composition of the cement samples

Phase	wt. %		
	Ecocem	CEM-1	CEM-2
C <sub>3</sub> S, monoclinic	58.6	54.5	59.6
C <sub>2</sub> S, monoclinic	8.6	18.4	11.1
C <sub>4</sub> AF, orthorhombic	16.0	10.9	10.1
C <sub>3</sub> A, cubic	1.9	5.2	4.9
C <sub>3</sub> A, orthorhombic	3.4	0.9	2.1
Anhydrite (CaSO <sub>4</sub> )	6.2	0.9	2.6
Dihydrate (CaSO <sub>4</sub> • 2H <sub>2</sub> O)	1.2	3.6	3.1
Hemihydrate (CaSO <sub>4</sub> • 0.5H <sub>2</sub> O)	0	0.3	0.1
Calcite (CaCO <sub>3</sub> )	2.3	3.0	2.3
Dolomite (CaMg(CO <sub>3</sub> ) <sub>2</sub> )	0	1.1	1.0
Arcanite (K <sub>2</sub> SO <sub>4</sub> )	0	0	0.2
Quartz (SiO <sub>2</sub> )	0.9	0.9	0.4
Free lime ( <i>Franke</i> )	0.7	0.1	0.7
Portlandite (Ca(OH) <sub>2</sub> )	0	0	0.8
Periclase (MgO)	0	0	0.5
Total	99.8	99.8	99.5
$d_{50}$ (μm)	10.65	18.13	20.25
density (g/cm <sup>3</sup> )	3.15	3.13	3.15

LCC cement (Limestone calcined clay blended cement) used in this thesis within the DFG SPP 2005 program consists of 70 % LC compound and 30 % calcined clay. The CEM I, 42.5 R sample used in **Section 5.4.1** and **Section 5.4.2** has been reported in the publication [147].

Three composite cements (CEMIII/A, 42.5 N and CEMIII/B, 42.5 N from Heidelberg; CEMII/A-LL, 32.5 R from Schwenk Cement) were chosen for the low-carbon cement characterization. The physical composition and chemical properties of these cements are characterized at the Technical University of Munich thoroughly outlined in **Section 5.4.3**.

### Slag

The GGBFS sample and its oxide composition in **Table 2** were provided by Ecocem company (from the plant of Fos sur mer, France).

**Table 2** Oxide composition (wt %) of granulated blast furnace slag used in this study

CaO	SiO <sub>2</sub>	Al <sub>2</sub> O <sub>3</sub>	MgO	FeO	TiO <sub>2</sub>	MnO	Na <sub>2</sub> O	SO <sub>3</sub>	Total
43.4	37.1	10.8	6.7	0.6	0.5	0.3	0.5	0.1	100

### 4.1.2 Chemicals

Acrylic acid (**AA**), methacrylic acid (**MAA**), maleic anhydride (**MAH**), 2-hydroxyethyl acrylate (**HEA**), ammonium persulphate (**APS**) and ascorbic acid (**VC**) were all purchased from Sigma-Aldrich Chemie GmbH, Steinheim, Germany. 2-acrylamido-2-methylpropane sulfonic acid (**AMPS**) was obtained from Merck-Schuchardt Company (Darmstadt, Germany). **DADMAC** from SNF FLOERGER<sup>®</sup> company, and the solid content is 65 %. **HPEG** macromonomer (EO7, EO10, EO23), **HPEG precast** and **HPEG ready mix** commercial PCE products obtained from Jilin Zhongxin Chemical Group Co. (China).

**HPEG 2400/4000** was provided by Marla Chemicals Company, Istanbul, Turkey. A PCE superplasticizer **VP 2020/15.2** provided by MBCC group (Mannheim / Germany).

## **4.2 Experimental method**

### **4.2.1 Size Exclusion Chromatography (SEC)**

The molecular weight ( $M_w$ ,  $M_n$ ), polydispersity index (PDI) of PCE copolymers, and conversion rate of macromonomers, were determined via Size Exclusion Chromatography (SEC) measurement via a Water 2695 Separation module and three Ultra hydro Gel<sup>TM</sup> columns (125, 250, 500). The fluid phase is 0.1 N NaNO<sub>3</sub> solution at a speed of 1.0 ml/min.

### **4.2.2 FT-IR spectra**

The FT-IR spectra were utilized for the chemical structure analysis especially for PCE polymers containing functional groups, this measurement was conducted in the transmittance mode with 64 scans at 25 °C with a VERTEX 70 Frourier transform infrared spectrometer (Bruker INVENIO, Germany), and the wavenumber ranged from 4000 cm<sup>-1</sup> to 400 cm<sup>-1</sup>.

### **4.2.3 <sup>1</sup>H NMR**

The <sup>1</sup>H NMR measurement was employed to distinguish different proton ions within various chemical environments. Prior to measurement, the PCE sample was dried in oven at 50 °C, then 30 mg powdered sample was dissolved in D<sub>2</sub>O (0.4 ml). An AVANCE-III 400MHz NMR instrument was used for the measurement with 16 scans.

### **4.2.4 Specific anionic charge amount**

The specific anionic charge of PCE polymer is an important parameter related to its dispersing effectiveness. Here, 0.1 g/L PCE superplasticizer solution was prepared in DI water and 0.01M aqueous NaOH solution (pH = 12), respectively. Then the PCE solution was titrated against a polydiallyl dimethyl ammonium chloride (polyDADMAC) fluid until charge neutralization was reached, this titration was conducted by a pH particle charge detector (PCD 03, Herrsching, Germany). The

negative charge amount per gram of polymer (= the specific anionic charge amount) was calculated based on the consumption of poly DADMAC compound [148].

#### **4.2.5 Phase separation of ion-pair system**

The phase separation of defoamers was detected in a climate chamber at 0, 22 and 50 °C, respectively. The phase separation between the Jeffamine defoamers and the HPEG type PCEs was checked after 5 days of aging.

#### **4.2.6 Defoaming performance and foaming behavior**

The defoaming performance of defoamers (graft copolymers and ion pair complexes), including defoaming activity and defoaming durability, were tested in an aqueous solution with a concentration of 10 g/L.

The activity and durability of fast antifoams (less than 1 min) were tested through a shake method with a wobbler (Vortex Mixer, VWR International GmbH, Darmstadt/Germany). First, 100 ml PCE or ion-pair solutions were added to a 250 ml glass bottle. Each shake cycle has 10 s agitation and then 60 s rest. Record the time until the water-gas interface is clean without any bubbles. The average time of the first three tests represents the defoaming activity, the cycles, in which the defoaming time exceeds 60 s, considered the defoaming durability. [149]. The foam stability can be characterized by the foam height as a function of time. 10 ml of defoamer solutions were placed in a 15 ml glass tube, and then shaken for 2 min in the wobbler, the foam height was recorded over 180 s.

#### **4.2.7 Defoaming performance in mortar**

The defoaming performance of PCE polymers in fresh mortar was tested in line with DIN EN 12350-7: 2009-08 [150]. The fresh mortar consisting of 450 g cement and 1350 g normal sand was mixed in a Toni-MIX agitator according to the DIN EN 196-1 standard [151]. The mortar was placed and compacted in the container of the air void tester instrument for 2 minutes, and then air pressure was applied to measure the amount of air voids.

#### **4.2.8 Dispersing effectiveness in paste**

The fluidity of cement paste was measured using the ‘mini-slump’ test as per DIN 1015-3 [152]. Here, the water-to-cement ratio was determined to achieve an  $18 \pm 0.5$  cm spread flow. The PCE dosages were selected to attain a  $26 \pm 0.5$  cm spread flow. The test was conducted as follows: firstly, the PCE polymer was dissolved in DI water in the container, 300 g of cement were added in to the solution and stirred with a spoon for 1 min. After 1 of min rest, the mixing was continued for 2 min. Then the cement paste was poured into a Vicat cone (40 mm, 70 mm, 80mm) on a glass. The spread flow was measured twice at  $90^\circ$  angles after lifting the cone vertically.

#### **4.2.9 Dispersing effectiveness in mortar**

The dispersing effectiveness of pure HPEG type PCEs and PCE-Jeffamine ion-pair systems was measured by a mortar spread flow test at a w/c ratio of 0.4 with the same dosage in line with the DIN EN 196-1 standard [22], and the dosages were determined by pure PCEs achieving a spread flow of  $20 \pm 5$  cm. In this experiment, the specific amount of PCEs was pre-dissolved in 180 g DI water in a steel cup, placed the cup into the mortar mixer machine (ToniMIX, Toni Technik, Berlin, Germany), and start the automatic program: mixing cement and PCEs solution at low speed (140 rpm) for 30 s, add sand at the same speed for another 30 s, then 90 s pause, continue mixing at high speed (285 rpm) for 60 s. The resulting mortar was fed into a slump cone (60 mm height, 70 mm top diameter, 100 mm bottom diameter), and vibrated 15 times on a shock table. The final mortar was measured twice, which is perpendicular to the first one, taking the average as the spread flow value.

#### **4.2.10 Surface tension test**

A Force Tensiometer K100 instrument (Krüss GmbH, Hamburg/Germany) was used for the surface tension test of PCE and defoamer solutions. The interfacial tension (IFT) was measured using the plate method as per Wilhelmy [153]. This involved measuring the force as a plate immersed vertically in a liquid was lifted out, and the result was determined as the average value of three repeated measurements.

#### **4.2.11 HLB value of the polymers**

The hydrophilic-lipophilic balance (HLB) value is useful to reveal the hydrophobic/hydrophilic property of PCE polymers. This value was computed through Griffin's method, and it is applicable to the surfactant polymer [154]:

$$\text{HLB} = 20 * M_h/M$$

Whereby  $M_h$  is the molecular weight of the hydrophilic portion of the molecule; and  $M$  is the molecular weight of the entire molecular.

#### **4.2.12 Compressive strength test in mortar**

The mechanical properties of standard mortar without and mixed with PCE admixture were tested via a Toni Technik (Berlin, Germany) instrument in line with the standard [86]. The mortar sample was fed in a  $40 \times 40 \times 160$  mm mold. All mortar samples were extracted from the mold after 1 day. The compressive strength was measured following a designated curing period. For measurements at 3 d, 7 d, and 28 d, the samples were removed from the mold and placed in water at  $20 \pm 1$  °C for the remaining curing duration. The compressive strength values were each tested three times as each mold holds three samples.

#### **4.2.13 Isothermal heat-flow calorimetry**

Isothermal calorimetry was used to capture the potential influence of PCE compounds on the hydration process of cement. Here, 4 g cement and the specific amount of pre-dissolved PCE solution were added into a 10 ml glass ampoule separately. Before the measurement with an isothermal conduction calorimeter (TAMair, Thermometric, Järfälla, Sweden), the mixture was shaken for 120 s in a wobbler and then immediately put into the calorimeter instrument.

#### **4.2.14 X-ray Diffraction analysis**

The formation of hydrate phases was analyzed via XRD at different hydration times and isopropanol was employed to terminate the hydration of cement pastes. After the

termination, the pastes were shaken in a wobbler for 2 min, and centrifuged at 8500 rpm for 10 min. The powder samples for the XRD test were obtained through freeze-drying (24 h) and grinding method. A D8 advance, Bruker AXS instrument (Bruker, Karlsruhe/Germany) with wave length of 1.54 Å was used for the test at a range of 5 ° to 70 °, with a 0.01 s/step. The total measuring time was ~ 80 min. The phase identification was obtained via the DiffraCEva software (BRUKER) [155], and the quantified phase composition of the cement was determined using Rietveld refinement in the TOPAS software, with 10 wt.% Al<sub>2</sub>O<sub>3</sub> as standard [156, 157].

### **4.2.15 Adsorption measurement**

The total organic carbon (TOC) measurement was applied to detect the adsorption amount of PCEs in different cement systems. First, a supernatant sample was obtained from a cement paste with a water-to-cement ratio of 0.5 (16 g of cement, 8.0 g water and pre-mixed PCE) after 10 min centrifugation at 2400 rpm. Then the supernatant was filtered through a 0.2 µm syringe filter, and 10 drops of 0.1 M HCl solution were added to remove inorganic carbonates and to prevent carbonation.

All the samples were measured by a LiquiTOC-II analyzer (Elementar Analysen systeme GmbH, Hanau, Germany). The TOC content was calculated from the difference between the reference PCE solution and the supernatant containing the same concentration of PCEs.

### **4.2.16 Zeta potential and pH values of cement paste**

The DT 1200 Electroacoustic Spectrometer (Dispersion Technology, Inc) was used for Zeta potential measurement. The calibration and ions background were conducted before measurement. The cement paste sample with a water-to-cement ratio of 0.5 was prepared according to the DIN EN 1015 standard [158].

For zeta potential measurement, the cement paste was poured into a glass container, then the zeta potential electrode, the titrator, the temperature probe and the pH meter were inserted into the paste and the mixture was stirred continuously at 200 rpm at room

temperature while the zeta potential measurement was taking. The pH values of cement paste were recorded at the same time.

#### **4.2.17 V-funnel empty times**

First, a standard mortar was prepared from 450 g 'Full binder', 1,350 g of norm sand and 139.5 g of water (including the water content of the PCE solution). Thereafter the mortar rested for 5 min, the V-funnel empty time test was conducted. The V-funnel empty time experiment was performed in line with the standard DIN EN 12350-9 [159]. The V-funnel, which was wiped with a wet towel to ensure a slightly moistened surface, was then filled with mortar. After removing the bottom plug, the time taken for the mortar to complete emptying was measured.

#### **4.2.17 Flow line test**

The flow line tests were conducted according to DIN EN 13995-2 [160]. First, standard 'Full binder' mortars were prepared and rested for 5 min. The mortar was then stirred for 5 s at 285 rpm and poured into the flow line cup. After that, the sliding plug was opened, and the flow behavior was evaluated using the D30 value (which indicates the distance the mortar traveled after 30 seconds) and the final maximum spread in the flow line.

## 5. Results and discussion

### 5.1 Synthesis and characterization of a non-air entraining PCE

The results in **Section 5.1** related to a non-air entraining PCE, which was published in 2022 by Lei Lei and Lin Zhang in the publication “synthesis and performance of a non-air entraining polycarboxylate superplasticizer” of “Cement and Concrete Research” journal.

#### 5.1.1 Synthesis of conventional graft polymer G45PC3 and G45PC5 and non-air entraining PCE G45PC5-g-Jeffamine

##### 5.1.1.1 Synthesis of conventional graft polymer G45PC3 and G45PC5

In this part, the abbreviations G45PC<sub>x</sub> ( $x = 3$  and  $5$ ) were used to denote the grafting copolymerized PCE polymer, with  $x$  representing the ratio of MAA to side chains and indicating the side chain density. Taking G45PC<sub>5</sub> as an example, the synthesis process is outlined as follows:

Firstly, G45PC<sub>5</sub> polymer was synthesized via grafting copolymerization as detailed in the publication [135]. Here, MPEG (M 2000) 21.2 g, 13.95 g of PMAA (39.2 wt.%,  $M_w = 4700$  g/mol) and 20 mL of DI water were weighed into a Schlenk flask. This solution was heated to 85 °C while stirring at 200 rpm for 1 hour. Then a vacuum ( $1.0 \times 10^{-2}$  mbar) was applied to remove by-product water, this can increase the conversion rate of this reversible reaction. The temperature was further increased to 150 °C to start the grafting reaction and kept at 150 °C for 5 hours. Thereafter, the grafted product was cooled to 80 °C, water was added to achieve a solid content around 30 wt.%, and the PCE solution was neutralized to  $\text{pH} \approx 7$  using 30 % NaOH solution. For the synthesis of G45PC<sub>5</sub>-g-Jeffamine with G45PC<sub>5</sub>, the dilution and pH adjustment are not required. The graft polymer G45PC<sub>3</sub> was also prepared following a similar scheme (see **Figure 11**) with the feeding molar ratio between MAA to MPEG of 4:1 (MPEG: 21.2 g, PMMA: 9.3 g), because this reaction consumed one molar of MAA unit in PMAA when graft with one molar of MPEG to obtain the product.

### 5.1.1.2 Synthesis of graft polymer G45PC5-g-Jeffamine

The non-air entraining PCE produced by grafting Jeffamine M1000 onto G45PC5 were additionally marked as G45PC5-g-Jeffamine. Here, 2 g (0.002 mol) of Jeffamine M1000 (Huntsman Germany) and 3.32 g of above synthesized G45PC5 (0.001 mol) are weighed with approx. 20 mL of DI water in a 250 mL Schlenk flask and stirred at 80 °C until a homogeneous solution has formed. The water is then removed by means of vacuum (0.1 mbar) and collected in a liquid nitrogen cooled cold trap.

To start the esterification or condensation reaction, the reaction mixture was heated to 180 °C for 5 h. After completion of the reaction, the polymer is cooled, diluted with water to a solids content of about 30%, and adjusted to a pH of ~ 7. The molar ratio between the PCE and defoamer refers to the number of repeat units in the PCE backbones, it means that for each repeat unit of the PCEs, two molecules of Jeffamine M1000 was grafted. The detailed synthesis process of these graft polymers is displayed in **Figure 11**. Furthermore, different Jeffamine polymers (Jeffamine M600, M1000 and M2005) were used for copolymerization with G45PC5 polymer at different feeding molar ratios, following the same synthesis procedure as G45PC5-g-Jeffamine. The feeding amounts of G45PC5 and Jeffamine polymers are listed in **Table 3**.

**Table 3** The feeding amounts of G45PC5 and Jeffamine polymers

Sample	Feeding molar ratio (COO <sup>-</sup> : MPEG : Jeffamine)	G45PC5	Jeffamine
		g	g
G45PC5-g-Jeffamine M600 (1mol)	4:1:1	3.32	0.6
G45PC5-g-Jeffamine M600 (2mol)	3:1:2	3.32	1.2
G45PC5-g-Jeffamine M1000 (1mol)	4:1:1	3.32	1
G45PC5-g-Jeffamine M1000 (2mol)	3:1:2	3.32	2
G45PC5-g-Jeffamine M1000 (3.5mol)	1.5:1:3.5	3.32	3.5
G45PC5-g-Jeffamine M2005 (1mol)	4:1:1	3.32	2
G45PC5-g-Jeffamine M2005 (3.5mol)	1.5:1:3.5	3.32	7

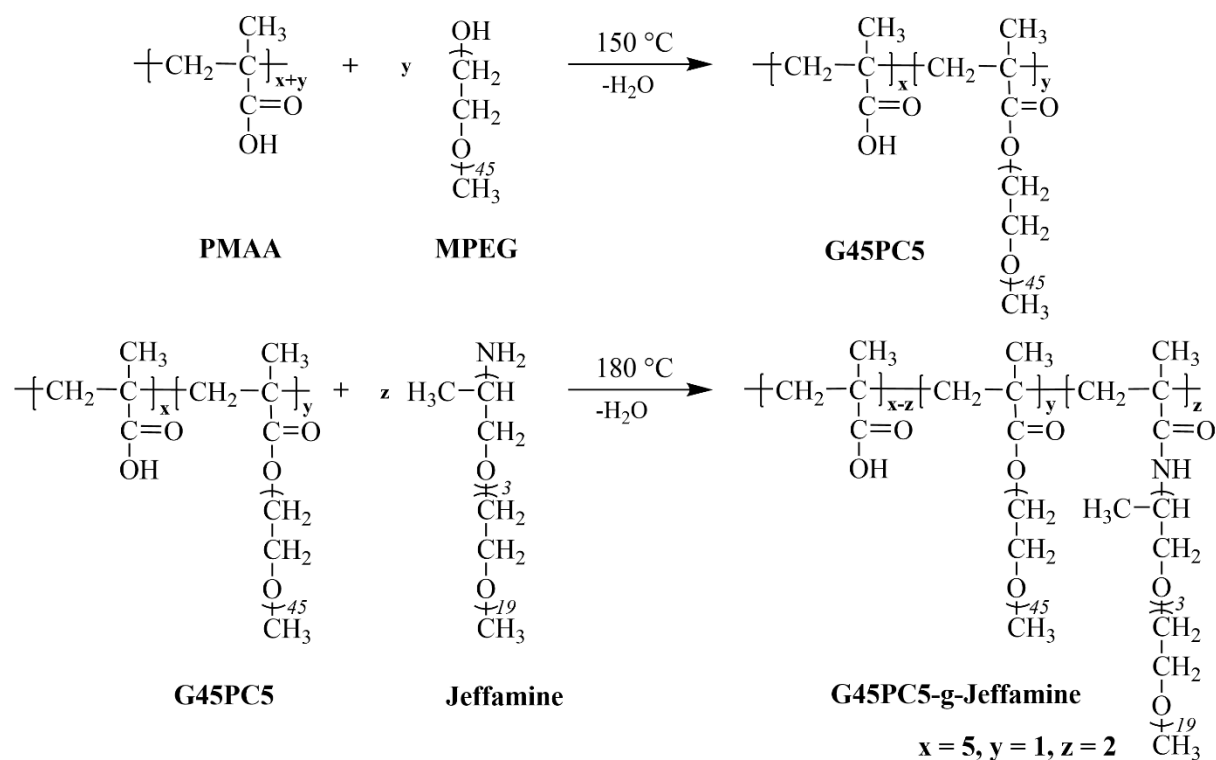


**Figure 11** Synthesis process of the graft polymer G45PC5 and G45PC5-g-Jeffamine

## 5.1.2 Characterization of the synthesized graft PCE polymers

### 5.1.2.1 SEC Results

The solid content, molecular weights ( $M_n$ ,  $M_w$ ), polydispersity index (PDI) and conversion rate of the polymer samples are listed in **Table 4**. The SEC spectra of grafted PCE polymers (G45PC5 and G45PC5-g-Jeffamine) are shown in the **Figure 12**. According to the results, all PCE samples exhibit low PDI values (1.6 - 2.0) and high rates for macromonomer conversion (91.3 - 98.1%).

The molecular weight of G45PC5 is 15290 g/mol ( $M_w$ ) and 9373 g/mol ( $M_n$ ) with 1.6 polydispersity index (PDI). The molecular weight of repeat units (AA-MPEG with 6:1 molar ratio) is around 2500 g/mol, so there are around 6 mol repeat units in 1 mol G45PC5 polymers. After Jeffamine M1000 was grafted at the main chain, the polymer G45PC5-g-Jeffamine has a molecular weight of 29280 g/mol ( $M_w$ ) and 14410 g/mol ( $M_n$ ) with polydispersity index (PDI) 2.0. The molecular weight increased by 13990

## Results and discussion

g/mol from G45PC5 to G45PC5-g-Jeffamine. Considering the number of repeat units, it can be calculated that around 2.3 mol Jeffamine M1000 molecular are grafted into 1 mol repeat units by reacting with the -COOH groups. It is slightly higher than the setting molar ratio (Jeffamine: repeat unit = 2: 1) because the Jeffamine M1000 is pure, but G45PC5 has a conversion rate of less than 100% in this grafting experiment.

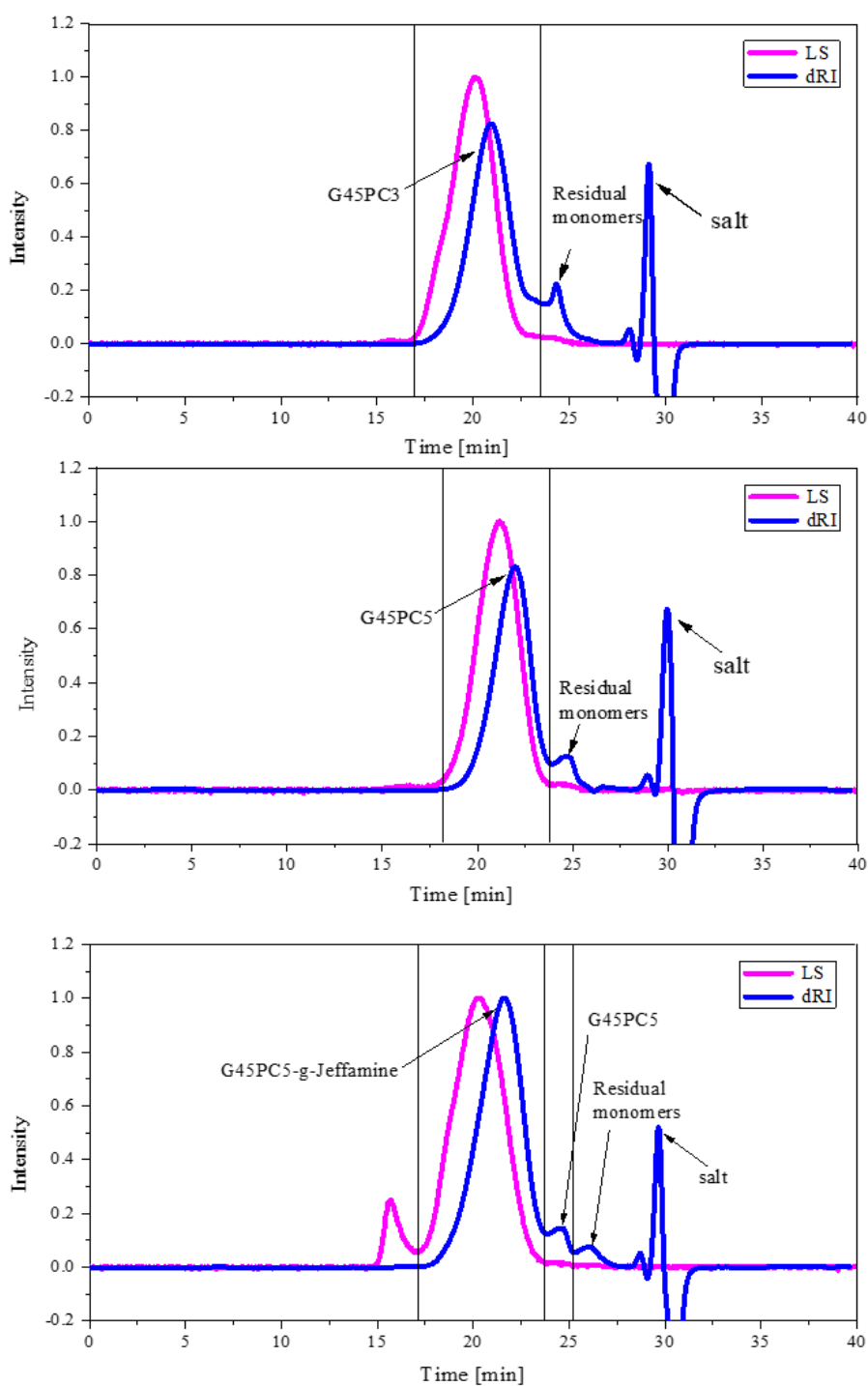


**Figure 12** SEC spectra of G45PC3, G45PC5 and G45PC5-g-Jeffamine polymers

**Table 4** Solid content, molar masses, polydispersity index (PDI) of the synthesized polymers, and the macromonomer conversion rate in the reaction

Sample	Solid content [%]	$M_w$ [g/mol]	$M_n$ [g/mol]	PDI [ $M_w/M_n$ ]	Conversion rate [%]
G45PC3	32.7	13,790	8,771	1.8	91.3
G45PC5	32.1	15,290	9,373	1.6	92.7
G45PC5-g-Jeffamine	33.6	29,280	14,410	2.0	98.1

### 5.1.2.2 $^1\text{H}$ NMR spectra

The chemical structure of G45PC5 and G45PC5-g-Jeffamine PCE samples was confirmed via  $^1\text{H}$  NMR spectroscopy. As marked in **Figure 13**, the proton peaks at 0.9 - 1.2 ppm and 1.7 - 2.2 ppm belong to the  $-\text{CH}_3$  and  $-\text{CH}_2$  groups respectively in MAA and MPEG repeat units, the strong and broad peaks around 3.6 ppm stem from protons in the ethylene oxide repeating units. Two additional peaks appearing at 3.8 ppm and 4.0 - 4.4 ppm can be assigned to the protons in the  $-\text{CH}_2$  groups adjacent to the formed ester group. All these characteristic peaks certificate the successful grafting of G45PC5 polymer.

In the spectrum of the G45PC5-g-Jeffamine polymer (see **Figure 14**), besides all characteristic peaks appearing in the G45PC5 polymer, a proton peak from the amide group ( $-\text{CONH}-$ ) at 7.9 ppm is also observed, confirming the successful graft of Jeffamine onto G45PC5 chemical structure.

Furthermore, the  $^1\text{H}$  NMR spectrum also provides the actual chemical composition of polymers based on the calculation of proton intensities at different chemical shifts. The feeding and actual molar ratios are calculated and shown in **Table 5**. It can be found that the actual molar ratio is nearly identical to the feeding molar ratio with respect to G45PC3 (3.04:1 vs. 3:1) and G45PC5 (5.06:1 vs. 5:1) polymers. The actual molar ratio of G45PC5-g-Jeffamine is also close to the feeding ratio (3.11: 1: 1.76 vs. 3: 1: 2). The reason behind this is the graft method typically produces a highly uniform statistical comb polymer [20, 74].

## Results and discussion

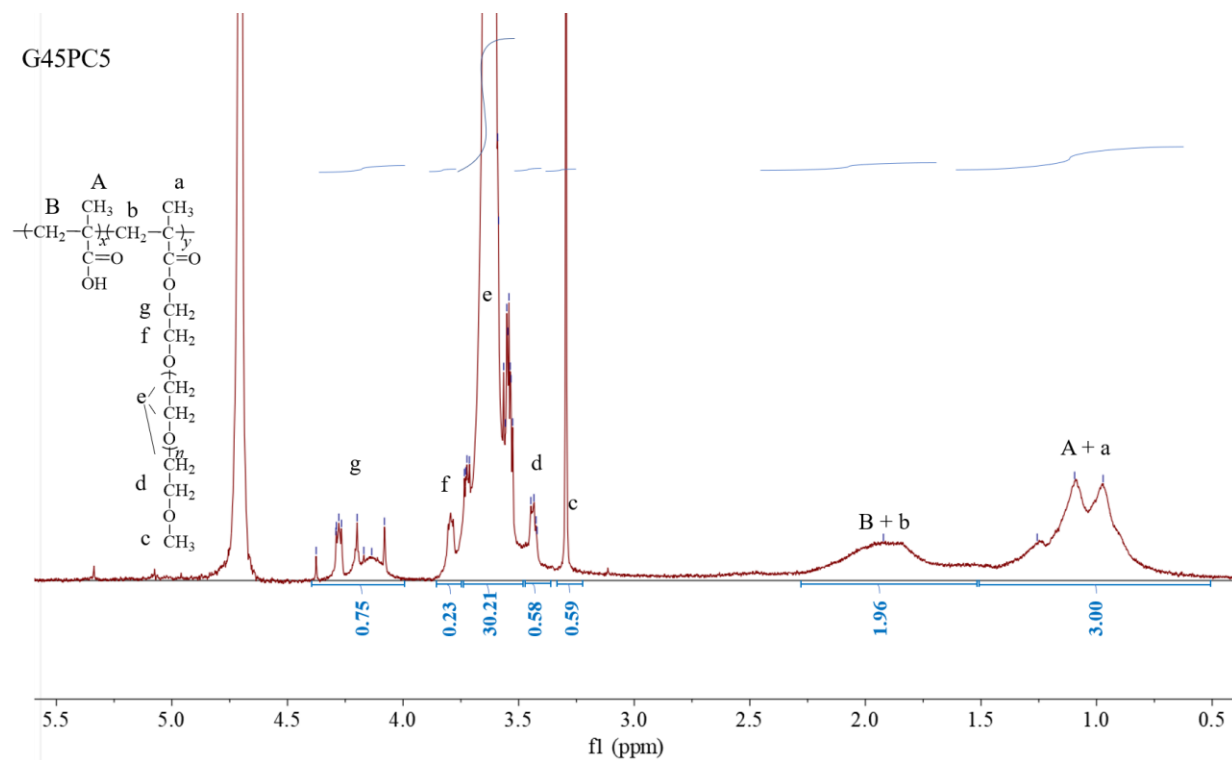


**Figure 13**  $^1\text{H}$  NMR spectrum and proton integrals of G45PC5 polymer

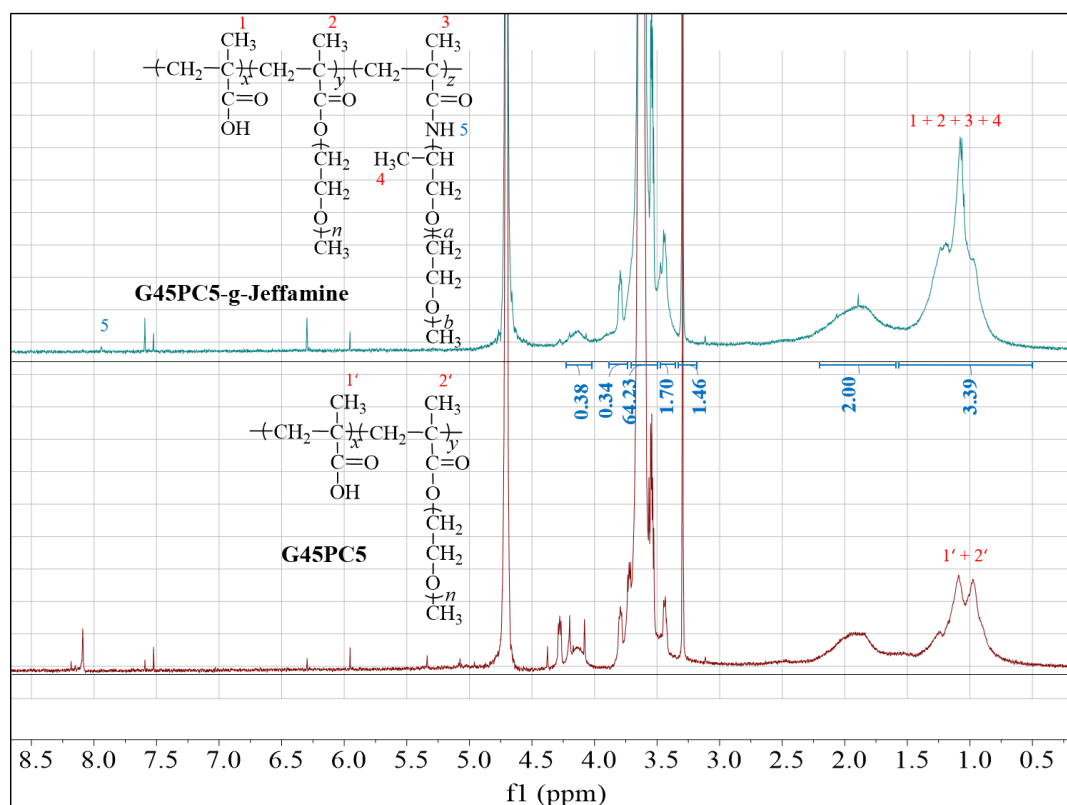


**Figure 14**  $^1\text{H}$  NMR spectra of G45PC5-g-Jeffamine and G45PC5 polymers

**Table 5** Structural/ compositional analysis of the PCE polymers

Sample	Feeding molar ratio (COO <sup>-</sup> : MPEG : Jeffamine)	Actual molar ratio (COO <sup>-</sup> : MPEG : Jeffamine)
G45PC3	3: 1: 0	3.04: 1: 0
G45PC5	5: 1: 0	5.06: 1: 0
G45PC5-g-Jeffamine	3: 1: 2	3.11: 1: 1.76

### 5.1.2.3 FT-IR spectroscopy

Then, the characteristic peaks of specific groups in the grafting copolymers were tested via the FTIR spectra and shown in **Figure 15**. In the G45PC5's FTIR spectrum, the broad bands between 1700 cm<sup>-1</sup> and 1726 cm<sup>-1</sup> originates from the stretching vibration of the C=O bond of carboxyl groups in the backbone, and the band at ~ 1081 cm<sup>-1</sup> is caused by the stretching vibration of the C–O from ethylene oxide side chain. All these characteristic bands confirm the successful synthesis of G45PC5 polymer through the graft method.

Furthermore, in the spectrum of G45PCE-g-Jeffamine, besides these characteristic bands in G45PC5 polymer, new bands at 1668 cm<sup>-1</sup> and 1281 cm<sup>-1</sup> (stretching vibration of C=O bond and C–N bond from –CONH group) suggest that the amide structure (–CONH) is successfully obtained in the G45PCE-g-Jeffamine polymer via esterification reaction.

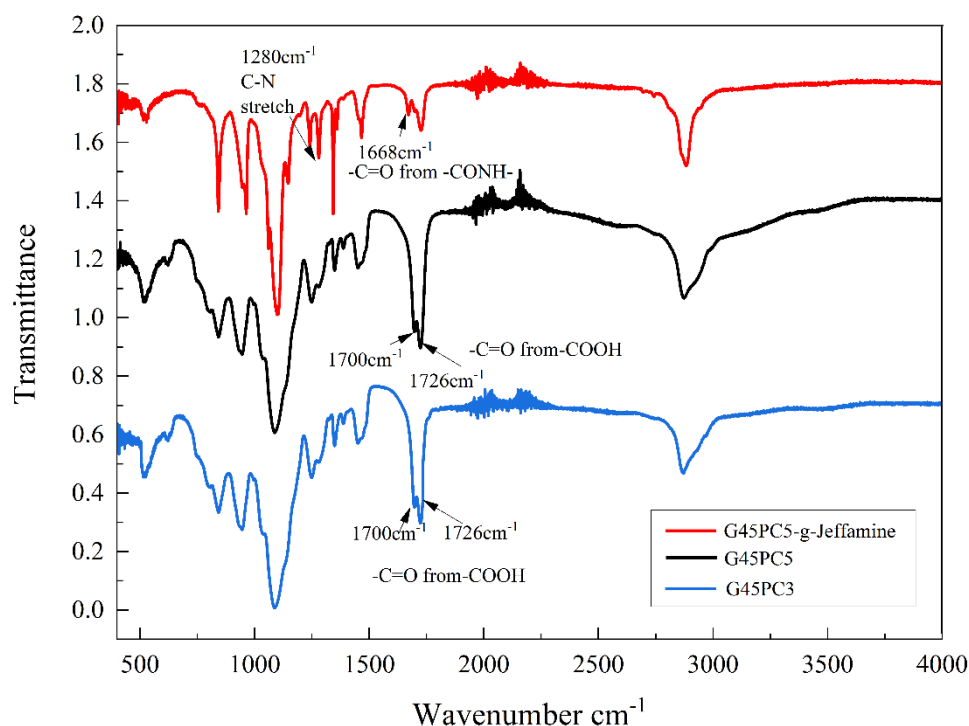


**Figure 15** The FT-IR spectra of G45PC5-g-Jeffamine, G45PC3 and G45PC5 PCEs

### 5.1.3 Phase separation of non-air entraining PCE

A compatibility test between defoamer and superplasticizer is necessary before its application [161]. This is because most defoamers are hydrophobic and may separate from the hydrophilic superplasticizers, this separation will compromise the defoaming effectiveness.

In this experiment, the phase separation of the synthesized G45PC5-g-Jeffamine polymer was tested using three tubes, each with a length of 20 cm and an inner diameter of 3 cm. The tubes were placed in a climate chamber at temperatures of 0, 22, and 50 °C, respectively. The results in **Table 6** demonstrate the phase separation of the G45PC5-g-Jeffamine polymer after 5 days of aging. It was observed that there was no visual separation at any of the three temperature conditions, indicating the excellent stability of this non-air-entraining PCE. This suggests that this defoamer will not degrade during long storage periods, maintaining its effectiveness over extended periods and indicating

a long shelf-life.

**Table 6** The phase separation of the G45PC5-g-Jeffamine defoamer

Sample	G45PC5-g-Jeffamine		
Temperature / °C	0	22	50
Phase separation	no	no	no

#### 5.1.4 Dispersing effectiveness of non-air entraining PCE

##### 5.1.4.1 Tests in paste

The dispersing performance of G45PC3, G45PC5, and G45PC5-g-Jeffamine superplasticizers was initially evaluated in cement paste using a “mini-slump” test. The water-to-cement ratio of 0.46 was determined by adjusting the flow value of the paste without any PCE to  $18 \pm 0.5$  cm. The dosages of PCE samples required to achieve a  $26 \pm 0.5$  cm cement paste flow are shown in **Figure 16**. The required dosages for the three PCEs are at 0.08% bwoc, indicating that all three PCE samples have similarly strong dispersing effectiveness in cement paste.

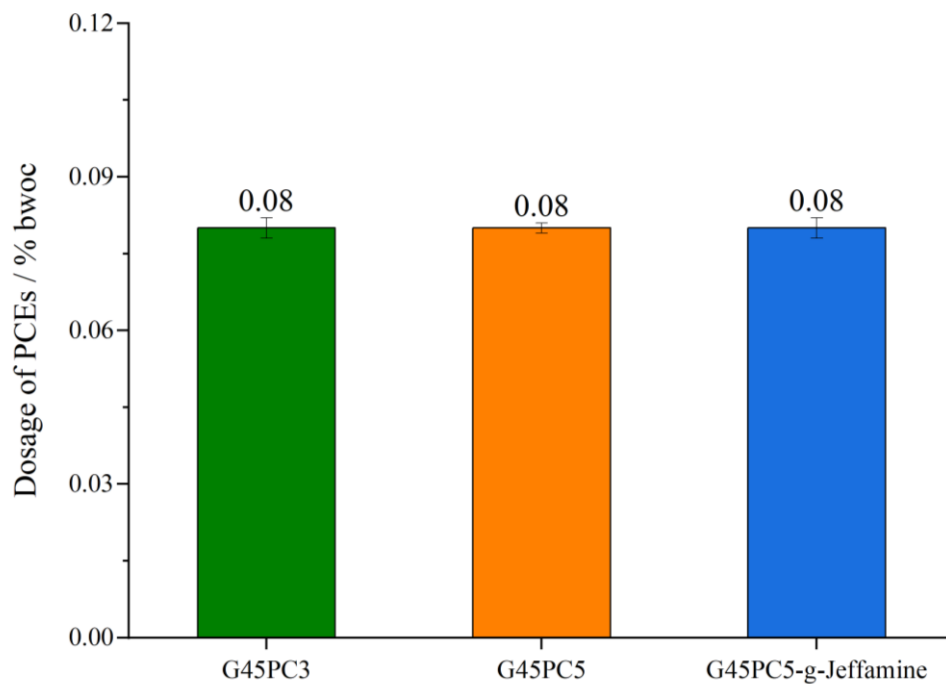


**Figure 16** Dosages required to obtain a  $26 \pm 0.5$  cm paste spread flow ( $w/c = 0.46$ )

#### 5.1.4.2 Tests in mortar

Next, the dispersing test of the superplasticizers was conducted in mortar with a water-to-cement ratio of 0.4, which has a 10.5 cm initial spread flow. In this part, the dosage of PCE samples was kept at 0.4% bwoc. It can be seen from **Figure 17**, the G45PC5-g-Jeffamine polymer has the strongest dispersing ability as it can provide the biggest spread flow (21.5 cm), followed by G45PC3 (20.3 cm), G45PC5 (19.0 cm).

As expected, the electrostatic repulsion and steric hindrance effect of superplasticizers determine their dispersing effectiveness. Previous publications confirmed that the electrostatic repulsion induced by repulsive forces between cement particles is so minor that can be easily neglected [162, 163]. While the steric hindrance dispersion mechanism stems from the non-adsorbing polyethylene glycol side chains have been proven to present the dominant effect [99, 164-166].

In this study, G45PC3 with higher side chain density exhibits stronger dispersing power than more anionic G45PC5. Similarly, G45PC5-g-Jeffamine polymers in this study with more side chains present better dispersion power than G45PC5, resulting from a stronger steric hindrance effect. The superior dispersing effectiveness of G45PC5-g-Jeffamine than G45PC3 can be ascribed to the extra jeffemine side chains. The comparison experiment of G45PC5 polymer and Jeffamine 1000 monomer mixture at a 1: 1 molar ratio produced a 17.8 cm spread flow, confirming that G45PC5-g-Jeffamine polymer benefits from its grafted Jeffamine side chains.

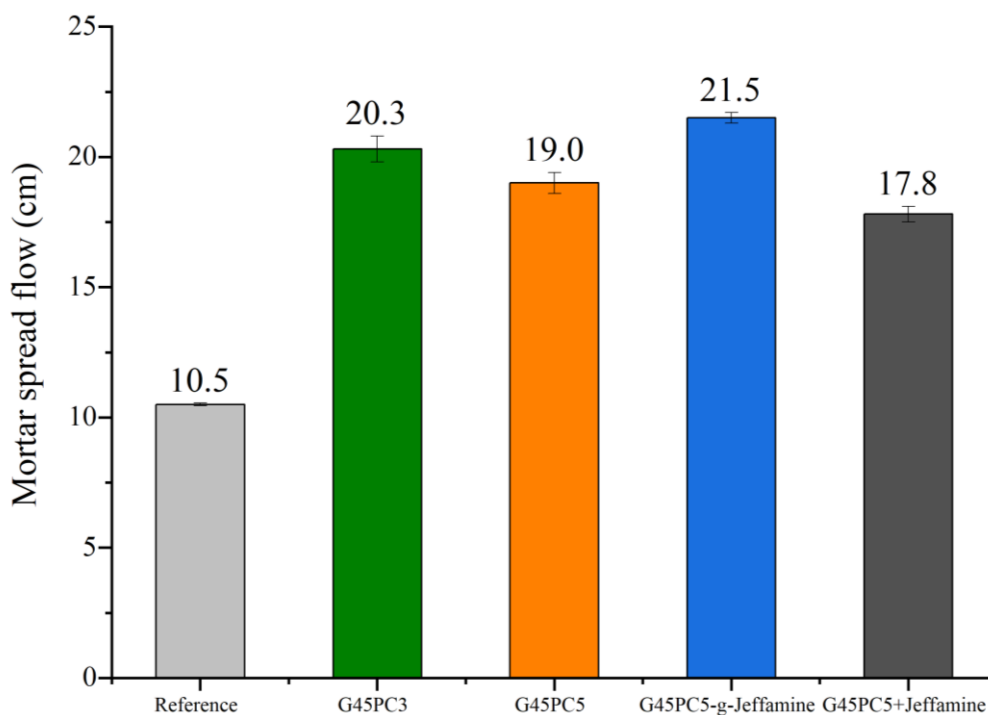


**Figure 17** Mortars spread flow without and admixed with PCE polymers

### 5.1.5 Foaming behavior of non-air entraining PCE

The foaming behavior of PCE polymers in aqueous solutions was first tested by shaking for 2 minutes in a tube, and then recording the foam height at different times. As shown in **Figure 18**, G45PC5 and G45PC3 polymers produced more foam than G45PC5-g-Jeffamine in the solution after 2 minutes of shaking, indicating that the air-entraining ability was inhibited by introducing hydrophobic Jeffamines into conventional G45PC5 PCE. Additionally, the G45PC5-g-Jeffamine polymer also effectively reduced the foam stability as bubbles in this solution collapsed faster than those in G45PC5 and G45PC3 PCE solutions.

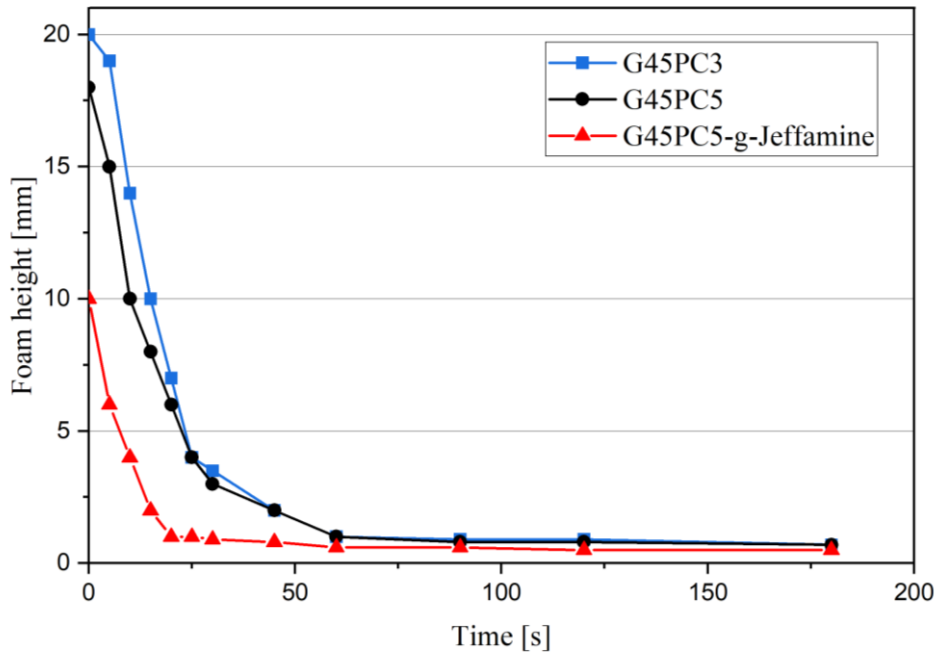


**Figure 18** Foam height of G45PC3, G45PC5 and G45PC5-g-Jeffamine PCEs

Secondly, the air-entraining ability of these PCE polymers was measured in mortar with the exact PCE dosage (0.4 % bwoc) at a water-to-cement ratio of 0.4 (see **Figure 19**). In the case of reference mortar without any admixture, 4.1% of air volume was observed, this value is inconsistent with previous researches [167, 168].

The admixture of G45PC5 PCE introduced more air (14.0 %) than reference, and similar results was observed for G45PC3 polymer (14.5 %), indicating strong air entrainment ability of conventional MPEG-type PCE. Lange et al. also reported the strong air entraining ability of conventional PCE polymers [168]. But there is no clear explanation for the mechanism of how the PCE affect the air entrainment. Łaźniewska-Piekarczyk reported that PCE increased the air voids in concrete via reducing the surface tension between the liquid and solid component [169]. Al Neshawy et.al think that PCE superplasticizer can increase the air entrainment since they partly reduce the adsorption of air entraining agent on the solid surface by competing with them [170].

However, after the Jeffamine molecular was grafted to this PCE polymer, G45PC5-g-Jeffamine is effective in decreasing the air-content of fresh mortar (4.6%). To make sure

whether the defoaming effect of G45PC5-g-Jeffamine is from unreacted Jeffamine, a G45PC5 polymer and Jeffamine 1000 monomer mixture with a 1: 1 molar ratio was applied in the air voids measurement, and 14 vol.% of air in the fresh mortar was produced. Therefore, Jeffamine M1000 monomer did not reduced the air stability when it was simply mixed with MPEG type PCE solution.

The molecular structure difference between G45PC5 and G45PC5-g-Jeffamine, as discussed in **Section 5.1.2**, is that G45PC5-g-Jeffamine polymer containing two kinds of side chains with different hydrophilic/ hydrophobic properties, and the number of side chains in G45PC5-g-Jeffamine polymer chain is more. So, it can be speculated that the defoaming effectiveness of G45PC5-g-Jeffamine polymer is related to their side chains.

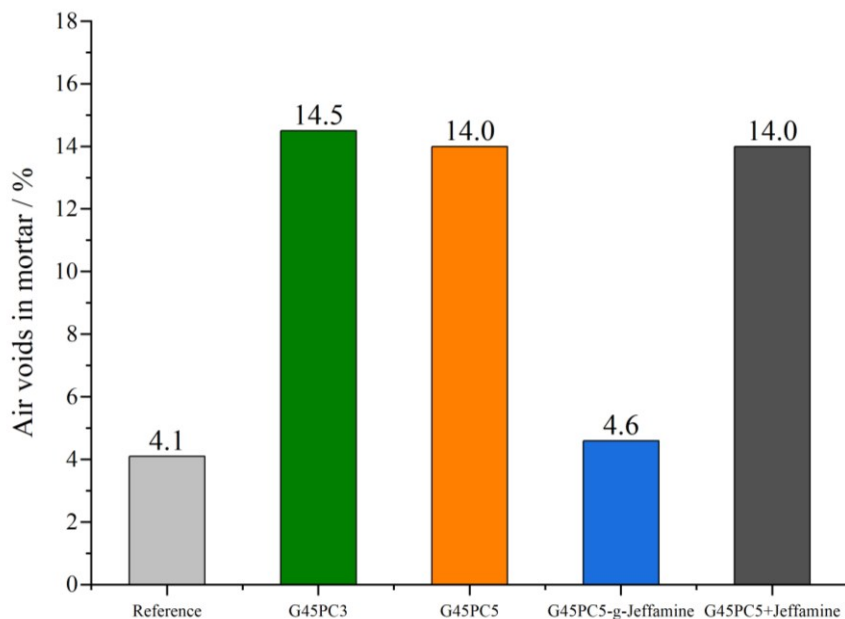


**Figure 19** Air voids of mortars without and admixed with PCE polymers at w/c ratio of 0.4

Furthermore, the HLB values which is related to the surface tension of these polymers was tested and listed in **Table 7**. The HLB value of DI water at 25 °C is 71.4 mN/m, similar result was reported in the previous literature [171]. The addition of G45PC5 and

G45PC5-g-Jeffamine decreased the HLB value to 59.1 and 48.0 respectively, because of the high surface activity of PCE polymers. This results is also in consistent with previous study form Pott et al. [172]. One plausible explanation for the non-air entraining properties of G45PC5-g-Jeffamine polymer could be its low HLB value.

**Table 7** The surface tension of different aqueous solutions.

Sample	Surface tension [mN/m]	HLB value
Water	71.4	-
G45PC5	59.1	18.5
G45PC5-g-Jeffamine	48.0	17.7

### 5.1.6 Compressive strength of mortars

The introduced Jeffamine side chains in G45PC5-g-Jeffamine decreased the air voids, the void ratio of mortar further affect its microstructure and mechanical properties. The compressive strength values of reference mortar and mortars admixed with G45PC5 and G45PC5-g-Jeffamine superplasticizers after 16 h, 3 d, 7 d and 28 d are shown in **Figure 20**.

The compressive strength of all samples increased as expected with hydration time. This is due to the hydration process, as longer curing time allows for more thorough hydration, resulting in higher compressive strength. After the same hydration time (16 hours, 3 days, 7 days, and 28 days), both mortars admixed with G45PC5 and G45PC5-g-Jeffamine polymers consistently exhibited higher compressive strength compared to reference mortars. This is because the MPEG type PCE can provide good fluidity to the cement, and the graft polymers do not have a retarding effect on the cement, as will be confirmed in the following hydration test. Furthermore, mortars admixed with G45PC5-g-Jeffamine always exhibited the highest compressive strength after the same hydration time. This is attributed to the defoaming properties, as higher porosity leads to lower compressive strength, and the G45PC5-g-Jeffamine defoamer reduced the air voids in fresh mortar, contributing to higher compressive strength compared to G45PC5.

However, it has been widely reported that the superplasticizer has retarding effect on the cement hydration, and the compressive strength were decreased with the addition of PCE samples [76, 173]. This negative effect is closely related to the PCE adsorption, which is determined by the chemical structure of PCE polymers. As mentioned in **Section 5.1.2.2**, graft method produced more uniform statistical comb polymer than free radical method. Those microstructural differences stemming from the synthesis methods inevitably lead to a distinct interaction with cement materials [174].

Therefore, the compressive strength of mortars admixed with 45PC5 and HPEG PCE polymers synthesized by free radical method were tested after 16 h, 3 d, 7 d and 28 d aging. As shown in **Figure 21**, the cement hydration at all ages except that of 28 days were delayed after the addition of these two PCE polymers.

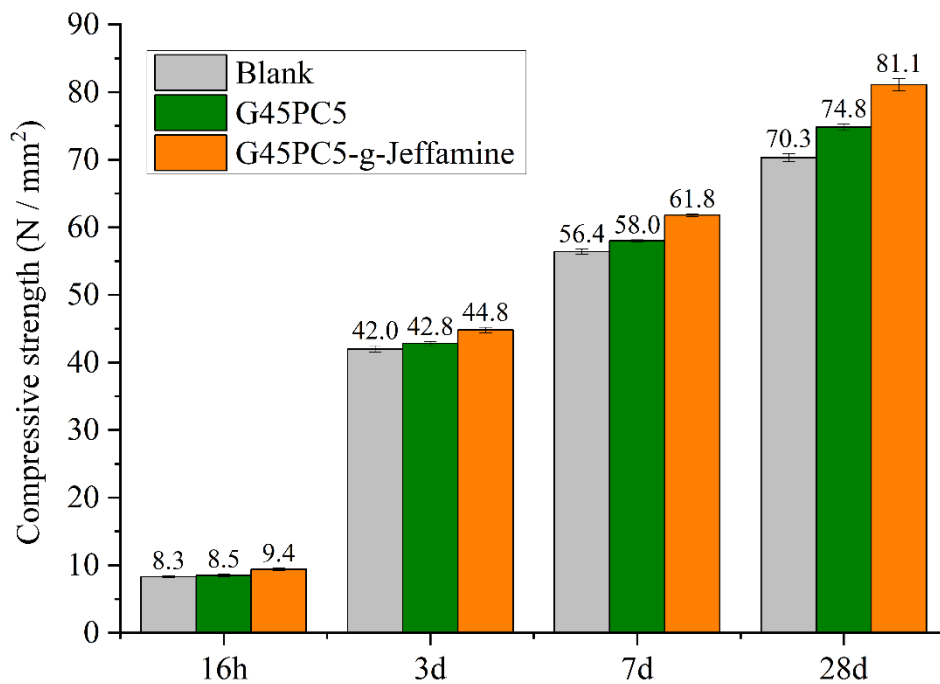


**Figure 20** Compressive strengths of mortars without and admixed with G45PC5 and G45PC5-g- Jeffamine superplasticizers after different curing times (w/c ratio = 0.4)

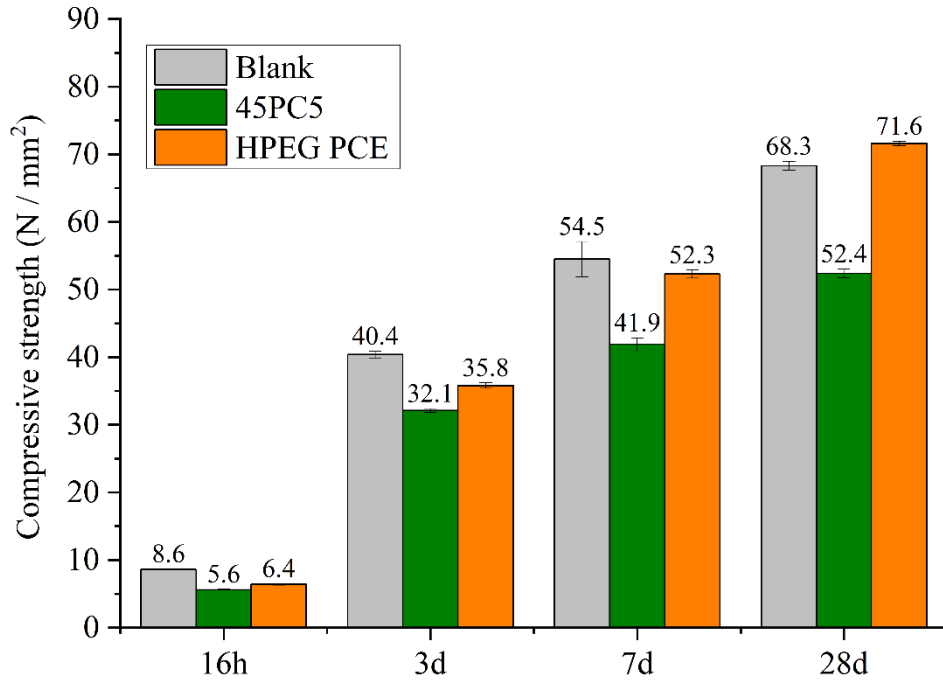


**Figure 21** Compressive strengths of mortars samples without and admixed with 45PC5 or HPEG PCE polymers after different curing times (w/c ratio = 0.4)

### 5.1.7 Isothermal heat-flow calorimetry test of cement paste

The heat flow represents the hydration rate, the first peak is mainly caused by rapid dissolution of  $C_3A$ , alkali- and calcium sulfates resulting in the precipitation of ettringite. After this initial hydration period, the induction (or dormant) period follows which is due to the hydration of alite (or  $C_3S$ ). Following the induction period, the main hydration period is established. It also includes the acceleration and deceleration period. This main hydration period is caused by the hydration of alite, but during the acceleration period significant amounts of C-S-H phases are formed causing the setting of the cement paste.

In accordance with the result from heat flow calorimetry (see **Figure 22**), no obvious delay in the induction period was observed for G45PC5 and G45PC5-g-Jeffamine polymers, indicating no retarding effect on the cement hydration. The maximum heat flow for G45PC5 and G45PC5-g-Jeffamine are similar, and both them are higher than

that of the reference paste without PCE.

The total hydration heat in **Figure 23** was increased when the cement paste was admixed with G45PC5 and G45PC5-g-Jeffamine polymers, which means this two PCE polymers has accelerate effect on the hydration of the silicate phases.

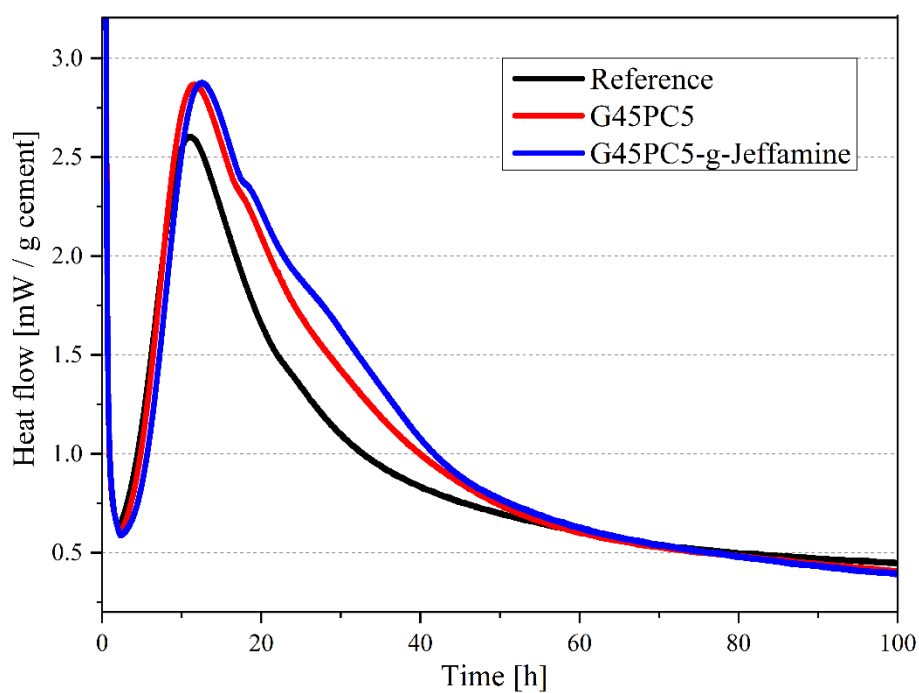


**Figure 22** Heat flow calorimetry of reference cement paste and admixed with 0.08 % bwoc of PCE samples (w/c ratio = 0.46)

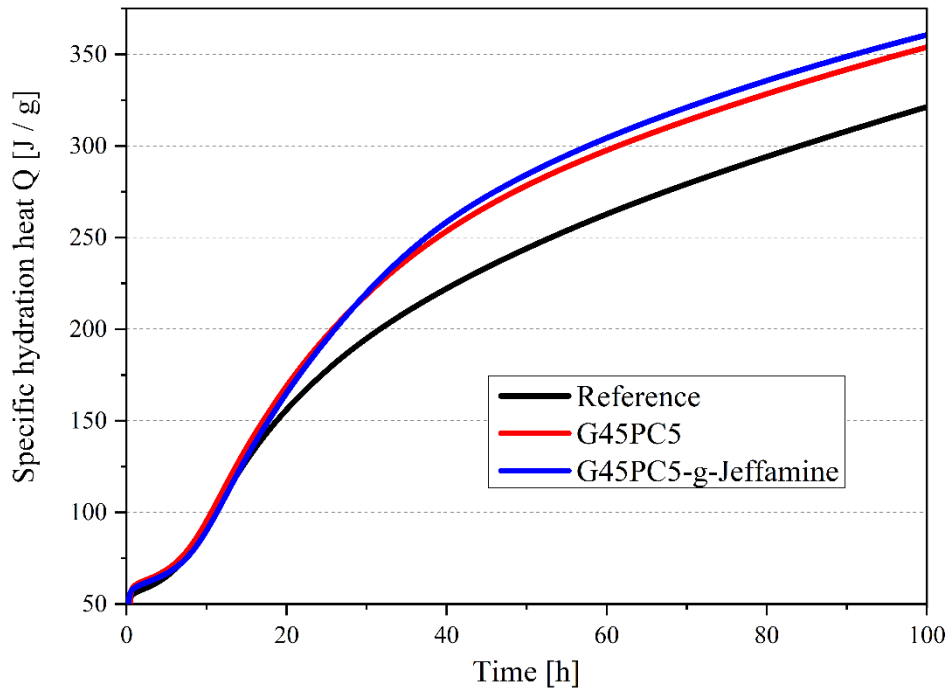


**Figure 23** Cumulative heat flow curves of reference cement paste and admixed with 0.08 % bwoc of PCE polymers (w/c ratio = 0.46)

### 5.1.8 X-ray analysis of cement hydration

The hydration kinetics of Portland cement can be influenced by various factors, such as hydration time, chemical admixtures, and temperature [175-177]. Complementary to the calorimetric test, the formation of crystalline hydrate phases during cement hydration was monitored for the first 30min, 60min, 4h, 8h, 16, 24h via XRD test.

**Figure 24** present the intensity of hydrate phase at different time.

As shown in **Figure 24**, the reflections of main phase (A: Alite) decreased and the hydration products such as portlandite (P) and ettringite increasingly formed with the hydration ongoing. In the cement paste containing G45PC5-g-Jeffamine, portlandite formation is significantly enhanced and ettringite formation is slightly increased compared to the reference. Thus, this XRD results confirmed an enhanced silicate reaction in paste admixed with G45PC5-g-Jeffamine polymer, which is responsible for the compressive strength development.

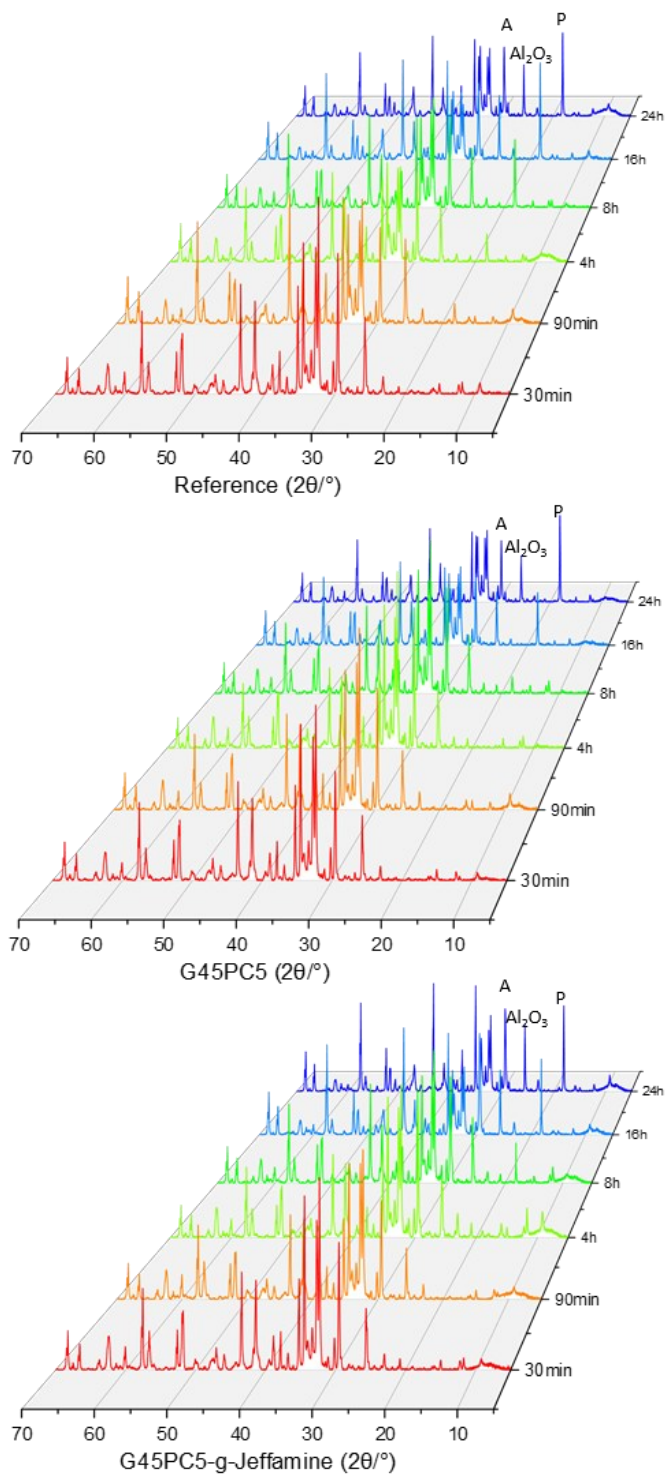


**Figure 24** The XRD diffractogram of cement pastes admixed with or without PCE polymers as a function of hydration time. (A: alite; P: portlandite)

QXRD measurement of cement hydration with 20 wt.% of aluminum oxide ( $\text{Al}_2\text{O}_3$ ) as

an internal standard was applied to track the specific mineral phase composition during hydration process. The content of C<sub>3</sub>S and Portlandite, which were recorded in **Table 8**, indicate that the hydration was delayed within the first 8h as the residual C<sub>3</sub>S amount in reference is the less compared to the sample admixed with G45PC5 or G45PC5-g-Jeffamine polymers. Afterwards, rapid formation of CH was recorded for the sample admixed with PCE polymers, which means G45PC5 and G45PC5-g-Jeffamine polymers promoted the hydration and compressive strength development after 16 h. It is worth noting that the presence of the Portlandite phase is rather undesirable and has a negative impact on the mechanical properties of the clinker. On the other hand, the addition of G45PC5 and G45PC5-g-Jeffamine polymers led to accelerated hydration and reduced air voids, which in turn promoted the development of compressive strength.

**Table 8** QXRD analysis of mineral content calculated by TOPAS (20 % Al<sub>2</sub>O<sub>3</sub>).

Sample	Mineral content (wt. %)	30 min	90 min	4 h	8h	16h	24h
Reference	C <sub>3</sub> S	33.7	27.9	23.1	21.2	11.5	10.6
	Portlandite	0.7	1.8	2.5	4.5	5.6	6.8
G45PC5	C <sub>3</sub> S	35.1	33.6	31.7	28.9	18.9	17.6
	Portlandite	0.2	0.8	1.0	2.0	4.7	7.5
G45PC5-g-Jeffamine	C <sub>3</sub> S	34.7	33.1	30.6	22.5	12.0	11.1
	Portlandite	0.7	1.1	1.4	4.5	5.7	7.8

In addition, a series of grafting PCE polymers incorporating different Jeffamines were synthesized, i.e. M600 (9/1 PO/EO), M2005 (29/6 PO/EO), as well as M1000 (3/19 PO/EO) respectively. Thereafter, the air-entraining property of the resulting PCE polymers was tested in fresh mortar and summarized in **Table 9**.

As is shown in **Table 8**, compared to its PO-rich Jeffamine cousins (Jeffamine M600 and M2005), Jeffamine-M1000 exhibited the least air entrainment. The possible explanation could be that Jeffamine M1000 chains with less hydrophobic PO units exhibited better compatibility with the conventional MPEG pendant chains. Typically,

the air bubbles were stabilized through the electrostatic repulsion induced by MPEG side chains, these Jeffamine side chains could enter water lamella, the hydrophobic PO segment cause a decrease of surface tension at specific points, as a result, the bubble burst. An in-depth investigation is still needed here. It is also clear from the table above that the substitution rate of Jeffamine has a great influence on the air entrainment of the G45PC5-Jeffamine polymers. In this study, the optimized molecular structure of the PCE polymer is COO<sup>-</sup>: MPEG: Jeffamine = 3: 1: 2. More experiments are required to investigate the defoaming mechanism.

**Table 9** Air voids in fresh mortar admixed with different G45PC5-g-Jeffamine polymer samples

Sample	Feeding molar ratio (COO <sup>-</sup> : MPEG : Jeffamine)	Air voids in mortar [%]
Reference	-	4.1
G45PC5-g-Jeffamine M600 (1mol)	4:1:1	20.0
G45PC5-g-Jeffamine M600 (2mol)	3:1:2	18.0
G45PC5-g-Jeffamine M1000 (1mol)	4:1:1	8.5
G45PC5-g-Jeffamine M1000 (2mol)	3:1:2	4.6
G45PC5-g-Jeffamine M1000 (3.5mol)	1.5:1:3.5	7.5
G45PC5-g-Jeffamine M2005 (1mol)	4:1:1	15.0
G45PC5-g-Jeffamine M2005 (3.5mol)	1.5:1:3.5	14.0

### 5.1.9 Summary of Section 5.1

In this part, a non-air entraining PCE containing Jeffamine side chains was synthesized through graft method. The chemical structure of this PCE polymer was confirmed through SEC, FT-IR and <sup>1</sup>H NMR measurements, its dispersing ability and influence on compressive strength of standard mortars were assessed via spread flow, air voids and compressive strength measurements. Further, the defoaming mechanism of this superplasticizer was explained by the HLB and surface tension values of the polymers. From the results obtained, the following conclusions can be drawn:

1. The graft method was successfully applied to obtained G45PC5-g-Jeffamine PCE polymer, which did not entrain extra air compared to the reference mortar without any PCE polymer.

## Results and discussion

---

2. The presence of more hydrophobic side chains in G45PC5-g-Jeffamine results in lower surface tension, allowing it to spread more quickly in the water film. The lower HLB value of the Jeffamine side chains disrupts the stability of the water film. Additionally, the hydrophobic side chains occupy some of the adsorption sites on the surface of cement particles, releasing more free water compared to a normal defoamer. As a result, mortar admixed with G45PC5-g-Jeffamine had very low air voids while still dispersing well at the same time.

3. G45PC3, G45PC5, and G45PC5-g-Jeffamine PCE polymers exhibit good dispersion power. The improved dispersing effectiveness of the G45PC5-g-Jeffamine PCE in mortar could be attributed to the additional polyamine pendant chains in the structure.

4. Both G45PC5 and G45PC5-g-Jeffamine samples with highly uniform statistical microstructure enhanced the compressive strength at all curing ages (16 h, 3 d, 7 d, and 28 d).

5. Calorimetric results, along with XRD analysis, confirmed that the enhanced cement hydration, especially concerning the silicate reaction, after 16 hours, can be achieved by adding the G45PC5 and G45PC5-g-Jeffamine polymer.

## **5.2 A novel defoaming system based on ion-pair complexes**

In this part, an ion pair complex based on 23HPEG7 PCE and Jeffamine 2005/2070 polymers were investigated. Qu [178] reported such ion pair complexes and investigated their performance in mortar spread flow and air voids. In this part, we focus on analyzing the defoaming behavior from various perspectives.

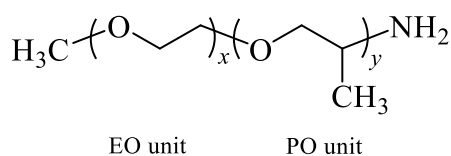
In this part, the research focuses on a new PCE-defoamer ion-pair defoaming system, which exhibits excellent formulation stability when utilized in cementitious materials. These ion-pair complexes are formed when the functional  $-COOH$  groups in PCE polymer react with  $-NH_2$  groups in Jeffamine defoamers at a relatively low pH ( $\sim 4$ ). This prevents phase separation of PCEs and defoamers during storage and transportation. When the ion-pair liquid is applied to cementitious materials with a higher pH ( $\sim 12$ ), the ion-pair dissociates. This allows the PCEs and Jeffamine defoamers to disperse and defoam simultaneously. Furthermore, the foam behavior of these ion-pair complexes was investigated from different perspectives, their influences on compressive strength and hydration degree were determined via isothermal heat-flow calorimetry and QXRD measurements. The influence of chemical structure parameters, such as side chain length and side chain density, on the dispersing effectiveness and defoaming performance were also analyzed.

### **5.2.1 Synthesis of PCE-Jeffamine ion-pair complexes**

Firstly, HPEG-type PCE (23HPEG7) was synthesized, the synthesis procedure at room temperature is described in the following:

First, 11 g of 23HPEG macromonomer dissolved in 10 g DI water in a three-neck flask was placed in an oil bath at room temperature. Once the macromonomer was dissolved, then a solution of 0.1 g of APS in 10 g of DI water was directly added to the flask. Five minutes later, start drooping solution A (5 g AA, 30 g DI water, 0.1 g 3-mercaptopropionic acid) and solution B (0.08 g ascorbic acid and 20 g DI water) for 3 hours. After the addition was completed, continue the reaction for another 2 hours (total reaction time is 5 hours).

The pH of the PCE solution was adjusted to 4 using a 30 wt.% sodium hydroxide solution before preparing ion-pair complexes. This PCE solution was then stirred with Jeffamines (Jeffamine 2005 or Jeffamine 2070) at different molar ratios. The chemical structures of Jeffamine 2005 and Jeffamine 2070 are displayed in **Figure 25**, and the synthesis route is shown in **Figure 26**.



Jeffamine	PO/EO mol ratio	Mw
2005	29/6	2000
2070	10/31	2000

**Figure 25** Chemical structure of Jeffamine 2005 and Jeffamine 2070

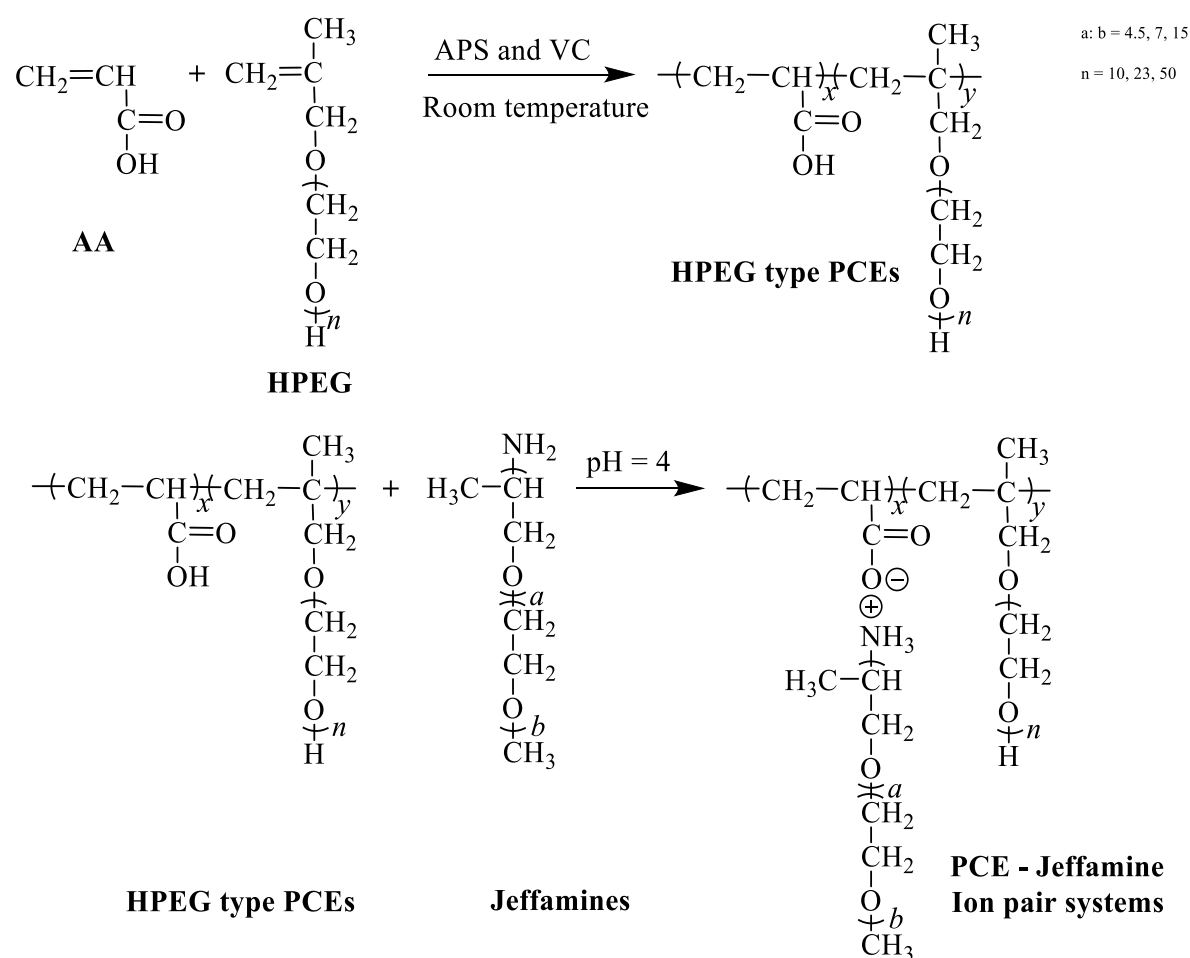


**Figure 26** Synthesis route for the ion-pair complexes

## 5.2.2 Characterization of PCE-Jeffamine ion-pair complexes

### 5.2.2.1 SEC Results

The molecular weights ( $M_n$ ,  $M_w$ ), polydispersity index (PDI) and conversion rate of 23HPEG7 PCE polymer were obtained via SEC and its SEC spectrum is shown in **Figure 27**. This PCE sample has relatively low PDI values (2.0) and high rates for macromonomer conversion (93 %), which are the characteristics of high-quality PCE superplasticizers (see **Table 10**).

**Table 10** Molecular weights, polydispersity index (PDI), and macromonomer conversion of the HPEG type PCEs.

Sample	$M_w$ [g/mol]	$M_n$ [g/mol]	PDI [ $M_w/M_n$ ]	Conversion rate [%]
23HPEG7	29,990	14,860	2.0	92.7

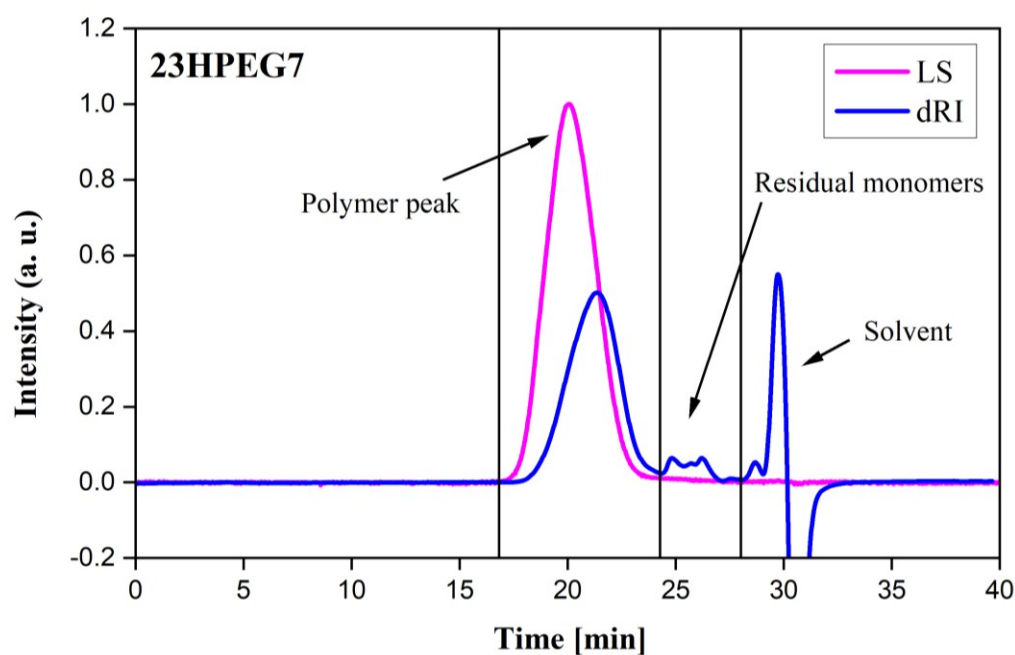


**Figure 27** SEC spectra of 23HPEG7 PCE

### 5.2.2.2 FT-IR

The PCE-Jeffamine ion-pair complexes were obtained by the ions reaction ( $-\text{COOH}$  and  $-\text{NH}_2$ ) in an aqueous solution at a specific pH. It can also be regarded as an ion-pair-induced self-assembly in an aqueous solvent with huge application potential [179]. FTIR instrument can be used to certify ion-pair formation and dissociation at different pH [180].

The FT-IR spectra of 23HPEG7, Jeffamine polymers (2005 or 2070) and their mixtures at different pH are shown in **Figure 28**. In the spectrum of 23HPEG7, the characteristic bands at  $1714\text{ cm}^{-1}$  and  $1638\text{ cm}^{-1}$  correspond to the stretching vibration band of  $-\text{C}=\text{O}$  derived from  $-\text{COOH}$  groups in the main chain. The bands that appear at  $2918\text{ cm}^{-1}$  and  $2874\text{ cm}^{-1}$  are the  $-\text{CH}_3$  and  $-\text{CH}_2$  respectively. The broad band appearing at  $3400\text{ cm}^{-1}$  is assigned to the stretching vibration band of  $-\text{OH}$  in  $-\text{COOH}$  groups. This band in both 23HPEG7-Jeffamine 2005 and 23HPEG7-Jeffamine 2070 ion-pair systems disappeared at the pH of 4.

Considering the cement pore solution has a pH of  $\sim 12$ , the pH of 23HPEG7-Jeffamine 2005 and 23HPEG7-Jeffamine 2070 polymers was readjusted to 12 to simulate the practical application. The band of the  $-\text{OH}$  group at  $3400\text{ cm}^{-1}$  reappeared (see **Figure 28**, purple lines). Another research related to alanine also certificated these intermolecular hydrogen bonds between the  $\text{NH}_3^+$  and  $\text{COO}^-$  groups, which are predominant in the zwitterionic form, and this zwitterionic form disappears in the higher pH [181].

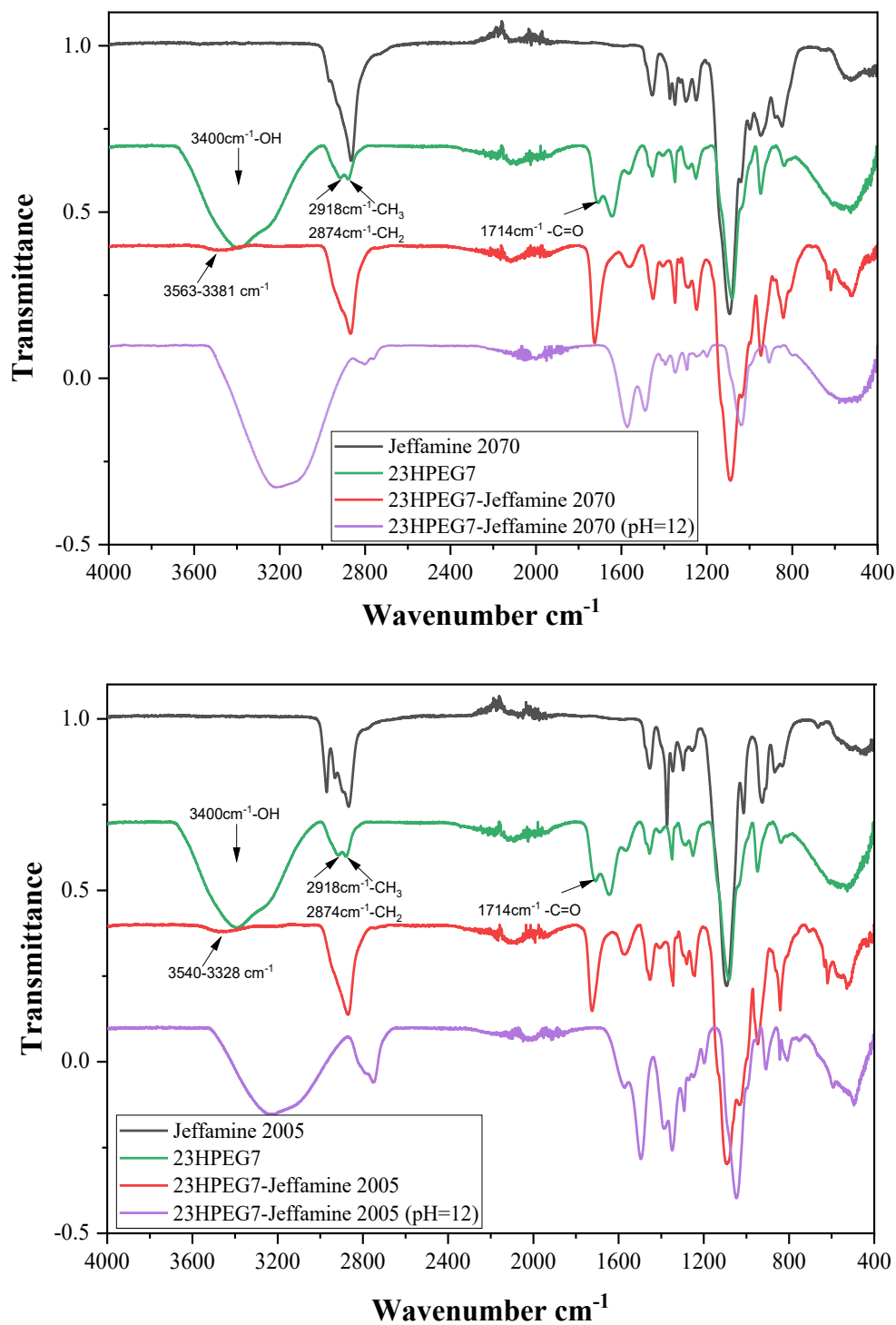


**Figure 28** FT-IR spectra of 23HPEG7 PCE and ion-pair systems at different pH

### 5.2.2.3 <sup>1</sup>H NMR

The structures of 23HPEG7-Jeffamine ion-pair complexes were further investigated by <sup>1</sup>H

## Results and discussion

NMR spectroscopy (see **Figure 29**). The typical proton peaks in 23HPEG7 polymer have been marked. The larger peak at 3.6 ppm stemmed from the characteristic ethylene oxide repeating units. The signals at 0.7 - 0.9 ppm and 2.3 - 2.5 ppm belong to the  $-\text{CH}_3$  group and the  $-\text{CH}$  in the backbone, respectively. Moreover, the protons in the  $-\text{CH}_2$  group of both AA and HPEG monomer in the backbone appeared at 1.6 - 2.0 ppm, and the proton peaks at 2.6 ppm, 3.5 ppm, and 3.8 ppm correspond to the  $-\text{CH}_2$  group adjacent to the ethylene oxide repeat unit in the side chains. These peaks indicate the successful synthesis of 23HPEG7 polymer by the free radical copolymerization method. Furthermore, two new peaks at 1.1 ppm and 3.3, which were assigned to the  $-\text{CH}_3$  in the PO units and the terminal groups of Jeffamines, now appeared in the  $^1\text{H}$  NMR spectra of the mixture (23HPEG7-Jeffamine 2005 and 23HPEG7-Jeffamine 20070), further certificate the formation of 23HPEG7 and Jeffamine ion-pair complexes.

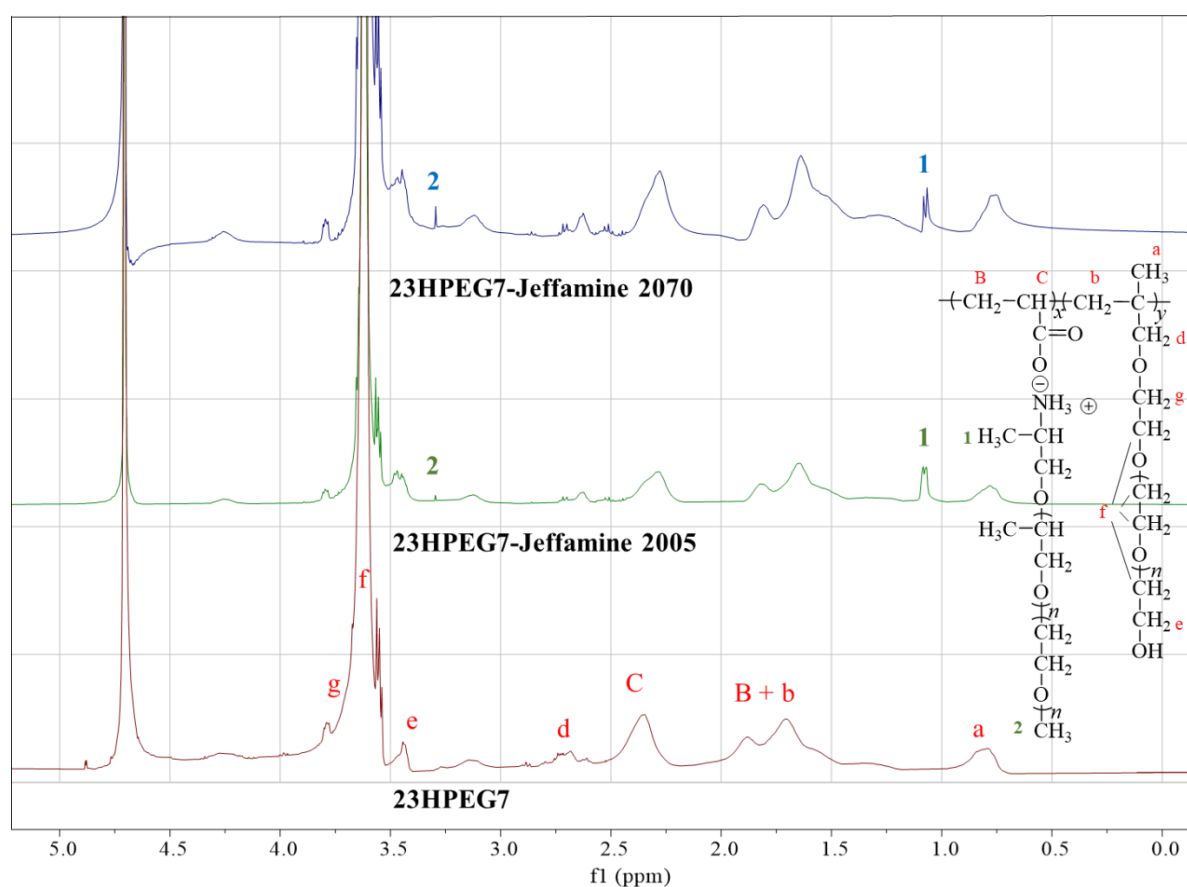


**Figure 29**  $^1\text{H}$  NMR spectra of the 23HPEG7 PCE and ion-pair systems

### 5.2.3 Phase separation test of PCE-Jeffamine ion-pair complexes

The product stability of the PCE and defoamer combinations is claimed to be up to one year under normal storage conditions according to industry requirements. In order to simulate the aging process, the ion-pair complexes and a conventional PCE-defoamer system were placed in a climate chamber and aged for 5 days under 0, 22 and 50 °C, respectively. The phase separation can be recognized by the eyes.

As shown in **Table 11**, no phase separation was observed in both 23HPEG7-Jeffamine 2005 and 23HPEG7-Jeffamine 2070 complexes over a wide temperature range, while the hydrophilic 23HPEG PCE separated with the hydrophobic Dow21A defoamer in the solution after 5 days aging test at each temperature. These results state the superiority of ion-pair complexes compared to the conventional defoaming system, and the ion-pair ensures the PCEs-Jeffamine defoaming complexes have good stability during storage, transport, and application stages.

**Table 11** The phase separation test of the ion-pair defoamers

Samples	Temperature/ °C	23HPEG7-Jeffamine 2005	23HPEG7-Jeffamine 2070	23HPEG7-Dow21A
Phase separation	0	no	no	yes
	22	no	no	yes
	50	no	no	yes

### 5.2.4 Foaming behavior of PCE-Jeffamine ion-pair complexes

#### 5.2.4.1 Defoaming activity and defoaming durability of ion-pair complexes

The foaming behavior of ion-pair systems was measured in an aqueous solution with a concentration of 10 g/L. For the defoaming activity in an aqueous solution, there is no obvious difference between 23HPEG7 PCE and 23HPEG7-Jeffamine ion-pair complex (see **Table 12**). Concerning the defoaming durability, as shown in **Table 12**, both 23HPEG7-Jeffamine 2005 and 23HPEG7-Jeffamine 2070 ion-pair complexes manifest longer defoaming durability than 23HPEG7 (> 30 times vs. 12 times). Therefore, the defoaming activity of Jeffamines could not be fully displayed when connected with the

PCE polymers in solution; in contrast, the defoaming durability was slightly affected by the ion-pair structure.

**Table 12** Defoaming activity and durability of ion-pair systems

PCE samples	Defoaming activity [s]	Defoaming durability
23HPEG7	16	12
23HPEG7-Jeffamine 2005	13	> 30
23HPEG7-Jeffamine 2070	14	> 30

#### 5.2.4.2 Foam stability of ion-pair systems

The foam stability of ion-pair complexes and 23HPEG7 PCE was tested in a solution, as shown in **Figure 30**. In terms of the initial bubble volume, pure 23HPEG7 PCE entrained the most air voids, followed by 23HPEG7-Jeffamine 2070, and 23HPEG7-Jeffamine 2005. Regarding foam stability, most of the bubbles in pure PCE and PCE-Jeffamine ion-pair solutions burst within one minute.

Obviously, the initial bubble volume is closely related to the hydrophilic/hydrophobic properties of the side chains of polymers, because it can directly change the stability of the water lamellar. In 23HPEG7 polymer, the polyethylene glycol ether (PEG) side chains just contain the hydrophilic EO units, which can fully stretch in the water lamellar, helping maintain the stability of the foams. After connecting 23HPEG7 with the Jeffamines through the ion-pairs, hydrophobic PO units and hydrophilic EO units with different ratios in the side chains were introduced. It is the hydrophobic PO unit, causing inhomogeneous surface tension of the water lamellar, disturbing the foam stability. That explained why 23HPEG7-Jeffamine 2070 and 23HPEG7-Jeffamine 2005 systems entrained less air than 23HPEG7 PCE. Further, Jeffamine 2005 is more hydrophobic than Jeffamine 2070, 23HPEG7-Jeffamine 2005 entrained the least initial bubble volume. For this reason, it is conceivable that introducing hydrophobic chains or segments in PCEs helps reduce the initial bubble volume [182].

In addition, the bubbles in 23HPEG7-Jeffamine 2070 and 23HPEG7-Jeffamine 2005

ion-pair systems burst faster than pure 23HPEG7 solution, and the final air voids in both is similar. The defoaming properties of different ion-pair systems were tested in mortar to certify the application of ion-pair system in cementitious materials.

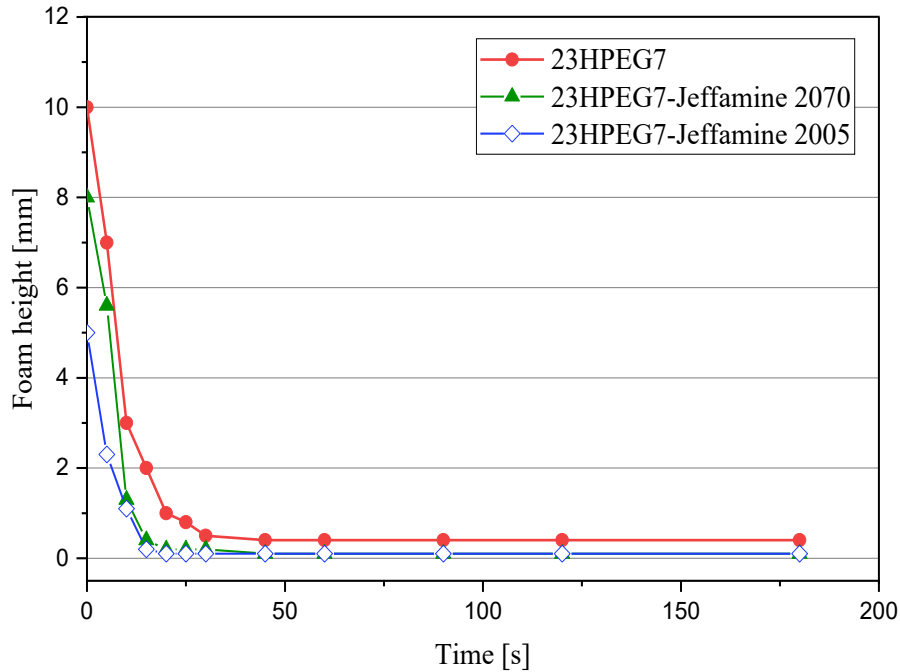


**Figure 30** Foaming behavior of pure 23HPEG7 PCE and ion-pair systems in an aqueous solution

#### 5.2.4.3 Defoaming effectiveness of ion-pair systems in mortar

The dosages needed for 23HPEG7 PCE polymer and ion-pair complexes to achieve a  $20 \pm 0.5$  cm mortar spread flow at a water-to-cement ratio of 0.4 are illustrated in **Figure 31**. It is observed that higher PCE dosages are necessary for ion-pair complexes (0.36 % bwoc) to achieve the same spread flow as 23HPEG7 (0.32 % bwoc).

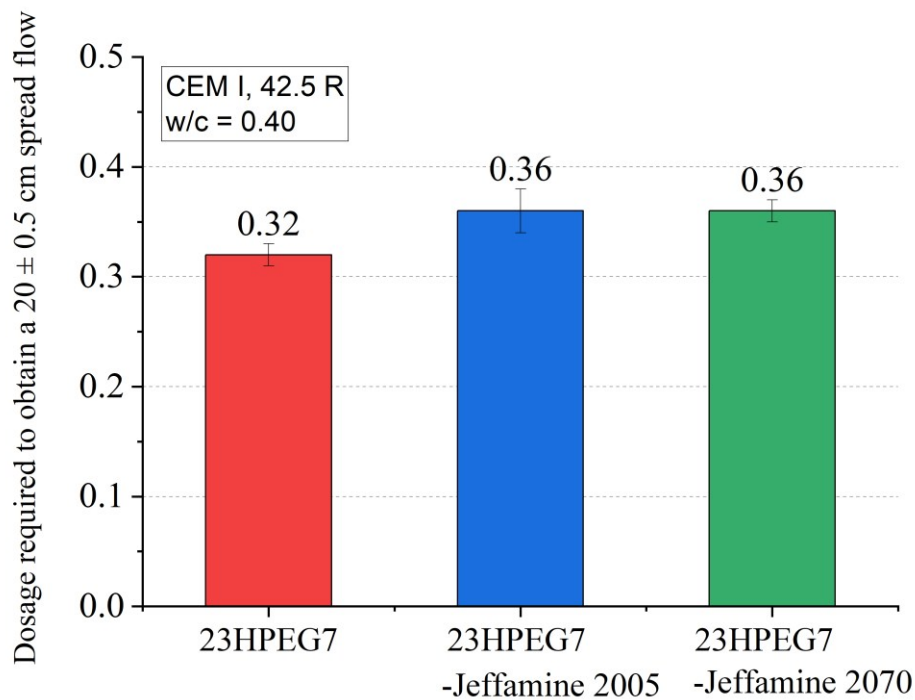


**Figure 31** Dosages required for 23HPEG7, 23HPEG7-jeffamine2005, 23HPEG7-Jeffamine2070 polymers to reach a spread flow of  $20 \pm 0.5$  cm

Regarding to the air voids in mortar, the reference mortar without any PCE contained 3.2 vol.% air voids. This value is comparable to the results of other research [167, 183]. As shown in **Figure 32**, Both pure 23HPEG7 PCE and the PCE-Jeffamine complexes introduced more air compared to the reference mortar. Mortars admixed with 23HPEG7 PCE have an air void of 18.8 vol.%, while the air voids of mortars added PCE-Jeffamine complexes are relatively low (4.6 - 5.1 vol.%). For PCE superplasticizers, it's the nature of surfactants leads to undesirable higher air voids [94], and the air-entraining ability of PCE polymer is chemical structure dependent. Qu reported that PCEs with higher side chain density and longer side chain length introduced less air [178]. For this reason, it can be considered that the anionic groups in the backbone stabilize the foam as it prevents the thinning of the water lamellar

Most mortars can achieve an air volume that is similar to the reference when mixed

with the PCE-Jeffamine complexes. On the one hand,  $-NH_2$  groups react with  $-COOH$  groups, destroying the stabilization effect of anionic for the water lamellar; on the other hand, the PO units cause inhomogeneous surface tension, accelerating the bubble to burst. Considering the influence of different Jeffamines on defoaming performance, it can be found that the ion-pairs complexes containing Jeffamine 2005 show slightly stronger defoaming performance than that containing Jeffamine 2070 at the same dosage. This result is inconsistent with the results tested in an aqueous solution. In addition, the ion-pairs show great defoaming effectiveness when the Jeffamine / PCE ratio was 0.1: 1, further increasing the Jeffamine content just has limited help in decreasing the air voids. Hence, it is a simple and practical method to obtain an efficient defoaming effect by introducing a small amount of Jeffamines to conventional HPEG-type PCEs.

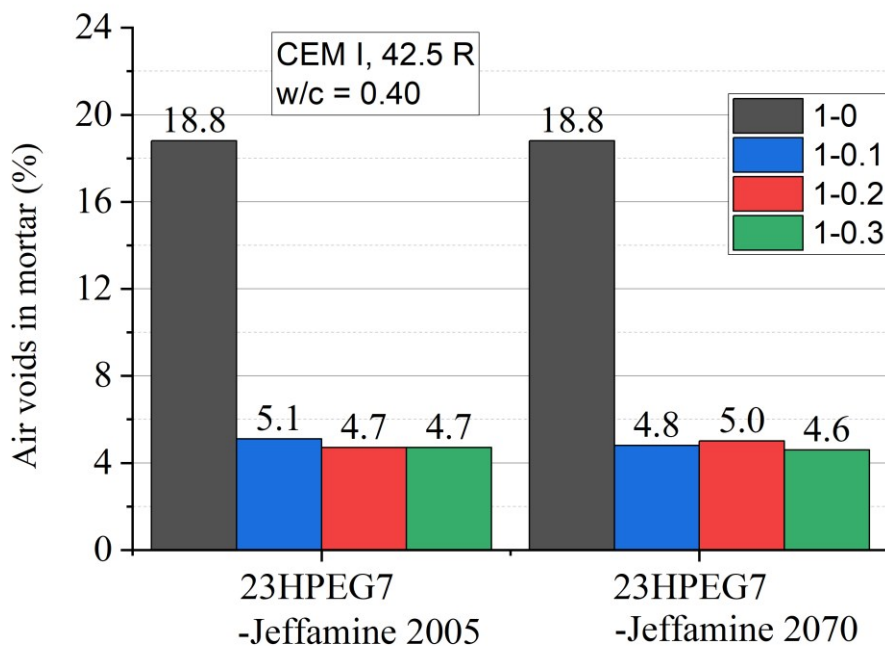


**Figure 32** Air voids in mortar when mixed 23HPEG7, 23HPEG7-jeffamine2005, 23HPEG7-Jeffamine2070 polymers

### 5.2.5 Dispersing effectiveness of ion-pair complex

As we all know, adding defoamer to the mixture will decrease the mortar fluidity because of the decreasing floatation force from the air, which leads to the settling and segregation of cement particles [82]. The fluidity of fresh mortar admixed with PCE-Jeffamine complexes is displayed in **Figure 33**.

PCEs-Jeffamine 2070 ion-pair complexes cause less reduction in dispersing ability than PCEs-Jeffamine 2005 complexes when the Jeffamine / PCE ratio was 0.1: 1. Therefore, the Jeffamine chain also plays an important role in the dispersing performance of the complexes, especially the hydrophilic Jeffamine 2070, which releases more free water and proves steric effect, can compensate for the fluidity loss from reducing air bubbles in some cases. Further increasing the Jeffamine content, PCEs-Jeffamine 2005 resulted in a slightly smaller mortar spread flow as the Jeffamine 2005 has stronger defoaming performance.

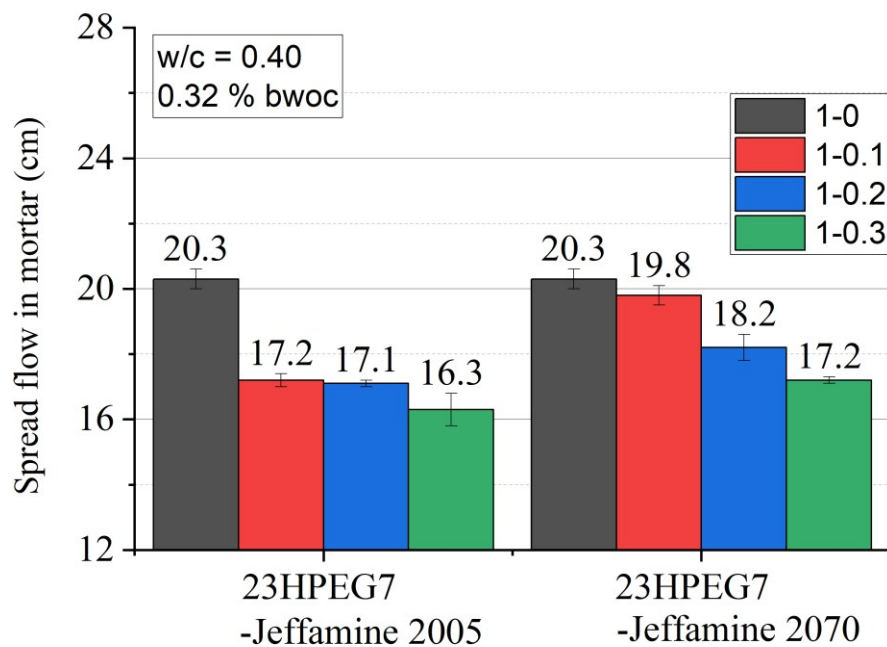


**Figure 33** Spread flow of mortars admixed with different PCE polymers

These complexes' HLB values and surface tension values were investigated to explain the different dispersing and defoaming performances between Jeffamine 2005 and Jeffamine 2070 (see **Table 13**). First, Jeffamine 2005 polymer with a higher PO proportion (PO/EO = 29/6), has an HLB value of 2.8, which means it is hydrophobic, while Jeffamine 2070 (PO/EO = 10/31) is more hydrophilic as its HLB value is 13.9. Then the hydrophilic/hydrophobic properties of Jeffamines affect the surface tension of these ion-pair complexes. The DI water has a surface tension of 71.4 N/m, close to the reference value [184]. After adding the 23HPEG7 polymer, the surface tension of the solution decreased to 48.8 N/m. Similar founding of MPEG PCE have been reported in another publication [185], and it is in accordance with the previous study of Pott et al. [172]. The ion-pair polymers further decreased the surface tension (34.2 N/m for 23HPEG7-Jeffamine 2005 complex and 40.9 N/m for 23HPEG7-Jeffamine 2070 complex), and hydrophobic Jeffamine 2005 contributed lower surface tension than hydrophilic Jeffamine 2070. Therefore, both Jeffamines can greatly reduce surface tension, then provide excellent deforming performance. The PO/EO ratio in Jeffamines has a great influence on the defoaming properties and leads to different dispersing effectiveness, but the optimal PO/EO ratio in Jeffamine to achieve excellent defoaming and dispersing properties is still not clear. Ma et al. also reported that the PO position and ratios remarkably affected the foam properties [186].

**Table 13** The surface tension of water, 23HPEG7 and ion-pair complexes

Ion-pair systems	Surface tension (N/m)	HLB values
Water	71.4	-
23HPEG7	48.8	-
23HPEG7-Jeffamine 2005	34.2	2.8 (Jeffamine 2005)
23HPEG7-Jeffamine 2070	40.9	13.9 (Jeffamine 2070)

### 5.2.6 Compressive strength of mortars

As different Jeffamines result in varying air voids and fluidity, they can alter the microstructure of fresh and hardened mortars, thereby affecting the mechanical

properties. In this part, the compressive strength of reference mortar and mortars admixing with 23HPEG7, 23HPEG7-Jeffamine 2005 and 23HPEG7-Jeffamine 2070 PCE polymers at curing times of 1 d, 3 d, 7 d and 28 d were investigated.

As shown in **Figure 34**, all the mortar strength increased with the aging time. The early strength (1 d) was reduced by the 23HPEG7 PCE, 23HPEG7-Jeffamine 2005 and 23HPEG7-Jeffamine 2070 complexes from 38.5 N/mm<sup>2</sup> to 30.2 N/mm<sup>2</sup>, 23.0 N/mm<sup>2</sup> and 23.8 N/mm<sup>2</sup>, respectively. When admixed with 23HPEG7 PCE, the compressive strength of standard mortars was reduced at different curing ages (1 d, 3 d, 7 d and 28 d); while the compressive strength with ion-pair complexes was improved a lot compared to 23HPEG7. In detail, the mortars containing ion-pair complexes have a similar compressive strength as the reference after 3 days of curing, the gain in 28 d strength achieved 11.1 % (23HPEG7-Jeffamine 2005) and 11.3 % (23HPEG7-Jeffamine 2070), respectively.

Comparing two Jeffamines, the mortars added 23HPEG7-Jeffamine 2070 have bigger compressive strength values than that with 23HPEG7-Jeffamine 2005 except at 1 day. Therefore, at the early stage, the hydrophilic Jeffamines 2070 did not improve the early strength even if it entrained less air, later it contributed to greater improvement in strength (even higher than reference) as it caused a denser microstructure as well as a good fluidity; the hydrophobic Jeffamines 2005 give a bigger compressive strength compared to 23HPEG7 PCE at whole curing stage because it causes a denser microstructure. Li et al. [187] also reported similar results that the defoamer agent enhances the development of strengths and volume density of hardened paste/mortar.

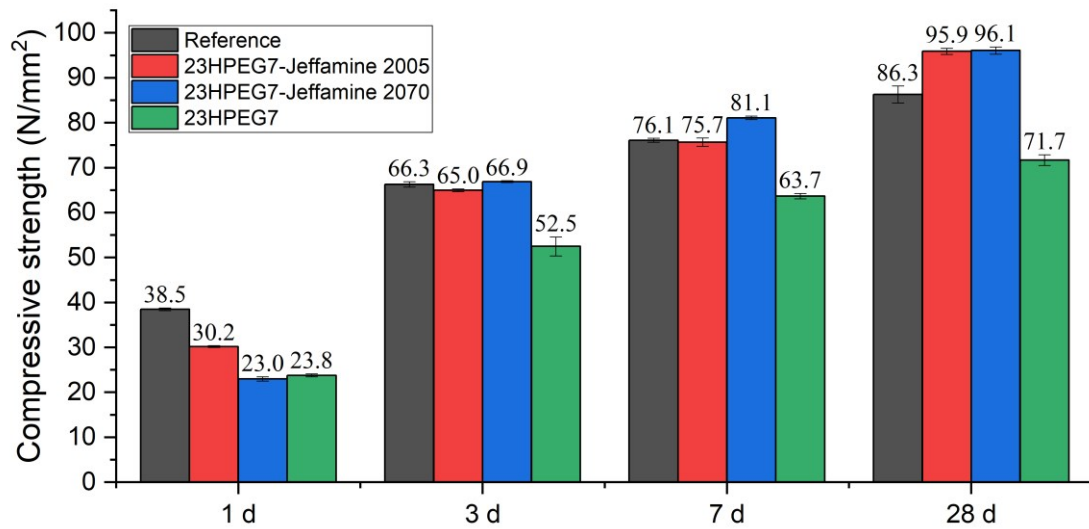


**Figure 34** Compressive strength of mortars admixed 23HPEG7 PCE and PCE-Jeffamine ion-pair complexes ( $w/c = 0.4$ )

### 5.2.7 Isothermal heat-flow calorimetry test of cement paste

The influence of ion-pair complexes on the cement hydration kinetic was captured via isothermal calorimetry (see **Figure 35** and **Figure 36**). The dosages for 23HPEG7 and ion-pair systems are the same (0.07 % bwoc), which is required to achieve a paste spread flow of  $26 \pm 0.5$  cm at a water-to-cement ratio of 0.5.

The 23HPEG7 PCE prolonged the induction period of cement hydration compared to the reference paste because of the retarding effect [188]. In detail, PCE adsorbed on the cement particle surface through the complexation between  $\text{COO}^-$  and  $\text{Ca}^{2+}$ , decreased the  $\text{Ca}^{2+}$  concentration in cement paste, and delayed the formation of the portlandite and C-S-H, which delayed the hydration process.

When adding the 23HPEG7-Jeffamines into the cement paste, the retarding effect is slightly reduced because the defoamer contributes to a denser structure, that helps the cement particles continue the hydration [189]. The hydrophobic Jeffamines 2005, which has stronger defoaming properties, performed better than Jeffamines 2070 in reducing retardation. But the retardation has not been eliminated as the 23HPEG7 and

Jeffamines dissociated under the alkaline conditions, so there is still some complexation of ions in the solution. another document found that the retardation effect of the PCEs on cement hydration is simply proportioned to their absolute adsorption amounts on the cement surface, while the complexation of the R-COO<sup>-</sup> group with Ca<sup>2+</sup>, which is independent of the PCE architectures, plays a minor role [190].

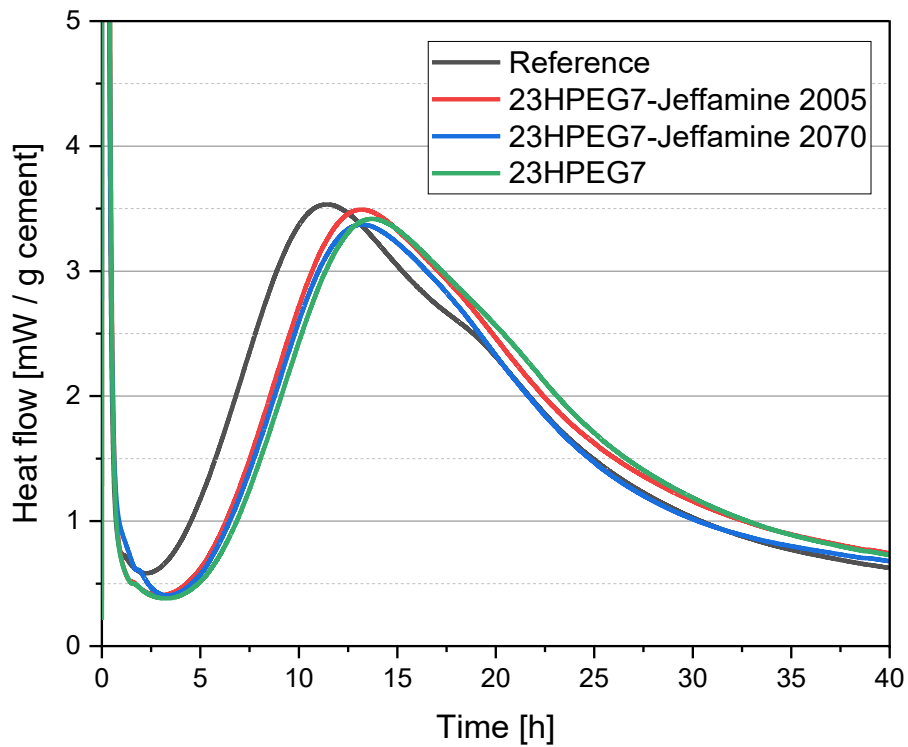


**Figure 35** Heat flow calorimetry of cement pastes admixed with PCE and ion-pair liquid (w/c ratio = 0.4)

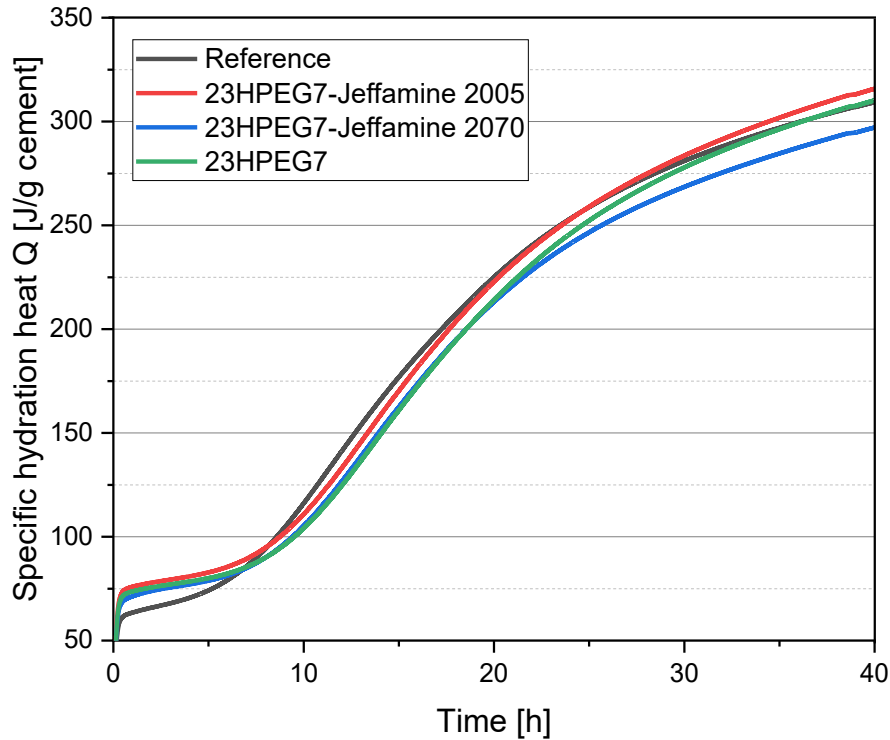


**Figure 36** Cumulative heat flow curves were recorded from cement pastes admixed with PCE and ion-pair liquid (w/c ratio = 0.4)

### 5.2.8 Q XRD

Quantitative X-ray diffraction analysis with 10 wt.%  $\text{Al}_3\text{O}_2$  as standard was used to monitor the consumption of the main reactant ( $\text{C}_3\text{S}$ ,  $\text{C}_2\text{S}$ ,  $\text{C}_3\text{A}$  and  $\text{C}_4\text{AF}$ ) and the formation of the crystalline hydration phase during the hydration process. As shown in **Figure 37**, the reflection intensity of hydration products portlandite increased over hydration time for all cement paste, while the reflections representing  $\text{C}_3\text{S}$ ,  $\text{C}_2\text{S}$ ,  $\text{C}_3\text{A}$  and  $\text{C}_4\text{AF}$  dropped over time.

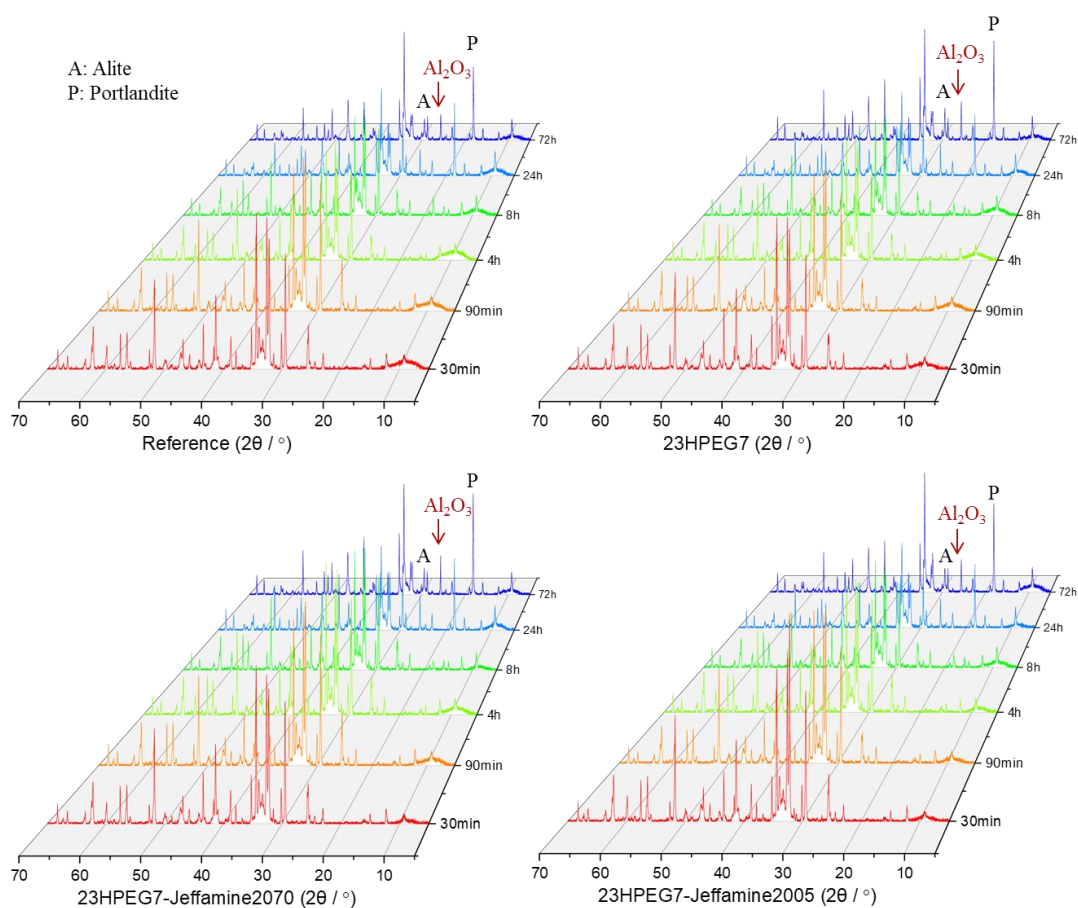


**Figure 37** X-ray diffractograms of cement paste admixed with or without 23HPEG7, 23HPEG7-Jeffamine 2005 and 23HPEG7-Jeffamine 2070 sample as a function of hydration time (the main reflection of alite and portlandite are marked)

Q-XRD measurement with 10 wt. %  $\text{Al}_2\text{O}_3$  as standard was applied to calculate the amounts of amorphous and other phases. The refinement quality is depicted in **Figure 38**. The close fit of the blue and red lines indicates a high-quality refinement. The Q-XRD results of some major phases are listed in **Table 14**, and plotted in **Figure 39**. The amount of unhydrated  $\text{C}_3\text{S}$ ,  $\text{C}_2\text{S}$  and the portlandite hydration product can reflect the hydration degree of cement to some extent [191]. The Rietveld calculations made on these diffraction patterns show that during the hydration of the cement paste, the amount of  $\text{C}_3\text{S}$ ,  $\text{C}_2\text{S}$ ,  $\text{C}_3\text{A}$  and  $\text{C}_4\text{AF}$  decreases, while the amounts of portlandite increases.

At the beginning, in the sample containing 23HPEG7, 23HPEG7-Jeffamine 2005 and 23HPEG7-Jeffamine 2070, there are more residual amounts of the reactant ( $C_3S$ ,  $C_2S$ ,  $C_3A$  and  $C_4AF$ ) and less portlandite product, that indicate the hindered hydration by the superplasticizer and the ion-pair defoamers. After 1 day, the main phase consumed more than the reference, but the amount of portlandite was less than the reference. Besides, there was the more amorphous phase in these samples, which has an irregular microstructure; consequently, the compressive strength was reduced.

Consider the influence of 23HPEG7 superplasticizer, 23HPEG7-Jeffamine 2005 and 23HPEG7-Jeffamine 2070 ion-pair defoamers on the hydration process. The hydrophilic 23HPEG7 and 23HPEG7-Jeffamine 2070 have a similar curve. They hindered the formation of portlandite at the initial stage, later the hydration was rapidly accelerated because of the sufficient dispersing. Hence, the compressive strength was greatly enhanced by 23HPEG7-Jeffamine 2070 as expected, whereas the mortar containing 23HPEG7 always had the lowest compressive strength because this superplasticizer entrained too much air. The hydrophobic 23HPEG7-Jeffamine 2005 shows a smaller hindrance to the formation of portlandite, and the improvement in the compressive strength is also limited.

Therefore, the ion-pair complexes with hydrophilic Jeffamine 2070 delay the hydration process at the beginning because of the hydrophilic and surfactant properties, later the hydration was rapidly accelerated due to the defoaming and dispersing effectiveness, which provides a denser microstructure and the good fluidity is good for the crystal growth, both enhanced the compressive strength; on the contrary, it is the 23HPEG7 not the hydrophobic 2070 in the complex delayed the initial hydration, and this complex accelerate the hydration later most rely on the denser microstructure giving by defoamer.

## Results and discussion

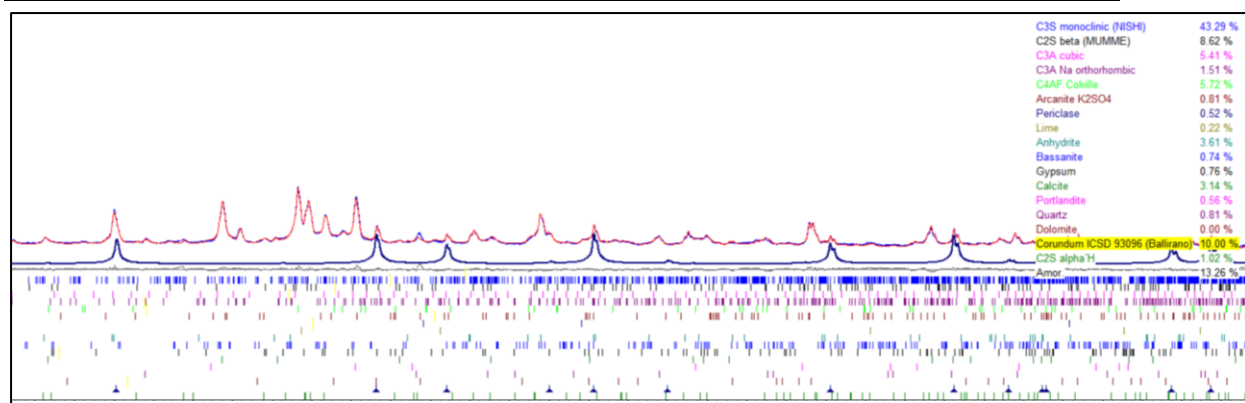


**Figure 38** Illustration of the refinement quality achieved with 10 wt. % Al<sub>2</sub>O<sub>3</sub> as the standard sample

**Table 14** Q XRD of mineral content (10% Al<sub>2</sub>O<sub>3</sub>)

Sample	Mineral content (wt. %)	90min	4h	8h	24h	72h
Reference	C <sub>3</sub> S	40.6	33.2	27.6	14.9	8.0
	C <sub>2</sub> S	6.8	4.6	4.7	5.0	3.4
	C <sub>3</sub> A	0.9	0.9	0.8	0.0	0.0
	C <sub>3</sub> A	2.0	1.5	1.5	1.1	0.6
	C <sub>4</sub> AF	10.9	9.4	8.7	7.4	5.1
23HPEG7	C <sub>3</sub> S	41.6	35.6	30.3	12.9	6.3
	C <sub>2</sub> S	5.4	5.0	4.1	3.2	3.1
	C <sub>3</sub> A	1.0	0.2	0.1	0.1	0.0
	C <sub>3</sub> A	2.2	1.9	1.8	1.0	0.3
	C <sub>4</sub> AF	11.1	9.6	9.4	5.5	3.8
23HPEG7- Jeffamine 2005	C <sub>3</sub> S	42.2	36.9	29.2	13.6	8.5
	C <sub>2</sub> S	5.9	3.8	3.7	3.4	3.6
	C <sub>3</sub> A	0.3	0.2	0.1	0.1	0.0
	C <sub>3</sub> A	2.6	2.5	1.9	1.2	0.2
	C <sub>4</sub> AF	9.7	8.0	8.0	6.1	5.2
23HPEG7- Jeffamine 2070	C <sub>3</sub> S	37.7	36.4	34.4	12.1	6.7
	C <sub>2</sub> S	4.9	4.2	4.1	3.3	3.1
	C <sub>3</sub> A	0.3	0.2	0.1	0.1	0.1
	C <sub>3</sub> A	2.6	2.2	2.4	0.7	0.3
	C <sub>4</sub> AF	9.3	8.9	8.6	5.2	3.7

## Results and discussion

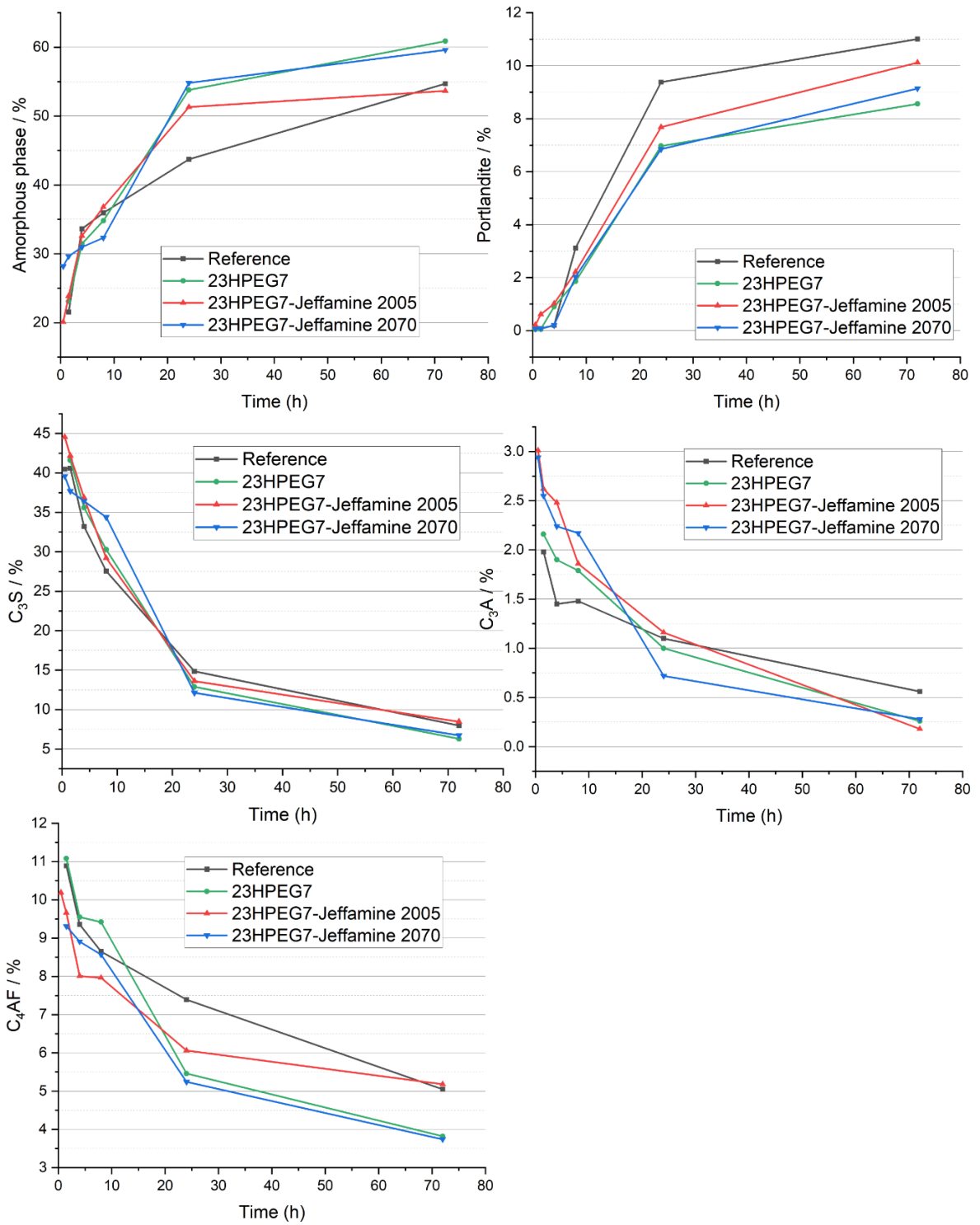


**Figure 39** Evolution of anhydrous and hydrated phase in cement paste admixed with 23HPEG7, 23HPEG7-Jeffamine 2005 and 23HPEG7-Jeffamine 2070 complexes

### 5.2.9 Summary of Section 5.2

The new PCE-Jeffamine ion-pair system was synthesized in this part to address the issues caused by the surfactant properties of HPEG-type PCE polymers in cementitious materials. The study confirmed the formation and dissociation of ion-pairs through FT-IR and  $^1\text{H}$  NMR spectroscopy. It also compared the foaming behavior and dispersing effectiveness of the ion-pair systems with the pure HPEG type PCE. Additionally, the study analyzed the influence of the ion-pair complexes on hydration kinetics using isothermal heat flow calorimetry and quantified X-Ray diffraction measurement. Based on the results, the following conclusions can be drawn:

1. Connecting Jeffamines to HPEG PCEs can provide additional defoaming properties for the superplasticizer, and the phase separation of this kind of polymer has also been confirmed.
2. In the PCE-Jeffamine complexes, the PO/EO ratio determines their defoaming and dispersing properties. The PO units are helpful for disrupting foam stability, while EO units dominate the dispersing performance.
3. All the 23HPEG PCE 23HPEG7-Jeffamine 2005 and 23HPEG7-Jeffamine 2070 ion-pair defoamers prolong the induction period in the cement hydration process.
4. Revealed calculations from the Q-XRD certificate show that the ion-pair complexes with hydrophilic Jeffamine 2070 delay the hydration process at the beginning due to their hydrophilic and surfactant properties; later, the hydration is rapidly accelerated due to the defoaming and dispersing effectiveness. In contrast, 23HPEG7-Jeffamine 2005 shows less hindrance on the portlandite formation, and the improvement in compressive strength is also limited.

### 5.3 Synthesis of HPEG-MAH PCE polymers

In this part, the maleic anhydride (MAH) monomer was selected as the backbone unit and copolymerized with HPEG macromonomer. MAH has a symmetrical structure caused by greater steric hindrance, so it has poor reactivity and is not prone to homopolymerization but copolymerization. Secondly, maleic anhydride monomer provides more  $-COOH$  groups in PCE, increases PCE's adsorption capacity and prolongs cement's setting time. Due to these particularities of maleic anhydride, the synthesis process is still difficult. A series of HPEG-MAH PCE polymers were synthesized via the free radical method with a redox initiator system; the research focuses on increasing the conversion rate of the macromonomer. The synthesis methods are introduced in the following:

#### 5.3.1 Synthesis of HPEG-MAH PCE via free radical copolymerization

##### HPEG-co-MA binary copolymerization

HPEG macromonomer, MAH monomer and DI water were first added to a four-neck flask, which was placed in an oil bath. Prepare solution A (APS and DI water), and solution B (VC and DI water). Solution A and solution B were pumped into the flask within 3.0 and 3.5 hours, respectively. Afterward, the reaction continued for another 2 hours. The pH of the copolymer solution was adjusted to 7 using 30 wt.% NaOH solution. The feeding amounts of monomers and initiators for each copolymer are listed in **Table 13**.

##### Ternary copolymerization

**Method-1:** HPEG macromonomer, MAH monomer, and DI water were first added to a four-neck flask, which was placed in an oil bath. Prepare solution A (5.5 g APS and 10.0 g water), and solution B (4.4 g VC, 20.0 g water and third comonomers). Solution A and solution B were pumped into the flask within 3.0 and 3.5 hours, respectively. Afterward, the reaction continued for another 2 hours. The pH of the copolymer solution was adjusted to 7 using 30 wt.% NaOH solution. The feeding amounts of

monomers and initiators for each copolymer are listed in **Table 15**.

**Method-2:** HPEG macromonomer, MAH monomer, and DI water were first added to a four-neck flask, which was placed in an oil bath. Prepare solution A (5.5 g APS and 10.0 g water), and solution B (4.4 g VC, 20.0 g water) and solution C (third comonomers and DI water). Solution A, solution B and solution C were pumped into the flask within 3.0 hours. Afterward, the reaction continued for another 2 hours. The pH value of the copolymer solution was adjusted to 7 using 30 wt.% NaOH solution. The feeding amounts of monomers and initiators for each copolymer are listed in **Table 15**.

**Table 15** The feeding amounts of monomers and initiators

Samples	HPEG g	MAH g	Third monomer g	APS g	VC g	Temperature °C
MAH-4	85.4	14.7		2.2	1.8	70
MAH-5	85.4	14.7		2.5	2.2	50
MAH-6	85.4	14.7		3.0	2.6	50
MAH-7	85.4	14.7		4.0	3.6	40
MAH-9	80.0	6.5		4.0	3.6	40
MAH-10	80.0	9.8		4.0	3.6	40
MAH-11	80.0	6.5		4.2	3.8	40
MAH-12	80.0	6.5		5.5	4.4	40
MAH2:1-1	80.0	6.5		3.0	2.4	40
MAH2:1-2	80.0	6.5		4.0	3.2	40
MAH2:1-3	80.0	6.5		5.5	4.4	40
MAH2:1-4	80.0	6.5		6.0	4.8	40
MAHEO7	77.7	21.8		5.5	4.4	40
MAHEO23	77.7	6.9		5.5	4.4	40
MAHEO45	80.0	3.3		5.5	4.4	40
MA-HPEG -AMPS	80.0	3.3	6.9	5.5	4.4	40
MA-HPEG -MAA	80.0	3.3	2.9	5.5	4.4	40
MA-HPEG -AMPS-2	80.0	3.3	6.9	5.5	4.4	40
MA-HPEG -MAA-2	80.0	3.3	2.9	5.5	4.4	40
MA-HPEG -MAA	80.0	6.5	1.4	5.5	4.4	40
MA-HPEG -MAA	80.0	6.5	0.7	5.5	4.4	40
70-MA-HPEG-MAA	80.0	6.5	1.4	6.5	0	70

### 5.3.2 HPEG-co-MAH copolymerization parameters

#### binary system: the influence of feeding molar ratio

The results in **Table 16** show the great influence of monomer feeding molar ratio on the conversion rate of HPEG macromonomers, which determines the quality of PCE polymers and their further performance in cement paste. The acid-to-ether (MAH:HPEG) ratios of 2:1 and 3:1 are suitable for obtaining high-quality MAH-co-HPEG copolymers. When the feeding ratio is 4.2:1, the actual acid/ether ratio is 8.4:1 because each MA monomer has two –COOH groups, it is too acid for the MAH and HPEG comonomers to copolymerization. When the feeding ratio is 1:1, the MAH monomer is not sufficient to achieve a high conversion rate. Therefore, the MAH:HPEG feeding ratio was determined at 2:1 in the following copolymerization experiments.

**Table 16** HPEG-co-MAH copolymers with different feeding molar ratios

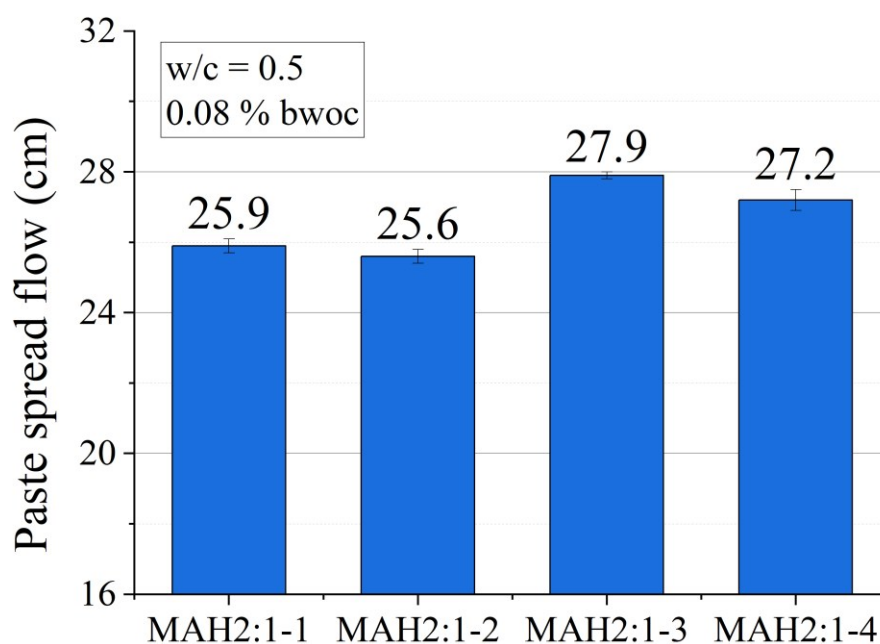
Samples	Conversion rate/ %	Solid content/ %	Mw [Da]	PDI	MAH:HPEG
MAH-7	77.4	40.9	22480	2.3	<b>4.2:1</b>
MAH-10	82.1	47.5	21940	2.4	<b>3:1</b>
MAH-9	87.2	46.2	29940	2.7	<b>2:1</b>
MAH-EO45	72.1	45.8	24420	2.4	<b>1:1</b>

#### The influence of APS-VC redox initiators amounts

It is worth noting that the chain transfer agent is not necessary for this MA-co-HPEG copolymerization, as both monomers have very low reactivity. The increasing number of APS-VC redox initiator systems resulted in a slight increase in conversion rate from 79.4 to 83.0 % (see **Table 17**). The molecular weight and PDI also increased; MAH2:1-3 and MAH2:1-4 PCE samples with higher  $M_w$  ( $\sim 30,000$ ) have better dispersing effectiveness in the mini-slump test (see **Figure 40**).

**Table 17** HPEG-co-MA copolymers with different initiator amounts

Samples	Conversion rate/ %	Solid content/ %	$M_w$ [Da]	PDI	MAH: HPEG	APS-VC g
MAH2:1-1	79.4	44.0	20030	2.1	2:1	<b>3-2.4</b>
MAH2:1-2	81.6	46.0	22920	2.2	2:1	<b>4-3.2</b>
MAH2:1-3	83.0	46.3	28210	2.3	2:1	<b>5.5-4.4</b>
MAH2:1-4	82.3	46.5	29960	2.4	2:1	<b>6-4.8</b>

**Figure 40** Mini slump test result of HPEG-co-MA copolymers with different initiator amounts

### The influence of macromonomers and copolymerization methods

In this part, MAH-co-HPEG copolymers obtained from bulk copolymerization were used as a reference, which required an MAH: HPEG feeding molar ratio of 1:1. When comparing these two synthesis methods, bulk copolymerization can provide PCE polymer with a higher molecular weight (see **Table 18**). However, the PCE copolymers (B-MAH EO10 and B-MAH EO23) obtained from bulk polymerization have very poor dispersing power in cement paste compared with those polymers (MAHEO7,

MAHEO23, MAHE45) obtained from free radical method (see **Figure 41**). It can be ascribed to the low conversion rate and wide molecular weight distribution of bulk copolymers, which means the bulk copolymerization method designed for MAH-APEG copolymer may not be suitable for the MAH-HPEG system.

When comparing different macromonomers, it is observed in both methods that HPEG macromonomers with smaller molecular weights contribute to higher conversion rates under the same conditions. Specifically, the conversion rate of MAHEO<sub>x</sub> copolymer increased from 72.1 to 90.2 % when replacing the HPEG monomer containing 45 EO units with 7 units. Nevertheless, HPEG macromonomers with smaller molecules provide poor steric hindrance, which also limits the dispersion ability of PCE copolymer.

**Table 18** HPEG-co-MA copolymers obtained from different synthesis methods

Samples	Conversion rate/ %	Solid content/ %	$M_w$ [Da]	PDI	MAH:HPEG
B-MAH EO10	70.6	34.0	1045000	14.0	1:1
B-MAH EO23	54.3	51.5	52910	5.6	1:1
MAHEO7	90.2	40.9	121000	10.6	1:1
MAHEO23	76.8	48.9	24130	2.8	1:1
MAHEO45	72.1	45.8	24420	2.4	1:1

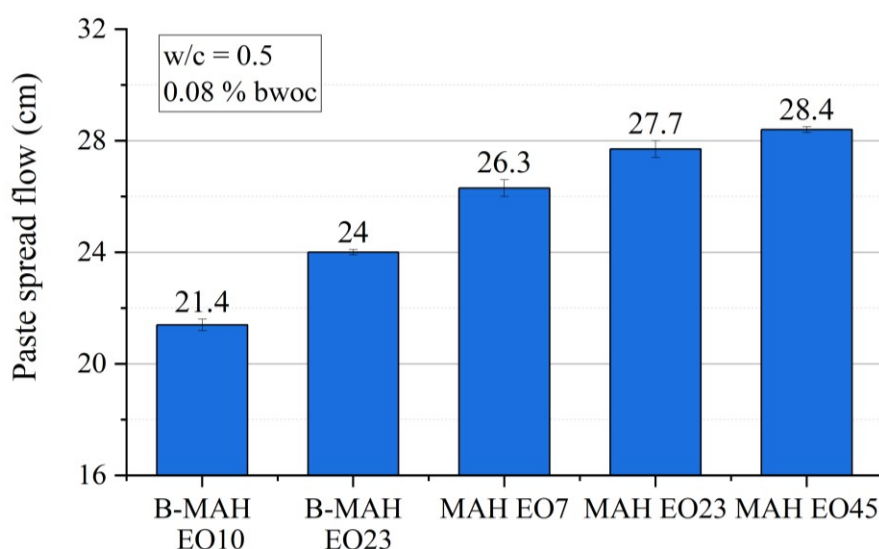


**Figure 41** Mini slump test result of HPEG-co-MA copolymers obtained from different synthesis methods

### 5.3.3 Ternary copolymerization system of MAH based PCE

In this part, Methacrylic acid (MAA) and 2-Acrylamido-2-methylpropane sulfonic acid (AMPS) monomers present relatively higher reactivity were choose to increase the conversion rate as third monomer to copolymerize with MAH and HPEG monomers respectively.

It can be seen from **Table 19** and **Figure 42** that MAA monomer contributed to a higher conversion rate and better dispersing effectiveness in cement paste than AMPS monomer. Again, MAH: HPEG: third monomer feeding molar ratio at 2:1:1 and 2:1:0.5 produced higher quality PCE than that at 1:1:1. Furthermore, the amount of third monomer also influenced the ternary copolymer's quality. In detail, the third comonomers are necessary to help generate free radicals more easily at the beginning of copolymerization in the ternary copolymerization system containing MAH and HPEG. However, too many third comonomers also consumed more free radicals and resulted in homo-polymerization, which also limited the conversion of HPEG macromonomers and influenced PCE quality. In addition, the 70-MA-HPEG-MAA PCE, which was synthesized at 70 °C initiated by the APS initiator, presents a lower conversion rate and worse dispersing effectiveness compared to MA-HPEG -MAA with the same feeding ratio of 2:1:1 (see **Figure 43**).

**Table 19** Ternary copolymerization system of MAH based PCE

Samples	Conversion rate/ %	Solid content/ %	$M_w$ [Da]	PDI	Feeding molar ratio
MA-HPEG -AMPS	70.1	49.7	29270	2.1	1:1:1
MA-HPEG -MAA	72.1	52.3	60750	3.3	1:1:1
MA-HPEG -AMPS-2	67.9	48.9	36520	2.2	1:1:1
MA-HPEG -MAA-2	70.4	48.2	47050	2.9	1:1:1
MA-HPEG -MAA	84.2	50.4	62100	4.2	2:1:1
MA-HPEG -MAA	83.6	55.6	52870	3.5	2:1:0.5
70-MA-HPEG-MAA	64.5	43.1	17500	2.2	2:1:1

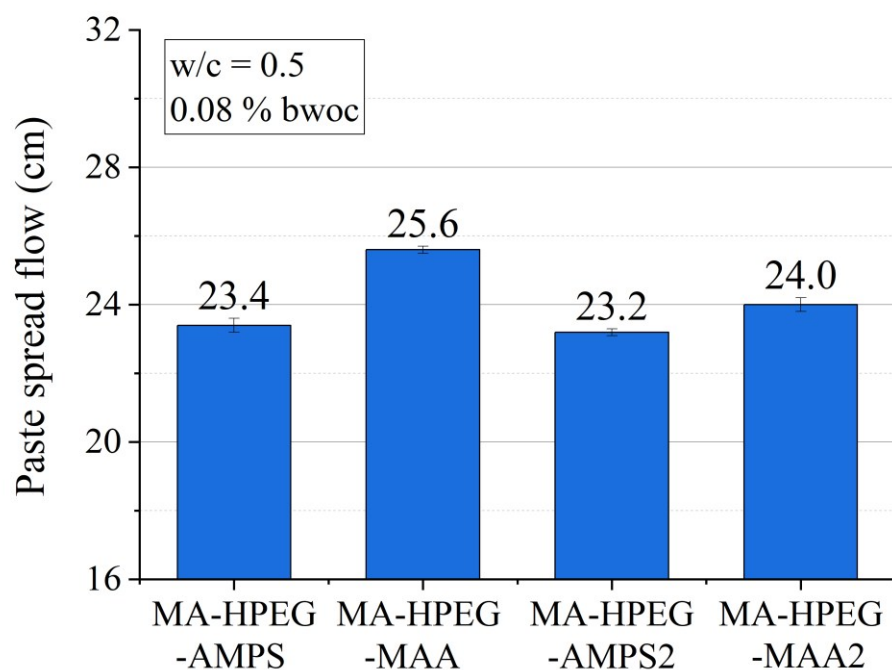


**Figure 42** Mini slump test result of copolymers obtained from ternary copolymerization system

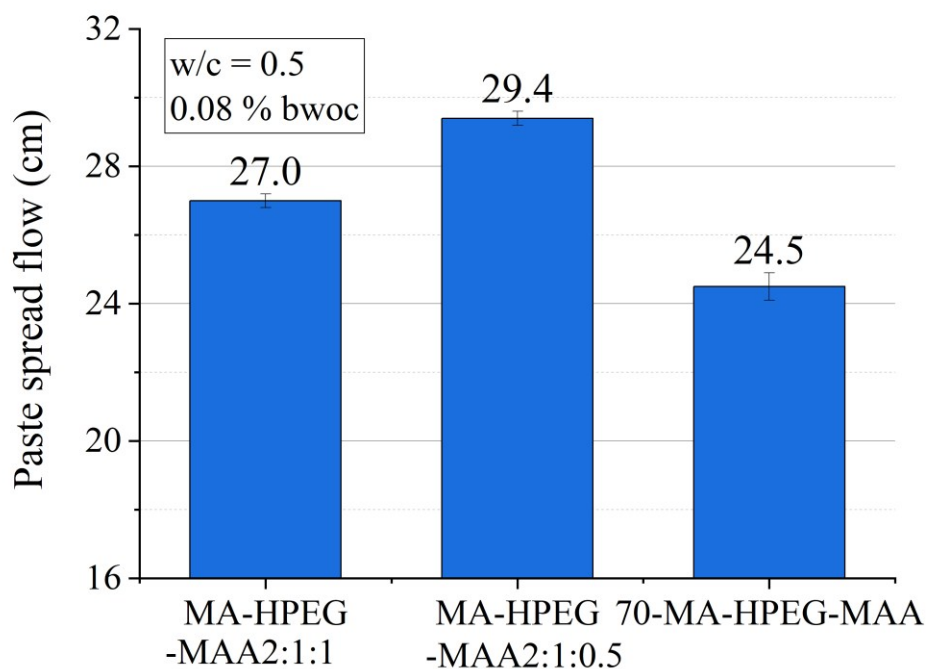


**Figure 43** Mini slump test result of copolymers obtained from ternary copolymerization system with different feeding molar ratios

#### 5.3.4 Summary of Section 5.3

In this section, the synthesis of MAH-co-HPEG PCE superplasticizers via the free radical method was investigated. There are limited reports on the binary copolymerization system of maleic anhydride and HPEG. This copolymerization is challenging because both monomers have low copolymerization reactivity. The results in this part show that the APS-VC redox initiator system can be used to polymerize MAH and HPEG without any chain transfer agent. This free radical polymerization method yields better PCE products than bulk polymerization. Moreover, it is discovered that the optimal MAH: HPEG monomer feeding ratio is 2:1 or 3:1. Using highly reactive HPEG monomer with low molecular weight can significantly improve the polymer conversion rate, but it limits the dispersion of the PCE superplasticizers. Additionally, the quality of PCE copolymers is closely related to their molecular weight distribution.

Introducing highly reactive MAA or AMPS monomer for terpolymerization enhances the conversion rate and dispersion performance to varying degrees. The best overall performance is observed when the monomer feeding ratio is 2:1:1 or 2:1:0.5. In the ternary system, controlling the amount of the third monomer is crucial to avoid self-polymerization or potential explosion.

## 5.4 Characterization and rheology of cementitious materials and their interaction with PCE polymers

The results in **Section 5.4.1** and **Section 5.4.2** relate to the Priority Program 2005 of the German Research Foundation (DFG SPP 2005), which was published in 2021 by Lin Zhang, Ran Li, Lei Lei and Johann Plank in the publication “Characterization data of reference industrial polycarboxylate superplasticizer VP 2020/15.2 used for Priority Program DFG SPP 2005 “Opus Fluidum Futurum - Rheology of reactive, multiscale, multiphase construction materials” of “Data in Brief” journal.

### 5.4.1 Characterization data of VP 2020/15.2 PCE polymer

A thorough characterization - including solid content, density, molecular properties, anionic charge and pH value - of one industrial ready-mix type PCE superplasticizer VP 2020/15.2 was conducted in this part.

#### 5.4.1.1 Physical and chemical properties

The chemical structure of this PCE is illustrated in **Figure 44**, it composites about 65 ethylene oxide units in the side chain. The SEC spectrum in **Figure 45** containing polymer peak, residual monomer peaks and solvent peak. The information listed in **Table 20** show that this PCE exhibits a relatively high macromonomer conversion rate and low polydispersity index (PDI), which are characteristics of high-quality PCE superplasticizer.

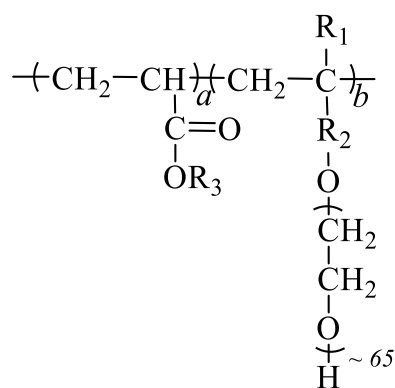


**Figure 44.** Chemical structure of the industrial PCE sample VP 2020/15.2

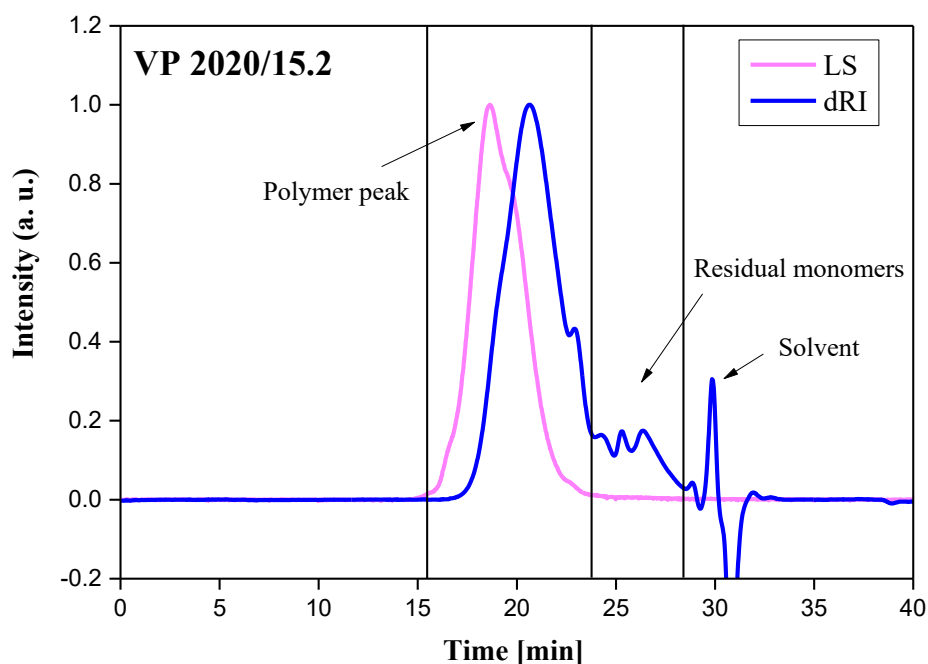


**Figure 45** SEC spectrum of VP 2020/15.2; eluent: 0.1 M NaNO<sub>3</sub>

**Table 20** Solid content, density, molecular weights, polydispersity index (PDI), macromonomer conversion and pH value of the industrial PCE sample VP 2020/15.2.

PCE	Solid content [wt.%]	Density [kg/L]	$M_w$ [g/mol]	$M_n$ [g/mol]	PDI	Macromonomer Conversion [%]	pH
VP 2020/15.2	20.5	1.01	78,100	28,560	2.7	86.1	5.6

#### 5.4.1.2 Anionic charge property

The specific anionic charge density of VP 2020/15.2 PCE sample are shown in **Figure 46** respectively. As expected, the charge density of PCEs in NaOH solution (1754  $\mu\text{eq/g}$ ) is notably higher than that in DI water (655  $\mu\text{eq/g}$ ). According to the titration mechanism, the anionic charges of PCEs are mainly contributed by the carboxylate groups in the polymer and highly rely on the pH value of the solution. Therefore, this

result can be ascribed to the deprotonation of the carboxylate groups in alkaline condition and it is consistent with the previous publication [79].

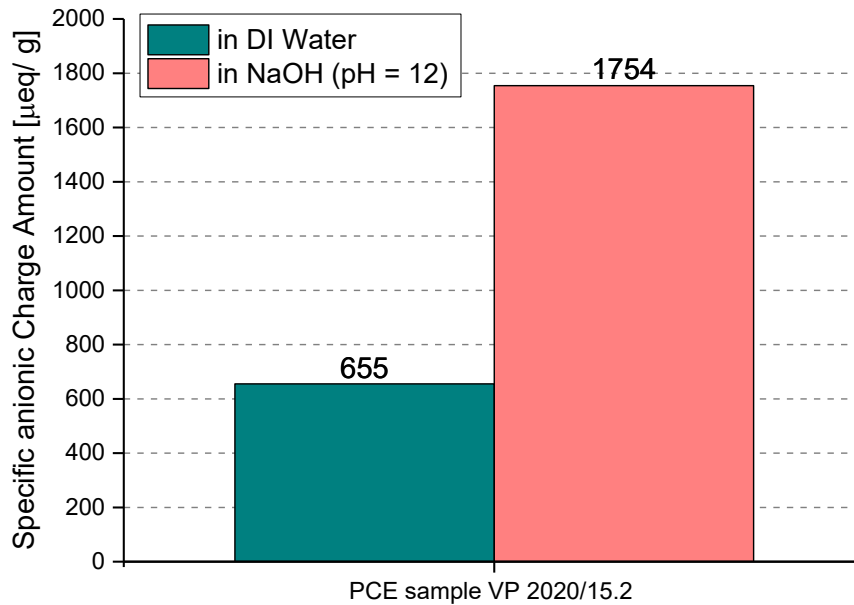


**Figure 46.** Specific anionic charge amount of PCE sample VP 2020/15.2

## 5.4.2 Interaction between PCE and cements

### 5.4.2.1 Dosage - dependent dispersing effect in OPC and LCC cement

The interaction between VP 2020/15.2 PCE and two types of cement CEM I 42.5 R and LCC cement was investigated in this part. The dispersing effectiveness of VP 2020/15.2 was first assessed in the paste at a water-to-cement ratio of 0.4.

The dosage-dependent dispersing capacity of VP 2020/15.2 in two cements is shown in **Figure 47**. The paste spread flow of CEM I 42.5 R and the LCC cements increased with increasing PCE dosages. The dosage of PCE required in LCC cement to reach maximum paste spread flow was around  $\sim 0.8$  % bwoc, while CEM I 42.5 R cement demand around 1.0 % bwoc of VP 2020/15.2 PCE.

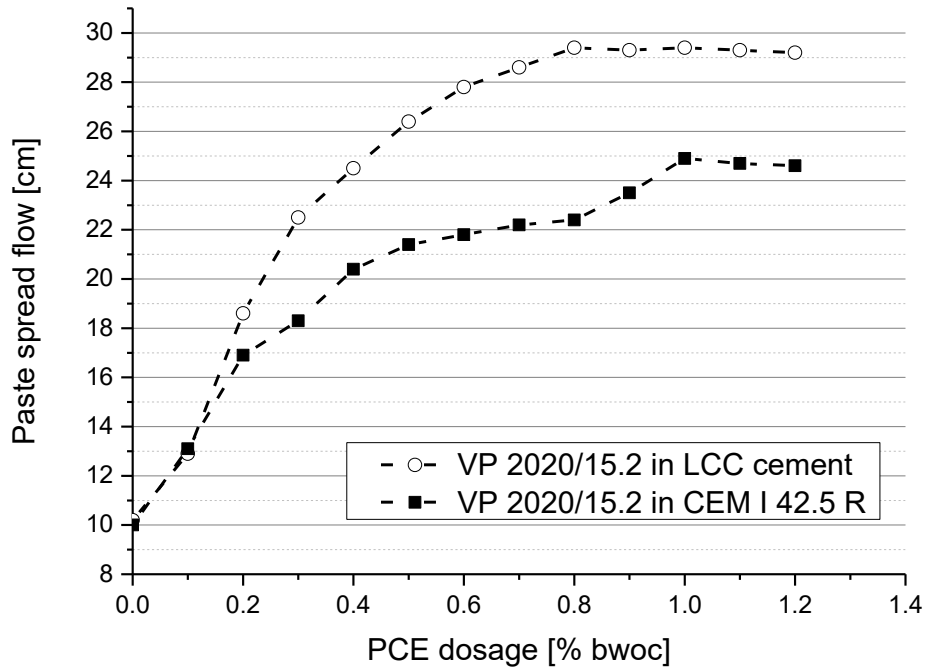


**Figure 47** Spread flow of PCE sample VP 2020/15.2 in CEM I 42.5 R and LCC cement pastes (w/c ratio = 0.4)

#### 5.4.2.2 Slump retention

Regarding the slump retention performance, the PCE dosages were varied to obtain the targeted initial spread flow of  $22 \text{ cm} \pm 0.5 \text{ cm}$  at water-to-cement ratio of 0.4. Specifically, the dosages required in CEM I 42.5 R cement was 0.7 % bwoc, while 0.3 % bwoc of VP 2020/15.2 PCE can provide the same spread flow in LCC cement, which means LCC cement is easier to disperse than OPC. As shown in **Figure 48**, the slump retention performances of VP 2020/15.2 PCE in LCC cement and CEM I 42.5 R cement were measured over 6 hours. Strongly delayed plastification was observed in both cement systems, and this phenomenon can be ascribed to the anionic charge density of the PCE sample at relatively high dosages.

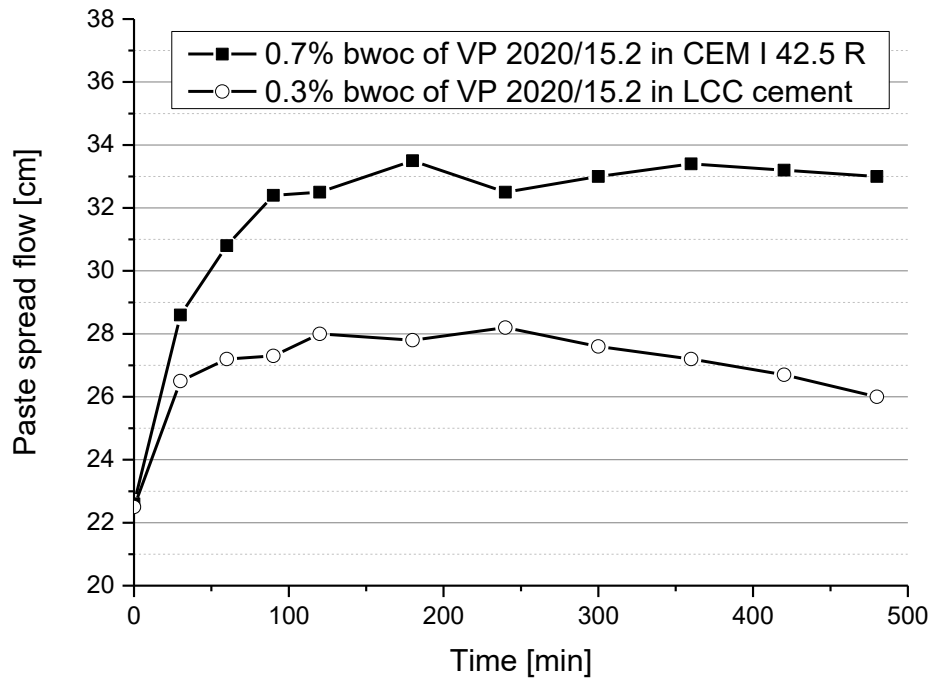


**Figure 48** Slump retention of VP 2020/15.2 PCE in CEM I 42.5 R and LCC cement pastes (w/c ratio = 0.4)

#### 5.4.2.3 Adsorption of PCE sample on CEM I 42.5 R and LCC cement

It is recognized that the adsorption behavior of superplasticizers is an important part contributing to the dispersion process [192]. Therefore, the dosage-dependent adsorption amounts of VP 2020/15.2 on both cements were measured to further explain its dispersing mechanism.

According to the adsorption mechanism, the cement particles are first negatively charged in paste, they may become positive later by adsorbing cations from the environment. This cationic layer allows the further adsorption of the superplasticizers' backbone containing  $\text{COO}^-$  groups, and also of the  $\text{SO}_4^{2-}$  ions present in solution [193, 194]. Research [195] about the thermodynamic parameters of the adsorption behavior demonstrated that PCE adsorption is energetically favorable and a spontaneous process. The driving force behind this is the gain in entropy, and the presence of  $\text{Ca}^{2+}$  ions in the pore solution strongly impacts PCE adsorption.

The TOC measurement result is displayed in **Figure 49**, less saturate adsorbed amount of VP 2020/15.2 PCE on CEM I 42.5 R than that on LCC cement was observed. This can be ascribed to their dissimilar mineral phrase composition, particle size, and surface charge, therefore different ion concentrations in cement pore solution.

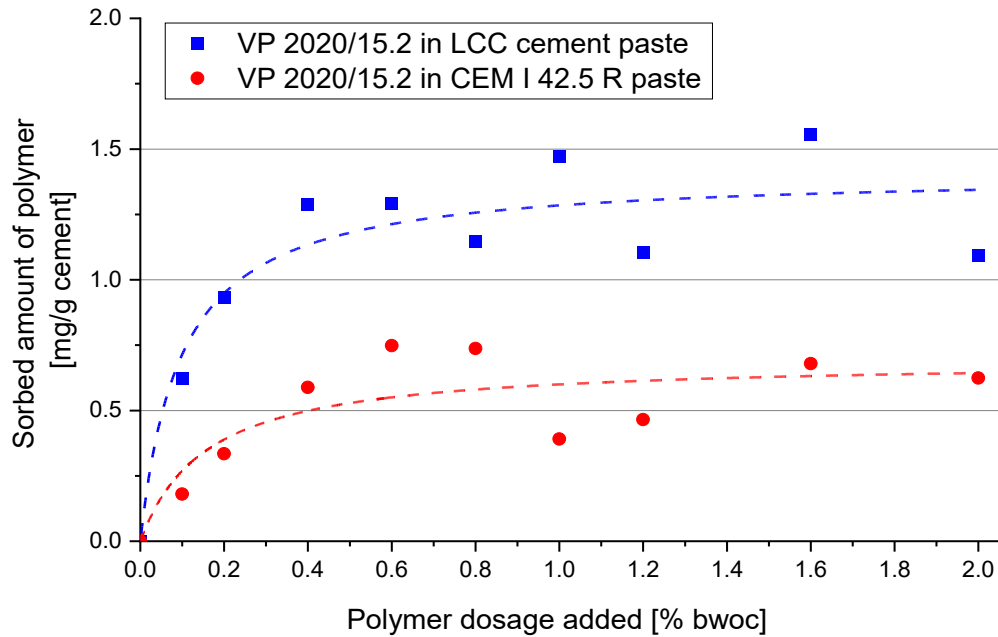


**Figure 49** Adsorption amount of VP 2020/15.2 PCE on CEM I 42.5 R and LCC cements

#### 5.4.2.4 Zeta potential of cement suspensions admixed with VP 2020/15.2

The zeta potential value of cement also affects the adsorption behavior. Here, a water-to-cement ratio of 0.5 was applied to achieve an 18 cm spread flow in both cements. As shown in **Figure 50**, LCC cement exhibits less negative initial zeta potential value (-4 mV), providing a more positive surface for further adsorption of superplasticizer molecules. With the addition of PCE polymer, the zeta potential values of both types of cement are towards less negative.

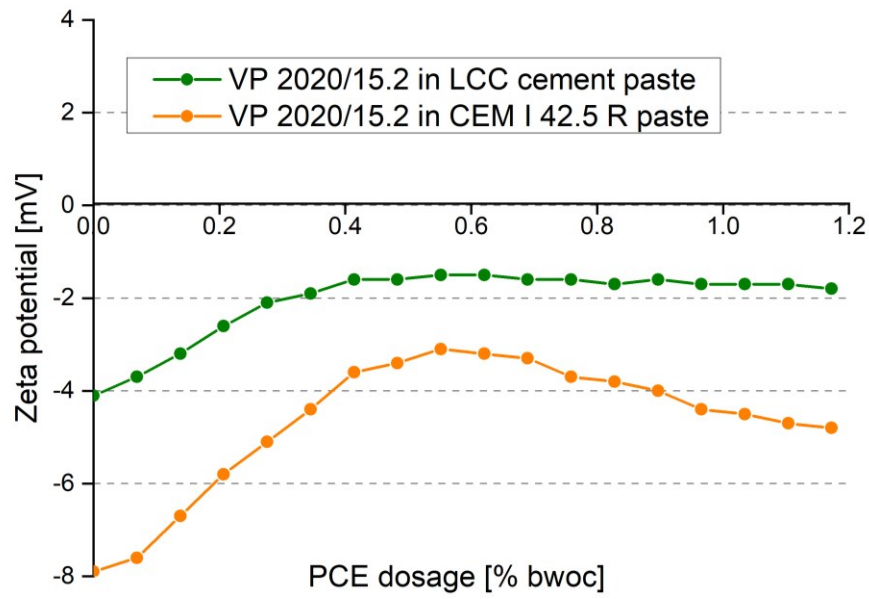


**Figure50** Dosage-dependent zeta potentials of CEM I 42.5 R and LCC cement pastes mixed with VP 2020/15.2 (w/c ratio = 0.5).

### 5.4.3 Phase composition and fluidity of composite cement CEM II/III

As mentioned before, the cement industry is transitioning from Ordinary Portland Cement (OPC) to low-carbon cement, for example composite cement. It is important to produce PCE superplasticizers that are suitable for this type of cement. Investigating the variation between composite cement and OPC is necessary to better understand which types of PCE will be optimal for this system. Here, one OPC cement CEM I 42.5 R from Schwenk cement company and three composite cements (CEM III/A 42.5 N and CEM III/B 42.5 N from Heidelberg; CEM II/A-LL 32.5 R from Schwenk Cement) were chosen for this study. Their physical properties including particle size, zeta potential values and pH values are listed in **Table 21**. The phase composition of these cement samples determined via Q-XRD, including Rietveld refinement, is shown in **Table 22**. Further, the particle sizes of these cements and cumulative value (red line) was confirmed by the laser granulometer (Cilas 1064, Cilas Company, Marseille, France) and shown in **Figure 51**. The OPC cement exhibits a  $d_{50}$  value of 20.25  $\mu\text{m}$ , while the  $d_{50}$  values of three types of composite cement are smaller (14.82  $\mu\text{m}$ , 9.32  $\mu\text{m}$ , and 15.78  $\mu\text{m}$ ), indicating that the composite cement contains finer particles.

The investigation was started by testing the initial spread flow in the mortar of OPC and three types of composite cement; the tests were conducted at a water-to-cement ratio of 0.4. It was observed that the fluidity of composite cement, specifically CEM II/A-LL 32.5R and CEM III/B 42.5N, was inferior to that of OPC (CEM I 42.5 R). This was evidenced by lower initial spread flows, as shown in **Table 21**. However, the CEM III/B 42.5 N cement displays a similar initial spread flow to OPC cement. The fluidity of cement paste is influenced by particle size and pH values. All three composite cements have smaller particle sizes, leading to increased surface area and higher water demand. The OPC paste has the highest pH value (13.1), releasing more ions into the pore solution. In contrast, the pH values of all composite cement are one order of magnitude lower (ranging from 11.8 to 12.0), with the CEM III/B 42.5 N cement sample having the lowest pH value (11.8). Additionally, less positive zeta potential values of composite cement are observed.

## Results and discussion

**Table 21** Physical properties of cement particles

Properties	CEM I 42.5 R	CEMIII/A 42.5 N	CEM III/B 42.5 N	CEM II/A-LL 32.5 R
Zeta potential (mV)	-12	-8	-3	-10
Particle size $d_{50}$ ( $\mu\text{m}$ )	20.25	14.82	9.32	15.78
pH value	13.1	12.0	11.8	12.0
Initial fluidity (cm)	14	14	12	13

**Table 22** Phase compositions of cement samples by means of Q-XRD analysis via *Rietveld* refinement

	CEM I 42.5 R	CEMIII/A 42.5 N	CEM III/B 42.5 N	CEM II/A-LL 32.5 R
Phase	wt. %	wt. %	wt. %	wt. %
C <sub>3</sub> S, monoclinic	<b>59.6</b>	<b>29.1</b>	<b>18.9</b>	<b>47.4</b>
C <sub>2</sub> S, monoclinic	11.1	7.1	2.7	13.4
C <sub>4</sub> AF, orthorhombic	<b>10.1</b>	<b>3.4</b>	<b>2.2</b>	<b>9.5</b>
C <sub>3</sub> A, cubic	4.9	1.7	0.7	3.4
C <sub>3</sub> A, orthorhombic	<b>2.1</b>	<b>3.5</b>	<b>1.7</b>	<b>2.5</b>
Anhydrite (CaSO <sub>4</sub> )	2.6	2.3	1.1	1.3
Dihydrate (CaSO <sub>4</sub> • 2H <sub>2</sub> O)	3.1	0.3	0.1	1.6
Hemihydrate (CaSO <sub>4</sub> • 0.5H <sub>2</sub> O)	0.1	2.0	1.3	0.5
Calcite (CaCO <sub>3</sub> )	<b>2.3</b>	<b>2.7</b>	<b>1.4</b>	<b>16.5</b>
Dolomite (CaMg(CO <sub>3</sub> ) <sub>2</sub> )	1.0	-	-	2.2
Arcanite (K <sub>2</sub> SO <sub>4</sub> )	0.2	0.6	0.5	-
Quartz (SiO <sub>2</sub> )	0.4	0.4	0.2	0.7
Free lime ( <i>Franke</i> )	0.7	0.8	0.2	0.4
Portlandite (Ca(OH) <sub>2</sub> )	0.8	-	0.6	-
Periclase (MgO)	0.5	-	0.2	0.6
Slag	-	<b>45.5</b>	<b>70.9</b>	-
Total	99.5	97.9	100.00	100.00

## Results and discussion

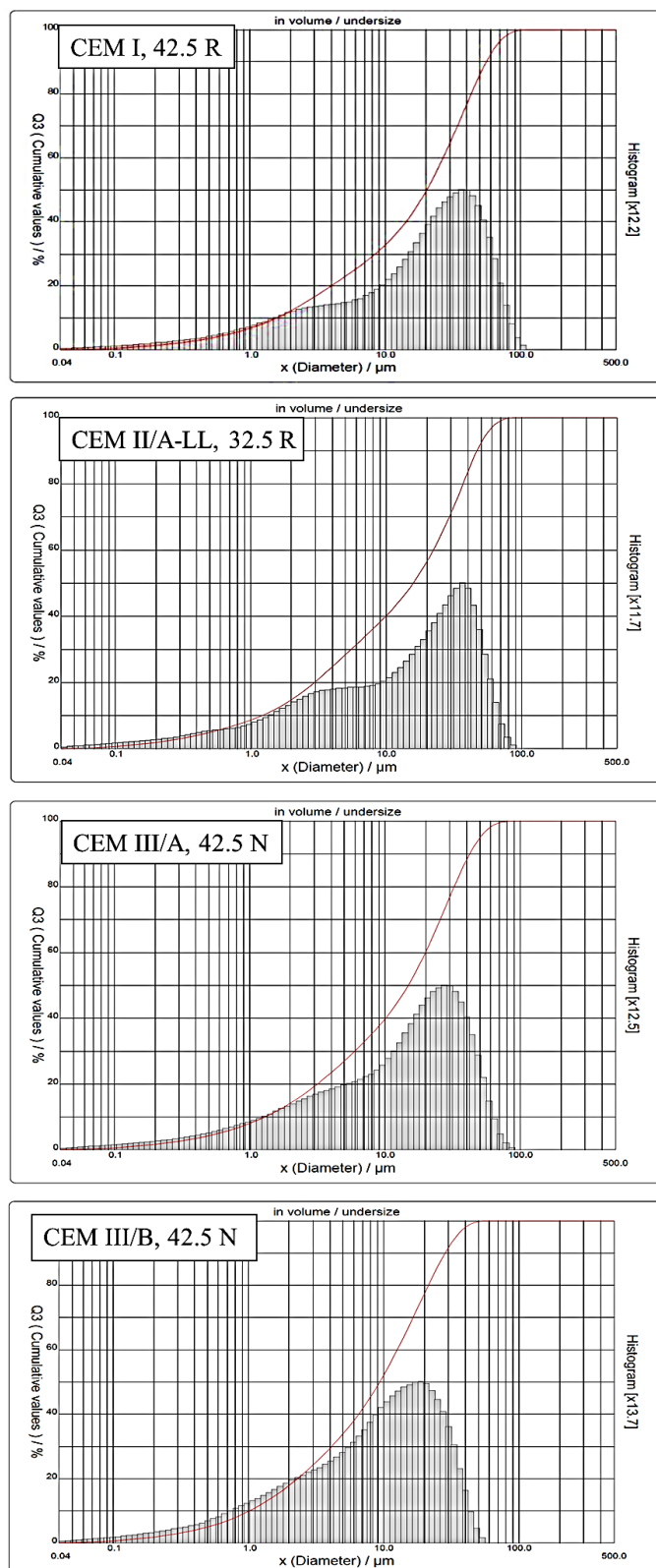


**Figure 51** Particle size distribution and cumulative value (red line) of CEM I, 42.5 R; CEM II/A-LL, 32.5 R; CEM III/A, 42.5 N and CEM III/B, 42.5 N cements

Furthermore, the pH values of all net cement pastes (OPC, CEM II/A-LL 32.5 R, CEM III/A 42.5 N and CEM III/B 42.5 N) obtained from zeta potential measurement over three hours were shown in **Figure 52**. All the composite cements have lower pH values than OPC, which is related to the lower alkali ions in blended systems [196, 197]. In the case of slag blended cement, the lower pH values of CEM III/A 42.5 N (12.0) and CEM III/B 42.5 N (11.8) are related to the reduced formation of sulphur species ( $\text{HS}^-$ ,  $\text{SO}_3^{2-}$ , and  $\text{S}_2\text{O}_3^{2-}$ ) [198, 199]. The pH values in the four cement systems increased with time; this can be attributed to the hydration of cement after contact with water, which promotes the dissolution of the precipitate to release more alkali ions [200, 201].

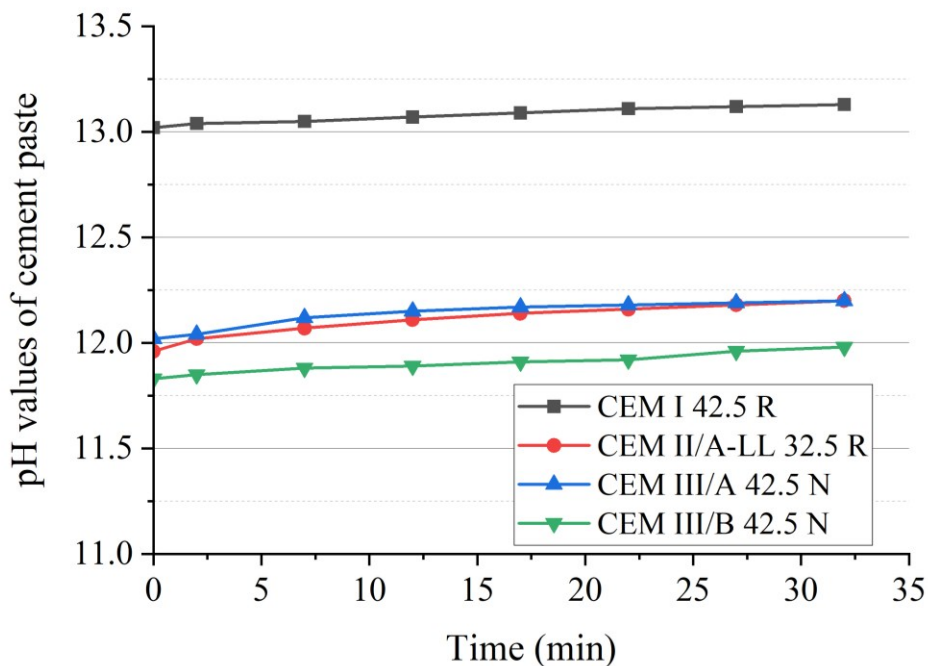


**Figure 52** Time dependent pH values of different cement pastes: CEM I 42.5 R; CEM II/A-LL 32.5 R; CEM III/A 42.5 N; CEM III/B 42.5 N

#### 5.4.4 Summary of Section 5.4

The low-carbon cement, such as LCC and composite cement, has lower carbon emissions and will be the future development direction of the cement industry. This chapter studied the interaction of VP 2020/15.2 PCE with LCC and OPC and characterized three composite cements. The results show that LCC and OPC have

different surface charges, which causes different adsorption behaviors of PCE on their surfaces, resulting in different dispersion and slump retention performances.

Three types of composite cement (CEM II/A-LL 32.5 R; CEM III/A 42.5 N and CEM III/B 42.5 N) have smaller particle sizes and lower pH values than OPC, making their initial fluidity worse than OPC. In addition, the surface charge of composite cement is also very different from OPC because of their distinct mineral phase composition, and they also contain large amounts of amorphous phases, which will affect their interaction with PCE. Studying the differences between composite cement and OPC will help in developing PCE admixtures suitable for low-carbon cement.

## **5.5 PCE superplasticizers for ‘slag + cement’ binder system**

The research work in this section was carried out in the Ecocem project from March 2021 to April 2023. The first part of the research focused on examining the dispersing effectiveness of various PCE polymers as well as PCE combinations, and evaluating their impact on the early strength of ‘slag + cement’ systems with different slag contents (85%, 70%, and 60% by weight). The second part investigated the dispersing effectiveness of PCE polymers in “Full binder” blended cement at a very low water-to-binder ratio (0.31 and 0.27). The initial phase of this project took place at TUM. Here, small-scale PCE polymers were synthesized and tested in paste and mortar; then large-scale PCE polymers were sent to Ecocem company for concrete testing. It should be noted that the results of the concrete tests are not included in this thesis

### **5.5.1 PCE superplasticizer for Na<sub>2</sub>SO<sub>4</sub> activated ‘slag + cement’ system**

The study in this part aimed to investigate and compare the dispersing and slump retention performance of different PCE polymers consisting of different chemical structures as well as PCE combinations in three ‘slag + cement’ systems with different slag content, and to check the retarding effect of these PCE polymers.

#### **5.5.1.1 Synthesis of the PCE Polymers**

A series of polycarboxylate superplasticizers with different molar ratios of acrylic acid to IPEG synthesized by aqueous free radical copolymerization and 45PC2 used in this section was provided by Prof. Plank and Dr. Lei, the chemical structure was shown in **Figure 53**. The polymers were designated as xIPEGy, whereby x represents the degree of polymerization of ethylene oxide in the macromonomer; while y represents the molar ratio of acrylic acid to the macromonomer. Ammonium persulfate was used as the initiator, and sodium methyl sulfonate was used as a chain transfer agent. The synthesis of IPEG PCE polymers was presented in [202]. The synthesis of 45PC2 was presented in [203].

The HPEG-type PCE polymers used in this part were synthesized by free radical method at 40 °C with APS and VC redox initiators and 3-Mercaptopropionic acid (3-

MPA) as a chain transfer agent. Take HPEG-AA-HEA3 as an example, 60 g of HPEG macromonomer and 60 g of DI water were added in a three-neck flask connected to a mechanical stirrer (400 rpm) and two separate inlets with peristaltic pumps. The flask was placed in an oil bath heated to 40 °C, and the string was for 30 min to dissolve the macromonomers. Then, a solution of 1.5 g of APS in 20 g of DI water was directly added to the flask. Next, two solutions were prepared for dropping by peristaltic pumps. Solution A: 5.4 g of AA, 8.7g of HEA, 0.6 g of 3-Mercaptopropionic acid (3-MPA) were dissolved in 30 g of DI water. Solution B: 1.2 g of VC was dissolved in 40 g of DI water. The reaction time started when solutions A and B were added dropwise into the reaction vessel over 3 hours. After the addition was completed, the reaction was continued for another 2 hours (the total reaction time is 5 hours). Finally, the PCE solution was cooled to room temperature. Dilute the PCE solution to obtain a solid content of around 30 %.

50HPEG3, 23HPEG3, HPEG-AA-HEA1and HPEG-AA-HEA2 PCE polymers were synthesized in the same way and same initiators. The copolymerization equation is illustrated in **Figure 54**. Their monomer feeding amounts are listed in **Table 23**.

The commercial products HPEG precast and HPEG ready mix were provided by Jilin Zhongxin Chemical Group Co. (China), MC PF26, and MC PF4 PCE polymer provided by MC-Bauchemie company (Germany). Sodium gluconate (>99% purity) was supplied by the China Academy of Building Research (CABR, Beijing), and a Sugar syrup sample was obtained from Südzucker AG - Werk Plattling company (Germany).

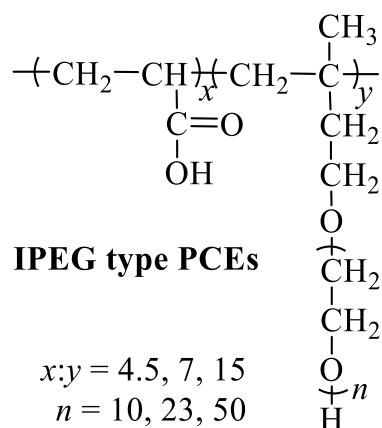


**Figure 53** Chemical structures of the IPEG-type PCE samples

## Results and discussion

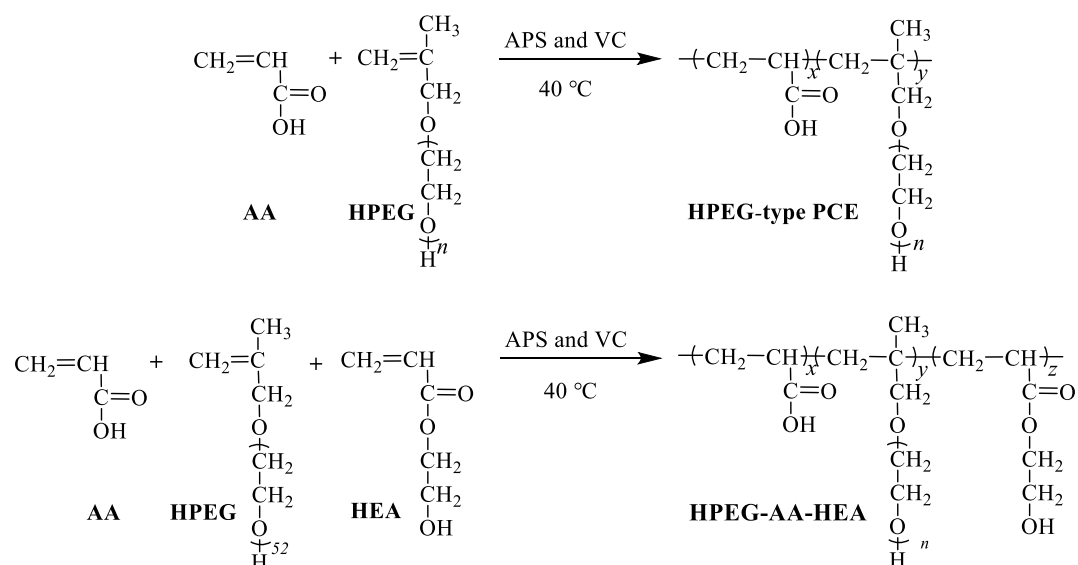


**Figure 54** Synthesis route of HPEG-type PCE and HPEG-AA-HEA polymers

**Table 23** Feeding amounts of the synthesized PCE polymers

Sample	HPEG	AA	HEA	Feeding molar ratio AA:HPEG:HEA
	g	g	g	
HPEG-AA-HEA 1	60	5.4	2.9	3:1:1
HPEG-AA-HEA 2	60	5.4	5.8	3:1:2
HPEG-AA-HEA 3	60	5.4	8.7	3:1:3
23HPEG3	27.5	5.4	-	3:1:0
50HPEG3	60	5.4	-	3:1:0

### 5.5.1.2 SEC characterization of PCE sample

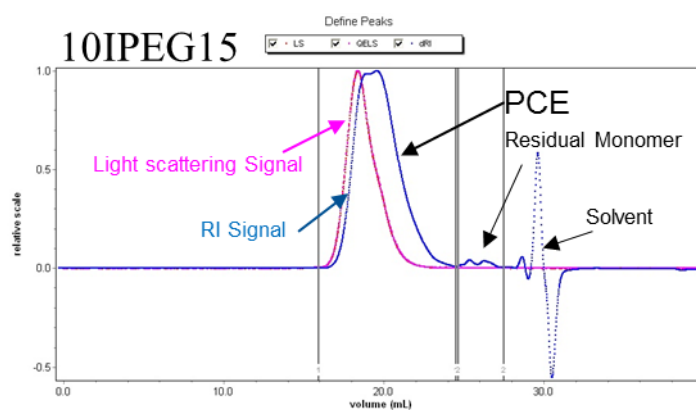
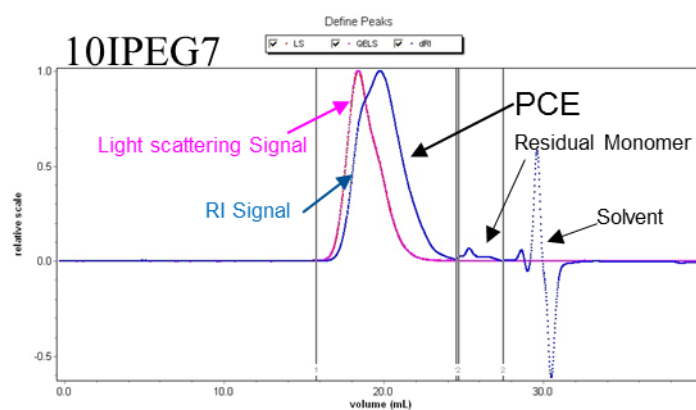
The solid content, molecular weights ( $M_n$ ,  $M_w$ ), polydispersity index (PDI) and conversion rate of the polymer samples are listed in **Table 24**. According to the results, all PCE samples exhibit low PDI values (1.6 - 2.4) and high rates for macromonomer conversion (85.0 - 98.1%), which are characteristic of high-quality PCE polymers.

In **Figure 55**, the SEC spectra of all synthesized PCE polymers are displayed. For all the polymer samples, a large peak appears at ~16 - 24 min elution time signifying the PCE polymer. Furthermore, two minor peaks representing the residual macromonomers and the solvent can be observed.

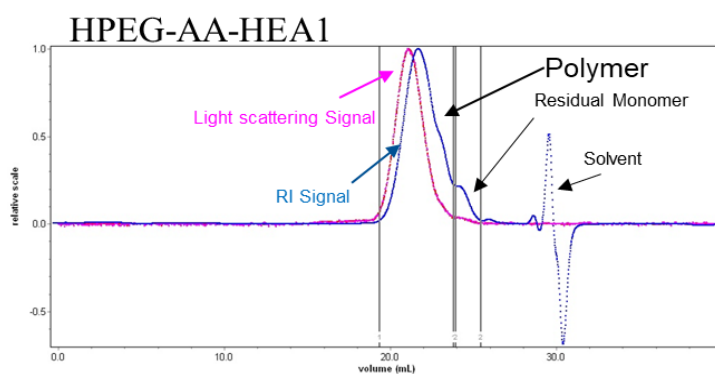
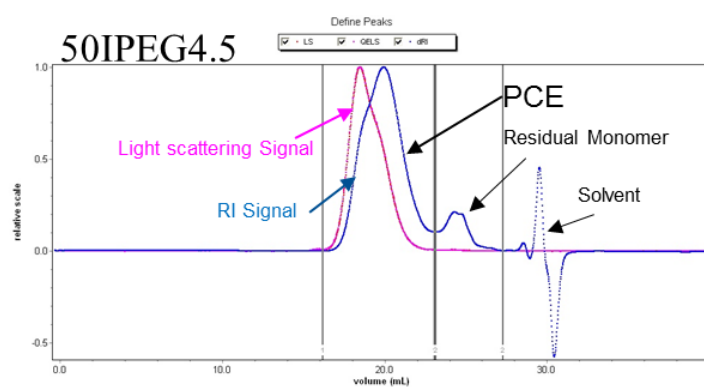
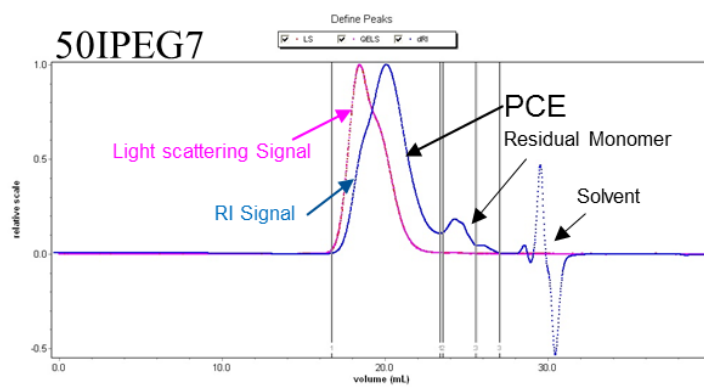
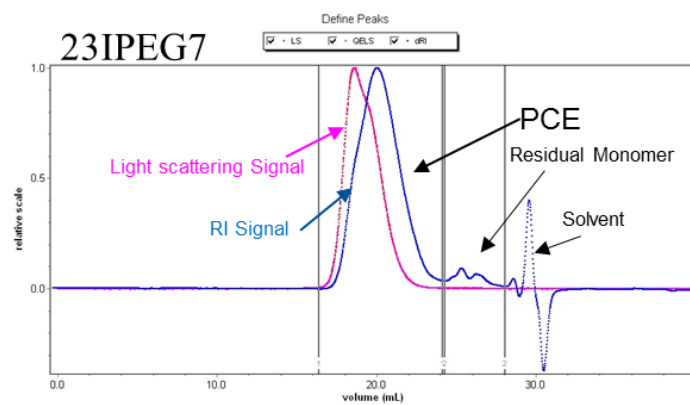
## Results and discussion

**Table 24** Solid content, molar masses and polydispersity index (PDI) of the synthesized PCE polymers and the conversion rate of the macromonomer

Sample	solid content		PDI		Conversion rate / %	Side chain length ( $n_{EO}$ )
	/ %	$M_w$	$M_n$	( $M_w/M_n$ )		
10IPEG7	36.0	83,570	35,110	2.4	97.9	10
10IPEG15	34.6	86,990	39,050	2.2	98.1	10
23IPEG7	41.0	71,720	29,920	2.4	95.9	23
50IPEG4.5	43.9	106,100	48,790	2.2	88.7	50
50IPEG7	45.3	90,360	36,960	2.4	90.9	50
HPEG-AA-HEA 1	30.5	14,040	8,580	1.6	92.5	50
HPEG-AA-HEA 2	31.2	15,410	9,414	1.6	94.5	50
HPEG-AA-HEA 3	31.3	15,120	9,500	1.6	96.6	50
23HPEG3	27.8	21,310	9,028	2.3	86.8	23
50HPEG3	26.9	30,560	14,040	2.2	85.0	50



## Results and discussion



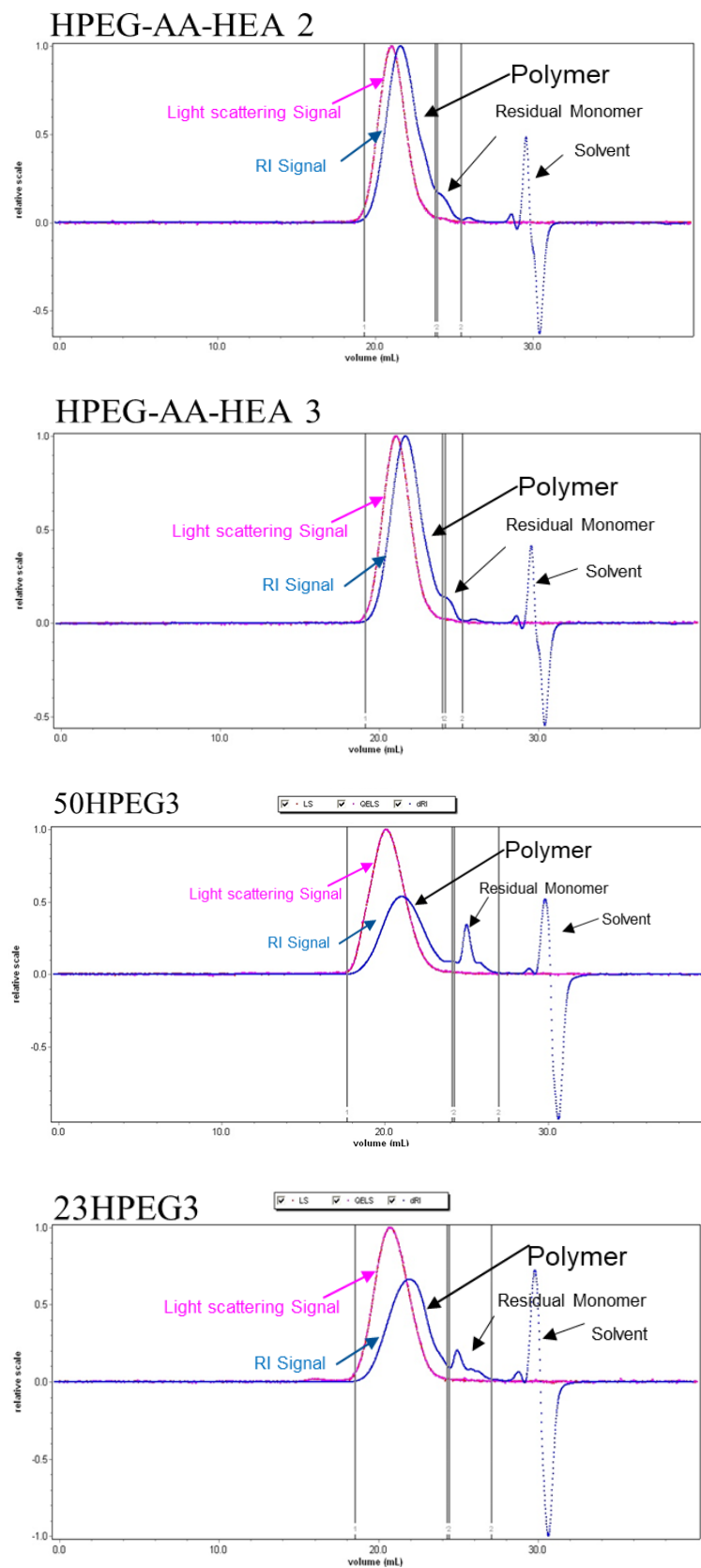
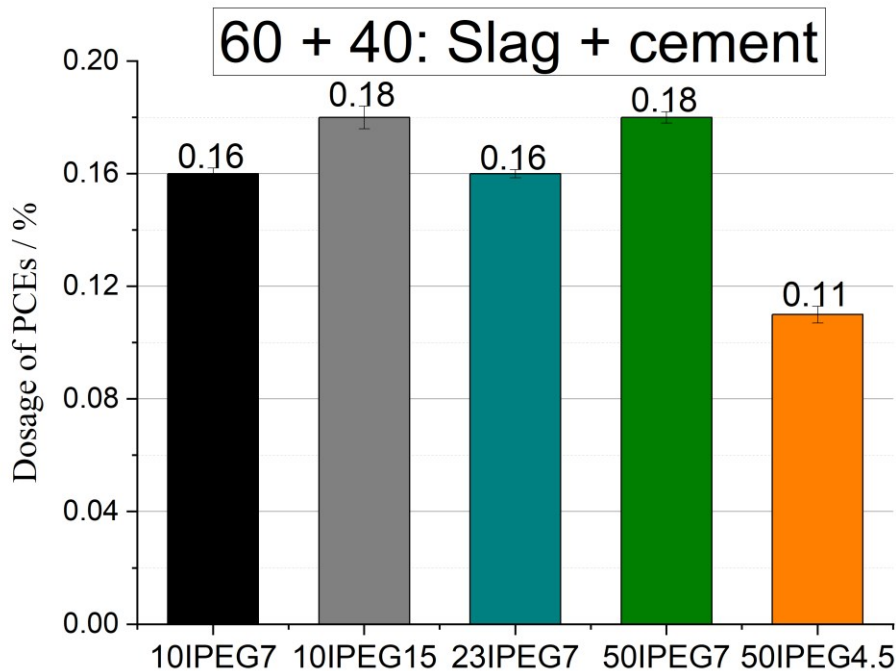


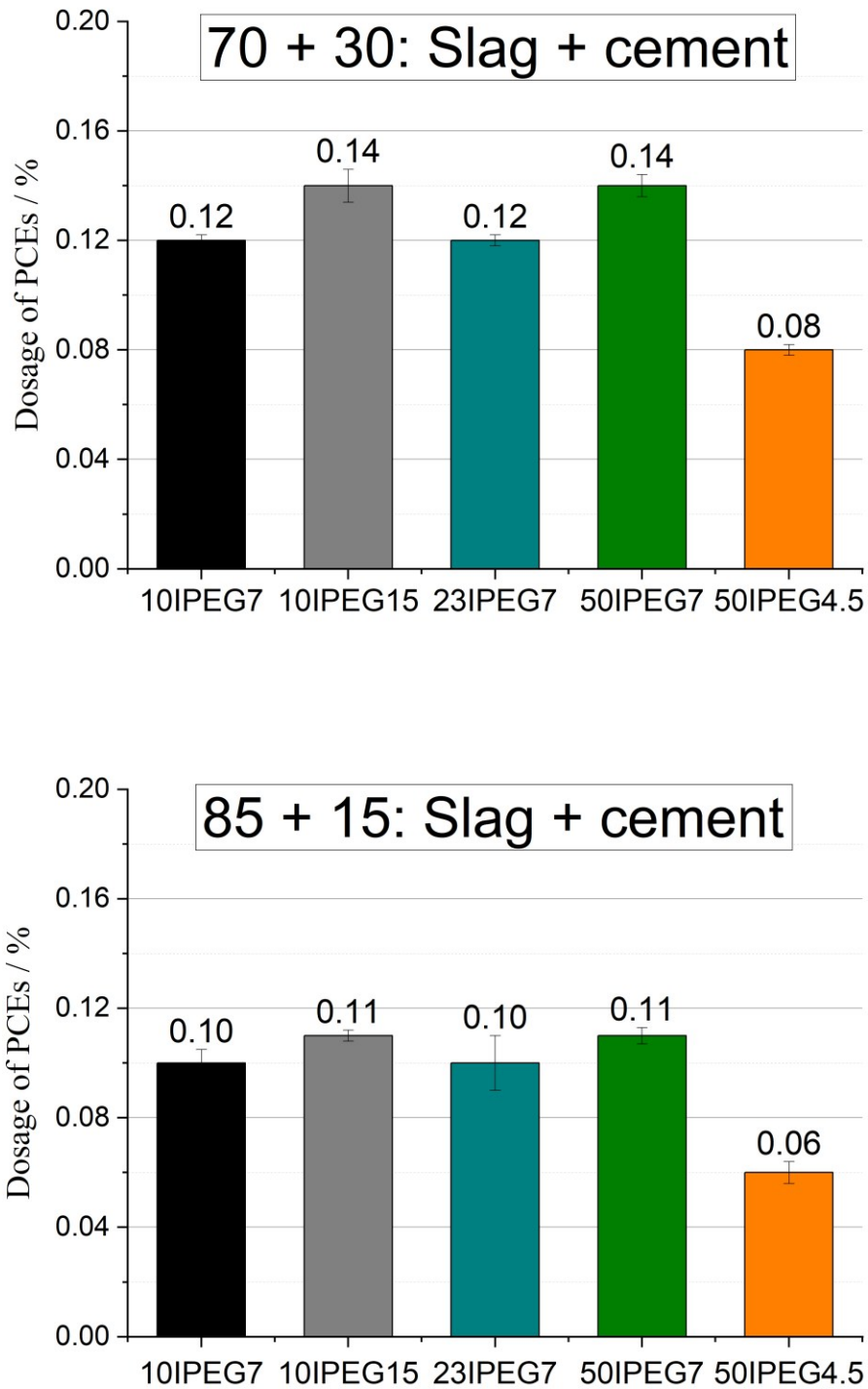
**Figure 55** SEC spectra of the synthesized PCE polymer samples

### 5.5.1.3 Dispersing performance of PCE polymers in paste and mortar

The dispersing performance of the IPEG superplasticizers was evaluated in ‘slag + cement’ pastes via “mini-slump” tests. There, the water-to-binder ratio was 0.4, and the flow value of the paste without any PCE (reference value) was 10 cm. The dosages required for all PCE polymers in the three ‘slag + cement’ binders to achieve  $26 \pm 0.5$  cm cement flow are shown in **Figure 56**.

The general observation as follows can be made: higher slag contents result in lower PCE dosage (which further improves the eco balance sheet of those binders), and IPEG PCEs of lower anionicity require lower dosages. Overall, the order of effectiveness of the PCE polymers is as follows: 50IPEG4.5 > 10IPEG7 = 23IPEG7 > 10IPEG15 = 50IPEG7. Further testing only the polymer 50IPEG7 and 50IPEG4.5 were used, because the macromonomer exhibiting 50 EO units is commercially most readily available.

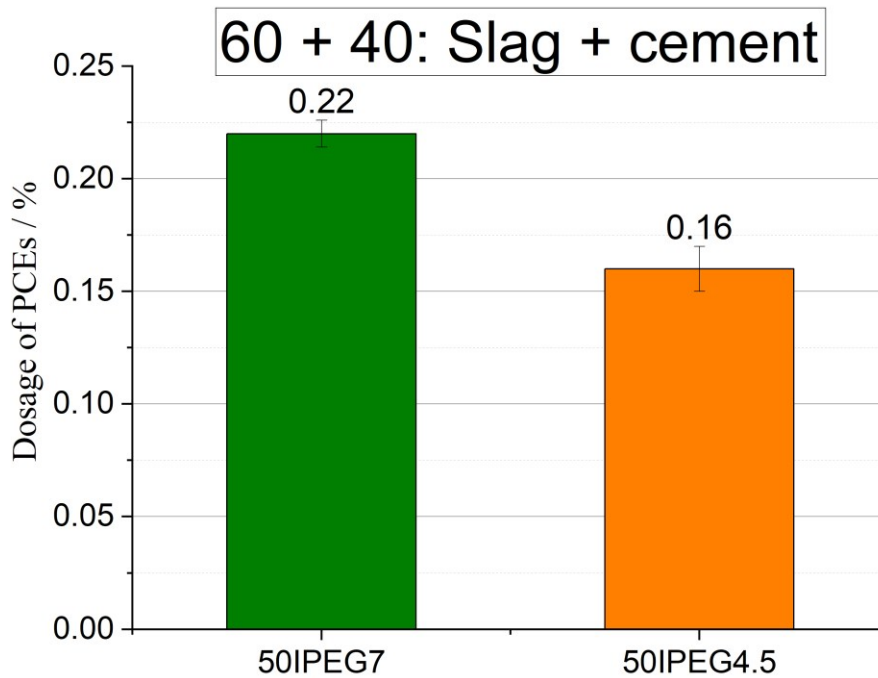




**Figure 56** Dosages of PCE required to obtain a paste spread flow of  $26 \pm 0.5$  cm (spread flow of reference pastes without PCE = 10 cm)

Next, the dispersing efficiency of 50IPEG7 and 50IPEG4.5 polymers was investigated in mortar. The water-to-binder ratio was 0.4, and the flow value of each mortar without any PCE was 10 cm. The PCE dosages required to achieve  $20 \pm 0.5$  cm mortar spread flow are shown in **Figure 57**.

It is observed that in mortar the PCE dosages required are generally higher than in paste, as was shown in section 4.3.1. However, similar to paste also, the PCE dosages decrease with increasing slag content, and the order of effectiveness of the PCEs is the same as in paste, with 50IPEG4.5 being clearly superior to 50IPEG7.



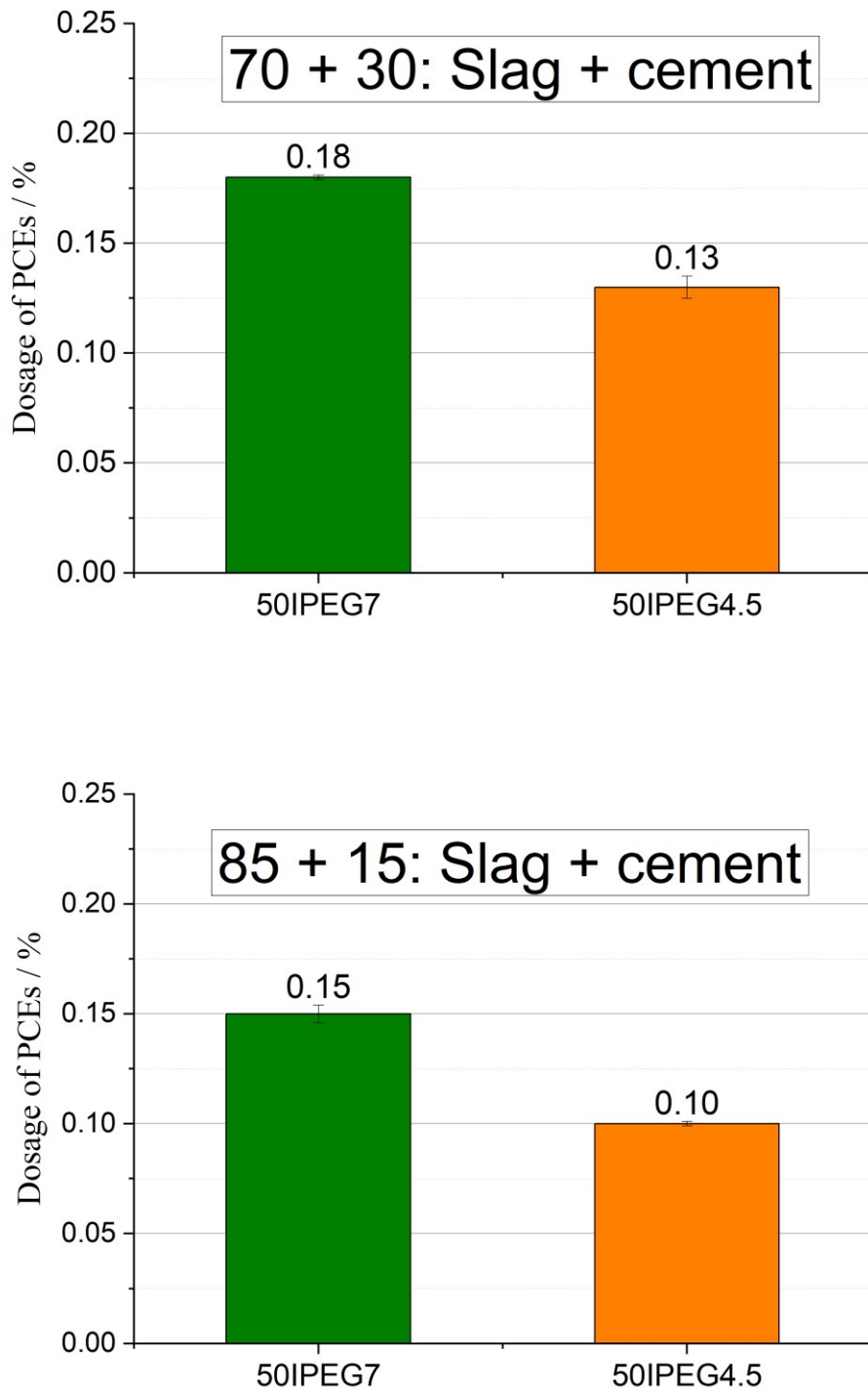


**Figure 57** Dosages of PCE required to obtain a mortar spread flow of  $20 \pm 0.5$  cm (all reference mortars without PCE have spread flow of 10 cm)

#### 5.5.1.4 Slump retention performance of PCE polymers in paste and mortar

The slump loss retention of ‘slag + cement’ pastes prepared at a water-to-binder ratio of 0.4 and a dosage corresponding to a paste flow of  $26 \pm 0.5$  cm was determined over a period of 2 h. According to **Figure 58**, 50IPEG4.5 and 50IPEG7 PCEs have different slump retention performance in the three binder systems.

Interestingly, in the 85 + 15 system, the stronger anionic PCE polymer 50IPEG7 performs better than the less anionic 50IPEG4.5; whereas in the 70 + 30 system, both PCEs exhibit similar performance; however, in the 60 + 40 system, the less anionic 50IPEG4.5 outperforms the more anionic 50IPEG7 polymer.

From Ordinary Portland Cement (OPC), it is known that PCEs of lower anionicity and higher side chain density, such as 50IPEG4.5, can provide larger slump retention than more anionic PCEs with less side chain density. Here, this rule only applies to the 60 + 40 system, which is relatively rich in cement (40%). However, in a slag rich system slump retention is better achieved by a more anionic PCE such as 50IPEG7. The mechanism behind this opposite behavior to OPC is completely unclear.

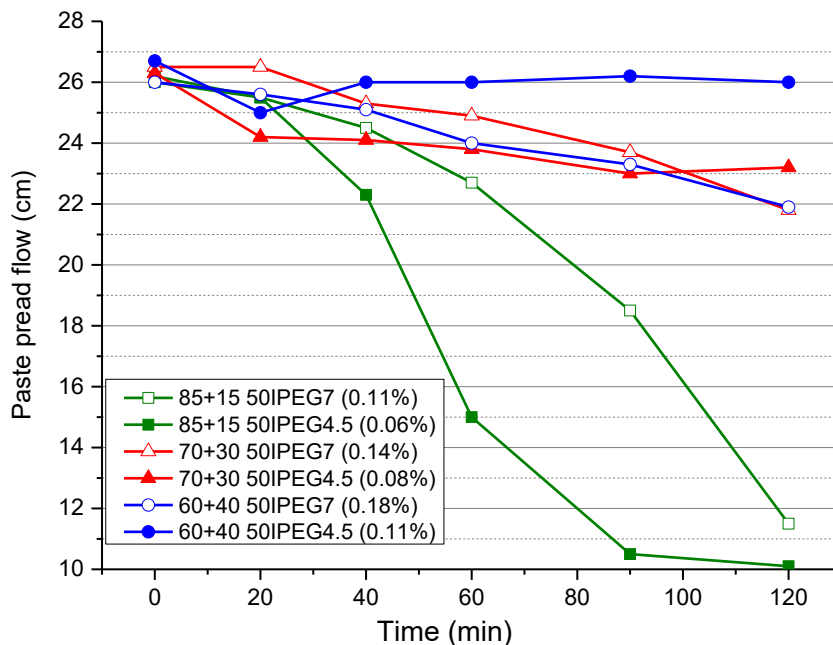


**Figure 58** Time-dependent evolution of the three ‘slag + cement’ spread flow of three pastes admixed with the synthesized polymers

Next, the slump retention behaviour was tested in mortar. At first, the individual IPEG PCEs were tested at dosages of the polymers to achieve a mortar spread flow of  $20 \pm 0.5$  cm. For these polymers, the evolution of mortar fluidity over time was measured. From **Figure 59**, it is evident that none of the PCE polymers 50IPEG7 and 50IPEG4.5 is able to maintain workability in all three systems for an extended period of time, this signifying a significant difference to the previous results in paste (**Figure 58**). Albeit, a comparable overall trend is observed, because also in mortar, the less anionic PCE is superior over the more anionic polymer 50IPEG7 as if can maintain fluidity over  $\sim 20$  min least. However, this is observed only for the systems which contain 30 or 40 % cement. For the slag rich system (85 + 15), none of these polymers can achieve any slump retention.

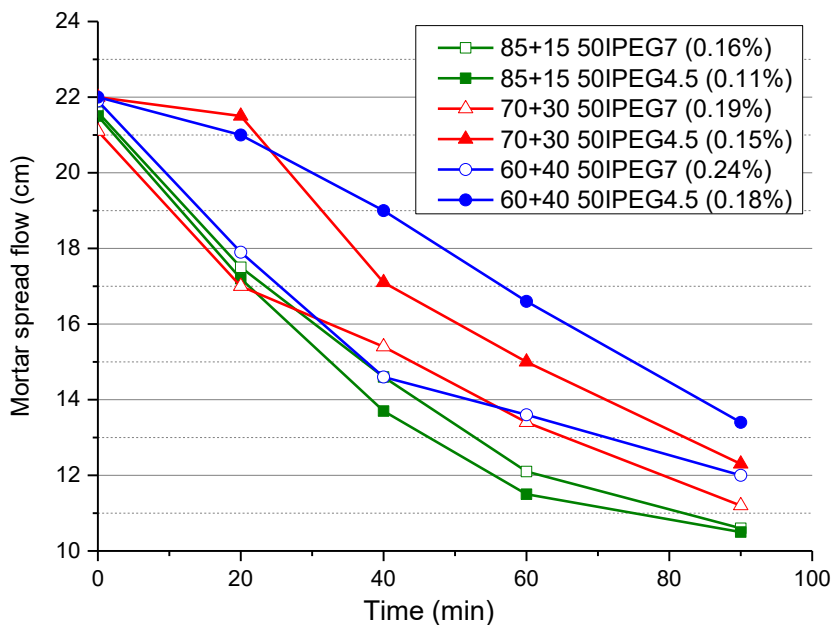


**Figure 59** Time-dependent evolution of the spread flow of the three ‘slag + cement’ mortars admixed with the synthesized polymers

To solve this problem, a commercial product HPEG ready mix superplasticizer, based on the so-called slow releasing mechanism was tested. The results are displayed in **Figure 60**. As expected, in the 70 + 30 and the 60 + 40 mortars, HPEG ready mix showed excellent slump retention over  $\sim 3$  hours, and the spread flow of the mortars even increased during the first hour which is not so desirable. Furthermore, in the slag

rich 85 + 15 system the HPEG ready mix superplasticizer could not provide any slump retention.

The results from both paste and mortar demonstrate that in system containing more than 70 % slag, the behaviour of PCEs become completely different as compared to OPC system. In order to solve this problem, in the next step combination of different PCEs were tested. At first, the combination of 50IPEG4.5 (which performed best in the paste and mortar test, see **Figure 58** and **Figure 59**) and HPEG ready mix was tested in the three mortars. The dosage of the HPEG ready mix polymer was fixed at 0.4 % while the addition of 50IPEG4.5 PCE was increased from 0.06 to 0.08 %.

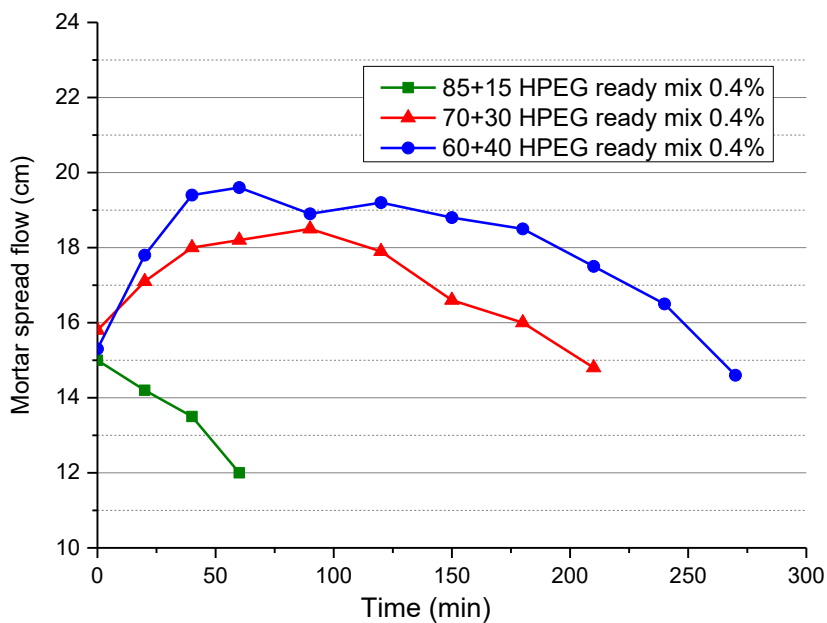


**Figure 60** Time-dependent evolution of the spread flow of the three ‘slag + cement’ mortars admixed with 0.4% HPEG Ready mix

According to **Figure 61** (a), this combination provides excellent slump retention over 3 hours in the system containing 30 or 40 % cement within the error range ( $\pm 0.5$  cm). Unfortunately, it did not work to satisfaction in the slag rich 85 + 15 mortar. In another test series, the dosage of 50IPEG4.5 was fixed at 0.06 % while the dosage of the HPEG ready mix PCE was varied between 0.3 and 0.4 %. There, workability was maintained for 3 hours (**Figure 61** (b)), but at spread flows which were lower than before. When

the dosage of HPEG ready mix was decreased even more to 0.15 – 0.2 %, the slump retention became much lower, as is shown in **Figure 61(c)**. This result signifies that a certain minimal threshold dosage of HPEG ready mix is required to achieve slump retention.

For the next step, lab-synthesized IPEG PCE 50IPEG4.5 was replaced by a commercial HPEG precast PCE. The results achieved for this combination of this commercial HPEG ready mix and the HPEG precast are shown in **Figure 62**. It is observed that this combination behavior is quite similar to that based on the self-synthesized IPEG PCE within the error range ( $\pm 0.5$  cm). Again, no satisfying slump retention was achieved in the slag rich 85 + 15 system.

To improve the workability over 2 hours, different retainers such as PCEs from MC company (MC PF26, MC PF4), PCEs with high side chain density (45PC2, 50HPEG3), retarders (Sodium Gluconate, Sugar syrup), HPEG-AA-HEAs PCEs with different composition were chosen to combine with HPEG precast and tested in mortar.

According to **Figure 63**, the combination HPEG precast + MC PCEs (MC PF26, MC PF4) provides lower initial spread flow and lower slump retention when using the same dosage as HPEG precast + HPEG ready mix. MC PF26 PCE performed better than MC PF4, and the combination of HPEG precast + MC PF26 behavior was quite similar to that of HPEG precast + HPEG ready mix combination via slightly increasing the dosage of HPEG precast and MC PF26 within the error range of  $\pm 0.5$  cm. As is shown in **Figure 64**, PCEs with high side chain density (45PC2, 23HPEG3 and 50HPEG3) can also work as retainer combined with HPEG precast, and the dosage for these retainers are different to achieve the same slump retention performance as HPEG precast + HPEG ready mix combination within the error range ( $\pm 0.5$  cm). HEPG type PCEs have stronger dispersing effectiveness, the required dosage of 23HPEG3 and 50HPEG3 to achieve good workability are lower than that of 45PC2.

Results and discussion

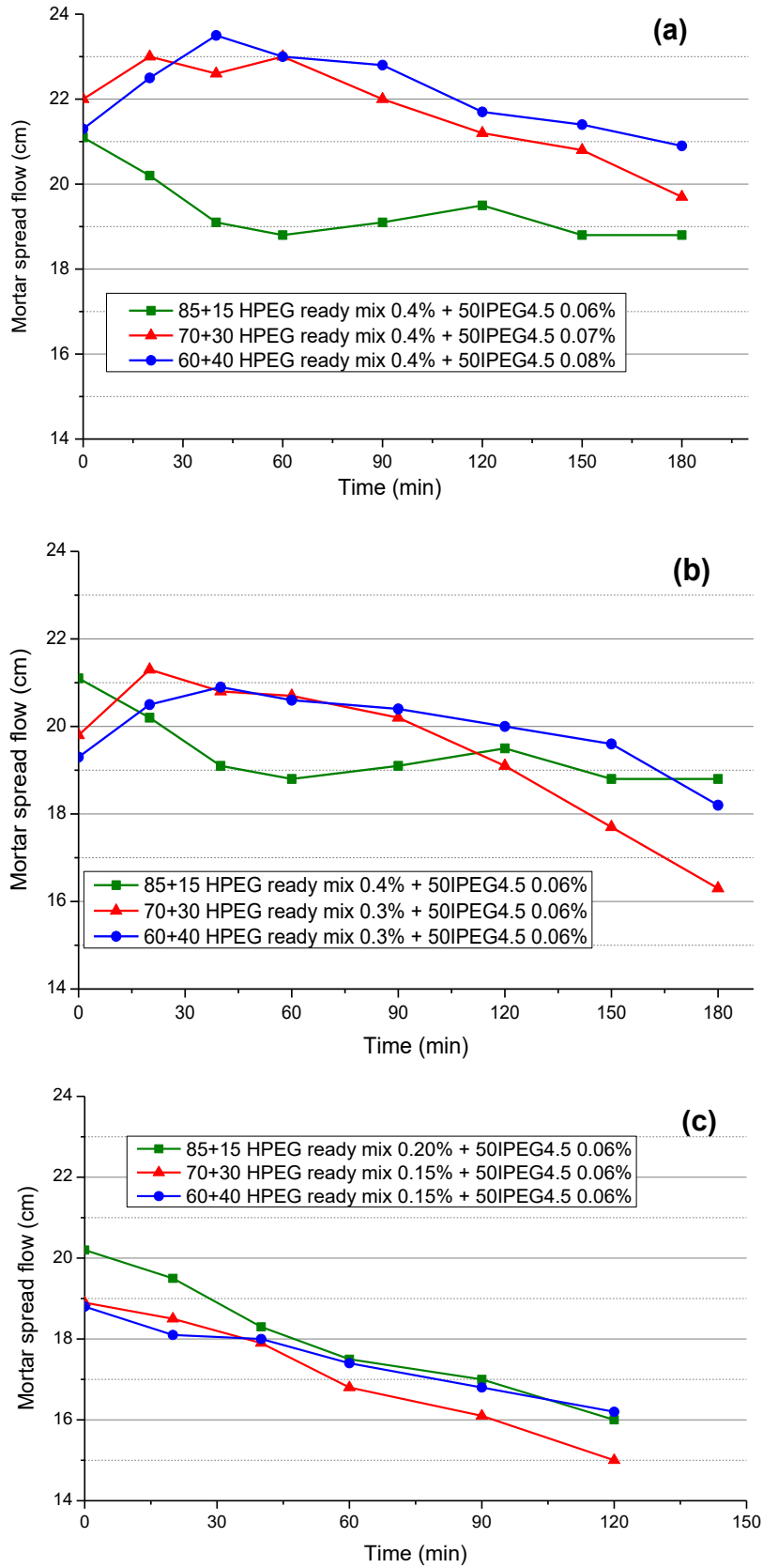


**Figure 61** Time-dependent spread flow of the three ‘slag + cement’ mortars admixed with a combination of HPEG Ready mix and 50IPEG4.5

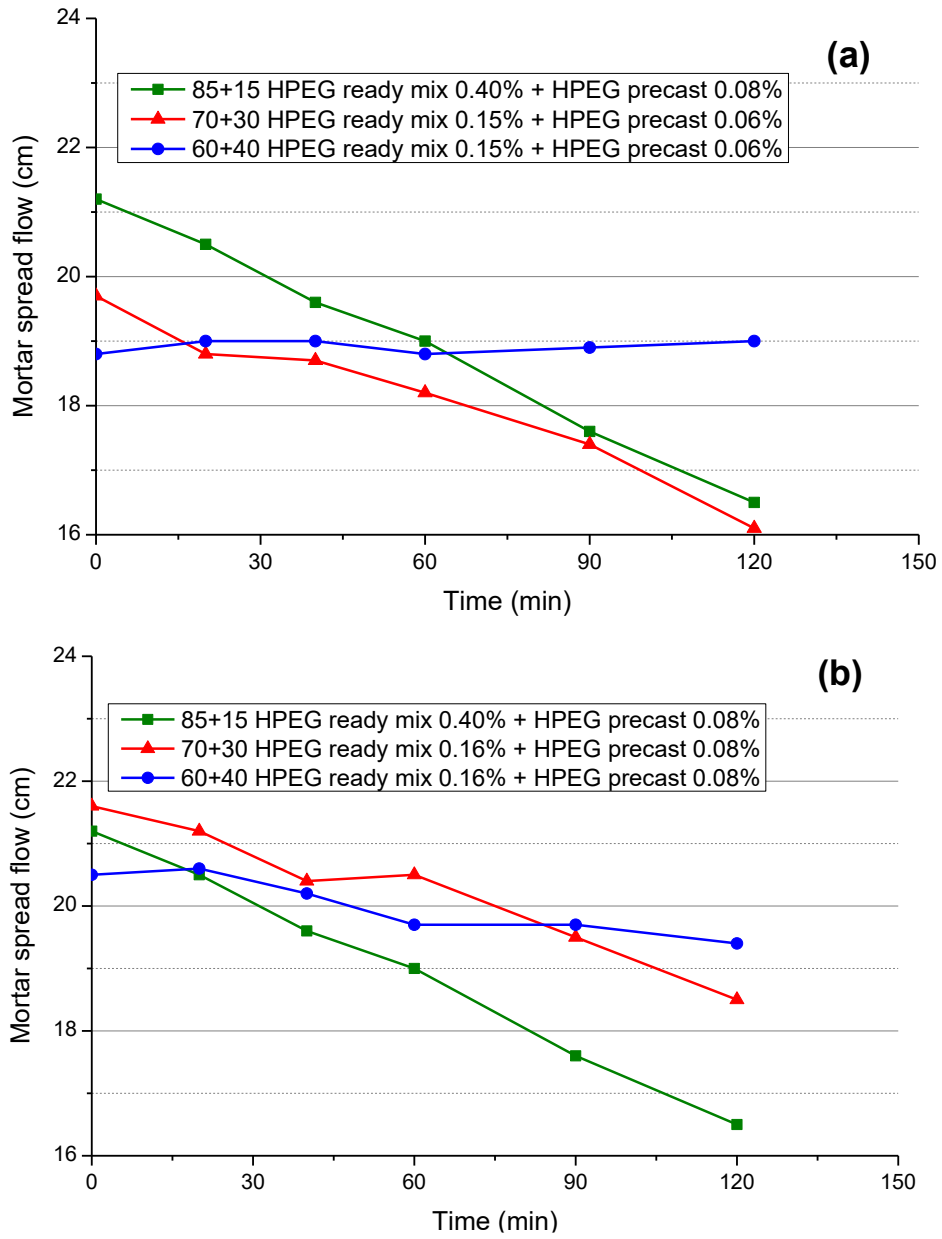


**Figure 62** Time-dependent spread flow of three ‘slag + cement’ mortars admixed with HPEG Ready mix and HPEG precast combination

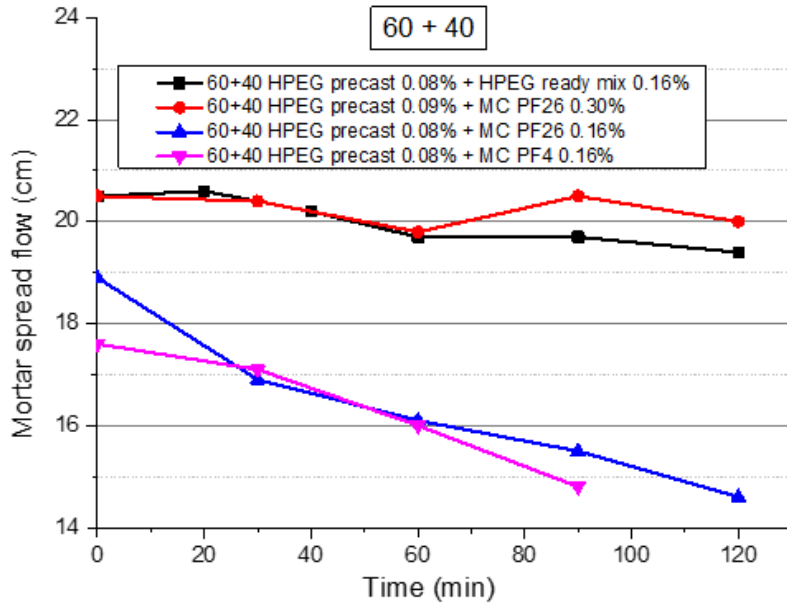


**Figure 63** Time-dependent spread flow of ‘60 + 40’ mortars admixed with PCEs combinations (HPEG ready mix + MC PCE)

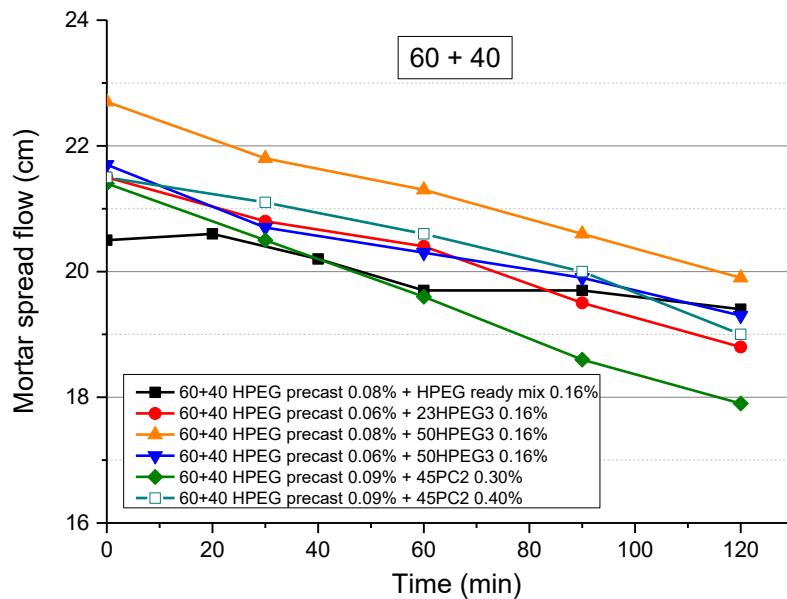


**Figure 64** Time-dependen spread flow of ‘60 + 40’ mortars admixed with PCEs combinations (HPEG ready mix + 45PC2 / 50HPEG3 / 25HPEG3)

Retarders such as sodium gluconate and sugar syrup, which slowed the hydration process of cement, can also work as retainers in this PCE combination. As is shown in **Figure 65**, sodium gluconate can provide perfect workability within the error range ( $\pm 0.5$  cm) at very low dosages (HPEG precast 0.12 % + sodium gluconate 0.10 %). While

none of the combinations of HPEG precast + sugar syrup can achieve good slump retention.

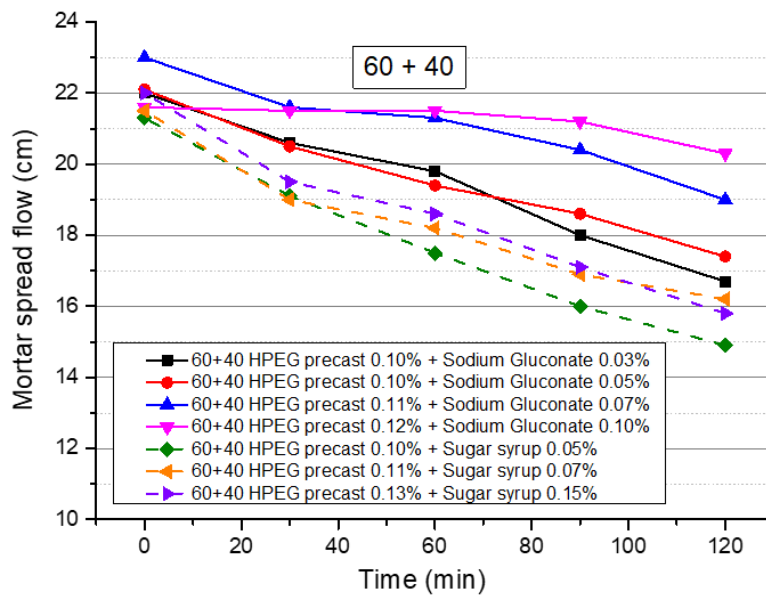


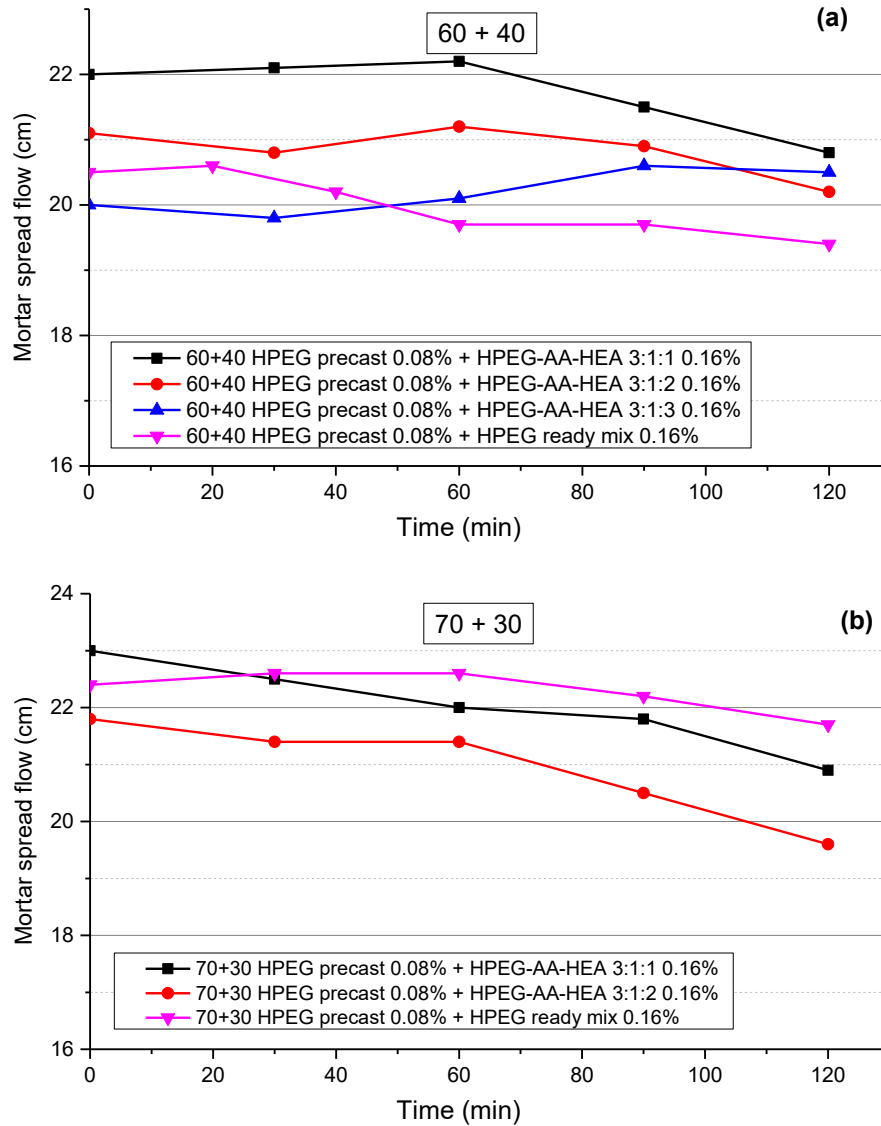
**Figure 65** Time-dependent spread flow of ‘60 + 40’ mortars admixed with PCEs combinations (HPEG ready mix + retarders)

The HPEG ready mix PCE, which is based on hydroxyethyl ester, can provide mortar with good workability but reduces the early strength (1 d). To solve this problem, HPEG-AA-HEAs with different compositions were synthesized and applied in ‘slag + cement’ systems.

According to **Figure 66 (a)**, All combinations of HPEG precast 0.08 % + HPEG-AA-HEAs 0.16 % ( $s = 1, 2, 3$ ) could maintain fluidity over 2 hours in ‘60 + 40’ mortars within the error range of  $\pm 0.5$  cm. HPEG-AA-HEAs with lower HEA content provide higher initial spread flow when same dosage was applied in ‘60 + 40’ mortars (HPEG-AA-HEA1 > HPEG-AA-HEA2 > HPEG-AA-HEA3), this is because HEA has lower adsorption on the binder. Mortar admixed combinations of HPEG precast + HPEG-AA-HEA1 and HPEG precast + HPEG-AA-HEA2 even have bigger spread flow than that of HPEG precast + HPEG ready mix combination in the ‘60 + 40’ system.

## Results and discussion

In 70 + 30 system, the same trend was observed that HEAs with lower HEA content provided higher initial spread flow when the same dosage was applied **Figure 66 (b)**. However, none of the combinations could maintain workability very well over 2 hours in '85 + 15' mortars **Figure 66 (c)**.



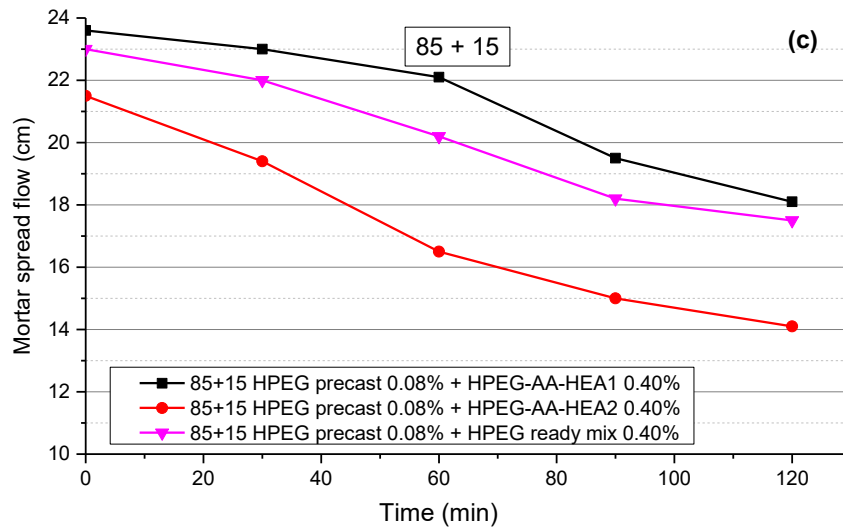


**Figure 66** Time-dependent spread flow of three ‘slag + cement’ mortars admixed with PCEs combinations (HPEG ready mix + HPEG-AA-HEAs)

#### 5.5.1.4 Compressive strength tests in mortar

In this part, the effect of the two IPEG PCEs 50IPEG4.5 and 50IPEG7 on the 1 d compressive strength of mortar was tested. The water-to-binder ratio was 0.4 and the PCE dosages were the same as that in slump retention tests.

As we can see from **Figure 67**, the low anionic PCE 50IPEG4.5 does not decrease the 1 d compressive strength, while the more anionic polymer 50IPEG7 induced a slight reduction in early strength. This negative effect increases with increased cement content in the binder and corresponds well with the known behavior of many anionic PCEs in OPC.

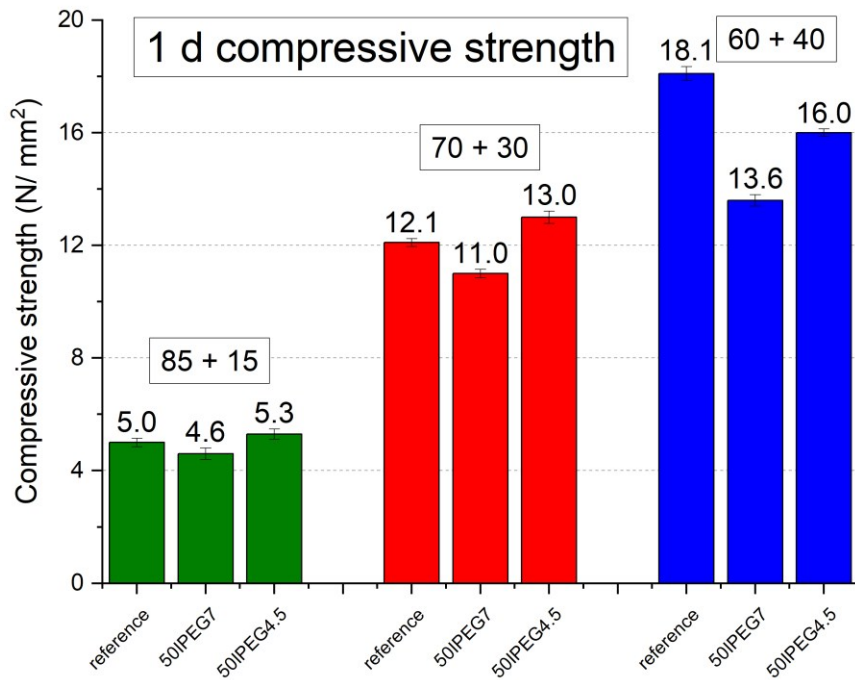


**Figure 67** 1 day compressive strengths of the mortar specimens admixed with 50IPEG4.5 or 50IPEG7 superplasticizers. (w/b = 0.4)

Thereafter, a combination of 50IPEG4.5 and HPEG ready mix were tested. Unfortunately, at the dosages where perfect workability was achieved for the mortars (**Figure 61(b)**), the 1 d strength values were much decreased, and even the 3d strength values were slightly decreased (**Figure 68**). This suggests that the HPEG ready mix PCE exercises a strong retarding effect which affects early strength (1 d). A possible solution is to decrease the dosage of this PCE.

When the dosage of HPEG ready mix was decreased, the 1 d compressive strength improved, as is shown in **Figure 69**. Compressive strength was measured at 10 ° C, as is shown in **Figure 70**. According to these results, the combination of HPEG ready mix and HPEG precast cannot fulfill the 1 d strength requirements of 3.5 N/ mm<sup>2</sup>, which corresponds to that of the reference.

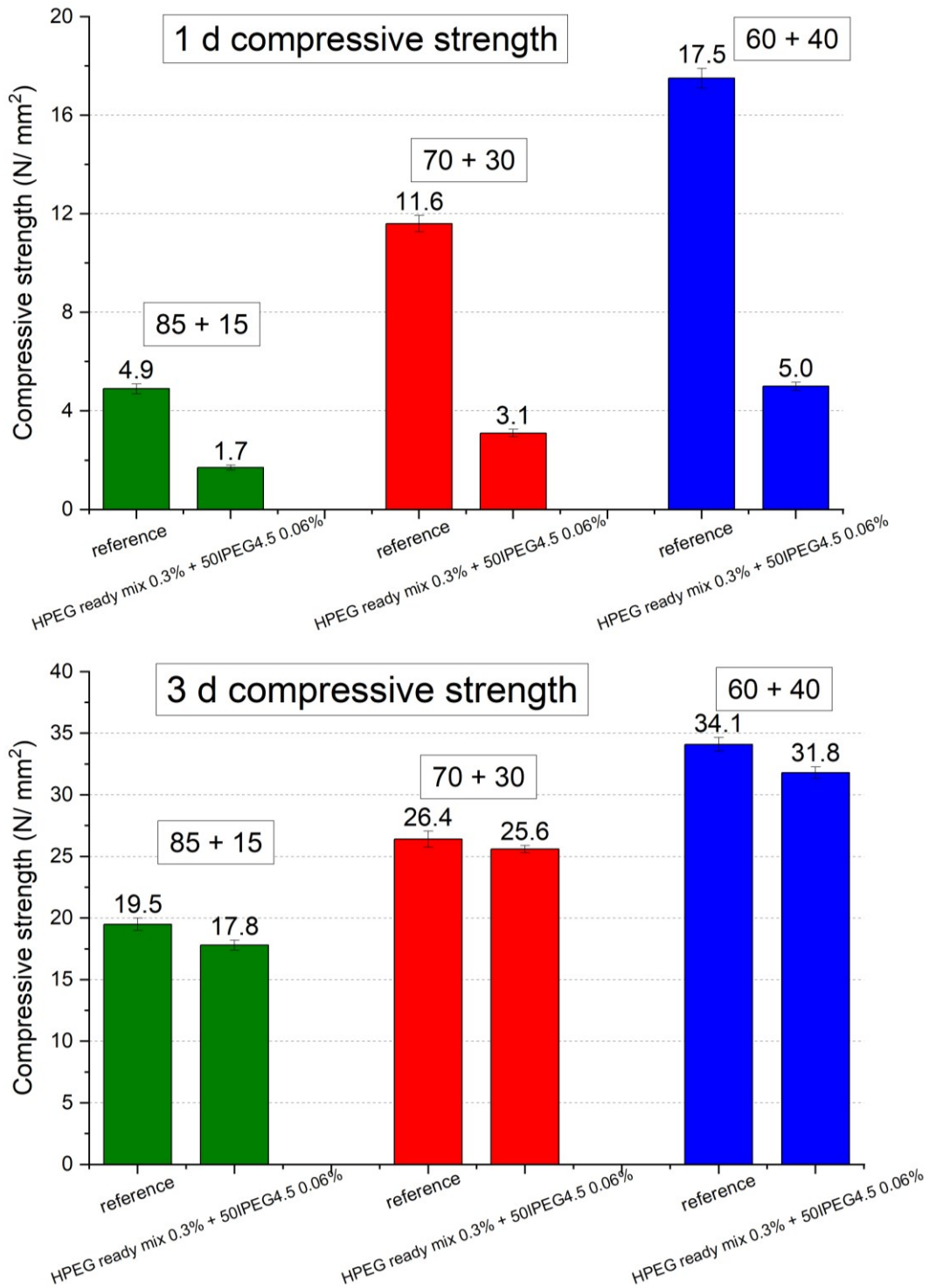


**Figure 68** Compressive strengths after 1 d or 3 days of the mortar admixed with PCE combinations (w/b = 0.4)

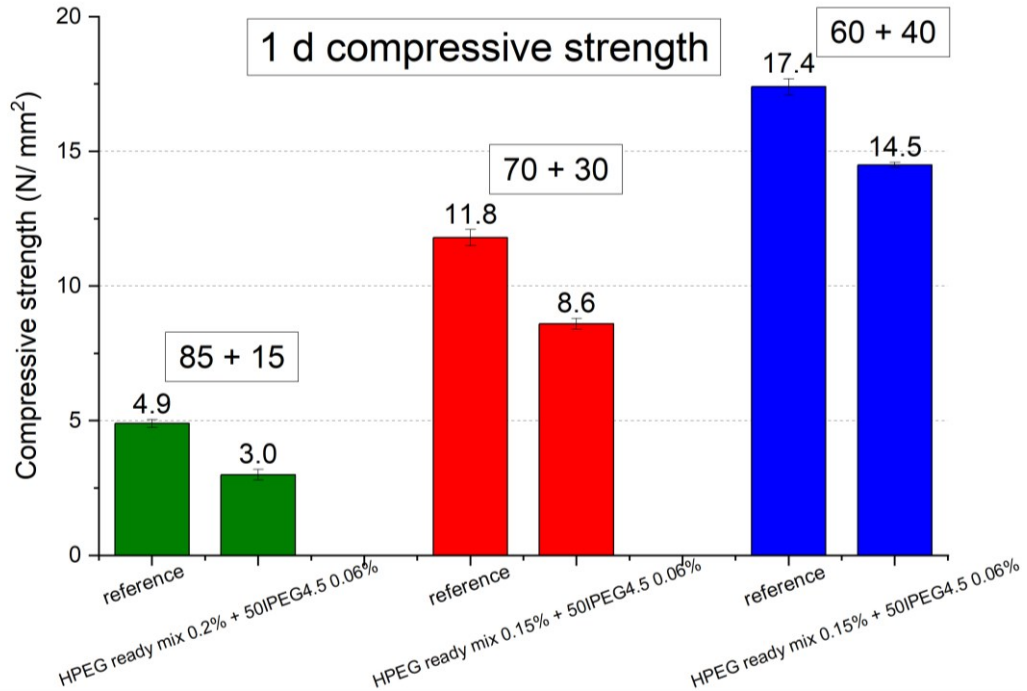


**Figure 69** 1 day compressive strengths of three mortar specimens admixed with a combination of HPEG ready mix and 50IPEG4.5. (w/b = 0.4)

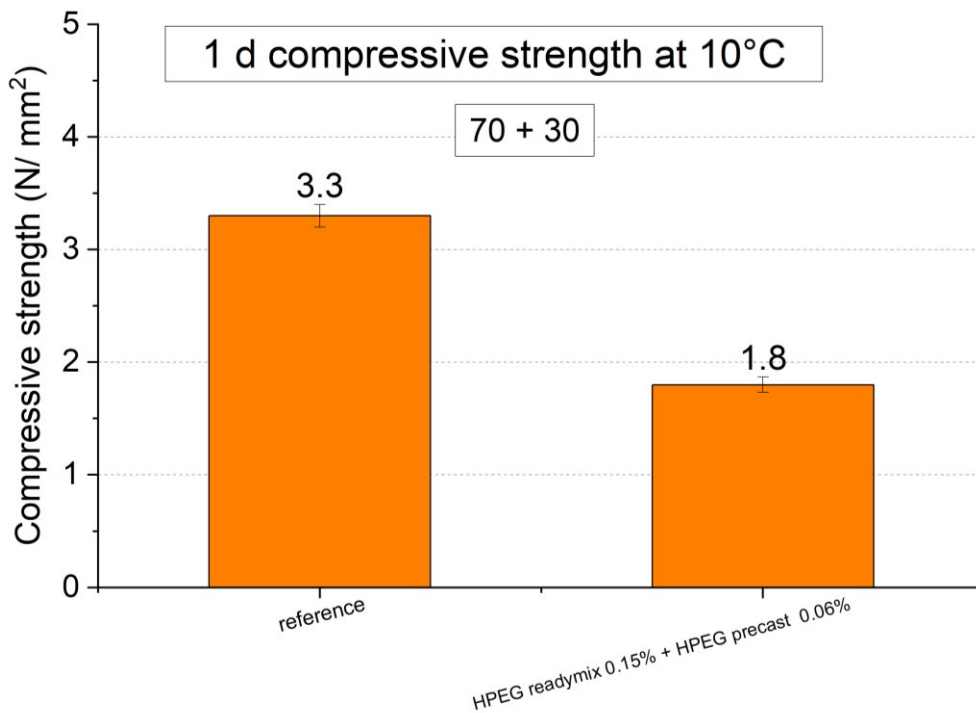


**Figure 70** 1 day compressive strengths of 70 + 30 mortars admixed with a combination of HPEG Ready mix and HPEG precast at 10 °C. (w/b = 0.4)

In this part, the effects of different PCEs combinations on the 1 d compressive strength of mortar were tested and compared with combination containing HPEG ready mix. The water to binder ratio was 0.4 and the PCE dosage was the same as that in slump retention tests.

As we can see from **Figure 71**, the HPEG precast + 45PC2 combination does not decrease the 1 d compressive strength, while the HPEG precast + MC PF26 combination induced a bigger reduction in early strength than the HPEG precast + HPEG ready mix combination. Therefore, 45PC2 with higher side chain density can achieve perfect workability through the steric hindrance, and the early strength can even be increased slightly.

After that, another two PCEs with relatively higher side chain density (50HPEG3 and 23HPEG3) were also chosen to be used in combination with HPEG ready mix and tested for the 1 d compressive strength. Unluckily, the early strength (1 d) was slightly decreased, as is shown in **Figure 72**, when the mortar was admixed with the combinations of HPEG precast + 50HPEG3 and HPEG precast + 23HPEG3.

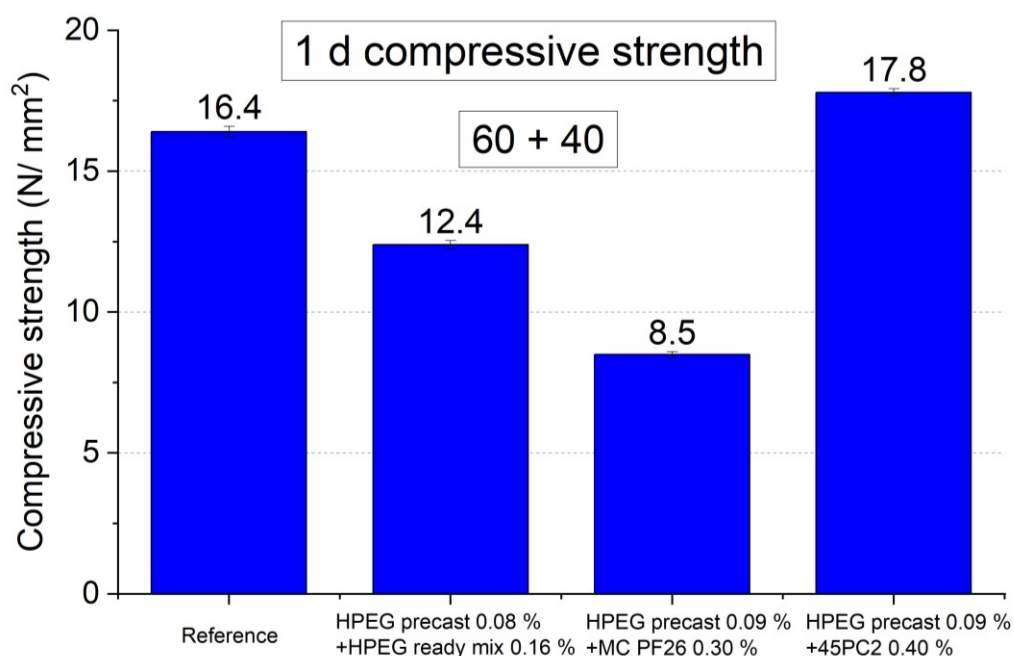


**Figure 71** 1 day compressive strengths of mortar specimens admixed with PCE combinations (water-to-binder ratio = 0.4)

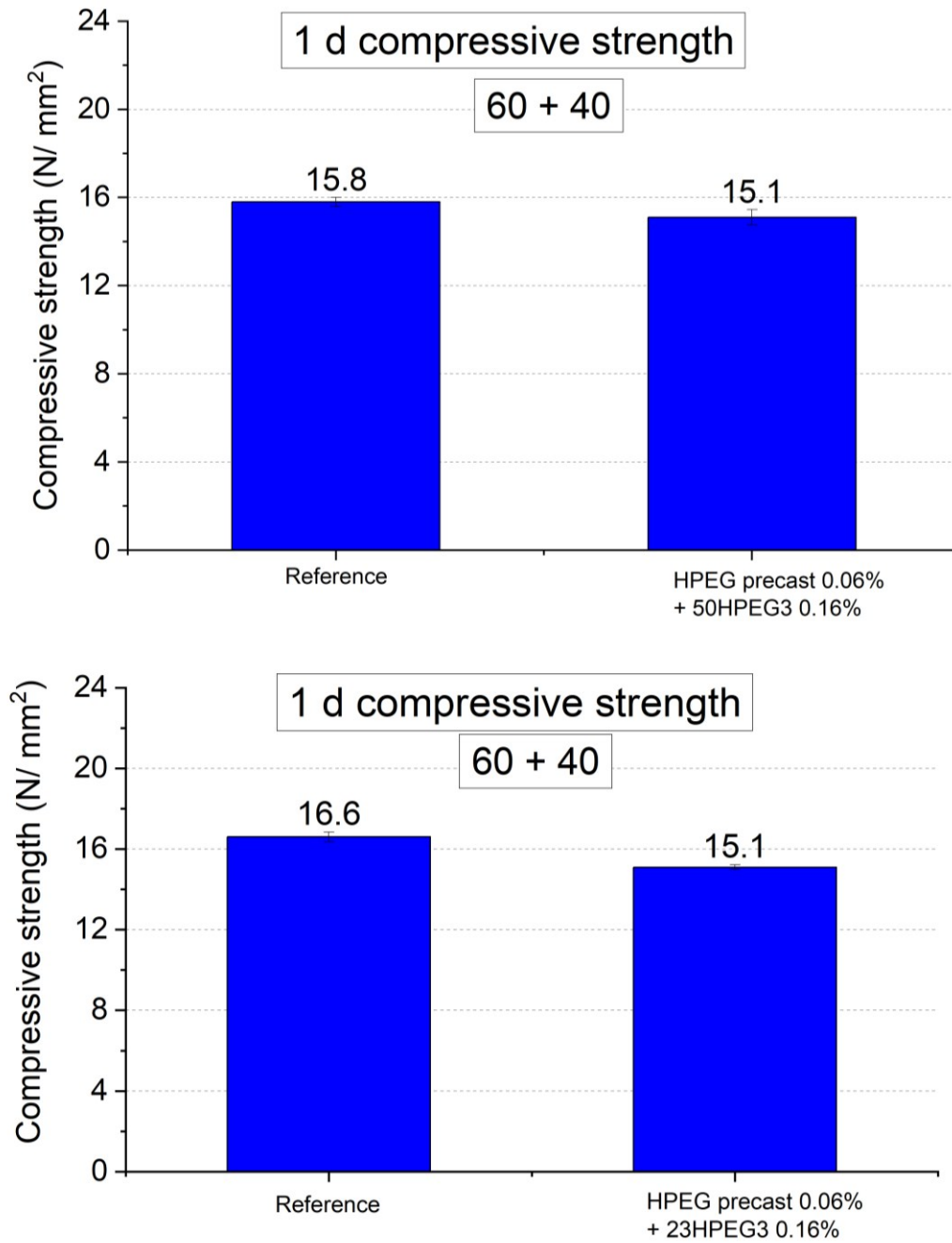


**Figure 72** 1 day compressive strengths of mortar specimens admixed with PCE combination of HPEG ready mix + 50HPEG3 / 23HPEG3 (w/b = 0.4)

Next, a combination of HPEG precast + sodium gluconate at different dosage were tested. As is shown in **Figure 73**, when the dosage of sodium gluconate increased from 0.05 % to 0.07 %, the 1 d strength decreased greatly. Continue increased the dosage of

sodium gluconate to 0.1%, the mortar specimens were not hardened because of the strong retarding effect of sodium gluconate.

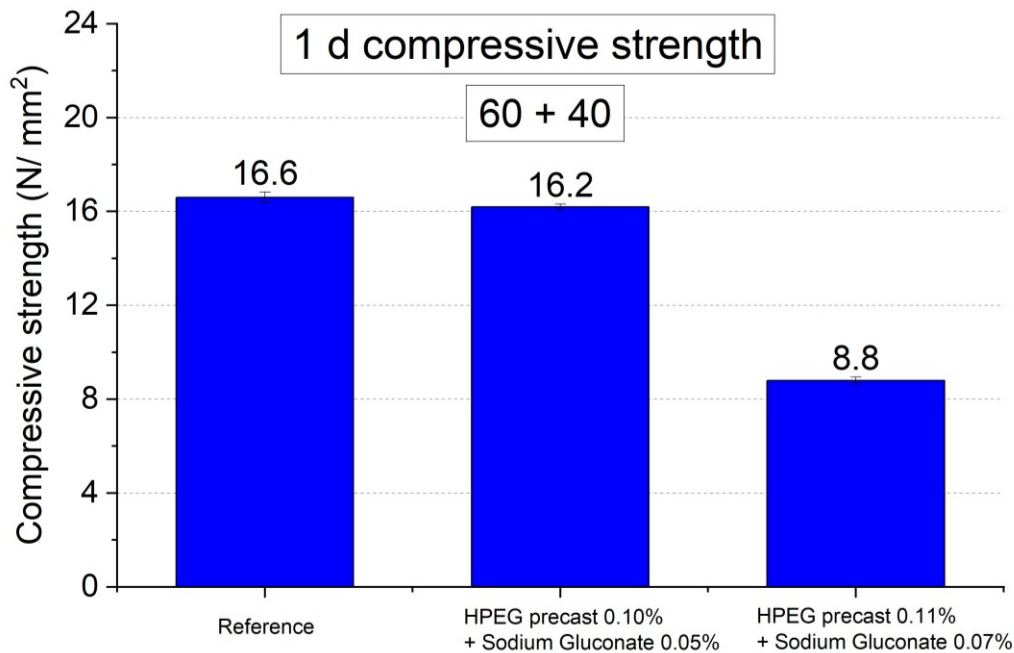


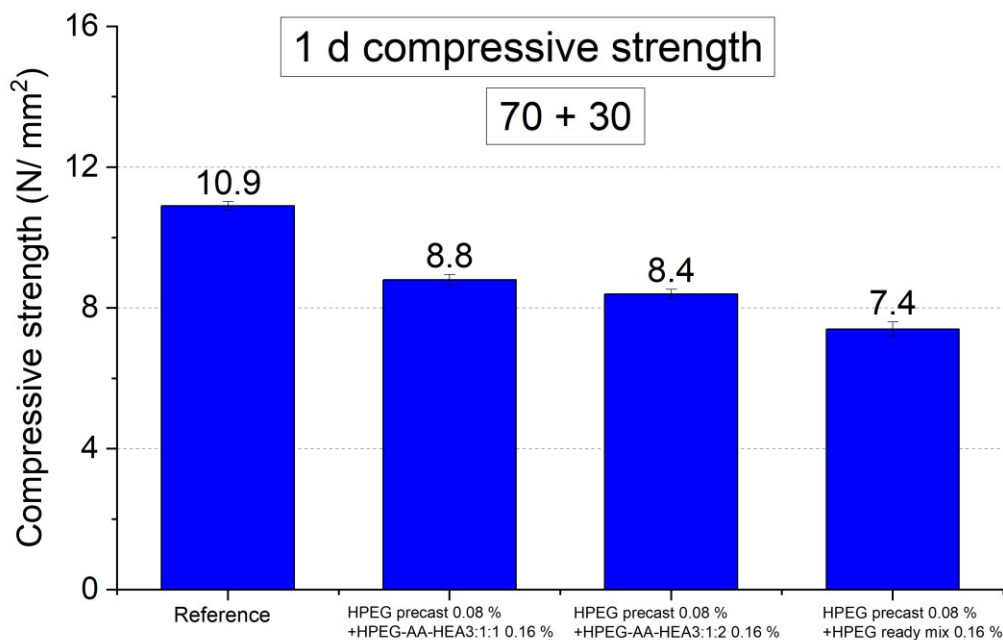
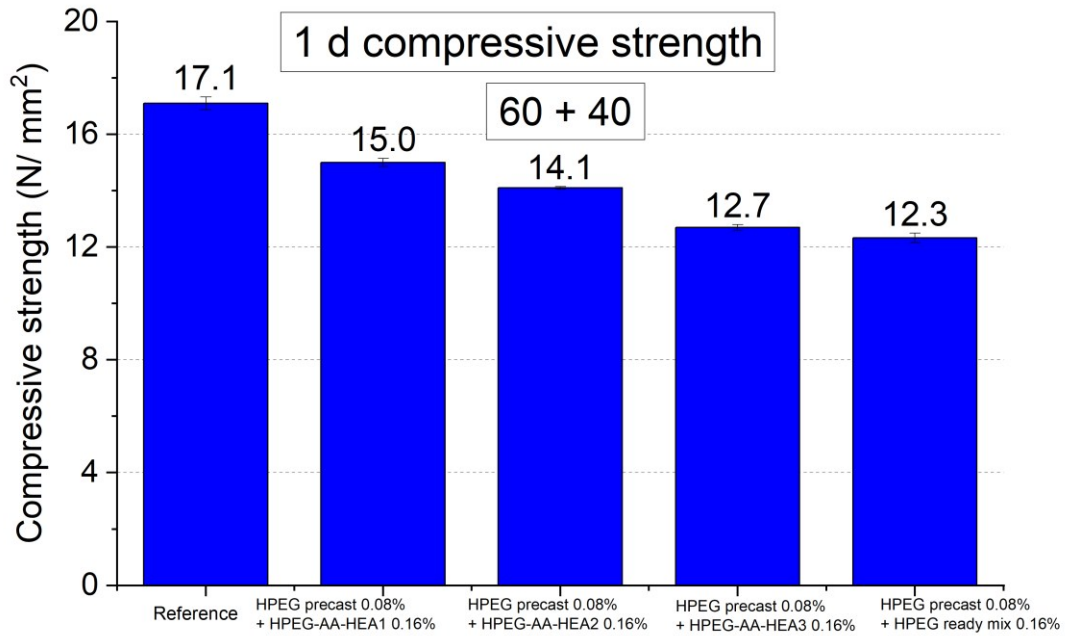
**Figure 73** 1 day compressive strengths of mortar specimens admixed with PCE combination of HPEG ready mix + sodium gluconate (w/b = 0.4)

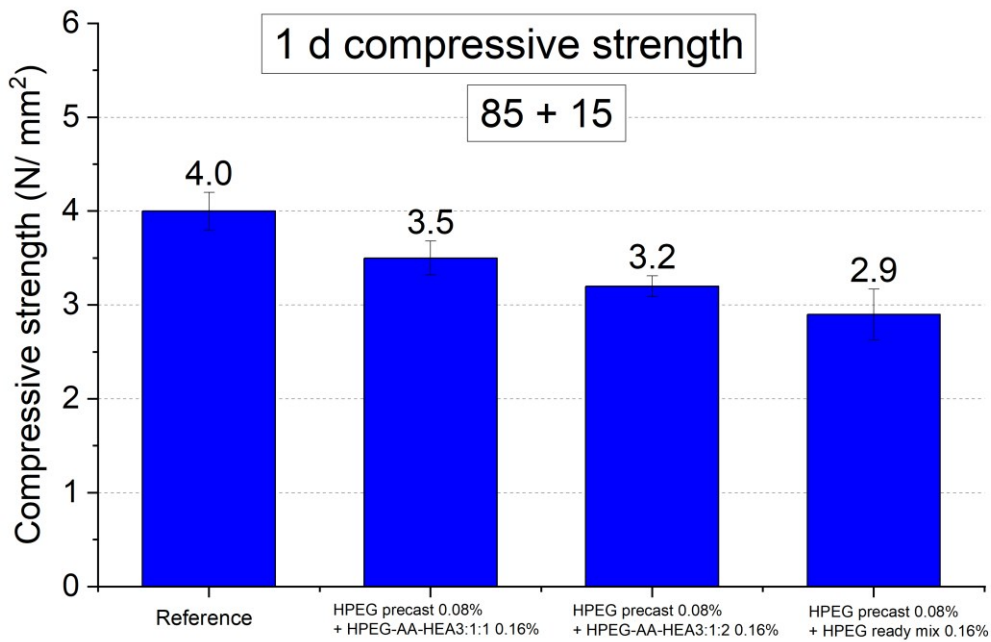
The HPEG-AA-HEAs with different compositions were synthesized and tested to research the influence of hydroxyethyl ester on early strength. It can be seen from **Figure 74**, the 1 d compressive strength for three ‘slag + cement’ systems can be improved by reducing the composition of hydroxyethyl ester. In more detail, the compressive strength of ‘60 + 40’ mortar at the same dosage: HPEG-AA-HEA1 > HPEG-AA-HEA2 > HPEG-AA-HEA3 = HPEG ready mix; the compressive strength of ‘70 + 30’ mortar at the same dosage: HPEG-AA-HEA1 > HPEG-AA-HEA2 > HPEG ready mix; the compressive strength of ‘85 + 15’ mortar at the same dosage: HPEG-AA-HEA1 > HPEG-AA-HEA2 > HPEG ready mix.

The compressive strength tests at low temperature (10 °C) were conducted in 60 + 40 and 70 + 30 mortar with combinations of HPEG precast + 45PC2 and HPEG precast + 50HPEG3 respectively (**Figure 75**). The HPEG precast + 45PC2 combination does not

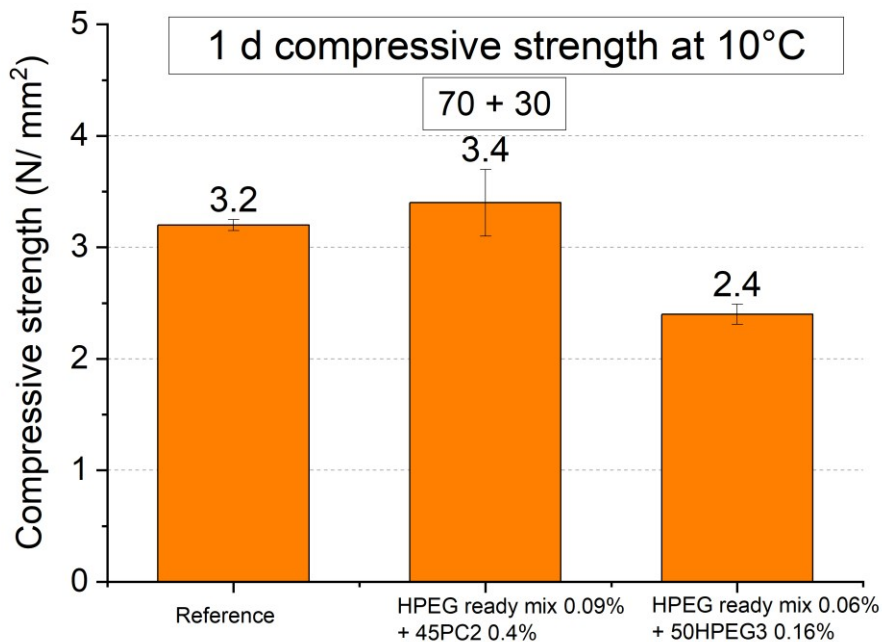
## Results and discussion

decrease the 1 d compressive strength at 10 °C, while the HPEG precast + 50HPEG3 combination induced a bigger reduction in early strength.





**Figure 74** 1 day compressive strengths of mortar specimens admixed with PCE combination of HPEG ready mix + HPEG-AA-HEAs (w/b = 0.4)



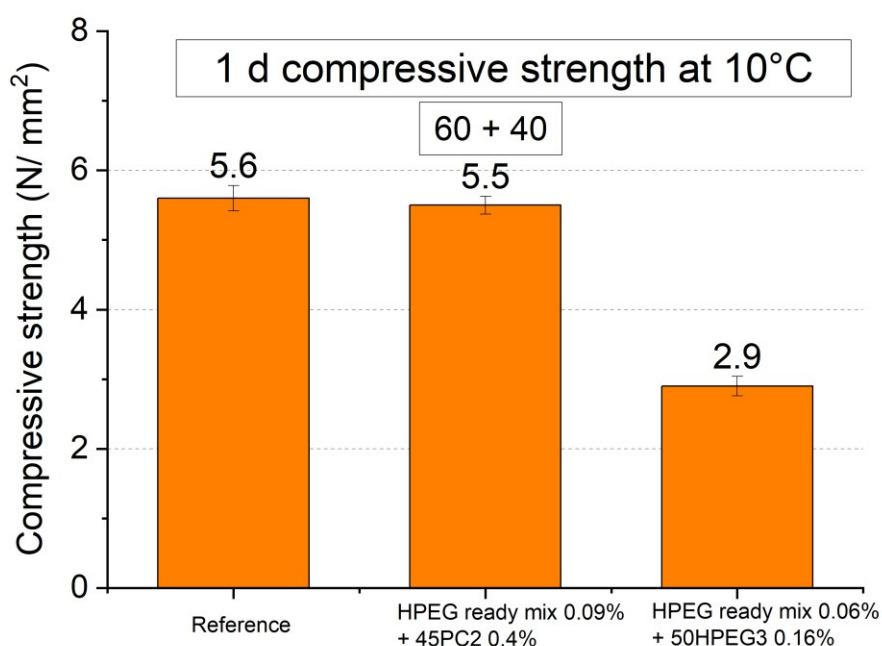


**Figure 75** 1 day compressive strengths of mortars admixed with PCE combination of HPEG ready mix + 45PC2 / 50HPEG3 at 10 °C (w/b = 0.4)

## 5.5.2 PCE superplasticizer for “Full binder” (w/b = 0.31)

### 5.5.2.1 Synthesis of the PCE Polymers

In this part, macromonomer (HPEG-2400/4000,  $M_w = 2400/4000$  Da) containing 52/89 ethylene oxide units was provided by Clariant Deutschland GmbH, Burgkirchen, Germany. The synthesis was conducted by free radical method at 40 °C with APS and VC redox initiators and 3-Mercaptopropionic acid (3-MPA) as a chain transfer agent. Take the synthesis of H-89HPEG8 PCE as an example: 40g of HPEG4000 macromonomer and 40 g of DI water were added in a three-neck flask connected to a mechanical stirrer (400 rpm) and two separate inlets with peristaltic pumps. The flask was placed in an oil bath heated to 40 °C, and the string was for 30 min to dissolve the macromonomers. Next, two solutions were prepared for dropping by peristaltic pumps. Solution A: 5.8 g of AA, 1.2 g of APS, 0.4 g of 3-Mercaptopropionic acid (3-MPA) were dissolved in 30 g of DI water. Solution B: 0.8 g of VC was dissolved in 40 g of

DI water. The reaction time started when solutions A and B were added dropwise into the reaction vessel over 3 hours. After the addition was completed, the reaction was continued for another 2 hours (the total reaction time is 5 hours). It is worth noting that APS in this method was dropped in solution A to avoid aggregation, which often happens when synthesis of HPEG PCE with higher anionic charge density and higher molecular weight. The molecular weight was adjusted by changing the amount of the 3-MPA chain transfer agent. All HPEG-type PCE polymers used in this part were synthesized in the same way with same initiators to get comparable results, their feeding amounts are listed in **Table 25**.

**Table 25** Feeding amounts of the lab synthesized PCE polymers

Samples	HPEG	AA	3-MPA	Feeding molar ratio
	g	g	g	AA: HPEG
L-52HPEG3	40	3.6	0.6	3:1
L-52HPEG4.5	40	5.4	0.8	4.5:1
L-52HPEG6	40	7.2	0.8	6:1
H-52HPEG3	40	3.6	0.3	3:1
H-52HPEG4.5	40	5.4	0.4	4.5:1
H-52HPEG6	40	7.2	0.4	6:1
H-52HPEG8	40	9.6	0.5	8:1
H-89HPEG6	40	4.3	0.4	6:1
H-89HPEG8	40	5.8	0.4	8:1

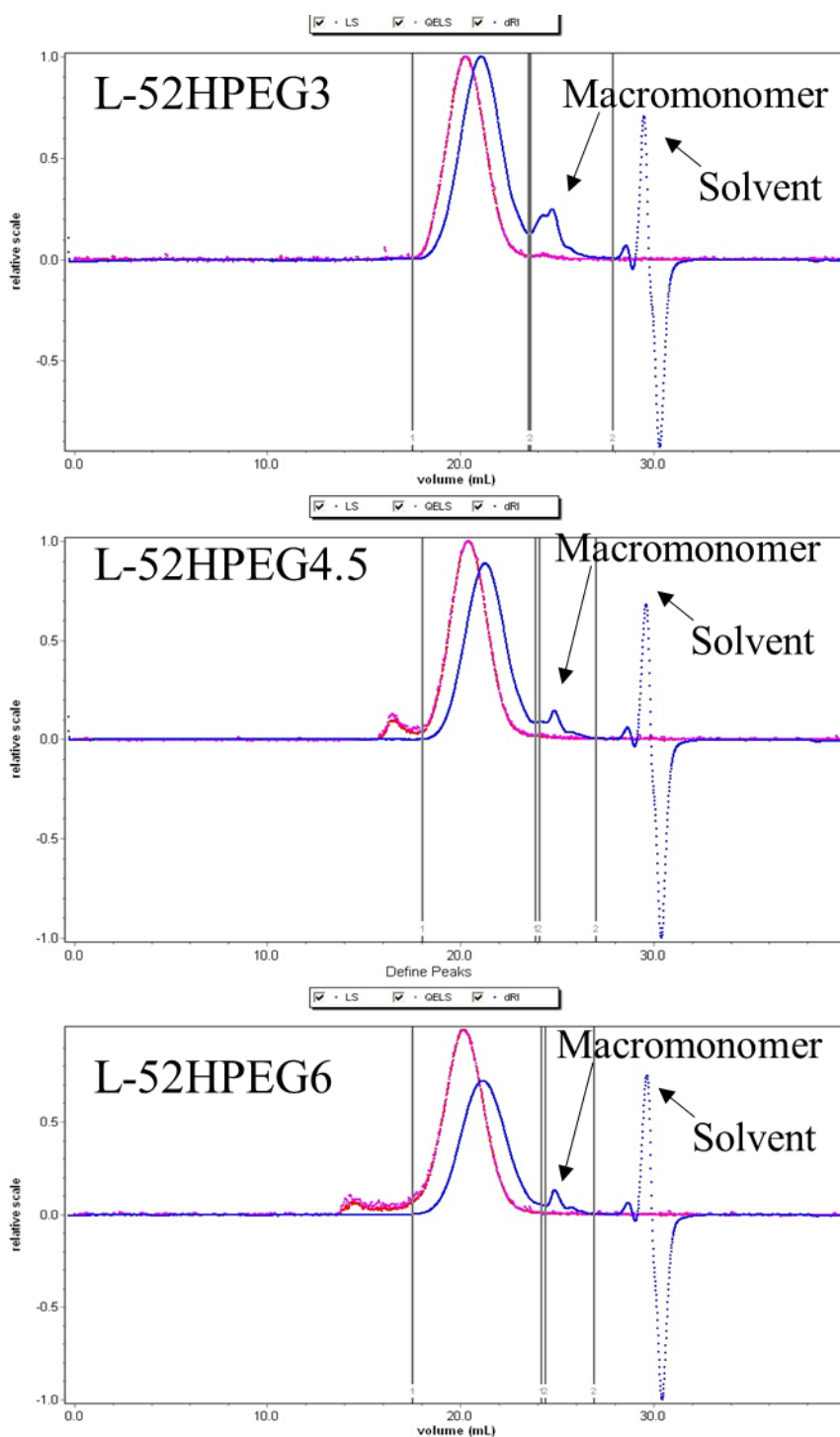
### 5.5.2.2 Characterization of the PCE Polymers

A series of HPEG type PCEs with different feeding molar ratios (AA: HPEG = 3:1, 4.5:1, 6:1 and 8:1) and different molecular weights were prepared applying the free radical synthesis method.

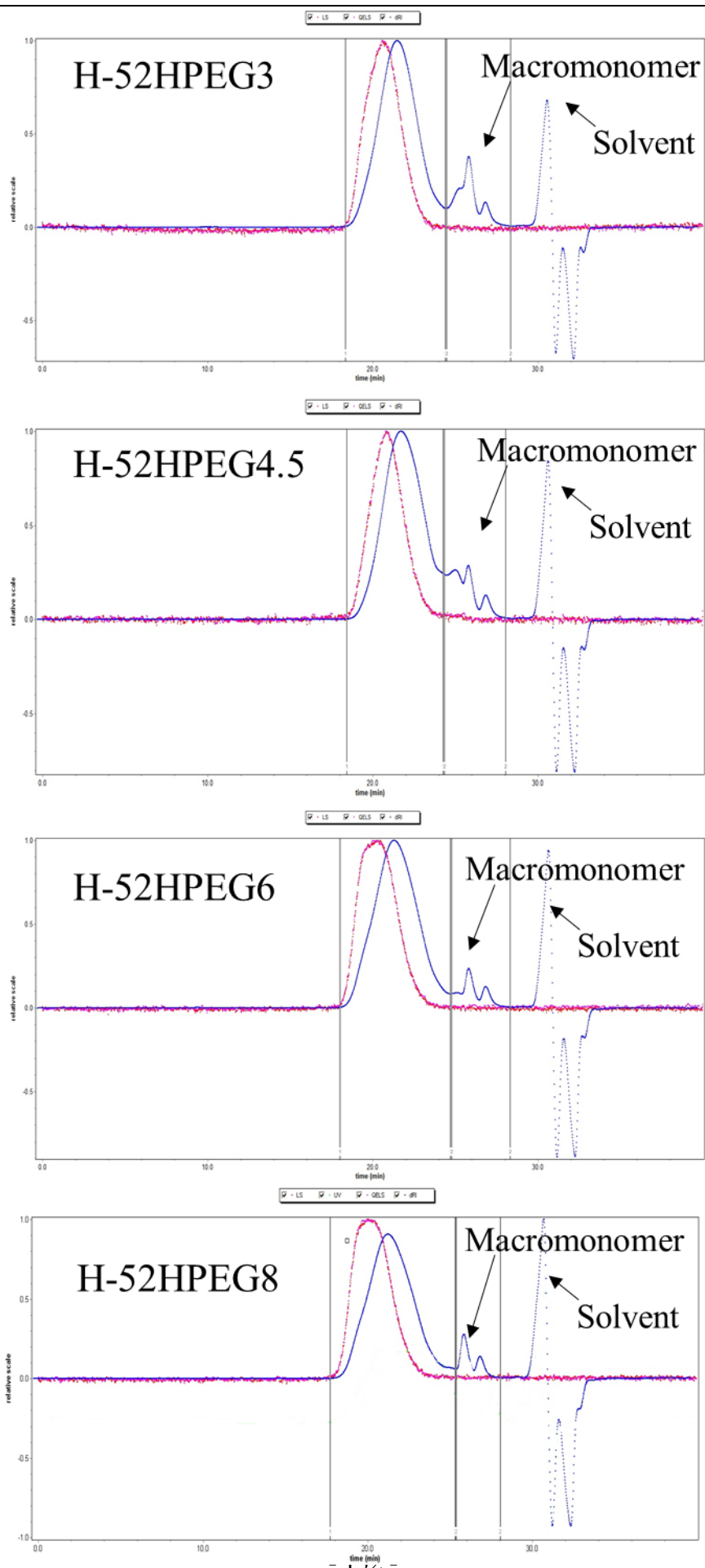
In **Figure 76**, the SEC chromatograms of all synthesized PCE polymers are displayed. For all samples, a large peak appears at ~18 - 26 min elution time signifying the PCE polymer. Furthermore, two minor peaks representing the residual macromonomer and the solvent can be observed. All the HPEG type PCE samples exhibited a relatively low

## Results and discussion

PDI (1.8 - 2.5) and high conversion rates of the macromonomer (84.6 - 93.2 %) which signifies high-quality superplasticizers (see **Table 26**).



## Results and discussion



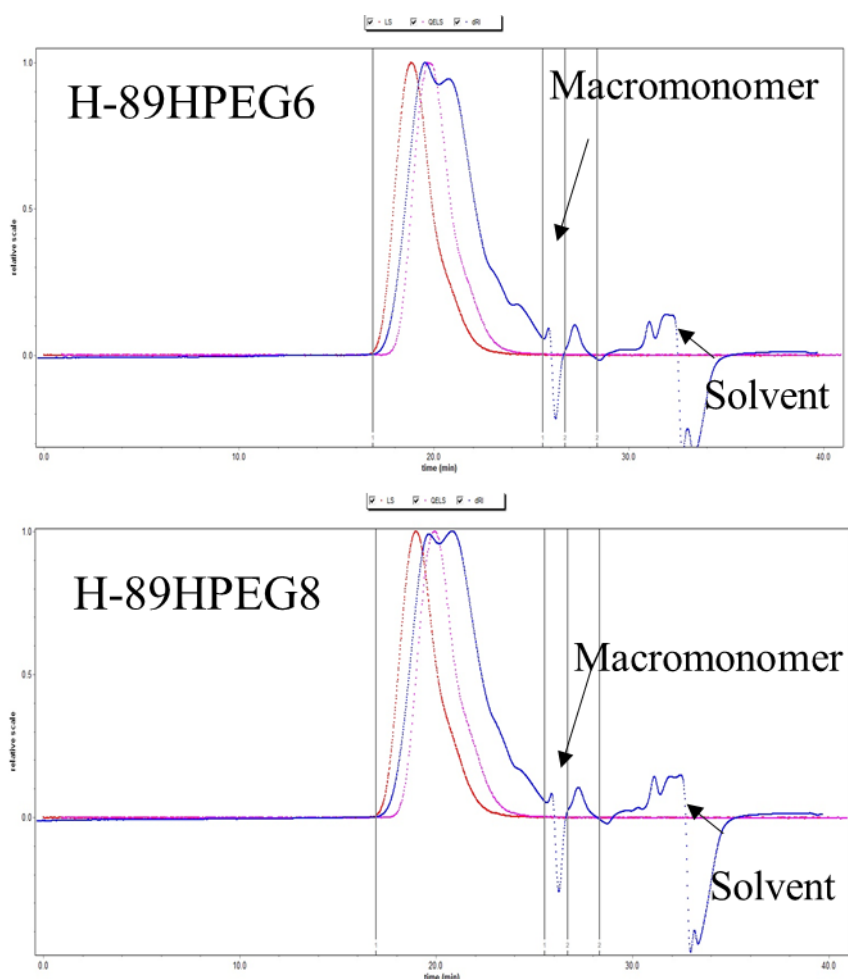


**Figure 76** SEC chromatograms of the synthesized PCE polymer samples

**Table 26** Solid content, molar masses and polydispersity index (PDI) of the lab-synthesized PCE polymers, and the conversion rate of the macromonomer

Sample	Solid content / wt. %	$M_w$ [Da]	$M_n$ [Da]	PDI ( $M_w/M_n$ )	Conversion rate / %
RB-1050	47.7	69,580	28,180	2.5	95.3
PC-1901	50.6	62,850	23,670	2.7	97.3
L-52HPEG3	35.0	29,510	16,120	1.8	87.3
L-52HPEG4.5	33.1	24,660	11,840	2.0	93.2
L-52HPEG6	35.3	28,440	11,210	2.5	94.6
H-52HPEG3	43.5	50,490	24,920	2.0	85.1
H-52HPEG4.5	42.1	50,140	21,610	2.3	84.6
H-52HPEG6	46.3	57,270	22,490	2.5	91.7
H-52HPEG8	43.2	57,550	25,480	2.3	92.0
H-89HPEG6	44.1	60,430	22,530	2.7	91.8
H-89HPEG8	43.6	59,780	23,140	2.5	91.9

### 5.5.2.3 Dispersing Performance of PCE Samples in ‘Full binder’ mortar

The dosage required for each PCE to obtain a  $20 \pm 0.5$  cm spread flow in the ‘Full binder’ mortar was tested at a water-to-binder ratio of 0.31. First, the reference sample RB-1050 exhibits very good dispersing effectiveness as it reaches the  $20 \pm 0.5$  cm spread flow at a dosage of 0.35 % bwob only (see **Figure 77**). Contrary to this, PC-1901 polymer presents no dispersing effectiveness in mortar, even at a dosage as high as 3 % bwob.

Second, the dispersing effectiveness of the lab synthesized HPEG type PCEs was measured and compared with that of RB-1050 polymer. As is shown in **Figure 77 (a)**, mortars containing HPEG type PCEs with low  $M_w$  (24,660 – 29,510 Da) can achieve the same spread flow, but require much higher dosage compared to RB-1050 polymer (0.65 % vs. 0.35 % bwob). The latter polymer has a significantly higher  $M_w$  value of 69,580 Da. Based on this observation, HPEG type PCEs possessing higher  $M_w$  were then synthesized. HPEG type PCEs of higher molecular weight exhibited superior dispersing effectiveness in the ‘Full binder’ mortar as compared to those of lower molecular weight (see **Figure 77 (b)**). Furthermore, their dispersing performance is even more improved when the feeding molar ratio of AA:HPEG is increased to 6:1 or 8:1. The reason behind this could be the higher anionicity leads to increased adsorbed amounts of PCEs on the surface of the ‘Full binder’ particles.

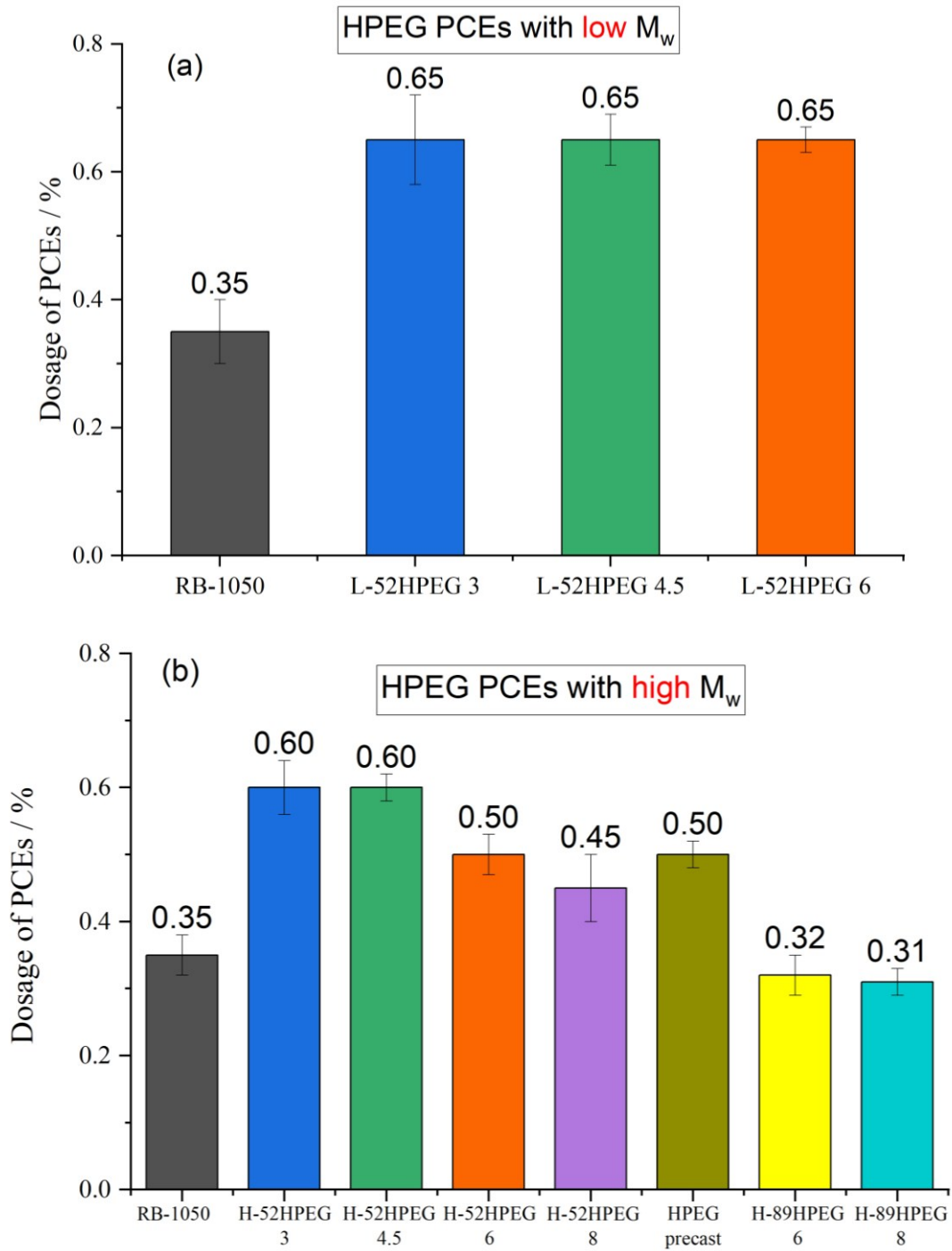
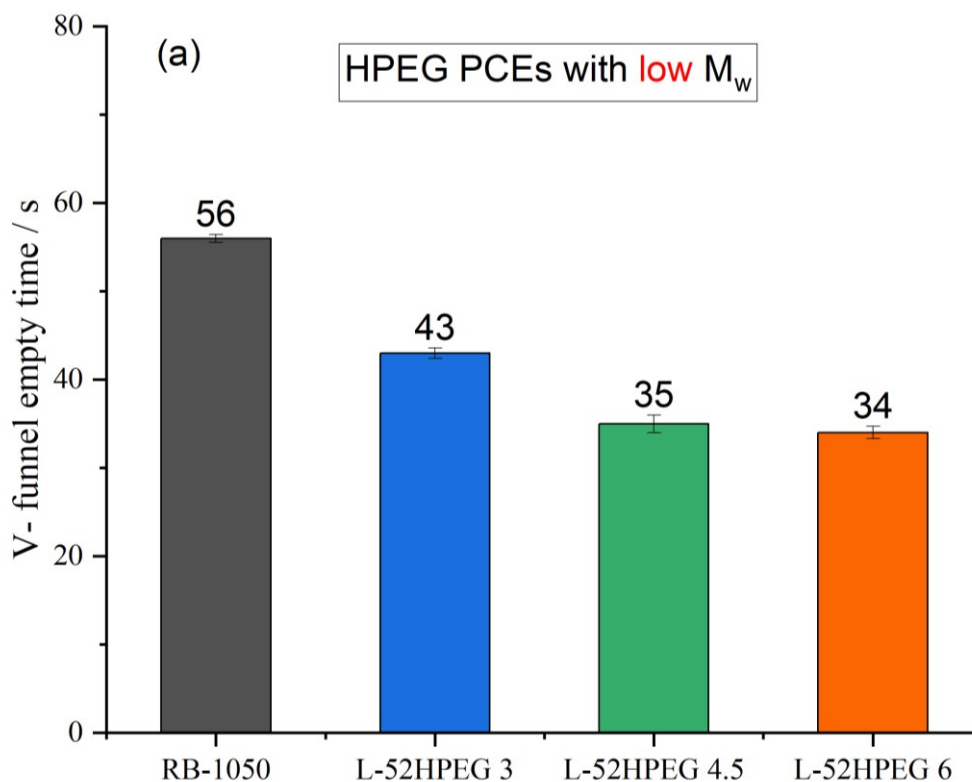


**Figure 77** Dosages of PCEs exhibiting low ( top) and high (bottom) molecular weight required to obtain a mortar spread flow of  $20 \pm 0.5$  cm

#### 5.5.2.4 V-funnel empty time tests

Furthermore, V-funnel empty time tests were conducted at the same water-to-binder ratio of 0.31 as in the mortar tests. Interestingly, most of the HPEG type PCE polymers (except H-52HPEG3 and H-52HPEG4.5) induced a less sticky consistency than RB-1050 polymer, as is demonstrated by significantly faster V-funnel empty times (see **Figure 78**).

Generally, all mortars admixed with lower  $M_w$  HPEG PCEs (L-52HPEG series) show faster V-funnel empty times. Meanwhile, in the H-52HPEG series, those with lower anionicity (molar ratio 3:1 and 4.5:1) contribute to longer empty times, while those with higher anionic character (molar ratio 6:1 and 8:1) result in very short empty times. Among all HPEG type PCEs, H-52HPEG8 produced the best performance regarding the V-funnel empty time test (27 sec vs. 56 sec for RB 1050). This result is similar to that from a commercial HPEG precast PCE (25 sec).



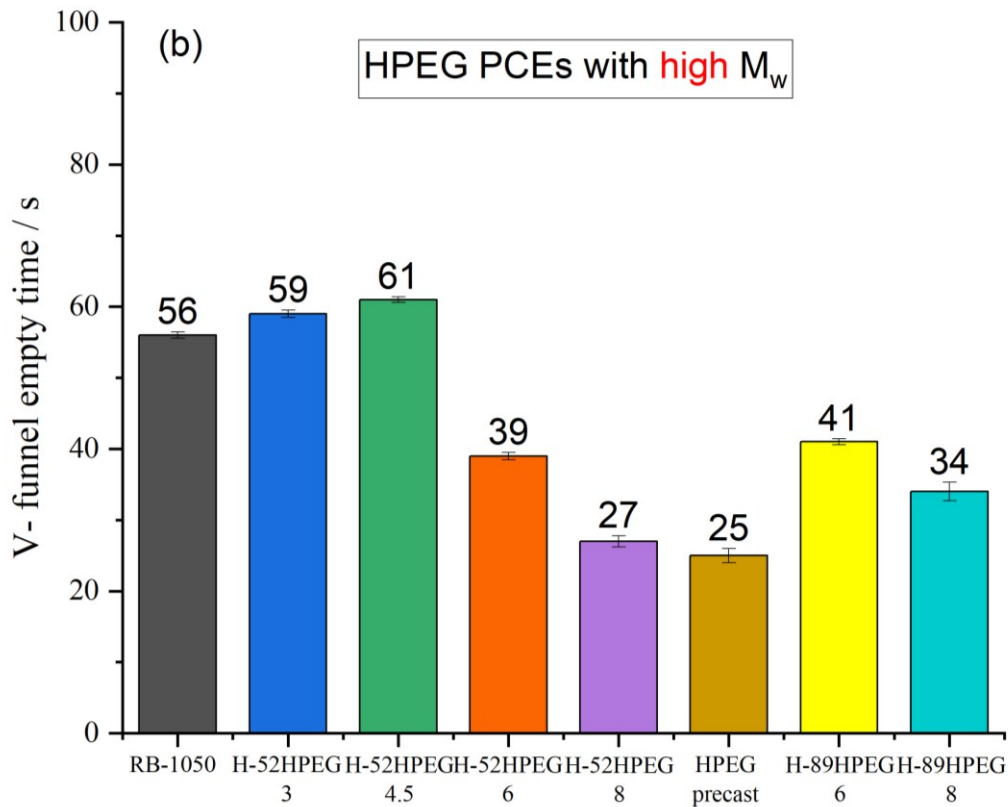


**Figure 78** V-funnel empty times of ‘Full binder’ mortars fluidized with different PCEs (w/b ratio = 0.31)

#### 5.5.2.5 Flow line tests

Next, the spreading behavior of ‘Full binder’ mortars containing different PCEs was investigated in the flow line. H-52HPEG6 produced the best results in the flow line (D30 = 35 cm, final flow = 41 cm), indicating that the mortar admixed with it flows fastest (see **Table 27**). H-52HPEG8 also greatly accelerates the flow in the flow line, presumably because of its higher anionic charge density, while the other HPEG type PCEs produce similar flow line results as RB-1050 polymer. All those samples exhibit similar D30 and final flow values.

The HLB values of all HPEG type PCEs were calculated and are shown in **Table 27**. Generally, their HLB values are close to 20 (18.8 - 19.2), indicating pronounced hydrophilic properties. Still, their chemical composition has an effect on the HLB values. HPEG type PCEs of higher acid-to-ether ratio exhibit lower HLB values, and

produce fast flowing mortars characterized by shorter V-funnel empty times as compared to those of lower acid-to-ether ratio. Furthermore, also the molecular weight strongly influences the flow speed. For example, L-52HPEG6 and H-52HPEG6 possess the same HLB value, but H-52HPEG6 with high molecular weight greatly accelerates the flow speed. Whether the molecular weight or anionic charge dominate the flow behavior of ‘Full binder’ mortar is not clear.

**Table 27** Flow line results of full binder mortar admixed with different PCEs (w/c ratio = 0.31)

Sample	HLB value	D30 (cm)	Final flow (cm)
RB-1050	-	23	30
L-52HPEG3	19.2	22	29
L-52HPEG4.5	19.1	21	24
L-52HPEG6	19.0	24	30.5
H-52HPEG3	19.2	23	29
H-52HPEG4.5	19.1	22	28
H-52HPEG6	19.0	35	41
H-52HPEG8	18.8	28	37
H-89HPEG6	19.3	27	38
H-89HPEG8	19.2	26	36
HPEG precast	-	22	30

### 5.5.3 PCE superplasticizer for “Full binder” (w/c = 0.27)

#### 5.5.3.1 Synthesis of the PCE Polymers

All HPEG-type PCE polymers except 52HPEG8-DADMAC0.1 (M2) used in this part were synthesized in the same way as described in **Section 5.5.2**. The feeding amounts are listed in **Table 28**. Take 89HPEG8-DADMAC0.1 as an example: 40g of HPEG4000 macromonomer and 30 g of DI water were added in a three-neck flask connected to a mechanical stirrer (400 rpm) and two separate inlets with peristaltic pumps. The flask was placed in an oil bath heated to 40 °C, and the string was for 30 min to dissolve the macromonomers. Next, two solutions were prepared for dropping

## Results and discussion

by peristaltic pumps. Solution A: 5.8 g of AA, 1.2g of APS, 0.25 g of DADMAC monomer (65 % solid content), 0.4 g of 3-Mercaptopropionic acid (3-MPA) were dissolved in 30 g of DI water. Solution B: 0.8 g of VC dissolved in 40 g of DI water. The reaction time started when solutions A and B were added dropwise into the reaction vessel over 3 hours. After the addition was completed, the reaction was continued for another 2 hours (the total reaction time is 5 hours). The synthesis of 52HPEG8-DADMAC0.1 (M2) was conducted in a way that the DADMAC monomer solution was directly added to the flask after the macromonomer was dissolved. Then, start adding solution A and solution B.

The synthesis of MPEG-type was realized at 80 °C with APS as initiator and 3-MPA as chain transfer agent. The synthesis procedure was published in [19]. Take 45PC6-DADMAC0.1 as an example: 50 g DI water was added in a 250 ml three-neck flask connected to a mechanical stirrer (380 rpm) and two separate inlets with peristaltic pumps. The flask was placed in an oil bath heated to 80 °C. Prepare solution A: 60 g MPEG2000, 15.4 g of AA, 0.75 g of DADMAC monomer (65 % solid content), 1.45 g of 3-MPA; Solution B: 1.67 g of APS and 65 g DI water. The reaction time started when solutions A and B were added dropwise into the reaction vessel over 4 hours and 5 hours, respectively. After the addition was completed, the reaction was continued for another 1 hour.

**Table 28** Feeding amounts of the synthesized PCE polymers

Sample	HPEG g	AA g	DADMAC g	3-MPA g	Feeding molar ratio
45PC6-DADMAC0.1	60	15.4	0.48	1.45	6:1:0.1
45PC6-DADMAC0.5	60	15.4	2.4	1.45	6:1:0.5
89HPEG8-DADMAC0.1	40	5.8	0.16	0.4	8:1:0.1
89HPEG8-DADMAC0.5	40	5.8	0.8	0.4	8:1:0.5
52HPEG8-DADMAC0.1	40	9.6	0.27	0.8	8:1:0.1
52HPEG8-DADMAC0.1 (M2)	40	9.6	1.35	0.8	8:1:0.1

### 5.5.3.2 Characterization of the PCE Polymers

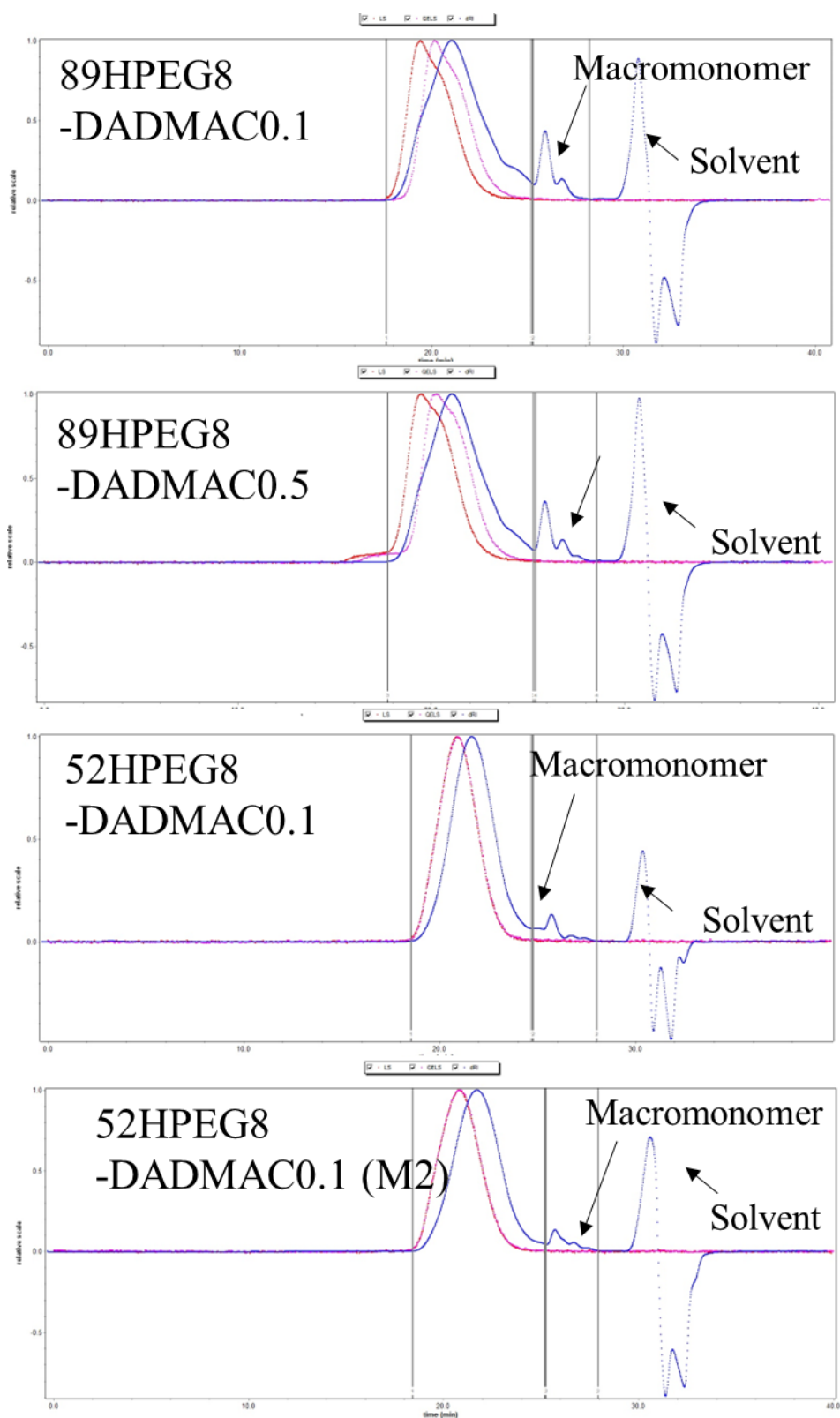
Series of HPEG and MPEG-types PCEs containing different feeding molar of DADMAC cationic monomers (DADMAC: macromonomer = 0.1:1 and 0.5:1) were synthesized by the free radical copolymerization method. The physical and chemical properties of such lab synthesized zwitterionic PCEs are listed in the **Table 29**. All of the PCE samples exhibited relatively high conversion rates of the macromonomer (83.8 - 95.2 %), which signifies high-quality superplasticizers.

The SEC chromatogram measurement was used to detect the chemical composition of PCE polymers, and the spectra are displayed in **Figure 79**. For all samples, a large peak appears at ~18 - 26 min elution time, signifying the PCE polymer. Furthermore, two minor peaks representing the residual macromonomer and the solvent can be observed.

**Table 29** Solid content, molar masses and polydispersity index (PDI) of the lab-synthesized PCE polymers, and the conversion rate of the macromonomer

Sample	Solid content / wt. %	$M_w$ [Da]	$M_n$ [Da]	PDI ( $M_w/M_n$ )	Conversion rate / %
45PC6-DADMAC0.1	29.5	80,700	20,210	3.9	83.8
45PC6-DADMAC0.5	38.6	111,110	22,530	4.9	84.6
89HPEG8-DADMAC0.1	44.2	52,000	17,330	3.0	89.8
89HPEG8-DADMAC0.5	44.5	49,610	17,800	2.8	91.0
52HPEG8-DADMAC0.1	40.4	28,450	14,460	1.9	94.9
52HPEG8-DADMAC0.1 (M2)	40.5	28,910	13,640	2.1	95.2

## Results and discussion



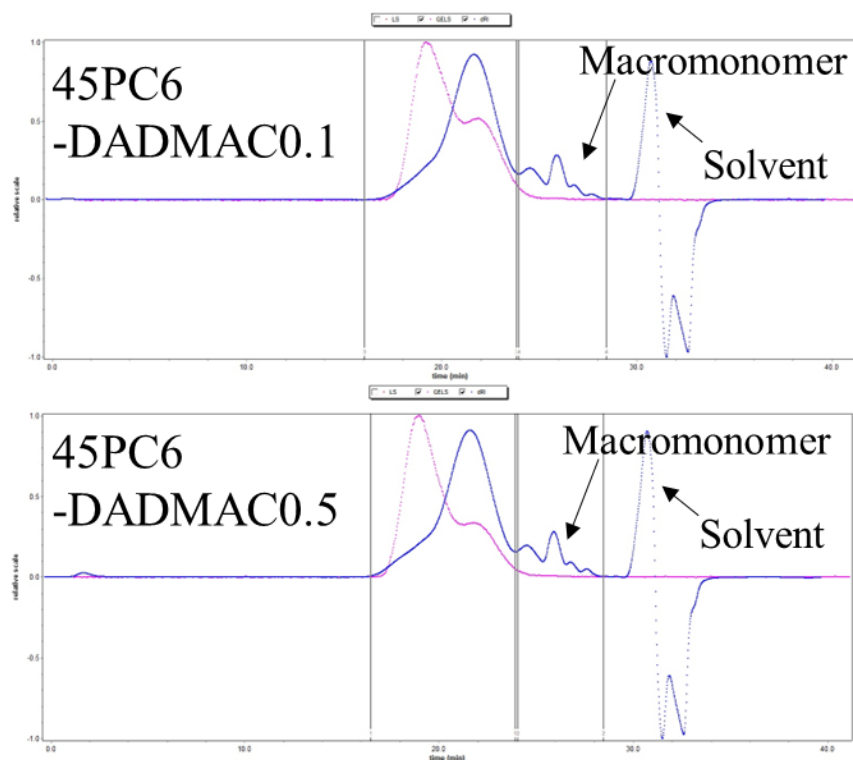


**Figure 79** SEC spectra of the synthesized zwitterionic PCE polymer samples

### 5.5.3.3 Dispersing Performance of zwitterionic PCE Samples in ‘Full binder’ mortar

The application properties of these zwitterionic PCEs was tested in mortar. Firstly, the initial spread flow value in the ‘Full binder’ mortar was tested at a lower water-to-binder ratio of 0.27. The 89HPEG8 superplasticizer was used as a reference. At the beginning, the mortar tests were conducted under normal mixing procedure (4 min), and the PCE dosage was set at 1 % bwob to check whether this superplasticizer could disperse the ‘Full binder’ mortar under such low water-to-binder ratio. As expected, all of the zwitterionic PCEs (45MPEG6-DADMAC0.1, 45MPEG6-DADMAC0.5, 89HPEG8-DADMAC0.1 and 89HPEG8-DADMAC0.5) could disperse the ‘Full binder’ mortar because of their high anionic charge density and long side chains (**Figure 80**). The zwitterionic PCEs even show slightly better dispersing effectiveness compared to the reference PCE 89HPEG8.

## Results and discussion

When compare the performance of different macromonomers, the zwitterionic PCEs based on 89HPEG macromonomer show better dispersing effectiveness than that of 45MPEG type zwitterionic PCEs. This superior dispersing effectiveness can be owed to the stronger steric effect from the longer side chains in 89HPEG macromonomer.

Additionally, the content of cationic monomer DADMAC seems had no obvious influence on the dispersing performance as the spread flows containing 45MPEG/89HPEG-DADMAC0.1 and 45MPEG/89HPEG-DADMAC0.5 are quite similar (18.7 cm vs. 18.1 cm; 20.1 cm vs. 19.9 cm). Therefore, introducing 0.1 molar DADMAC for one molar macromonomer was enough to provide PCEs with better dispersing effectiveness.

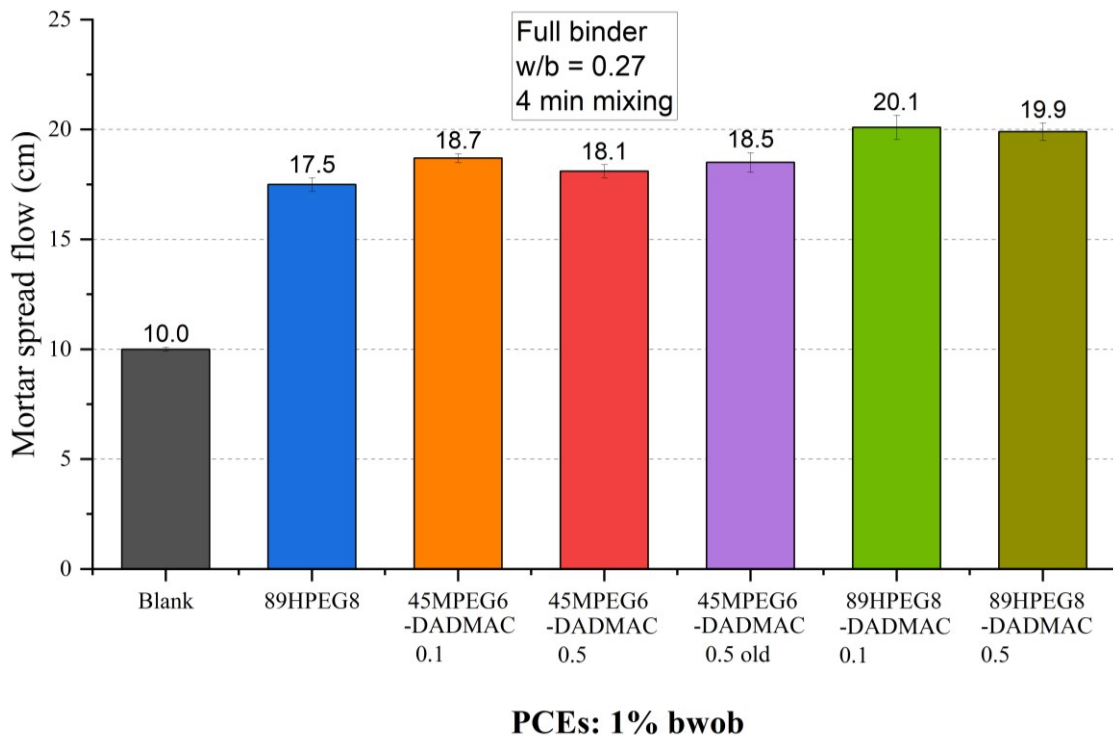


**Figure 80** Initial spread flow of PCEs at a 0.27 w/b ratio with 1 % bwob dosage

Secondly, the influence of PCE dosages on the initial spread flow of ‘Full binder’ mortar at a very low water-to-binder ratio was determined. As shown in **Figure 81**, the initial spread flow of the ‘Full binder’ mortar was slightly increased when increasing

the PCE dosage from 0.40 % bwob to 0.50 % bwob. Further increasing the PCE dosage to 0.65 % bwob did not improve the spread flow except 89HPEG8-DADMAC0.1 PCE. It seems that the saturated adsorption platform for 89HPEG8 and 45MPEG6-DADMAC0.1 are around 0.5 % bwob whereas 89HPEG8-DADMAC0.1 polymer has a higher saturated adsorption platform. In order to improve the initial spread flow of the ‘Full binder’ mortar at very low water-to-binder ratio, the 6.5 min mixing procedure (normal mixing procedure and 2.5 min fast speed mixing) was applied in the flowing tests.

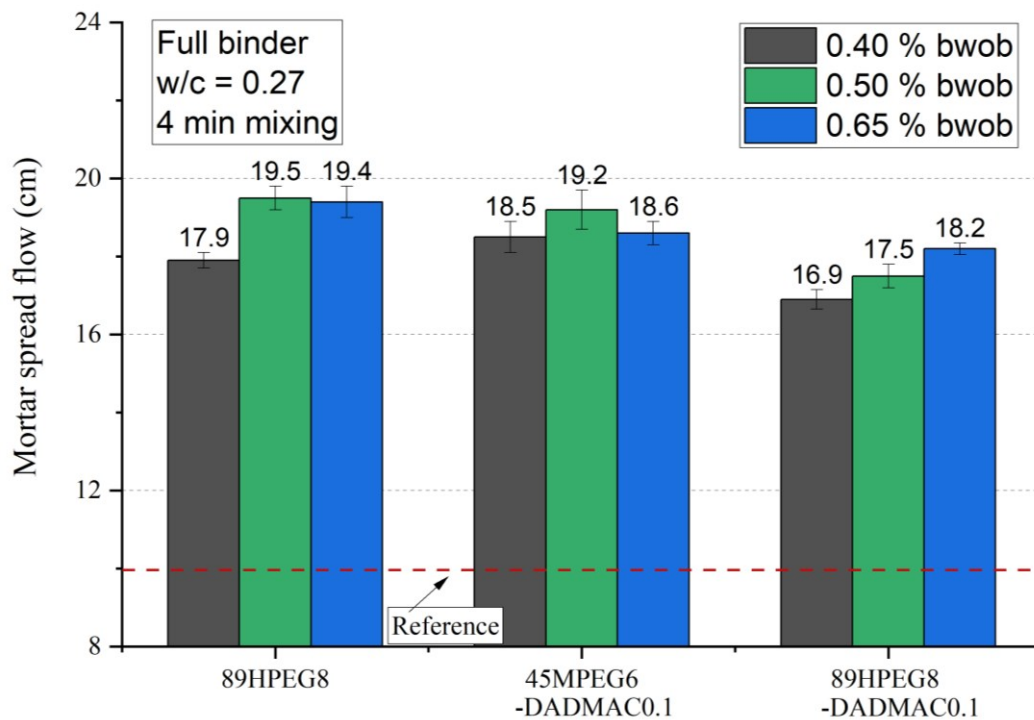


**Figure 81** Initial spread flow of PCEs at 0.27 w/b ratio with different dosages

In this part, another important application property - slump retention performance of zwitterionic PCE in the ‘Full binder’ mortar - was also tested at a water-to-binder ratio of 0.27. As mentioned before, the mixing procedure greatly influenced the spread flow of the mortars. As displayed in **Figure 82**, the 6.5 min mixing procedure provided a bigger initial spread flow within the error range ( $\pm 0.5$  cm) and eliminated the undesired retarding effect.

## Results and discussion

Next, the effect of HPEG-DADMAC PCEs' chemical compositions and side chain lengths on the slump retention performance was determined (see **Figure 83**). All of the zwitterionic PCEs exhibit superior slump retaining ability than that of Optima100 polymer and 'HPEG precast + 89HPEG3' PCE combination within the error range ( $\pm 0.5$  cm). 89HPEG8-DADMAC0.1 with longer side chains can achieve the same spread flow at a relatively lower dosage compared to 52HPEG8-DADMAC0.1 (0.9 % bwob vs. 1.2 % bwob). 52HPEG10-DADMAC0.1 polymer with higher anionic monomer (AA) amount exhibits better dispersing effectiveness but relatively worse slump retention performance. In addition, the influence of the synthesis methods on the slump retention performance of 52HPEG8-DADMAC0.1 PCEs was tested. It can be found from **Figure 84** that the initial spread flow was decreased when DADMAC was dissolved in flask with macromonomer, whereas the slump retention curve has a similar tendency to the 52HPEG8-DADMAC0.1 polymer.

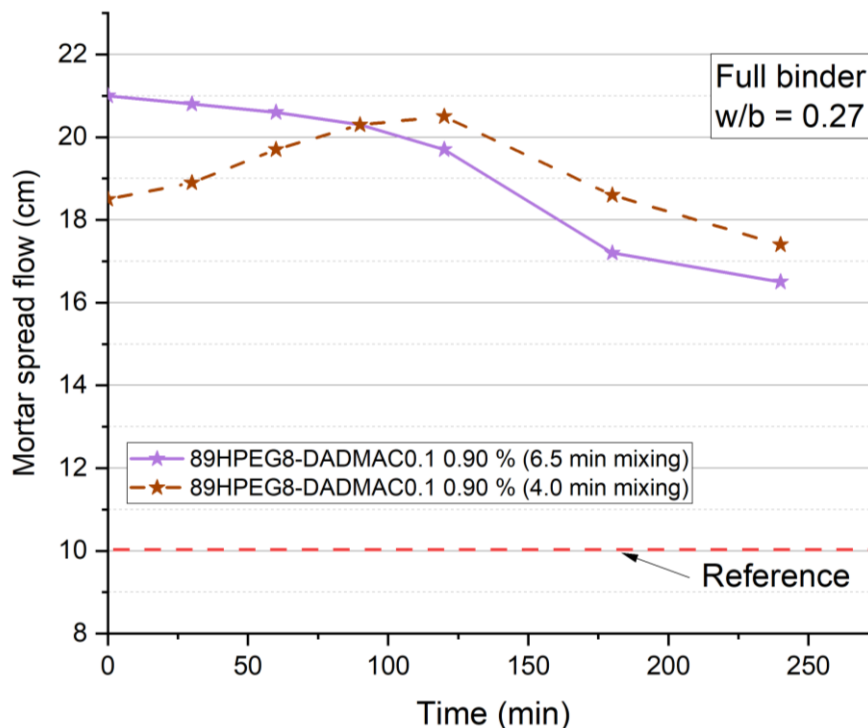


**Figure 82** Slump retention of 'Full binder' mortar containing 89HPEG8-DADMAC0.1 under different mixing procedures

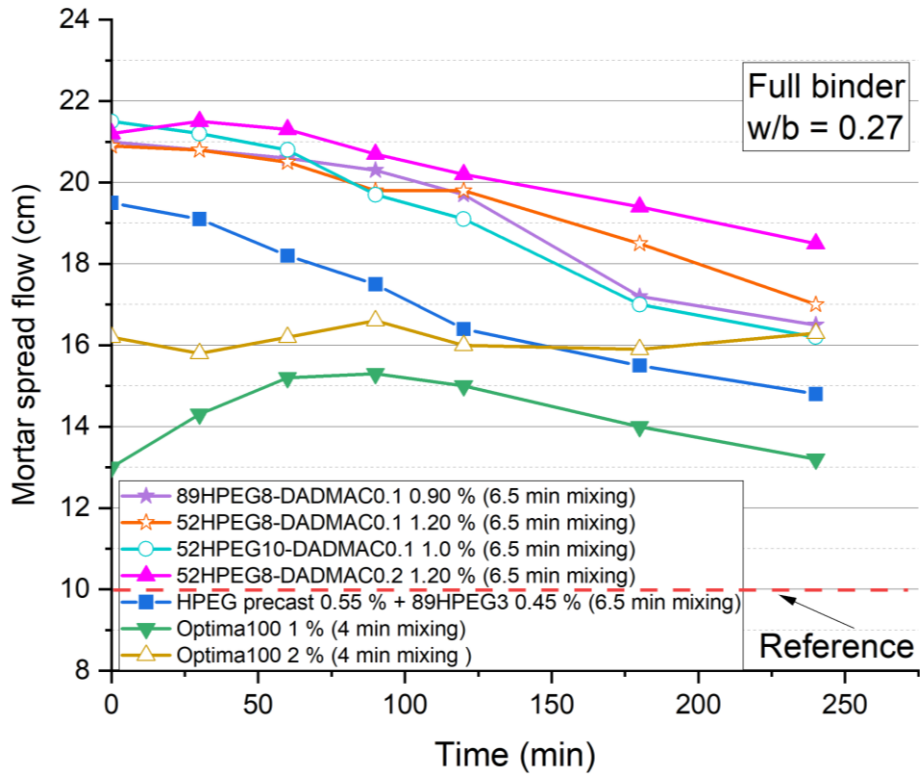


**Figure 83** Slump retention of ‘Full binder’ mortar containing different HPEG-DADMAC PCEs

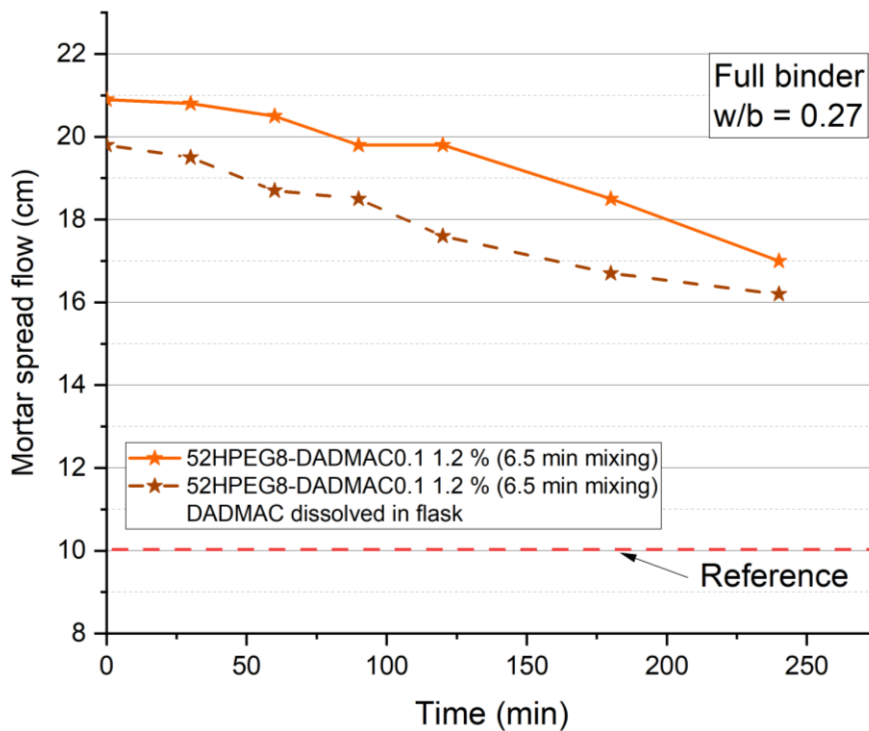


**Figure 84** Slump retention performance of 52HPEG8-DADMAC0.1 PCEs obtained by different synthesis methods

### 5.5.3.4 V-funnel empty time tests

As shown in **Figure 85**, all of the ‘Full binder’ mortar fluidized with HPEG-DADMAC zwitterionic PCEs have shorter V-funnel empty times (within 60 sec) than that with Optima100 (more than 300 sec) and ‘HPEG precast + 89HPEG3’ PCE combination (113 sec). The 89HPEG8-DADMAC0.1 zwitterionic PCE has the shortest V-funnel empty times. Further increasing the DADMAC amount to 0.2 can slightly shorten the empty times from 35 sec to 33 sec.

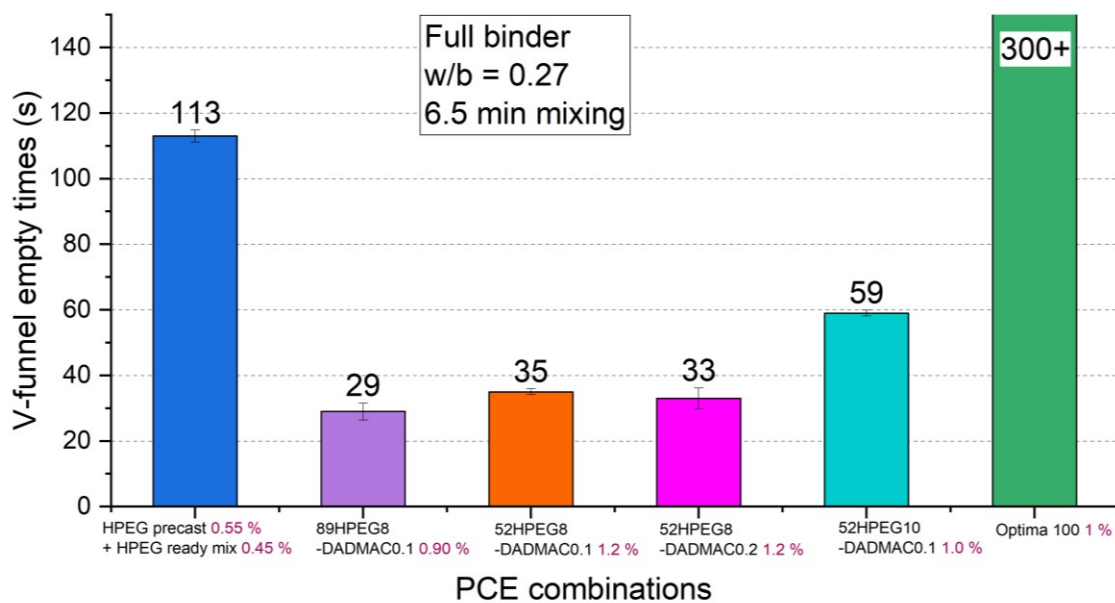


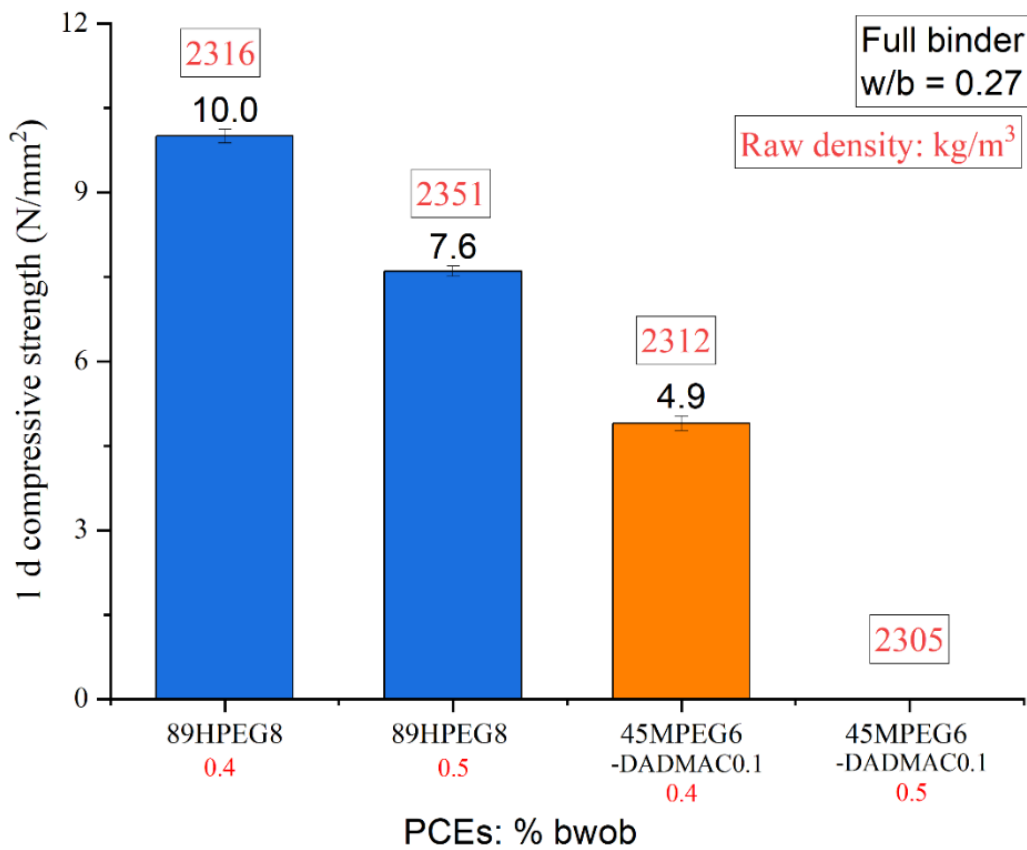
**Figure 85** V-funnel empty times of ‘Full binder’ mortar fluidized with different HPEG-DADMAC PCEs

### 5.5.3.5 Compressive strength tests

The early compressive strength is another critical property for the ‘Full binder system’. As shown in **Figure 86**, the 1 d compressive strength was greatly decreased as the PCE dosage increased from 0.4 % bwob to 0.5 % bwob. Thereafter, the PCE dosage was set at 0.4 % bwob to check the influence of different PCEs on 1 d and 3 d compressive strength (see **Figure 87**). The 1 d compressive strength of mortars admixed with HPEG-type zwitterionic PCEs 89HPEG8-DADMAC were slightly strengthened compared to

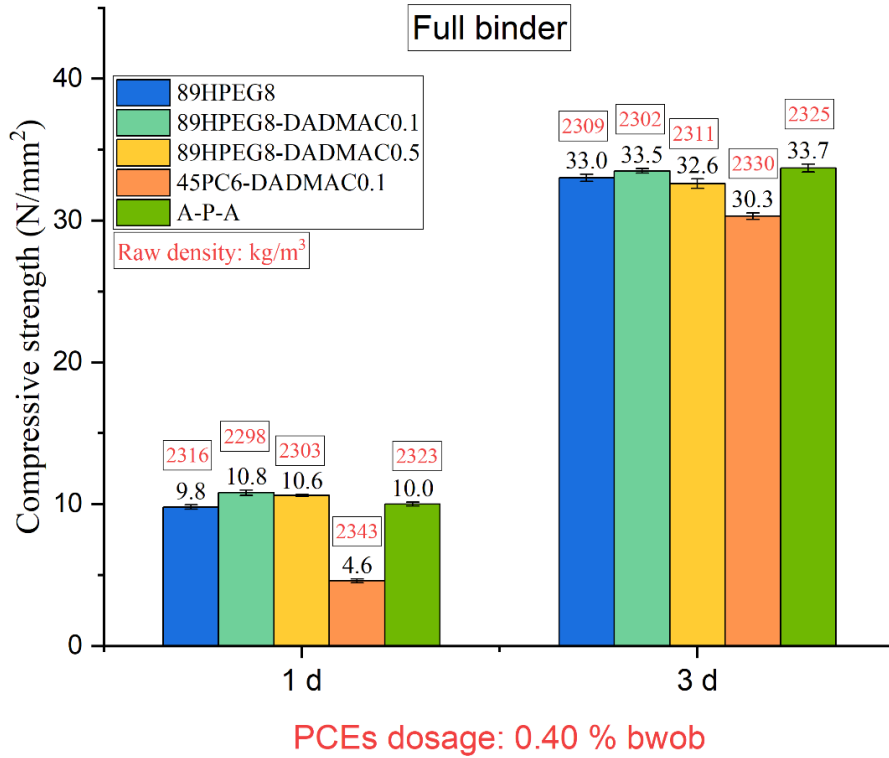
that with 89HPEG8 polymer, while the addition of 45PC6-DADMAC PCE causes a great reduction in the early strength, and this reduction in compressive strength was not apparent after 3 days hydration.

However, the spread flow at such a lower dosage is not good enough for application (around 18 cm). Some PCE combinations were applied in this test, unfortunately, only the ‘HPEG precast + 89HPEG3’ PCE combination could provide ‘Full binder’ mortar good workability without significantly hindering the early compressive strength (see **Figure 88**).

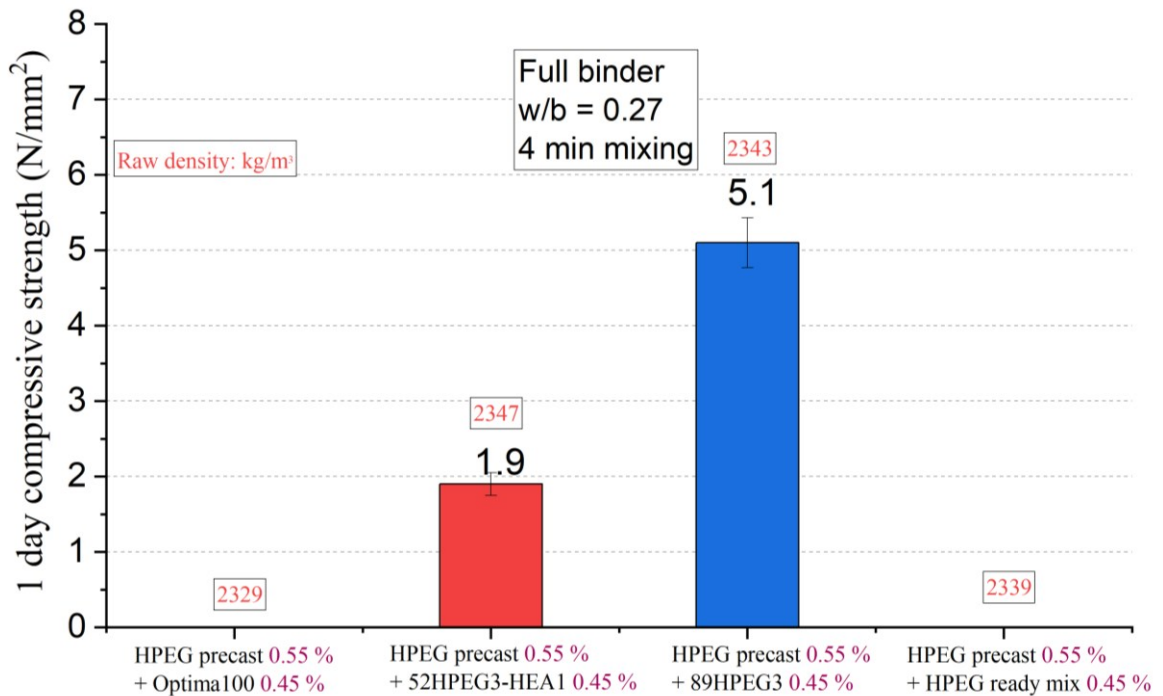


**Figure 86** 1 d compressive strength of ‘Full binder’ mortar admixed with PCEs at different dosage

Results and discussion



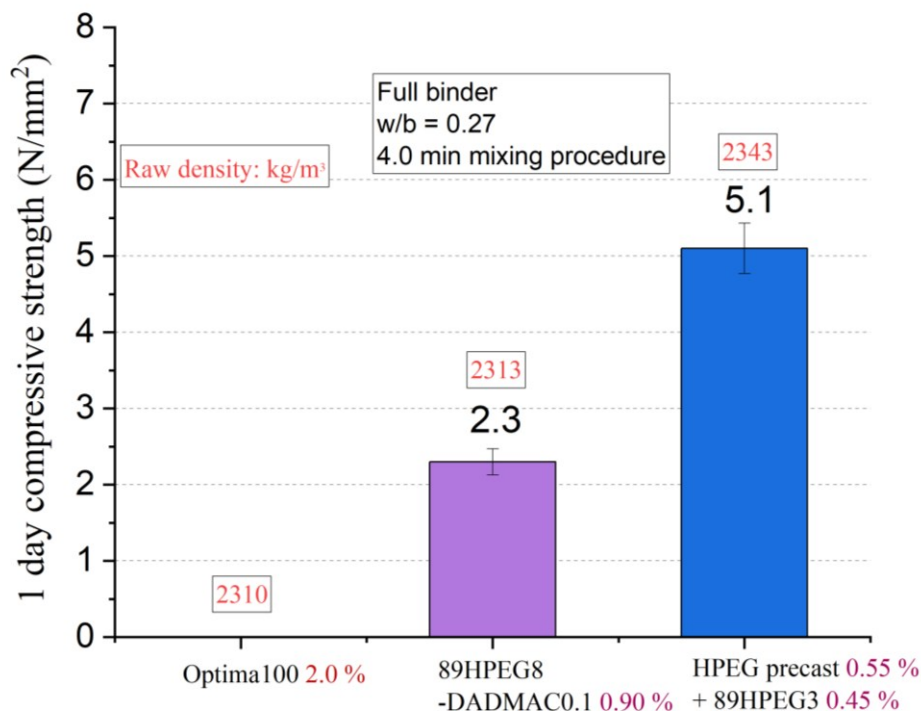
**Figure 87** Compressive strength (1 d and 3 d) of ‘Full binder’ mortar containing different PCEs



**Figure 88** Early compressive strength (1 d) of ‘Full binder’ mortar containing different PCE combinations

## Results and discussion

As discussed, extending the mixing time will help the PCE superplasticizer better adsorb on the surface of cement particles, thereby increasing the mortar spread flow. The 6.5 min mixing procedure also strengthens the 1 d compressive strength (**Figure 89**). Therefore, all of the following tests were conducted under a 6.5 min mixing procedure. The early compressive strength (1 d and 3 d) of standard mortar admixed with 89HPEG8-DADMAC0.1 and 'HPEG precast + 89HPEG3' PCE combination were shown in **Figure 90**. 'HPEG precast + 89HPEG3' PCE combination had less retarding effect than 89HPEG8-DADMAC0.1 superplasticizer. Next, zwitterionic PCEs based on 52HPEG macromonomer, which is more available in commercial production, were tested. Unfortunately, all of the standard mortars containing 52HPEG-DADMAC PCEs did not harden after 1 day of hydration, so the instrument could not detect the values. The 3 d compressive strength were still weaker than that with 89HPEG8-DADMAC0.1 zwitterionic PCE (see **Figure 91**).



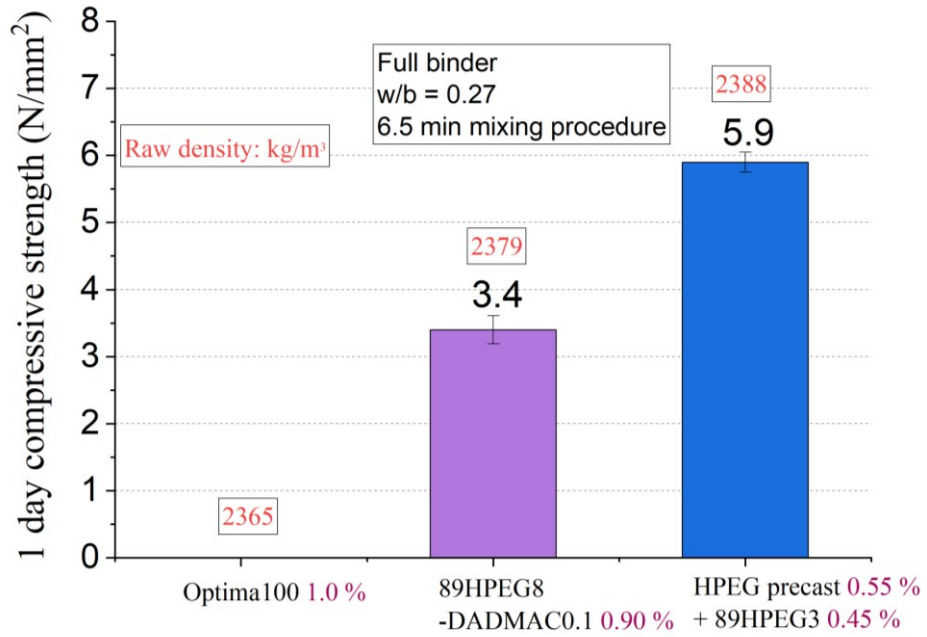


**Figure 89** Early strength (1 d) of ‘Full binder’ mortar under different mixing procedure: 4.0 min mixing (top); 6.5 min mixing procedure (bottom)

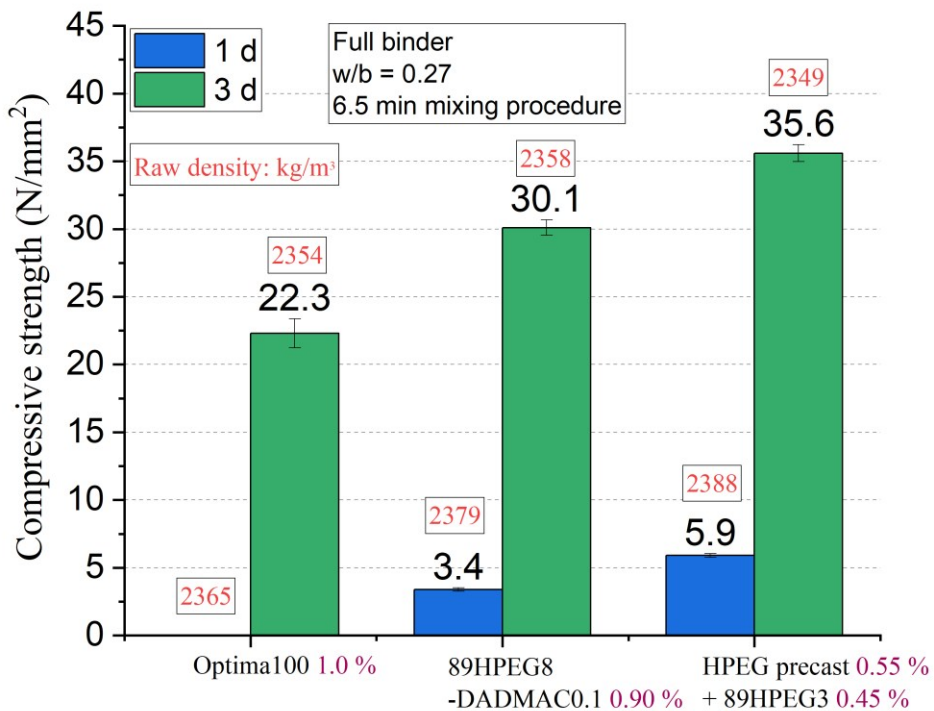


**Figure 90** Compressive strength (1 d, 3 d) of ‘Full binder’ mortar under 6.5 min mixing procedure

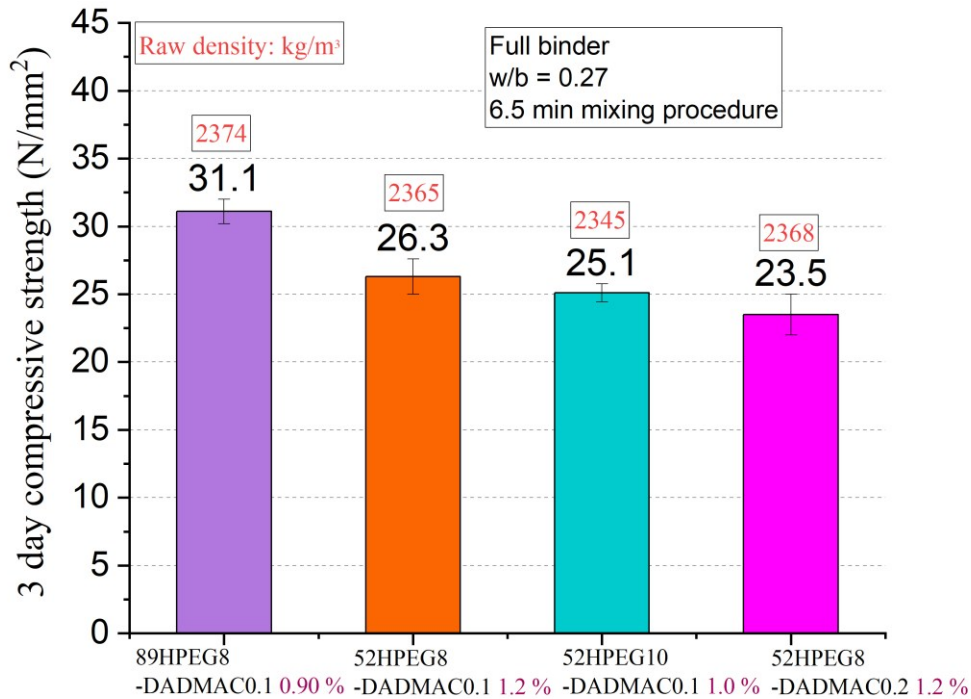


**Figure 91** 3 d compressive strength of ‘Full binder’ mortar containing different PCEs

#### 5.5.4 Summary of Section 5.5

In this Section, PCE superplasticizers and PCE combinations were successfully synthesized and applied in the slag blended cementitious material. Slag is easier to be fluidized than OPC cement. Hence lower PCE dosages are required as the slag content increase. On the other hand, the slump retention becomes increasingly difficult with increasing slag content.

PCE polymers with low anionicity are more effective slump retention than these with less anionic character. This behaviour is similar as OPC. To achieve 2 - 3 hours of slump retention, low dosage PCEs based on hydroxyethyl ester are required. Unfortunately, these slump retainers strongly reduce early strength (1 d). For the slag rich 85 + 15 binder, new PCE polymers without ester need to be developed which are less or not at all retarding.

The study of “Full binder” cementitious materials with a water-to-binder ratio of 0.31 indicates that HPEG-type PCE polymers with higher molecular weight and greater anionic charge demonstrate better dispersing ability. On the other hand, PCE superplasticizers with lower molecular weight leads to a quicker V-funnel empty time. When the water-to-binder ratio was further reduced to 0.27, HPEG-type PCE struggled to disperse this binder effectively, even at a high PCE dosage (1 %). Increasing the mixing time from 4 min to 6.5 min can enhance the flow of mortar by aiding the full distribution and adsorption of PCE polymer on the surface of the binder particles. The ‘Full binder’ requires novel and optimized superplasticizers, successful identification of suitable HPEG PCE and zwitterionic PCE products achieved.

## 5.6 Novel structured PCE superplasticizers

In this part, PCE superplasticizer with novel structure were synthesized and tested in mortar. Gradient or block structured copolymers have special thermal and interfacial properties because they exhibit gradual changes in sequence structure. Controlled radical polymerization (CRP) techniques, including nitroxidemediated polymerization (NMP), atom transfer radical polymerization (ATRP) and reversible addition-fragmentation chain transfer (RAFT) methods, were widely used to synthesize gradient copolymers. These methods are very useful, but they are not easy to apply in the real industry. Therefore, this part investigated the potential of free radical methods to produce PCE polymer with novel structure.

### 5.6.1 Synthesis of PCE via free radical copolymerization

There are two main strategies to synthesize gradient polymers: 1) when two monomers with similar reactivity ratio continuously feed one monomer into the solution of the second monomer through the polymerization, also called the forced gradient method; 2) the batch method takes advantage of two monomers with a big difference in reactivity ratio. Theoretical reactivity of HPEG and AA monomers used in this thesis are quite different. The designed segment sequence of three PCE copolymers is illustrated in **Figure 92**.

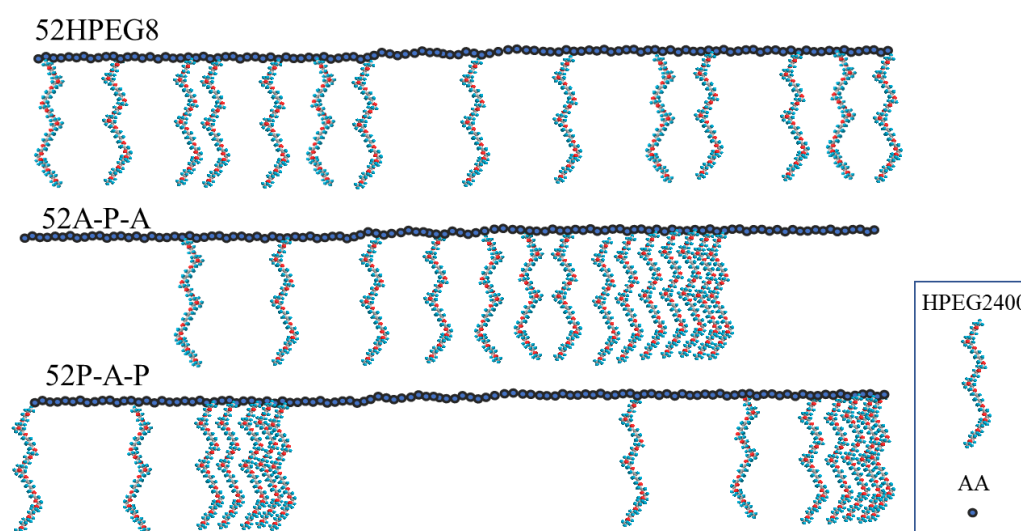


**Figure 92** Conceptual sketch of three PCEs with different sequence structures

The synthesis process of these three polymers is described as follows:

52HPEG8: 40g of HPEG macromonomer and 40 g of DI water were added in a three-neck flask connected to a mechanical stirrer (400 rpm) and two separate inlets with peristaltic pumps. The flask was placed in an oil bath heated to 40 °C, and the string was for 30 min to dissolve the macromonomers. Next, two solutions were prepared for dropping by peristaltic pumps. Solution A: 9.6 g of AA, 1.2 g of APS, 1 g of 3-MPA were dissolved in 30 g of DI water. Solution B: 0.8 g of VC was dissolved in 40 g of DI water. The reaction time started when solutions A and B were added dropwise into the reaction vessel over 3 hours. After the addition was completed, the reaction was continued for another 2 hours (the total reaction time is 5 hours). It is worth noting that APS in this method was dropped in solution A to avoid aggregation, which often happens when synthesis of HPEG PCE with higher anionic charge density and higher molecular weight.

In synthesis novel structured 52A-P-A polymer, three solutions were prepared before the copolymerization, solution A: AA (1.5 g), DI water (20 g), VC (0.2 g), 3-MPA (0.3 g); solution B: HPEG (40 g), DI water (40 g), AA (6.6 g), VC (0.4 g), 3-MPA (0.4 g); solution C: APS (1.2 g), DI water (20 g). First, add solution A and 5 g of solution C to the flask and keep the reaction for 30 min at the temperature of 40 °C; then add solution B and 11.2 g of solution C to the flask and react for 1.5 h; next, prepare the same solution A, drop it into the flask within 30 min and add 5 g of solution C. After the addition was completed, the reaction was continued for another 2 hours. Finally, the PCE solution was cooled to room temperature.

In the synthesis of 52P-A-P polymer, three solutions were prepared before the copolymerization, solution A: AA (3 g), DI water (20 g), VC (0.4 g), 3-MPA (0.6 g); solution B: HPEG (40 g), DI water (40 g), AA (6.6 g), VC (0.4 g), 3-MPA (0.4 g); solution C: APS (1.2 g), DI water (20 g). Half of solution B and 5 g of solution A were first added to the reaction flask, and the reaction was for 1h at the temperature of 40 °C, then solution A and 11.2 g of solution C were added to the flask and reacted for 30 min,

next the residual solution B and 5 g of solution C was added. After the addition was completed, the reaction was continued for another 2 hours. Finally, the PCE solution was cooled to room temperature.

## 5.6.2 Characterization of PCE polymers

### 5.6.2.1 SEC Results

The chemical composition of PCE samples (52HPEG8, 52A-P-A and 52P-A-P) was confirmed by size exclusion chromatography (SEC) instrument with differential refractive index (dRI) and light-scattering (LS) detectors [204, 205]. The SEC spectra in **Figure 93** displayed the different chemical phase (polymer and residual monomers) in three PCE polymers. They only consist of one copolymer peak (~18 min - ~25 min) and the residual monomer peaks (~25 min - ~28 min), their high conversion rate of macromonomers (85 - 95 %) and low molecular weight distribution (PDI: 1.9 - 2.2) in **Table 30** characterized the successful polymerization without significant amounts of unreacted residual monomers.

The free-radical copolymerization was usually considered to be an instant reaction, and the copolymer could be a blend of homopolymer and copolymer (P(AA) and HPEG-AA copolymer) in the feeding method as described in **Section 5.6.1**. However, the 40 °C free-radical copolymerization, together with APS and AA free radical, which have longer half-lives than the copolymerization times, make it possible to obtain the novel structured PCE by changing the feeding sequence of monomers [206].

Regarding to the block structure of PCE polymers, both 52A-P-A and 52P-A-P polymers exhibit higher molecular weight than 52HPEG8 PCE (see **Table 29**). In addition, the 52A-P-A and 52P-A-P PCE polymers synthesized in this study have similar PDI values to 52HPEG8 (1.9), unlike polymers from CRP methods usually with a PDI around 1.0. Therefore, the novel structured PCE polymers synthesized in this study do not exhibit strictly controlled chain sequence distribution, and kinetic measurements on model systems and detailed polymer fragmentation were not performed in this part. The study in this part focused on synthesizing PCE polymers using a low-cost method and comparing their characteristic and performance to

## Results and discussion

conventional products.

**Table 30** Solid content, molar masses and polydispersity index (PDI) of the synthesized PCE polymers, and the conversion rate of the macromonomer

Sample	Solid content / wt. %	$M_w$ [Da]	$M_n$ [Da]	PDI ( $M_w/M_n$ )	Conversion rate / %
52A-P-A	39.9	27,130	13,900	1.9	91.7
52P-A-P	36.3	31,610	14,330	2.2	84.5
52HPEG8	38.2	26,410	14,110	1.9	95.2

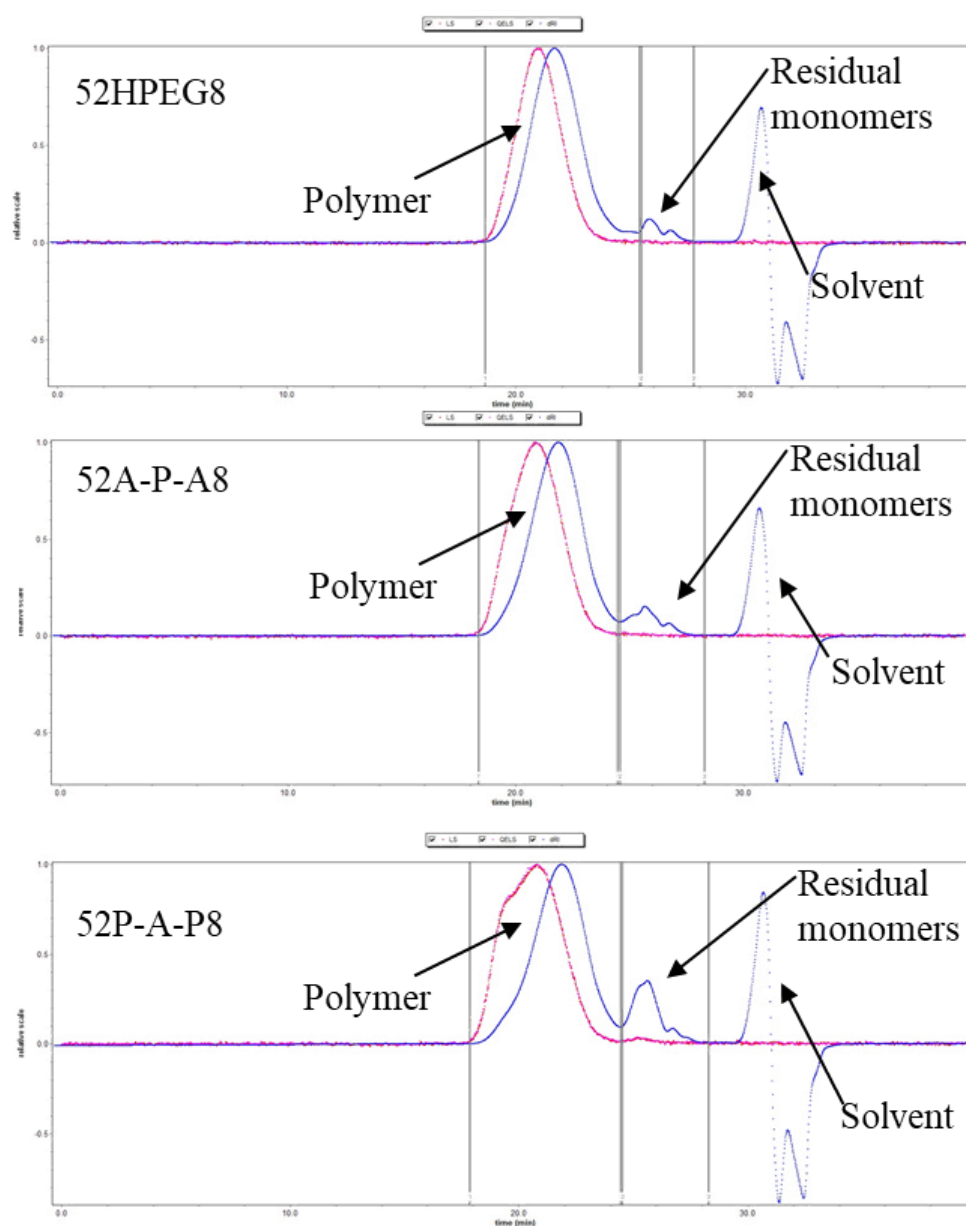


**Figure 93** SEC spectra of PCE polymers with different microstructure

### 5.6.2.2 $^1\text{H}$ NMR measurement

$^1\text{H}$  NMR measurement, which can provide the types and amount of the proton under different chemical environments, successfully distinguished 52A-P-A and 52P-A-P copolymers from the 52HPEG8 random polymer based on the difference in chain segment. The typical proton peaks in 52HPEG8 polymer have been marked (**Figure 94**). The larger peak at 3.6 ppm stemmed from the characteristic ethylene oxide repeating units. The signals at 0.7 - 0.9 ppm and 2.3 - 2.5 ppm belong to the  $-\text{CH}_3$  group and the  $-\text{CH}$  in the backbone, respectively. Moreover, the protons in  $-\text{CH}_2$  group of both AA and HPEG monomer in the backbone appeared at 1.3 - 2.0 ppm, and the proton peaks at 2.6 ppm, 3.4 ppm and 3.8 ppm correspond to the  $-\text{CH}_2$  group adjacent to the ethylene oxide repeat unit in the side chains.

The  $^1\text{H}$  NMR spectra of 52A-P-A and 52P-A-P copolymers (orange and blue curve) exhibited the same characteristic peak that existed in 52HPEG8 copolymer, certifying the successful copolymerization of HPEG and AA monomers under different feeding method. In addition, one sharp peak at 1.6 ppm was observed in both spectra, certifying the existence of poly (acrylic acid) segment in both copolymers. This sharp comes from the methylene ( $-\text{CH}_2-\text{CH}_2$ ) in the poly (acrylic acid) segment, and its strength is positively related to the length of the poly (acrylic acid) segment, as the peak in 52P-A-P copolymer is more obvious because it has a longer poly (acrylic acid) segment in the middle of the polymer chain according to the feeding amounts. Therefore, it can be concluded that the free radical method can realize the redistribute of AA monomers in the polymer chain by changing the feeding sequence of monomers.

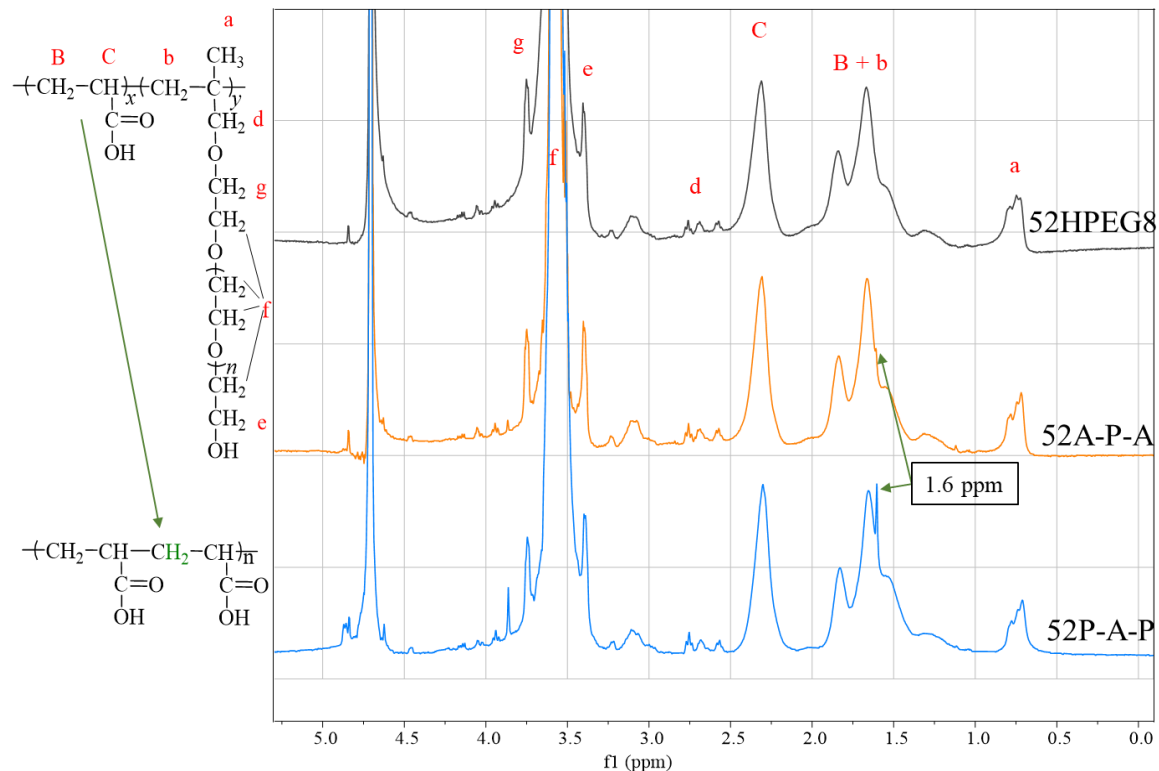


**Figure 94**  $^1\text{H}$  NMR spectra of 52HPEG8, 52A-P-A and 52P-A-P copolymers

### 5.6.2.3 FT-IR measurement

The FT-IR spectra can provide the vibration information of different groups in the copolymer chain (**Figure 95**). First, the bands that appear at  $2797\text{ cm}^{-1}$  and  $2758\text{ cm}^{-1}$  are the  $-\text{CH}_3$  and  $-\text{CH}_2$  respectively. The broad band appearing between  $3587\text{ cm}^{-1}$  and  $2860\text{ cm}^{-1}$  is assigned to the stretching vibration band of  $-\text{OH}$  in  $-\text{COOH}$  groups from AA monomer. The broad and strong band around  $1032\text{ cm}^{-1}$  is related to  $-\text{C}-\text{O}$  in the HPEG macromonomer in the side chains. These typical bands in three polymers (52HPEG8, 52A-P-A and 52P-A-P) indicate the successful copolymerization of AA and HPEG monomers by free radical method. Another band at  $1634\text{ cm}^{-1}$  is from the stretching vibration of  $-\text{C}=\text{O}$  form  $-\text{COOH}$  groups, and this band in 52A-P-A copolymer is more obvious. One possible explanation is that most of the  $-\text{COOH}$  groups in the 52A-P-A copolymer are located at the end of polymer chains, whose vibration was less influenced by the long side chains of the HPEG monomer.

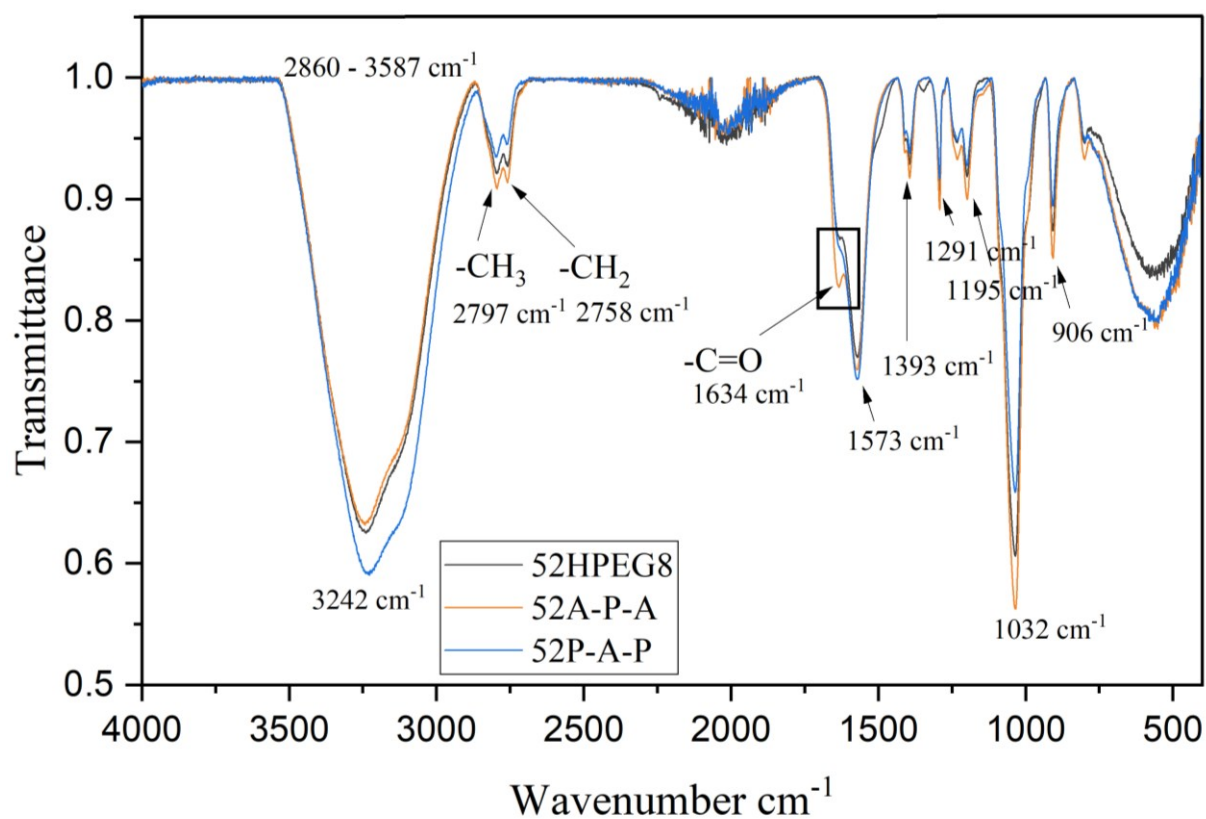


**Figure 95** FT-IR spectra of 52HPEG8, 52A-P-A and 52P-A-P copolymers

#### 5.6.2.4 Specific anionic charge amounts

The specific anionic charge amounts of 52HPEG8, 52A-P-A, and 52P-A-P copolymers were tested in DI water, 0.01 M NaOH, and cement pore solution (**Table 31**). Three copolymers exhibit similar specific anionic charge amount values when tested in DI water, whereas 52A-P-A copolymers have the highest values when tested in NaOH and cement pore solution.

**Table 31** Specific anionic charge amount of superplasticizer samples

PCE sample	Specific anionic charge amount [ $\mu\text{eq/g}$ ]	
	in DI water	in 0.01 M NaOH pH = 12
52HPEG8	893	3214
	904	3220
	897	3211
52A-P-A	874	3483
	861	3566
	865	3512
52P-A-P	758	3492
	740	3460
	744	3475

#### 5.6.2.5 Surface tension measurement

Gradient polymers have special interfacial phase properties because of the gradual change of the composition in the polymer chain. The surface tension measurement was used to detect the critical micelle concentration (CMC) of three copolymers. As the concentration of a surfactant increases, adsorption takes place at the surface until it is fully overlaid, which corresponds to the minimum value of the surface tension. As shown in **Figure 96**, random copolymer 52HPEG8 has a critical micelle concentration (CMC) between 0.015 % to 0.02 %, while 52A-P-A polymer did not show an obvious decrease in surface tension when the polymer concentration was increased.

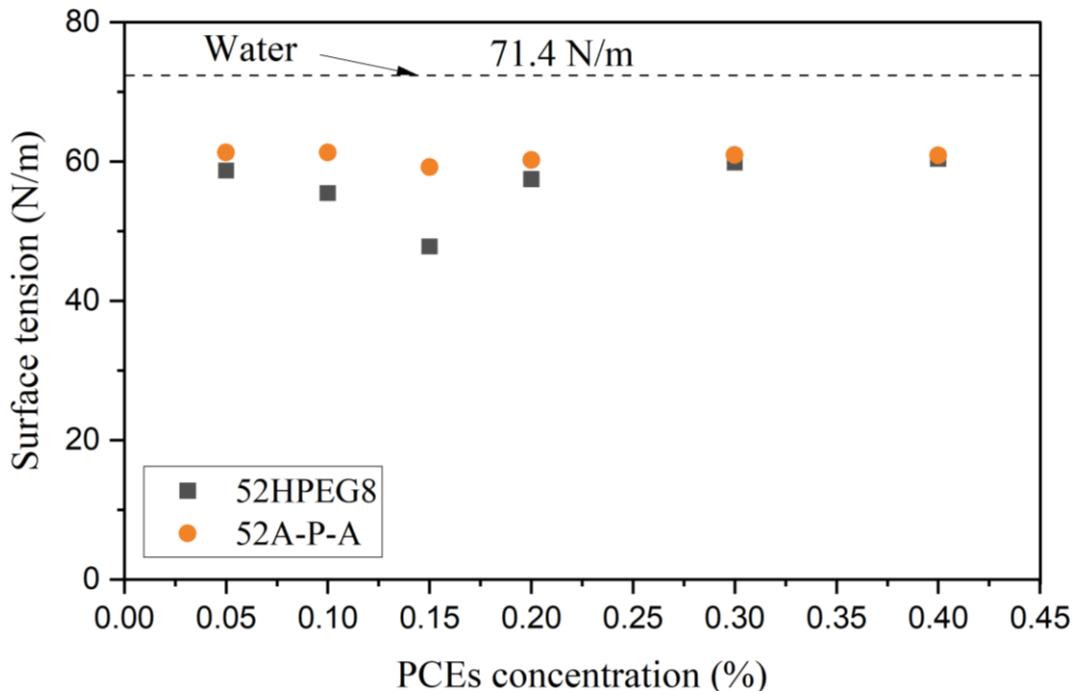


**Figure 96** Surface tension value of 52HPEG8 and 52A-P-A polymers with increasing PCE concentration

### 5.6.3 Performance of novel structured PCE in OPC

#### 5.6.3.1 Dispersing effectiveness

First, the dispersing effectiveness of PCE superplasticizer was tested in mortar at different water-to-cement ratios. As expected, more dosages of all three PCE samples (52HPEG8, 52A-P-A and 52P-A-P) are required at a w/c ratio of 0.40 than that at 0.45 to reach the same spread flow of 20 cm (see **Figure 97**). When comparing three PCE samples with different microstructures, 52HPEG8 and 52A-P-A exhibit stronger dispersing power than 52P-A-P polymer.

Secondly, the dispersing effectiveness was assessed at the same dosage and compared with one commercial precast-type PCE HPEG precast at a water-to-cement ratio of 0.40. 52HPEG8 and 52A-P-A PCE polymers provide similar dispersing capacity as HPEG precast (see **Figure 98**).

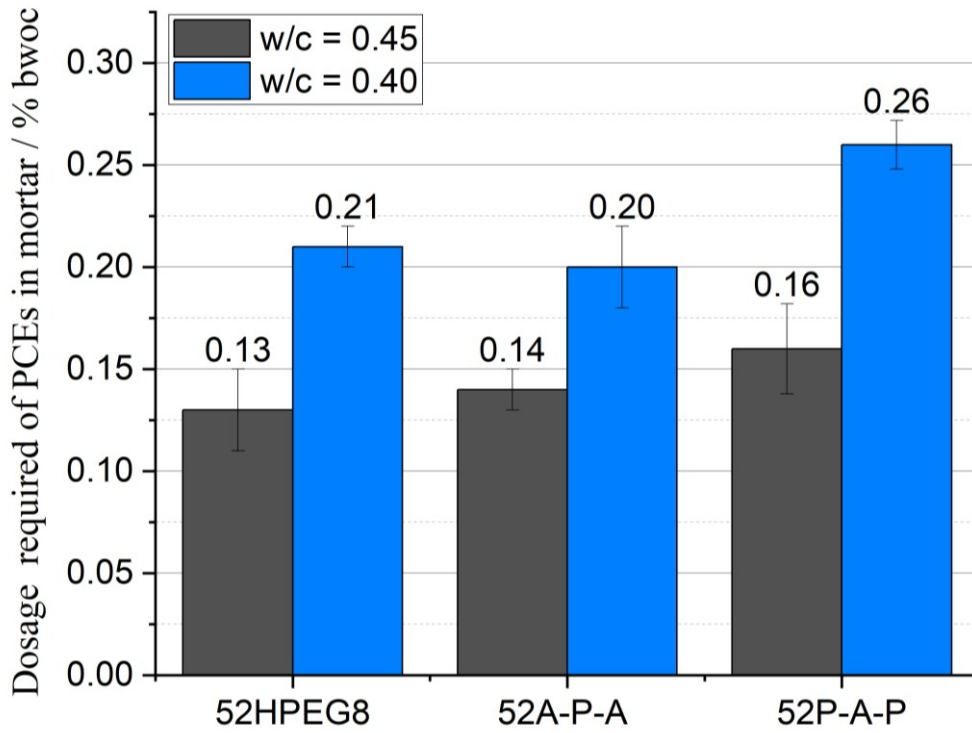


Figure 97 Dosage required to obtain a 20 cm spread flow with different w/c ratios

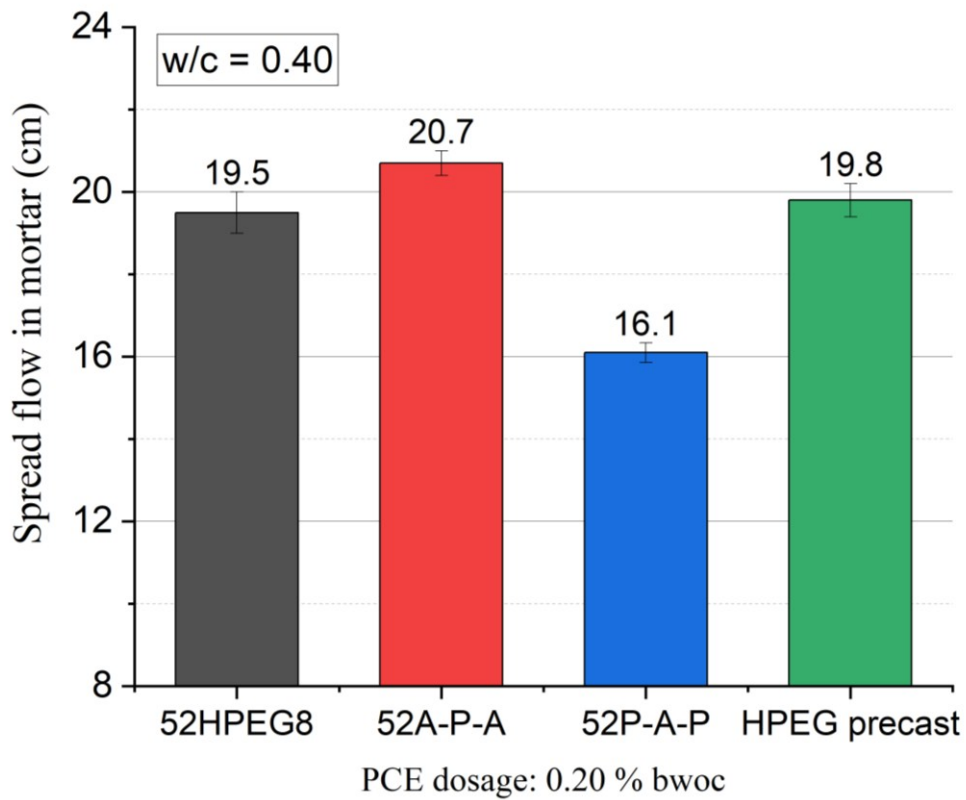
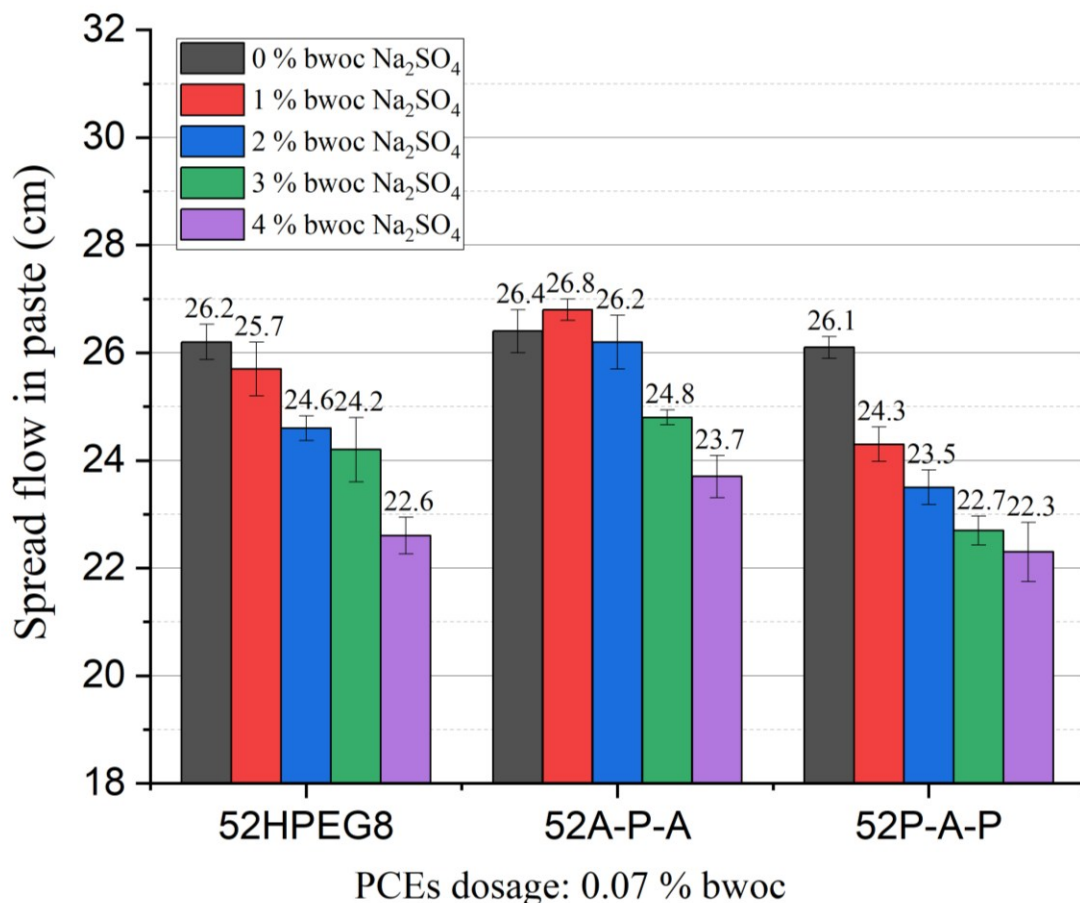


Figure 98 Dispersing effectiveness of different PCEs at the same dosage

### 5.6.3.2 Sulfate resistance of PCE polymers

Next, the sulfate resistance of gradient PCE was assessed in paste at a water-to-cement ratio of 0.45, which can provide a spread flow of 18 cm. The PCE dosage was set at 0.07 % bwoc to obtain an initial spread flow of ~ 26 cm. The spread flows of cement paste containing different sulfate content (1 %, 2 %, 3 % and 4 %) and 0.07 % bwoc PCE were shown in **Figure 99**.

52A-P-A exhibits good sulfate resistance when the sulfate content is not more than 2 % bwoc. While the spread flow of cement pastes admixing 52HPEG8 and 52P-A-P decreased to different degree with increasing sulfate content. The order of sulfate resistance of three PCE polymers is 52A-P-A > 52HPEG8 > 52P-A-P.



**Figure 99** Mini slump test of 52HPEG8, 52A-P-A and 52P-A-P polymers in paste

#### 5.6.4 Summary of Section 5.6

it is possible to synthesis PCE with specific block through free radical copolymerization method. Changing the feeding sequence of monomers affect the formation of polymer microstructure and the properties of the final PCE product. This provides a new idea for the development of novel structured PCE superplasticizer in the future.

This part studied the preparation of optimal PCE product by only changing the feeding sequence while controlling the total mass. A series of block-structured PCE (52A-P-A, 52P-A-P) were obtained from the free-radical method by changing monomers' feeding sequence. Their dispersing effectiveness was tested in CEM I. The SEC, <sup>1</sup>H NMR and FT-IR spectra confirmed the distinct chemical composition of these PCE samples. In addition, PCE samples with block structure have higher dosage effectiveness than random ones. It can be ascribed to the faster adsorption behavior caused by the higher anionic charge according to the specific anionic charge amount measurements. Such PCE samples with a block structure also exhibit sulfate robustness at low sulfate concentrations (1 % bwoc).



## **6. Summary and outlook**

The PCE polycarboxylate superplasticizers have greatly broadened the application of cementitious materials. This thesis aims to solve the defoaming problem of OPC cement and make up for the shortage of PCE polymers suitable for low-carbon cement. Different polymerization methods such as free radical copolymerization, graft and ion-pair complex were used to realize molecular design purpose and corresponding PCE products were copolymerized. The physical and chemical structural properties of these PCE samples were characterized, and their performance in cementitious materials was assessed in paste and mortar. Their working mechanism related to defoaming behavior, hydration process, and adsorption was further analyzed. Various types of low-carbon cement were characterized, in detail, their phase composition, particle size distribution, surface charge, and pH value were analyzed. Based on these characterizations, a series of randomly structured and novel structured PCE superplasticizers for slag blended cement and composite cement were synthesized and tested.

### **Non-air entraining PCE for OPC cement**

The introduction of Jeffamine side chains in PCE structure through the grafting method successfully synthesized a series of G45PC5-g-Jeffamine PCE polymers, therefore realizing air voids controlling purpose in the OPC cement system. The mortar admixed G45PC5-g-Jeffamine 1000 had very low air voids but still dispersed well at the same time. This prior dispersing effectiveness could be ascribed to the steric hindrance from extra polyamine pendant chains, and the hydrophobic side chain also occupied more adsorption sites on the surface of cement particles, which released more free water. Such graft polymer presented no prolongation of the hydration induction period and enhanced the compressive strength at all curing ages (16 h, 3 d, 7 d, and 28 d) due to the different microstructure of the grafted polymer.

For the ion-pair defoamer, pH value is an important parameter in forming and decomposing of PCE-jeffamine complex polymers, The research work in this part focuses on investigating the foaming behavior from different dimensions. Specifically,

two complex polymers 23HPEG7-Jeffamine 2005 and 23HPEG7-Jeffamine 2070 were synthesized and characterized. The foaming behaviors of these two polymers, including defoaming activity, defoaming durability, foam stability and air voids in mortar, were assessed and compared with the pure 23HPEG7 PCE. It was found that 23HPEG7-Jeffamine 2005 and 23HPEG7-Jeffamine 2070 complex exhibited similar defoaming activity as 23HPEG7 PCE but better defoaming durability. The PO/EO ratio in Jeffamine determined their defoaming and dispersing properties, PO units are helpful for disturbing foam stability, while EO units dominate the dispersing performance. Unlike graft polymers, the ion-pair defoamers prolong the induction in the cement hydration process.

With respect to the future development of defoamers based on PCE polymers, the compatibility problem of PO-rich Jeffamine with conventional PCE structure should be taken into consideration, and an in-depth investigation will be interesting for future research.

### **Synthesis of MA-co-HPEG PCE superplasticizers via free radical method**

In this part, a series of MA-co-HPEG PCE superplasticizers was synthesized with the APS-VC redox initiator system. The conversion rate of HPEG macromonomer was increased to ~ 90 % by adjusting the feeding molar ratio, initiator amounts, and molecular weight of HPEG and introducing third comonomers. The optimal MA:HPEG monomer feeding ratio is 2:1 or 3:1. Using highly active third comonomers (MAA/AMPS) or small molecular weight HPEG monomer can greatly accelerate polymerization. The dispersing effectiveness of maleic-based superplasticizers was measured in mini-slump tests. More measurements of different performances, such as viscosity reducing or defoaming behavior, will be interesting for future investigation.

### **Characterization and rheology of cementitious materials and their interaction with PCE polymers**

This part examined the interaction of VP 2020/15.2 PCE with low-carbon cement, LCC and OPC cement, and three types of composite cement were also characterized. The

results indicate that LCC and OPC have different surface charges, leading to varied adsorption behaviors of PCE on their surfaces. This, in turn, affects dispersion and slump retention performances.

Three types of composite cement (CEM II/A-LL 32.5 R; CEM III/A 42.5 N and CEM III/B 42.5 N) have smaller particle sizes and lower pH values compared to OPC, resulting in poorer initial fluidity. Additionally, the surface charge of composite cement differs from that of OPC due to their distinct mineral phase composition and the presence of large amounts of amorphous phases, which impacts their interaction with PCE. Understanding these variations between composite cement and OPC will aid in the development of PCE admixtures suitable for low-carbon cement.

### **PCE superplasticizer designed for slag blended cement**

In the  $\text{Na}_2\text{SO}_4$ -activated “slag + cement” system, the slag is easier to fluidize than OPC, so lower PCE dosages are needed as the slag content increases. However, it becomes increasingly difficult to retain the slump with higher slag content. The PCE polymers with low anionicity are more effective in retaining slump performance. PCE superplasticizers based on hydroxyethyl ester were successfully synthesized and can achieve a retained slump for 2 - 3 hours but significantly reduce early strength (1 d). For the slag-rich ‘85 + 15’ binder, new PCE polymers without ester that are less or not at all retarding are needed.

The study of ‘Full binder’ cementitious materials with a water-to-binder ratio of 0.31 suggests that HPEG type PCE polymers with higher molecular weight and greater anionic charge have better dispersing ability. Conversely, PCE superplasticizers with lower molecular weight lead

to a quicker V-funnel empty time. When the water-to-binder ratio was further reduced to 0.27, HPEG-type PCE struggled to effectively disperse this binder even at a high PCE dosage (1 %). Increasing the mixing time from 4 min to 6.5 min can enhance the flow of mortar by aiding the full distribution and adsorption of PCE polymer on the surface of the binder particles. HPEG type zwitterionic PCE polymers were synthesized

and can disperse the “Full binder” well.

### **Novel structured PCE**

This section focused on the development of novel structured PCE products by altering the feeding sequence. The SEC, <sup>1</sup>H NMR, and FT-IR spectra confirmed the distinct segment sequence between gradient and random PCE samples. Furthermore, the A-P-A PCE sample with a novel structure showed greater dosage effectiveness, especially in sulfate resistance, compared to the 52HPEG8 PCE. This is attributed to faster adsorption behavior due to the higher anionic charge, as indicated by the specific anionic charge amount measurement. It was confirmed that the free radical copolymerization method is useful tool to synthesize PCE polymer with specific structure for different application in the future.

## **7. Zusammenfassung und Ausblick**

Die Polycarboxylat-Superplastifizierer haben die Anwendung von zementösen Materialien erheblich erweitert. Diese Dissertation zielt darauf ab, das Entschäumungsproblem von OPC-Zement zu lösen und den Mangel an PCE-Polymeren, die für kohlenstoffarmen Zement geeignet sind, auszugleichen. Verschiedene Polymerisationsmethoden wie freie Radikal-Copolymerisation, Pfropfung und Ion-Paar-Komplex wurden verwendet, um das Ziel des Moleküldesigns zu verwirklichen, und entsprechende PCE-Produkte wurden copolymerisiert. Die physikalischen und chemischen Strukturmerkmale dieser PCE-Proben wurden charakterisiert und ihre Leistung in zementösen Materialien in Paste und Mörtel bewertet. Ihr Wirkmechanismus in Bezug auf Entschäumungsverhalten, Hydratationsprozess und Adsorption wurde weiter analysiert. Verschiedene Arten von kohlenstoffarmem Zement wurden detailliert charakterisiert, ihre Phasenzusammensetzung, Partikelgrößenverteilung, Oberflächenladung und pH-Wert wurden analysiert. Auf der Grundlage dieser Charakterisierungen wurden Serien von zufällig strukturierten und neu strukturierten PCE-Superplastifizierern für Schlacke-Blended-Zement und Kompositzement synthetisiert und getestet.

### **Nicht-luftporenbildende PCE für OPC-Zement**

Die Einführung von Jeffamin-Seitenketten in die PCE-Struktur durch die Pfropfungsmethode ermöglichte erfolgreich die Synthese einer Reihe von G45PC5-g-Jeffamin PCE-Polymeren und realisierte somit das Ziel der Luftgehaltskontrolle im OPC-Zementssystem. Der mit G45PC5-g-Jeffamin 1000 gemischte Mörtel hatte einen sehr geringen Luftgehalt, verteilte sich aber gleichzeitig gut. Diese vorrangige Dispergiereffektivität könnte auf den sterischen Effekt der zusätzlichen Polyamin-Seitenketten zurückzuführen sein, und die hydrophobe Seitenkette belegte auch mehr Adsorptionsstellen auf der Oberfläche der Zementpartikel, was mehr freies Wasser freisetzte. Ein solches Pfropfpolymer verlängert die Hydratationsinduktionszeit nicht und erhöht die Druckfestigkeit in allen Aushärtungsstufen (16 h, 3 d, 7 d und 28 d)

aufgrund der unterschiedlichen Mikrostruktur des Pffropfpolymers.

Für den Ion-Paar-Entschäumer ist der pH-Wert ein wichtiger Parameter bei der Bildung und Zersetzung von PCE-Jeffamin-Komplexpolymeren. Die Forschungsarbeit in diesem Teil konzentriert sich auf die Untersuchung des Schaumbildungsverhaltens aus verschiedenen Dimensionen. Insbesondere wurden zwei Komplexpolymere 23HPEG7-Jeffamin 2005 und 23HPEG7-Jeffamin 2070 synthetisiert und charakterisiert. Die Schaumbildungsverhalten dieser beiden Polymere, einschließlich Entschäumungsaktivität, Entschäumungsdauerhaftigkeit, Schaumstabilität und Luftgehalt im Mörtel, wurden bewertet und mit dem reinen 23HPEG7 PCE verglichen. Es wurde festgestellt, dass 23HPEG7-Jeffamin 2005 und 23HPEG7-Jeffamin 2070 eine ähnliche Entschäumungsaktivität wie 23HPEG7 PCE, aber eine bessere Entschäumungsdauerhaftigkeit aufweisen. Das PO/EO-Verhältnis in Jeffamin bestimmt deren Entschäumungs- und Dispergiereigenschaften, wobei PO-Einheiten zur Störung der Schaumstabilität beitragen, während EO-Einheiten die Dispergiereigenschaften dominieren. Im Gegensatz zu Pffropfpolymeren verlängern die Ion-Paar-Entschäumer die Induktionszeit im Zementhydratationsprozess.

Hinsichtlich der zukünftigen Entwicklung von Entschäumern auf Basis von PCE-Polymeren sollte das Kompatibilitätsproblem von PO-reichen Jeffaminen mit der herkömmlichen PCE-Struktur berücksichtigt werden, und eine eingehende Untersuchung wird für zukünftige Forschungen interessant sein.

### **Synthese von MA-co-HPEG PCE-Superplastifizierern mittels freier Radikalmethode**

In diesem Teil wurde eine Serie von MA-co-HPEG PCE-Superplastifizierern mit dem APS-VC-Redoxinitiatorsystem synthetisiert. Die Umwandlungsrate des HPEG-Makromonomers wurde auf ~ 90 % erhöht, indem das Molverhältnis der Zuführung, die Initiator Mengen und das Molekulargewicht von HPEG sowie die Einführung dritter Comonomere angepasst wurden. Das optimale MA

ührungsverhältnis beträgt 2:1 oder 3:1. Die Verwendung hochaktiver dritter Comonomere (MAA/AMPS) oder kleinerer HPEG-Monomere kann die Polymerisation erheblich beschleunigen. Die Dispergiereffektivität der maleinsäurebasierten Superplastifizierer wurde in Mini-Slump-Tests gemessen. Weitere Messungen unterschiedlicher Leistungen wie Viskositätsreduzierung oder Entschäumungsverhalten werden für zukünftige Untersuchungen interessant sein.

### **Charakterisierung und Rheologie zementöser Materialien und deren Interaktion mit PCE-Polymeren**

Dieser Teil untersuchte die Interaktion von VP 2020/15.2 PCE mit kohlenstoffarmem Zement: LCC und OPC-Zement; und drei Arten von Kompositzement wurden ebenfalls charakterisiert. Die Ergebnisse zeigen, dass LCC und OPC unterschiedliche Oberflächenladungen aufweisen, was zu unterschiedlichen Adsorptionsverhalten von PCE auf deren Oberflächen führt. Dies wiederum beeinflusst die Dispergier- und Setzverhaltensleistungen.

Drei Arten von Kompositzementen (CEM II/A-LL 32,5 R; CEM III/A 42,5 N und CEM III/B 42,5 N) haben kleinere Partikelgrößen und niedrigere pH-Werte im Vergleich zu OPC, was zu einer schlechteren anfänglichen Fließfähigkeit führt. Zudem unterscheidet sich die Oberflächenladung des Kompositzements von der des OPC aufgrund ihrer unterschiedlichen Mineralphasen-Zusammensetzung und des Vorhandenseins großer amorpher Phasen, was ihre Interaktion mit PCE beeinflusst. Das Verständnis dieser Unterschiede zwischen Kompositzement und OPC wird zur Entwicklung von PCE-Zusätzen beitragen, die für kohlenstoffarmen Zement geeignet sind.

### **PCE-Superplastifizierer für schlackengebundenen Zement**

Im Na<sub>2</sub>SO<sub>4</sub>-aktivierten „Schlacke + Zement“-System ist die Schlacke leichter zu verflüssigen als OPC, daher werden bei steigendem Schlackengehalt niedrigere PCE-Dosierungen benötigt. Allerdings wird es zunehmend schwieriger, mit höherem Schlackengehalt den Ausbreitmaß zu erhalten. PCE-Polymere mit niedriger Anionizität sind effektiver bei der Erhaltung der Ausbreitmaßleistung. PCE-Superplastifizierer auf

Basis von Hydroxyethylester wurden erfolgreich synthetisiert und können einen erhaltenen Ausbreitmaß von 2 - 3 Stunden erreichen, reduzieren jedoch die Frühfestigkeit (1 Tag) erheblich. Für das schlackenreiche „85 + 15“-Bindemittel sind neue PCE-Polymere ohne Ester erforderlich, die weniger oder gar nicht verzögernd wirken.

Die Untersuchung von „Vollbindemittel“-zementösen Materialien mit einem Wasser-Bindemittel-Verhältnis von 0,31 legt nahe, dass HPEG-Typ-PCE-Polymere mit höherem Molekulargewicht und größerer anionischer Ladung eine bessere Dispersionsfähigkeit haben. Umgekehrt führen PCE-Superplastifizierer mit niedrigerem Molekulargewicht zu einer schnelleren V-Trichter-Entleerungszeit. Wenn das Wasser-Bindemittel-Verhältnis weiter auf 0,27 reduziert wurde, hatten HPEG-Typ-PCEs Schwierigkeiten, dieses Bindemittel selbst bei einer hohen PCE-Dosierung (1 %) effektiv zu dispergieren. Eine Erhöhung der Mischzeit von 4 Minuten auf 6,5 Minuten kann den Fluss des Mörtels verbessern, indem die vollständige Verteilung und Adsorption des PCE-Polymers auf der Oberfläche der Bindemittelpartikel unterstützt wird. HPEG-Typ-zwitterionische PCE-Polymere wurden synthetisiert und können das „Vollbindemittel“ gut dispergieren.

### **Neu strukturierte PCE**

Dieser Abschnitt konzentriert sich auf die Entwicklung neu strukturierter PCE-Produkte durch Änderung der Zuführungsreihenfolge. Die SEC-, <sup>1</sup>H-NMR- und FT-IR-Spektren bestätigten die unterschiedliche Segmentsequenz zwischen den gradienten und zufälligen PCE-Proben. Darüber hinaus zeigte die A-P-A-PCE-Probe mit einer neuartigen Struktur eine größere Dosiseffektivität, insbesondere in der Sulfatbeständigkeit, im Vergleich zum 52HPEG8-PCE. Dies wird auf ein schnelleres Adsorptionsverhalten aufgrund der höheren anionischen Ladung zurückgeführt, wie durch die spezifische anionische Ladungsmessung angezeigt.

**Reference**

- [1] R.M. Andrew, Global CO<sub>2</sub> emissions from cement production, *Earth System Science Data*, 10 (2018) 195-217.
- [2] N. Mahasanan, S. Smith, K. Humphreys, The Cement Industry and Global Climate Change Current and Potential Future Cement Industry CO<sub>2</sub> Emissions, *Greenhouse Gas Control Technologies - 6th International Conference*, (2003) 995-1000.
- [3] M. Schneider, The cement industry on the way to a low-carbon future, *Cement and Concrete Research*, 124 (2019) 105792.
- [4] M. Amran, N. Makul, R. Fediuk, Y.H. Lee, N.I. Vatin, Y.Y. Lee, K. Mohammed, Global carbon recoverability experiences from the cement industry, *Case Studies in Construction Materials*, 17 (2022) e01439.
- [5] P. Friedlingstein, M.W. Jones, M. O'Sullivan, et al, Global Carbon Budget 2021, *Earth Syst. Sci. Data*, 14 (2022) 1917-2005.
- [6] R. Guo, J. Wang, L. Bing, D. Tong, P. Ciais, S.J. Davis, R.M. Andrew, F. Xi, Z. Liu, Global CO<sub>2</sub> uptake by cement from 1930 to 2019, *Earth Syst. Sci. Data*, 13 (2021) 1791-1805.
- [7] R. Chaudhury, U. Sharma, P. Thapliyal, L. Singh, Low-CO<sub>2</sub> emission strategies to achieve net zero target in cement sector, *Journal of Cleaner Production*, (2023) 137466.
- [8] A. Adesina, Recent advances in the concrete industry to reduce its carbon dioxide emissions, *Environmental Challenges*, 1 (2020) 100004.
- [9] S.P. Deolalkar, Chapter 2 - Composite Cements, in: S.P. Deolalkar (Ed.) *Designing Green Cement Plants*, Butterworth-Heinemann 2016, pp. 41-44.
- [10] M. Saafi, L. Tang, J. Fung, M. Rahman, J. Liggat, Enhanced properties of graphene/fly ash geopolymeric composite cement, *Cement and Concrete Research*, 67 (2015) 292-299.
- [11] P. Gonnon, D. Lootens, Toward net zero carbon for concrete and mortar: Clinker substitution with ground calcium carbonate, *Cement and Concrete Composites*,

- 142 (2023) 105190.
- [12] E. Gartner, H. Hirao, A review of alternative approaches to the reduction of CO<sub>2</sub> emissions associated with the manufacture of the binder phase in concrete, *Cement and Concrete Research*, 78 (2015) 126-142.
- [13] M. Heikal, M.A. Ali, S.M. Ibrahim, H.I. Bendary, Sustainable composite cement prepared by two different types of iron slag, *Journal of Material Cycles and Waste Management*, (2023) 1-15.
- [14] S. Ibrahim, A. Meawad, Towards green concrete: Study the role of waste glass powder on cement/superplasticizer compatibility, *Journal of Building Engineering*, 47 (2022) 103751.
- [15] T. Kropyvnytska, M. Sanytsky, I. Heviuk, L. Kripka, Study of the Properties of Low-Carbon Portland-Composite Cements CEM II/CM, *International Scientific Conference EcoComfort and Current Issues of Civil Engineering*, Springer, 2022, pp. 230-237.
- [16] T. Hirata, Cement dispersants, JP patent, 842022 (S59-018338), 1981.
- [17] L. Lei, T. Hirata, J. Plank, 40 years of PCE superplasticizers-History, current state-of-the-art and an outlook, *Cement and Concrete Research*, 157 (2022) 106826.
- [18] J.W.C. K.C. Hsu, F.T. Jiang, D.S. Hwung, An amphoteric copolymer as a concrete admixture, in: V.M. Malhotra (Ed.), *8th CanMET/ACI International Conference of Superplasticizers and Other Chemical Admixtures in Concrete*, Sorrento, Italy, (2006) 309-320.
- [19] J. Stecher, J. Plank, Novel concrete superplasticizers based on phosphate esters, *Cement and Concrete Research*, 119 (2019) 36-43.
- [20] L. Lei, M. Palacios, J. Plank, A.A. Jeknavorian, Interaction between polycarboxylate superplasticizers and non-calcined clays and calcined clays: A review, *Cement and Concrete Research*, 154 (2022) 106717.
- [21] M. Ilg, J. Plank, Synthesis and properties of a polycarboxylate superplasticizer with a jellyfish-like structure comprising hyperbranched polyglycerols, *Industrial & Engineering Chemistry Research*, 58 (2019) 12913-12926.

## Reference

---

- [22] R. Ma, Y. Wang, H. Li, Y. Bai, Progress in the polycarboxylate superplasticizer and their structure-activity relationship–A review, *Materials Today Communications*, (2023) 105838.
- [23] X. Wang, Y. Yang, X. Shu, Y. Wang, Q. Ran, J. Liu, Tailoring polycarboxylate architecture to improve the rheological properties of cement paste, *Journal of Dispersion Science and Technology*, 40 (2019) 1567-1574.
- [24] F. Dalas, A. Nonat, S. Pourchet, M. Mosquet, D. Rinaldi, S. Sabio, Tailoring the anionic function and the side chains of comb-like superplasticizers to improve their adsorption, *Cement and Concrete Research*, 67 (2015) 21-30.
- [25] M. Ezzat, X. Xu, K. El Cheikh, K. Lesage, R. Hoogenboom, G. De Schutter, Structure-property relationships for polycarboxylate ether superplasticizers by means of RAFT polymerization, *Journal of colloid and interface science*, 553 (2019) 788-797.
- [26] B. Yu, Z. Zeng, Q. Ren, Y. Chen, M. Liang, H. Zou, Study on the performance of polycarboxylate-based superplasticizers synthesized by reversible addition–fragmentation chain transfer (RAFT) polymerization, *Journal of molecular structure*, 1120 (2016) 171-179.
- [27] S. Ramanathan, M. Croly, P. Suraneni, Comparison of the effects that supplementary cementitious materials replacement levels have on cementitious paste properties, *Cement and Concrete Composites*, 112 (2020) 103678.
- [28] B. Lothenbach, K. Scrivener, R.D. Hooton, Supplementary cementitious materials, *Cement and Concrete Research*, 41 (2011) 1244-1256.
- [29] M.M.A. Elahi, C.R. Shearer, A. Naser Rashid Reza, A.K. Saha, M.N.N. Khan, M.M. Hossain, P.K. Sarker, Improving the sulfate attack resistance of concrete by using supplementary cementitious materials (SCMs): A review, *Construction and Building Materials*, 281 (2021) 122628.
- [30] S.R. Satone, D.K. Parbat, A.M. Badar, V.P. Varghese, D.S. Satone, M.A. Kawalkar, Application of green material on durability behaviour of green concrete, *Materials Today: Proceedings*, (2023).

## Reference

---

- [31] M.R. Ahmad, B. Chen, S. Farasat Ali Shah, Investigate the influence of expanded clay aggregate and silica fume on the properties of lightweight concrete, *Construction and Building Materials*, 220 (2019) 253-266.
- [32] D. Ndahirwa, H. Zmamou, H. Lenormand, N. Leblanc, The role of supplementary cementitious materials in hydration, durability and shrinkage of cement-based materials, their environmental and economic benefits: A review, *Cleaner Materials*, 5 (2022) 100123.
- [33] A. Alaskar, R.D. Hooton, Effect of binder fineness and composition on length change of high-performance concrete, *Construction and Building Materials*, 237 (2020) 117537.
- [34] M.C.G. Juenger, R. Snellings, S.A. Bernal, Supplementary cementitious materials: New sources, characterization, and performance insights, *Cement and Concrete Research*, 122 (2019) 257-273.
- [35] M.C. Juenger, R. Siddique, Recent advances in understanding the role of supplementary cementitious materials in concrete, *Cement and concrete research*, 78 (2015) 71-80.
- [36] R. Snellings, G. Mertens, J. Elsen, Supplementary cementitious materials, *Reviews in Mineralogy and Geochemistry*, 74 (2012) 211-278.
- [37] R. Snellings, Assessing, understanding and unlocking supplementary cementitious materials, *RILEM Technical Letters*, 1 (2016) 50-55.
- [38] K.L. Scrivener, V.M. John, E.M. Gartner, Eco-efficient cements: Potential economically viable solutions for a low-CO<sub>2</sub> cement-based materials industry, *Cement and Concrete Research*, 114 (2018) 2-26.
- [39] S. Kumar, S. Dhara, V. Kumar, A. Gupta, A. Prasad, K. Keshari, B. Mishra, Recent trends in slag management & utilization in the steel industry, *Minerals & Metals Review*, 1 (2019) 94-102.
- [40] Supriya, R. Chaudhury, U. Sharma, P.C. Thapliyal, L.P. Singh, Low-CO<sub>2</sub> emission strategies to achieve net zero target in cement sector, *Journal of Cleaner Production*, 417 (2023) 137466.

## Reference

---

- [41] R.J. Flatt, N. Roussel, H. Bessaies-Bey, L. Caneda-Martínez, M. Palacios, F. Zunino, From physics to chemistry of fresh blended cements, *Cement and Concrete Research*, 172 (2023) 107243.
- [42] M.S. Imbabi, C. Carrigan, S. McKenna, Trends and developments in green cement and concrete technology, *International Journal of Sustainable Built Environment*, 1 (2012) 194-216.
- [43] O. Boukendakdji, E.-H. Kadri, S. Kenai, Effects of granulated blast furnace slag and superplasticizer type on the fresh properties and compressive strength of self-compacting concrete, *Cement and Concrete Composites*, 34 (2012) 583-590.
- [44] Z. Xu, Z. Guo, Y. Zhao, S. Li, X. Luo, G. Chen, C. Liu, J. Gao, Hydration of blended cement with high-volume slag and nano-silica, *Journal of Building Engineering*, 64 (2023) 105657.
- [45] M. Königsberger, J. Carette, Validated hydration model for slag-blended cement based on calorimetry measurements, *Cement and Concrete Research*, 128 (2020) 105950.
- [46] E. Douglas, A. Bilodeau, J. Brandstetr, V. Malhotra, Alkali activated ground granulated blast-furnace slag concrete: preliminary investigation, *Cement and concrete research*, 21 (1991) 101-108.
- [47] J.M. Etcheverry, Y.A. Villagran-Zaccardi, P. Van den Heede, V. Hallet, N. De Belie, Effect of sodium sulfate activation on the early age behaviour and microstructure development of hybrid cementitious systems containing Portland cement, and blast furnace slag, *Cement and Concrete Composites*, 141 (2023) 105101.
- [48] C.B. Cheah, L.E. Tan, M. Ramli, Recent advances in slag-based binder and chemical activators derived from industrial by-products—A review, *Construction and Building Materials*, 272 (2021) 121657.
- [49] F. Puertas, B. González-Fonteboa, I. González-Taboada, M.M. Alonso, M. Torres-Carrasco, G. Rojo, F. Martínez-Abella, Alkali-activated slag concrete: Fresh and hardened behaviour, *Cement and Concrete Composites*, 85 (2018) 22-31.
- [50] M.S. Konsta-Gdoutos, S.P. Shah, Hydration and properties of novel blended

## Reference

---

- cements based on cement kiln dust and blast furnace slag, *Cement and Concrete Research*, 33 (2003) 1269-1276.
- [51] L. Li, J. Yang, H. Li, Y. Du, Insights into the microstructure evolution of slag, fly ash and condensed silica fume in blended cement paste, *Construction and Building Materials*, 309 (2021) 125044.
- [52] M. Palacios, F. Puertas, P. Bowen, Y.F. Houst, Effect of PCs superplasticizers on the rheological properties and hydration process of slag-blended cement pastes, *Journal of Materials Science*, 44 (2009) 2714-2723.
- [53] M. Şahmaran, H.A. Christianto, İ.Ö. Yaman, The effect of chemical admixtures and mineral additives on the properties of self-compacting mortars, *Cement and Concrete Composites*, 28 (2006) 432-440.
- [54] M.M. Alonso, M. Palacios, F. Puertas, Compatibility between polycarboxylate-based admixtures and blended-cement pastes, *Cement and Concrete Composites*, 35 (2013) 151-162.
- [55] A. Danish, M.A. Mosaberpanah, Influence of cenospheres and fly ash on the mechanical and durability properties of high-performance cement mortar under different curing regimes, *Construction and Building Materials*, 279 (2021) 122458.
- [56] A. Hallal, E.-H. Kadri, K. Ezziane, A. Kadri, H. Khelafi, Combined effect of mineral admixtures with superplasticizers on the fluidity of the blended cement paste, *Construction and Building Materials*, 24 (2010) 1418-1423.
- [57] S. Ng, H. Justnes, Influence of plasticizers on the rheology and early heat of hydration of blended cements with high content of fly ash, *Cement and concrete composites*, 65 (2016) 41-54.
- [58] M. Sharma, S. Bishnoi, F. Martirena, K. Scrivener, Limestone calcined clay cement and concrete: A state-of-the-art review, *Cement and Concrete Research*, 149 (2021) 106564.
- [59] K. Scrivener, F. Avet, H. Maraghechi, F. Zunino, J. Ston, W. Hanpongpun, A. Favier, Impacting factors and properties of limestone calcined clay cements (LC3), *Green Materials*, 7 (2018) 3-14.

## Reference

---

- [60] F. Zunino, F. Martirena, K. Scrivener, Limestone Calcined Clay Cements (LC<sup>3</sup>), *ACI Materials Journal*, 118 (2021).
- [61] <https://lc3.ch/about-lc3/>, (accessed April 17, 2024).
- [62] I.M. Krieger, T.J. Dougherty, A mechanism for non-Newtonian flow in suspensions of rigid spheres, *Trans. Soc. Rheol.*, 3 (1959) 137-152.
- [63] L. Struble, G.-K. Sun, Viscosity of Portland cement paste as a function of concentration, *Advanced Cement Based Materials*, 2 (1995) 62-69.
- [64] O. Burgos-Montes, M.M. Alonso, F. Puertas, Viscosity and water demand of limestone- and fly ash-blended cement pastes in the presence of superplasticisers, *Construction and Building Materials*, 48 (2013) 417-423.
- [65] F. Winnefeld, S. Becker, J. Pakusch, T. Götz, Effects of the molecular architecture of comb-shaped superplasticizers on their performance in cementitious systems, *Cement and Concrete Composites*, 29 (2007) 251-262.
- [66] A. Zingg, F. Winnefeld, L. Holzer, J. Pakusch, S. Becker, R. Figi, L. Gauckler, Interaction of polycarboxylate-based superplasticizers with cements containing different C3A amounts, *Cement and Concrete Composites*, 31 (2009) 153-162.
- [67] Q. Zhang, J. Chen, J. Zhu, Y. Yang, D. Zhou, T. Wang, X. Shu, M. Qiao, Advances in Organic Rheology-Modifiers (Chemical Admixtures) and Their Effects on the Rheological Properties of Cement-Based Materials, *Materials*, 15 (2022) 8730.
- [68] M.J. de Hita, M. Criado, Influence of superplasticizers on the workability and mechanical development of binary and ternary blended cement and alkali-activated cement, *Construction and Building Materials*, 366 (2023) 130272.
- [69] I. Bhandari, R. Kumar, A. Sofi, N.S. Nighot, A systematic study on sustainable low carbon cement–Superplasticizer interaction: Fresh, mechanical, microstructural and durability characteristics, *Heliyon*, (2023).
- [70] F.F. Ataie, M.C.G. Juenger, S.C. Taylor-Lange, K.A. Riding, Comparison of the retarding mechanisms of zinc oxide and sucrose on cement hydration and interactions with supplementary cementitious materials, *Cement and Concrete Research*, 72 (2015) 128-136.

## Reference

---

- [71] A. Papageorgiou, G. Tzouvalas, S. Tsimas, Use of inorganic setting retarders in cement industry, *Cement and Concrete Composites*, 27 (2005) 183-189.
- [72] D.A. Hall, R. Stevens, B. El-Jazairi, The effect of retarders on the microstructure and mechanical properties of magnesia–phosphate cement mortar, *Cement and Concrete Research*, 31 (2001) 455-465.
- [73] M. Zajac, J. Skocek, F. Bullerjahn, M. Ben Haha, Effect of retarders on the early hydration of calcium-sulpho-aluminate (CSA) type cements, *Cement and Concrete Research*, 84 (2016) 62-75.
- [74] J. Plank, E. Sakai, C.W. Miao, C. Yu, J.X. Hong, Chemical admixtures — Chemistry, applications and their impact on concrete microstructure and durability, *Cement and Concrete Research*, 78 (2015) 81-99.
- [75] P.G. Ng, C.B. Cheah, E.P. Ng, C.W. Oo, K.H. Leow, The influence of main and side chain densities of PCE superplasticizer on engineering properties and microstructure development of slag and fly ash ternary blended cement concrete, *Construction and Building Materials*, 242 (2020) 118103.
- [76] K. Yamada, T. Takahashi, S. Hanehara, M. Matsuhisa, Effects of the chemical structure on the properties of polycarboxylate-type superplasticizer, *Cement and concrete research*, 30 (2000) 197-207.
- [77] A. Lange, J. Plank, Formation of nano-sized ettringite crystals identified as root cause for cement incompatibility of PCE superplasticizers, *Nanotechnology in Construction: Proceedings of NICOM5*, Springer, 2015, pp. 55-63.
- [78] R. Li, L. Lei, T. Sui, J. Plank, Approaches to achieve fluidity retention in low-carbon calcined clay blended cements, *Journal of Cleaner Production*, 311 (2021) 127770.
- [79] C. Chomyn, J. Plank, Impact of different pH-values of polycarboxylate (PCE) superplasticizer solutions on their dispersing effectiveness, *Construction and Building Materials*, 246 (2020) 118440.
- [80] N. Li, B. Ding, The Performance of Low Air-Entraining Polycarboxylate Superplasticizer, *Advanced Materials Research*, 1129 (2015) 361-366.

## Reference

---

- [81] X. Zeng, X. Lan, H. Zhu, H. Liu, H. Umar, Y. Xie, G. Long, M. Cong, A Review on Bubble Stability in Fresh Concrete: Mechanisms and Main Factors, *Materials*, 13 (2020) 1820.
- [82] L. Du, K.J. Folliard, Mechanisms of air entrainment in concrete, *Cement and Concrete Research*, 35 (2005) 1463-1471.
- [83] M.T. Hasholt, M.H.S. Jespersen, O.M. Jensen, Mechanical properties of concrete with SAP. Part I: Development of compressive strength, International RILEM conference on use of superabsorbent polymers and other new additives in concrete, Rilem publications, 2010, pp. 117-126.
- [84] N. Denkov, K. Marinova, N. Denkov, K. Marinova, Antifoam effects of solid particles, oil drops and oil-solid compounds in aqueous foams, *Colloidal Particles at Liquid Interfaces*, (2006).
- [85] N.D. Denkov, K.G. Marinova, S.S. Tcholakova, Mechanistic understanding of the modes of action of foam control agents, *Adv Colloid Interface Sci*, 206 (2014) 57-67.
- [86] W. Wang, X. Fan, For the preparation method of the defoamer of water-based system CN105148571B, 2017.
- [87] F. Xu, A kind of preparation method of defoamer easy to use CN107177351A, 2017.
- [88] G.A. Smith, Defoamer compositions and uses therefor WO2001076729A2, 2001.
- [89] J. Ma, Y. Shang, C. Peng, H. Liu, S. Zheng, H. Yan, Q. Ran, Foam and rheological behavior of polydentate phosphonate-modified polymers under cement system, *Construction and Building Materials*, 290 (2021) 123205.
- [90] E.C. Galgoci, S.Y. Chan, K. Yacoub, Innovative, gemini-type molecular defoamer technology for improved coating aesthetics, *JCT Research*, 3 (2006) 77-85.
- [91] P.R. Garrett, Defoaming: Antifoams and mechanical methods, *Current Opinion in Colloid & Interface Science*, 20 (2015) 81-91.
- [92] R.D. Kulkarni, E.D. Goddard, B. Kanner, Mechanism of antifoaming action, *Journal of Colloid and Interface Science*, 59 (1977) 468-476.

## Reference

---

- [93] R. Pelton, T. Flaherty, Defoamers: linking fundamentals to formulations, *Polymer International*, 52 (2003) 479-485.
- [94] A.J. Ara, Overview of Defoaming Technologies for Polycarboxylate-Based Superplasticizers, *ACI Symposium Publication*, 329 (2018) 185-200.
- [95] S.M. Shendy, J.R. Bury, T.M. Vickers, F. Ong, WO 2001042162A1, Solubilized defoamers for cementitious compositions, 2005.
- [96] D.C. Darwin, R.T. Taylor, A.A. Jeknavorian, D.F. Shen, Emulsified comb polymer and defoaming agent composition and method of making same US6139623A, 1998.
- [97] P.-H. Chuang, S. Zhang, Y. Ke, Y. Guo, Effect of different macromonomer molecular size in polycarboxylate superplasticizer by molecular dynamics simulation, *IOP Conference Series: Materials Science and Engineering*, 738 (2020) 012033.
- [98] Q. Ran, F. Song, T. Wang, S. Fan, J. Ma, Y. Yang, J. Liu, Effect of the different hydrophobic groups of polycarboxylate superplasticizers on the properties in cement mortars, *Polymer Composites*, 38 (2017) 1783-1791.
- [99] H. Uchikawa, S. Hanehara, D. Sawaki, The role of steric repulsive force in the dispersion of cement particles in fresh paste prepared with organic admixture, *Cement and Concrete Research*, 27 (1997) 37-50.
- [100] A. Kauppi, K.M. Andersson, L. Bergström, Probing the effect of superplasticizer adsorption on the surface forces using the colloidal probe AFM technique, *Cement and Concrete Research*, 35 (2005) 133-140.
- [101] H. Tian, X. Kong, T. Su, D. Wang, Comparative study of two PCE superplasticizers with varied charge density in Portland cement and sulfoaluminate cement systems, *Cement and Concrete Research*, 115 (2019) 43-58.
- [102] R. Flatt, Analysis of superplasticizers used in concrete, *Analisis*, 26 (1998) 28-34.
- [103] L. Lei, H.-K. Chan, Investigation into the molecular design and plasticizing effectiveness of HPEG-based polycarboxylate superplasticizers in alkali-activated

## Reference

---

- slag, *Cement and Concrete Research*, 136 (2020) 106150.
- [104] E. Sakai, A. Ishida, A. Ohta, New trends in the development of chemical admixtures in Japan, *Journal of Advanced Concrete Technology*, 4 (2006) 211-223.
- [105] J.B. Martin Ebner, A. Ohta, Polycarboxylate Based Admixture's Trend in Europe, (2004).
- [106] A. Lange, T. Hirata, J. Plank, Influence of the HLB value of polycarboxylate superplasticizers on the flow behavior of mortar and concrete, *Cement and Concrete Research*, 60 (2014) 45-50.
- [107] Y. Li, C. Yang, Y. Zhang, J. Zheng, H. Guo, M. Lu, Study on dispersion, adsorption and flow retaining behaviors of cement mortars with TPEG-type polyether kind polycarboxylate superplasticizers, *Construction and Building Materials*, 64 (2014) 324-332.
- [108] Z. Wang, Y. Xu, WuHao, X. Liu, F. Zheng, H. Li, S. Cui, M. Lan, Y. Wang, A room temperature synthesis method for polycarboxylate superplasticizer, CN Patent 101974135 B, 2013.
- [109] A. Gerhard, W. Josef, P. Johann, Kern Alfred, Copolymers based on oxyalkyleneglycol alkenyl ethers and derivatives of unsaturated dicarboxylic acids, EP 0736553 B1, (1996).
- [110] L. Lei, J. Plank, Synthesis and properties of a vinyl ether-based polycarboxylate superplasticizer for concrete possessing clay tolerance, *Industrial & Engineering Chemistry Research*, 53 (2014) 1048-1055.
- [111] G. Liu, X. Qin, X. Wei, Z. Wang, J. Ren, Study on the monomer reactivity ratio and performance of EPEG-AA (ethylene-glycol monovinyl polyethylene glycol-acrylic acid) copolymerization system, *Journal of Macromolecular Science, Part A*, 57 (2020) 646-653.
- [112] H. Feng, Z. Feng, W. Wang, Z. Deng, B. Zheng, Impact of polycarboxylate superplasticizers (PCEs) with novel molecular structures on fluidity, rheological behavior and adsorption properties of cement mortar, *Construction and Building Materials*, 292 (2021) 123285.

## Reference

---

- [113] H. Feng, Z. Feng, Y. Mao, Z. Deng, B. Zheng, Study on the polymerization process and monomer reactivity of EPEG-type polycarboxylate superplasticizer, *Journal of Applied Polymer Science*, 139 (2022) e52697.
- [114] T. Amaya, A. Ikeda, J. Imamura, A. Kobayashi, K. Saito, W.M. Danzinger, T. Tomoyose, Cement dispersant and concrete composition containing the dispersant, Google Patents, 2004.
- [115] M. Mosquet, Y. Chevalier, S. Brunel, J.P. Guicquero, P. Le Perchec, Polyoxyethylene di-phosphonates as efficient dispersing polymers for aqueous suspensions, *Journal of applied polymer science*, 65 (1997) 2545-2555.
- [116] O. Akhlaghi, T. Aytas, B. Tatli, D. Sezer, A. Hodaei, A. Favier, K. Scrivener, Y.Z. Menciloglu, O. Akbulut, Modified poly (carboxylate ether)-based superplasticizer for enhanced flowability of calcined clay-limestone-gypsum blended Portland cement, *Cement and Concrete Research*, 101 (2017) 114-122.
- [117] Y. He, X. Zhang, R. Hooton, Effects of organosilane-modified polycarboxylate superplasticizer on the fluidity and hydration properties of cement paste, *Construction and Building Materials*, 132 (2017) 112-123.
- [118] G. De Schutter, M. Ezzat, K. Lesage, R. Hoogenboom, Responsive superplasticizers for active rheology control of cementitious materials, *Cement and Concrete Research*, 165 (2023) 107084.
- [119] Z. Lu, X. Kong, H. Liu, Z. Wang, Y. Zhang, B. Dong, F. Xing, Interaction of silylated superplasticizers with cementitious materials, *Journal of Applied Polymer Science*, 133 (2016).
- [120] S. Sha, Y. Zhang, Y. Ma, Y. Liu, C. Shi, Effect of molecular structure of maleic anhydride, fumaric acid–Isopentenyl polyoxyethylene ether based polycarboxylate superplasticizer on its properties in cement pastes, *Construction and Building Materials*, 308 (2021) 125143.
- [121] X. Chen, Z. Liu, X. Fu, X. Xie, T. Wang, Z. Rong, Y. Nong, Z. Lu, Enhanced adsorption and properties of TPEG-type superplasticizers modified by maleic anhydride: A perspective from molecular architecture and conformation, *Materials*

## Reference

---

- and Structures, 57 (2024) 4.
- [122] A. Habbaba, A. Lange, J. Plank, Synthesis and performance of a modified polycarboxylate dispersant for concrete possessing enhanced cement compatibility, Journal of applied polymer science, 129 (2013) 346-353.
- [123] T. Kitano, S. Kawaguchi, K. Ito, A. Minakata, Dissociation behavior of poly (fumaric acid) and poly (maleic acid). 1. Potentiometric titration and intrinsic viscosity, Macromolecules, 20 (1987) 1598-1606.
- [124] X. Liu, Z. Wang, Y. Zheng, S. Cui, M. Lan, H. Li, J. Zhu, X. Liang, Preparation, characterization and performances of powdered polycarboxylate superplasticizer with bulk polymerization, Materials, 7 (2014) 6169-6183.
- [125] A.A. Jeknavorian, A. Arfaei, N.S. Berke, D.C. Darwin, E.M. Gartner, L.A. Jardine, J.F. Lambert, L.R. Roberts, High early-strength-enhancing admixture for precast hydraulic cement and compositions containing same, Google Patents, 1998.
- [126] T.M. Vickers Jr, R. Packe-Wirth, J.R. Bury, J. Osborne, R. Lu, J. Moreau, L.E. Brower, S.M. Shendy, J. Pickett, Derivatized polycarboxylate dispersants, Google Patents, 2001.
- [127] I. Schober, T.A. Bürge, U. Velten, J. Widmer, C.M. Bürge, U. Mäder, Cement admixture for improved slump life, Google Patents, 2006.
- [128] X. Liu, Z. Wang, J. Zhu, Y. Zheng, S. Cui, M. Lan, H. Li, Synthesis, characterization and performance of a polycarboxylate superplasticizer with amide structure, Colloids and Surfaces A: Physicochemical and Engineering Aspects, 448 (2014) 119-129.
- [129] K. Hsu, J. Chen, F. Jiang, D. Hwung, An amphoteric copolymer as a concrete admixture, Special Publication, 239 (2006) 309-320.
- [130] M. Schmid, N. Beuntner, K.-C. Thienel, J. Plank, Amphoteric Superplasticizers for Cements Blended with a Calcined Clay, Special publication, (2018) 41-54.
- [131] R. Li, L. Lei, T. Sui, J. Plank, Effectiveness of PCE superplasticizers in calcined clay blended cements, Cement and Concrete Research, 141 (2021) 106334.
- [132] G. Lai, X. Liu, X. Song, J. Guan, Z. Wang, S. Cui, S. Qian, Q. Luo, H. Xie, C.

## Reference

---

- Xia, A mechanistic study on the effectiveness of star-like and comb-like polycarboxylate superplasticizers in cement pastes, *Cement and Concrete Research*, 175 (2024) 107389.
- [133] T. Zhou, H. Duan, Z. Li, Y. Jin, H. Liu, Y. Pang, H. Lou, D. Yang, X. Qiu, Reconfiguring Molecular Conformation from Comb-Type to Y-Type for Improving Dispersion Performance of Polycarboxylate Superplasticizers, *Macromolecules*, 57 (2024) 727-738.
- [134] Q. Ran, X. Wang, X. Shu, Q. Zhang, Y. Yang, J. Liu, Effects of Sequence Structure of Polycarboxylate Superplasticizers on the Dispersion Behavior of Cement Paste, *Journal of Dispersion Science and Technology*, 37 (2016) 431-441.
- [135] M. Werani, L. Lei, Influence of side chain length of MPEG-based polycarboxylate superplasticizers on their resistance towards intercalation into clay structures, *Construction and Building Materials*, 281 (2021) 122621.
- [136] I. Emaldi, E. Erkizia, J.R. Leiza, J.S. Dolado, Understanding the effect of MPEG-PCE's microstructure on the adsorption and hydration of OPC, *Journal of the American Ceramic Society*, 106 (2023) 2567-2579.
- [137] T. Hirata, T. Yuasa, K. Shiote, K. Nagare, S. Iwai, Cement dispersant, method for producing polycarboxylic acid for cement dispersant and cement composition, Google Patents, 2001.
- [138] T. Fukuda, K. Kubo, Y.-D. Ma, Kinetics of free radical copolymerization, *Progress in polymer science*, 17 (1992) 875-916.
- [139] K.F. O'Driscoll, Free radical polymerization kinetics - revisited, *Pure and Applied Chemistry*, 53 (1981) 617-626.
- [140] N. Hadjichristidis, H. Iatrou, M. Pitsikalis, J. Mays, Macromolecular architectures by living and controlled/living polymerizations, *Progress in Polymer Science*, 31 (2006) 1068-1132.
- [141] G. Moad, E. Rizzardo, S.H. Thang, Toward living radical polymerization, *Accounts of chemical research*, 41 (2008) 1133-1142.
- [142] K. Matyjaszewski, J. Spanswick, Controlled/living radical polymerization,

## Reference

---

- Handbook of Polymer Synthesis, CRC Press 2004, pp. 907-954.
- [143] D.J.M. Flower, J.G. Sanjayan, Green house gas emissions due to concrete manufacture, *The International Journal of Life Cycle Assessment*, 12 (2007) 282-288.
- [144] X. Liu, G. Lai, J. Guan, S. Qian, Z. Wang, S. Cui, F. Gao, Y. Jiao, R. Tao, Technical optimization and life cycle assessment of environment-friendly superplasticizer for concrete engineering, *Chemosphere*, 281 (2021) 130955.
- [145] C. Schiefer, J. Plank, CO<sub>2</sub> emission of polycarboxylate superplasticizers (PCEs) used in concrete, *Journal of Cleaner Production*, 427 (2023) 138785.
- [146] C. Schiefer, J. Plank, On the CO<sub>2</sub> footprint of polycarboxylate superplasticizers (PCEs) and its impact on the eco balance of concrete, *Construction and Building Materials*, 409 (2023) 133944.
- [147] Z.C. Lu, M. Haist, D. Ivanov, C. Jakob, D. Jansen, S. Leinitz, J. Link, V. Mechtcherine, J. Neubauer, J. Plank, W. Schmidt, C. Schilde, C. Schröfl, T. Sowoidnich, D. Stephan, Characterization data of reference cement CEM I 42.5 R used for priority program DFG SPP 2005 “Opus Fluidum Futurum – Rheology of reactive, multiscale, multiphase construction materials”, *Data in brief*, 27 (2019) 104699.
- [148] J. Plank, B. Sachsenhauser, Experimental determination of the effective anionic charge density of polycarboxylate superplasticizers in cement pore solution, *Cement and Concrete Research*, 39 (2009) 1-5.
- [149] <mechanisms of foam destruction by oil based antifoams 2004-08-ND-ReviewCov.pdf>.
- [150] DIN EN 12350-7:2009-08 Prüfung von Frischbeton - Teil 7: Luftgehalt - Druckverfahren;, Germany, 2009.
- [151] DIN EN 196-1 Prüfverfahren für Zement - Teil 1: Bestimmung der Festigkeit, Germany, 2016.
- [152] DIN EN 1015-3, Prüfverfahren für Mörtel und Mauerwerk-Teil 3: Bestimmung der Konsistenz von Frischmörtel (mit Ausbreittisch), Deutsche Norm, Beuth-

- Verlag, Berlin, 2007.
- [153] L. Wilhelmy, Ueber die Abhängigkeit der Capillaritäts-Constanten des Alkohols von Substanz und Gestalt des benetzten festen Körpers, *Annalen der Physik*, 195 (1863) 177-217.
- [154] W.C. Griffin, Classification of Surface-Active Agents by “HLB”, *Journal of Cosmetic Science*, 1 (1949) 311-326.
- [155] X-ray Diffraction (XRD) DIFFRAC.EVA, <https://www.bruker.com/de/products-and-solutions/diffractometers-and-x-ray-microscopes/x-ray-diffractometers/diffrac-suite-software/diffrac-eva.html>.
- [156] H.M. Rietveld, Line profiles of neutron powder-diffraction peaks for structure refinement, *Acta Crystallographica*, 22 (1967) 151-152.
- [157] H.M. Rietveld, A profile refinement method for nuclear and magnetic structures, *Applied Crystallography*, 2 (1969) 65-71.
- [158] D.E. 1015-3, Prüfverfahren für Mörtel und Mauerwerk-Teil 3: Bestimmung der Konsistenz von Frischmörtel (mit Ausbreittisch), Deutsche Norm, Beuth-Verlag, Berlin, 2007.
- [159] DIN EN 12350-9: 2010: Testing fresh concrete - Part 9: Self-compacting concrete - V funnel test.
- [160] DIN EN 13395-2: 2002: Products and systems for the protection and repair of concrete structures - Test methods - Determination of workability - Part 2: Test for flow of grout or mortar.
- [161] B. Łażniewska-Piekarczyk, The methodology for assessing the impact of new generation superplasticizers on air content in self-compacting concrete, *Construction and Building Materials*, 53 (2014) 488-502.
- [162] G. Gelardi, R. Flatt, Working mechanisms of water reducers and superplasticizers, *Science and technology of concrete admixtures*, Elsevier 2016, pp. 257-278.
- [163] K. Yoshioka, E.-i. Tazawa, K. Kawai, T. Enohata, Adsorption characteristics of superplasticizers on cement component minerals, *Cement and concrete research*, 32 (2002) 1507-1513.

## Reference

---

- [164] Y. Zhang, X. Kong, Correlations of the dispersing capability of NSF and PCE types of superplasticizer and their impacts on cement hydration with the adsorption in fresh cement pastes, *Cement and concrete research*, 69 (2015) 1-9.
- [165] M. Palacios, P. Bowen, M. Kappler, H.-J. Butt, M. Stuer, C. Pecharromás, U. Aschauer, H. Puertas, F. Puertas, Repulsion forces of superplasticizers on ground granulated blast furnace slag in alkaline media, from AFM measurements to rheological properties, *Materiales de Construcción*, 62 (2012) 489-513.
- [166] R.J. Flatt, Dispersion forces in cement suspensions, *Cement and Concrete Research*, 34 (2004) 399-408.
- [167] F. Özcan, M. Emin Koç, Influence of ground pumice on compressive strength and air content of both non-air and air entrained concrete in fresh and hardened state, *Construction and Building Materials*, 187 (2018) 382-393.
- [168] A. Lange, J. Plank, Study on the foaming behaviour of allyl ether-based polycarboxylate superplasticizers, *Cement and Concrete Research*, 42 (2012) 484-489.
- [169] B. Łaźniewska-Piekarczyk, The effect of superplasticizers and anti-foaming agents on the air entrainment and properties of the mix of self compacting concrete, *Cement, Wapno, Beton*, 29 (2009) 133-147.
- [170] F. Al-Neshawy, T. Ojala, J. Punkki, Stability of Air Content in Fresh Concretes with PCE-Based Superplasticizers, *Nordic Concrete Research*, 60 (2019) 145-158.
- [171] N. Vargaftik, B. Volkov, L. Voljak, International tables of the surface tension of water, *Journal of Physical and Chemical Reference Data*, 12 (1983) 817-820.
- [172] J. Pott, L. Lohaus, Development strategies for foamed cement paste, Tailor made concrete structures. London: Taylor & Francis Group, (2008) 457-460.
- [173] L. Xia, M. Zhou, T. Ni, Z. Liu, Synthesis and characterization of a novel early-strength polycarboxylate superplasticizer and its performances in cementitious system, *Journal of Applied Polymer Science*, 137 (2020) 48906.
- [174] J. Pickelmann, H. Li, R. Baumann, J. Plank, A <sup>13</sup>C NMR Spectroscopic Study on the Repartition of Acid and Ester Groups in MPEG Type PCEs Prepared via

## Reference

---

- Radical Copolymerization and Grafting Techniques, Eleventh international conference on superplasticizers and other chemical admixtures in concrete, 2015.
- [175] C. You, J. Qian, J. Qin, H. Wang, Q. Wang, Z. Ye, Effect of early hydration temperature on hydration product and strength development of magnesium phosphate cement (MPC), *Cement and Concrete Research*, 78 (2015) 179-189.
- [176] J. Cheung, A. Jeknavorian, L. Roberts, D. Silva, Impact of admixtures on the hydration kinetics of Portland cement, *Cement and concrete research*, 41 (2011) 1289-1309.
- [177] L. Lei, R. Li, A. Fuddin, Influence of maltodextrin retarder on the hydration kinetics and mechanical properties of Portland cement, *Cement and Concrete Composites*, 114 (2020) 103774.
- [178] Q. Zitao, Evaluation of ion pair defoaming system for HPEG-type polycarboxylate superplasticizers, Chemistry department, Technical University of Munich, 2019.
- [179] T.H. Rehm, C. Schmuck, Ion-pair induced self-assembly in aqueous solvents, *Chemical Society Reviews*, 39 (2010) 3597-3611.
- [180] J. Coates, Interpretation of Infrared Spectra, A Practical Approach, *Encyclopedia of Analytical Chemistry* 2006.
- [181] A.R. Garcia, R.B. de Barros, J.P. Lourenço, L.M. Ilharco, The Infrared Spectrum of Solid l-Alanine: Influence of pH-Induced Structural Changes, *The Journal of Physical Chemistry A*, 112 (2008) 8280-8287.
- [182] N.D. Denkov, K.G. Marinova, S.S. Tcholakova, Mechanistic understanding of the modes of action of foam control agents, *Advances in Colloid and Interface Science*, 206 (2014) 57-67.
- [183] A. Lange, J. Plank, Study on the foaming behaviour of allyl ether-based polycarboxylate superplasticizers, *Cement and Concrete Research*, 42 (2012) 484–489.
- [184] N.B. Vargaftik, B.N. Volkov, L.D. Voljak, International Tables of the Surface Tension of Water, *Journal of Physical and Chemical Reference Data*, 12 (1983)

- 817-820.
- [185] L. Lei, L. Zhang, Synthesis and performance of a non-air entraining polycarboxylate superplasticizer, *Cement and Concrete Research*, 159 (2022) 106853.
- [186] J. Ma, Y. Shang, C. Peng, H. Liu, Q. Ran, Synthesis and foaming performance of one high-efficient air content regulator of concrete, *Colloids and Surfaces A: Physicochemical and Engineering Aspects*, 586 (2020) 124245.
- [187] H. Li, Z. Xue, H. Liang, Y. Guo, G. Liang, D. Ni, Z. Yang, Influence of defoaming agents on mechanical performances and pore characteristics of Portland cement paste/mortar in presence of EVA dispersible powder, *Journal of Building Engineering*, 41 (2021) 102780.
- [188] F.-r. Kong, L.-s. Pan, C.-m. Wang, D.-l. Zhang, N. Xu, Effects of polycarboxylate superplasticizers with different molecular structure on the hydration behavior of cement paste, *Construction and Building Materials*, 105 (2016) 545-553.
- [189] W. Mao, C. Cao, X. Li, J. Qian, C. You, Preparation of Magnesium Ammonium Phosphate Mortar by Manufactured Limestone Sand Using Compound Defoaming Agents for Improved Strength and Impermeability, *Buildings*, 12 (2022) 267.
- [190] L. Zhang, X. Miao, X. Kong, S. Zhou, Retardation effect of PCE superplasticizers with different architectures and their impacts on early strength of cement mortar, *Cement and Concrete Composites*, 104 (2019) 103369.
- [191] H. Ahmadi Moghadam, A. Mirzaei, Z. Abedi Dehghi, The relation between porosity, hydration degree and compressive strength of Portland cement pastes in the presence of aluminum chloride additive, *Construction and Building Materials*, 250 (2020) 118884.
- [192] Y. Houst, R. Flatt, P. Bowen, H. Hofmann, U. Mäder, J. Widmer, U. Sulser, T. Bürge, Influence of superplasticizer adsorption on the rheology of cement paste, *Proceedings of the International RILEM Conference on " The Role of Admixtures in High Performance Concrete"*, RILEM Publications sarl, Cachan, France., 1999, pp. 387-402.

## Reference

---

- [193] J. Plank, C. Hirsch, Impact of zeta potential of early cement hydration phases on superplasticizer adsorption, *Cement and Concrete Research*, 37 (2007) 537-542.
- [194] A. Zingg, F. Winnefeld, L. Holzer, J. Pakusch, S. Becker, L. Gauckler, Adsorption of polyelectrolytes and its influence on the rheology, zeta potential, and microstructure of various cement and hydrate phases, *Journal of Colloid and Interface Science*, 323 (2008) 301-312.
- [195] J. Plank, B. Sachsenhauser, J. de Reese, Experimental determination of the thermodynamic parameters affecting the adsorption behaviour and dispersion effectiveness of PCE superplasticizers, *Cement and Concrete Research*, 40 (2010) 699-709.
- [196] R. Rostami, A. Klemm, F. Almeida, The Effect of SCMs in Blended Cements on Sorption Characteristics of Superabsorbent Polymers, *Materials*, 14 (2021) 1609.
- [197] E. Berodier, K. Scrivener, Evolution of pore structure in blended systems, *Cement and Concrete Research*, 73 (2015) 25-35.
- [198] M. Thomas, The effect of supplementary cementing materials on alkali-silica reaction: A review, *Cement and Concrete Research*, 41 (2011) 1224-1231.
- [199] A. Vollpracht, B. Lothenbach, R. Snellings, J. Haufe, The pore solution of blended cements: a review, *Materials and Structures*, 49 (2016) 3341-3367.
- [200] H. Tian, X. Kong, X. Miao, L. Jiang, X. Pang, A new insight into the working mechanism of PCE emphasizing the interaction between PCE and  $\text{Ca}^{2+}$  in fresh cement paste, *Construction and Building Materials*, 275 (2021) 122133.
- [201] B. Wu, B.-W. Chun, L. Gu, T.L. Kuhl, Effect of  $\text{Ca}^{2+}$  ion concentration on adsorption of poly (carboxylate ether)-based (PCE) superplasticizer on mica, *Journal of colloid and interface science*, 527 (2018) 195-201.
- [202] J. Plank, H. Li, M. Ilg, J. Pickelmann, W. Eisenreich, Y. Yao, Z. Wang, A microstructural analysis of isoprenol ether-based polycarboxylates and the impact of structural motifs on the dispersing effectiveness, *Cement and Concrete Research*, 84 (2016) 20-29.
- [203] J. Plank, K. Pöllmann, N. Zouaoui, P.R. Andres, C. Schaefer, Synthesis and

## Reference

---

- performance of methacrylic ester based polycarboxylate superplasticizers possessing hydroxy terminated poly(ethylene glycol) side chains, *Cement and Concrete Research*, 38 (2008) 1210-1216.
- [204] H.G. Barth, C. Jackson, B.E. Boyes, Size exclusion chromatography, *Analytical chemistry*, 66 (1994) 595-620.
- [205] L.K. Kostanski, D.M. Keller, A.E. Hamielec, Size-exclusion chromatography—a review of calibration methodologies, *Journal of biochemical and biophysical methods*, 58 (2004) 159-186.
- [206] A.P. Freidig, H.J. Verhaar, J.L. Hermens, Quantitative structure-property relationships for the chemical reactivity of acrylates and methacrylates, *Environmental Toxicology and Chemistry: An International Journal*, 18 (1999) 1133-1139.